A DEEP SKY SURVEY AT 2700 MHZ

Jasper V. Wall

1970

A Thesis Submitted for the Degree of

Doctor of Philosophy

The Australian National University

Canberra

For J & K

ACKNOWLEDGEMENTS

It is a pleasure to thank Mr. J. G. Bolton, my supervisor during the course of this investigation, for his sustained interest in each phase of the work. I am indebted to him for his continued advice, and the generous amount of time which he has devoted to the reading, discussion, and criticism of the manuscript of this thesis.

Mr. A. J. Shimmins likewise gave freely of advice and devoted a considerable amount of time to discussion and criticism of drafts of the thesis, for which I am grateful. In addition, he has made a considerable amount of unpublished data available to me.

I thank Dr. Beverley Harris for generously communicating her accurate observations of flux densities of Parkes catalogue sources to me in advance of publication. I should also like to thank Drs. D. Wills, J. B. Whiteoak, F. F. Gardner, B. A. Peterson, and R. N. Manchester for communicating observational results to me prior to publication.

During the earlier stages of this work Drs. Leonard Searle and Bengt Westerlund offered valuable advice and assistance for which I am grateful. The advice and encouragement of Dr. D. S. Mathewson during the final stages of the work has also been much appreciated.

I acknowledge very valuable discussions with Dr. Allan Sandage and Professor F. Hoyle. I also acknowledge useful

discussions on certain specific aspects of the investigation with Mr. B. F. C. Cooper, Dr. Beverley Harris, and Dr. J. B. Whiteoak.

I thank all members of the receiver group of the Division of Radiophysics, CSIRO, who assisted in the preparation, installation, and testing of the receivers used. In this regard I acknowledge in particular the generous assistance of Mr. D. Cooke and Mr. W. Butler.

During the course of this investigation the observational and computational facilities of the Division of Radiophysics, CSIRO, were generously made available to me by Dr. E. G. Bowen, Chief of the Division, and Mr. J. G. Bolton, Director of the ANRAO. I thank the Director of Mount Stromlo and Siding Spring Observatories, Professor O. J. Eggen, and his predecessor, Professor B. J. Bok, for the arrangement with CSIRO whereby I was able to use these facilities to obtain the observational material for this thesis.

I gratefully acknowledge a Research Scholarship from the Australian National University during the course of this work.

In the final preparation of this thesis, I am indebted to Miss Sue Khouri for her help in typing part of the final copy; to Miss Flora Ogsten; and to Mr. P. Linstead.

I owe my greatest debt of gratitude to my wife Jenny for her patience and encouragement during this work. She deciphered and typed all first and subsequent drafts, and typed the greater part of the final copy of this thesis; her assistance throughout has been invaluable.

The text of this thesis contains full acknowledgement of any part of this investigation which is not solely my own work.

J. V. Wall

CONTENTS

		PAGE
CHAPTER 1 INTRODUCTION		1
1.1	Extragalactic Source Surveys	2
1.2	Observational Programmes in the Present Investigation	9
1.3	A Summary of the Investigation	12
CHAPTER 2 THE PARKES 2700 MHZ SURVEY: SELECTED REGIONS, AND THE ±4° DECLINATION ZONE		17
2.1	Telescope and Receiver	17
2.2	The Survey Observations	18
2.3	The Source Position/Flux Density Observations	22
2.4	The Source Positions	26
2.5	The Accuracy of the Catalogue Positions	32
2.6	Comparison with Other Observations	35
2.7	The 2700 MHz Flux Densities	38
2.8	Errors in the Flux Densities	42
2.9	Comparison with Other Observations	48
2.10	Reliability and Completeness	50
CHAPTER 3 OPTICAL IDENTIFICATIONS		55
3.1	Galaxy Identifications from the Parkes 2700 MHz Survey: the Selected Regions and the ±4° Declination Zone	55
3.2	Quasi-Stellar Objects in the Parkes 2700 MHz Survey: the Selected Regions, and the ±4° Declination Zone	61
CHAPTER 4 THE SPECTRA OF SOURCES IN THE PARKES 2700 MHZ SURVEYS I. THE OBSERVATIONS, AND SPECTRA OF INDIVIDUAL SOURCES		67
4.1	Flux Densities at 5009 MHz	67
4.2	Flux Densities at 2700 MHz	85
4.3	Flux Densities at 1403 MHz and 468 MHz	86

4.4 Other Flux Densities between 1400 and 1425 MHz 91
4.5 Flux Densities at 635 MHz 92
4.6 Flux Densities at 408 MHz 94
4.7 Flux Densities at 178 MHz 95
4.8 The Spectra of Individual Sources in the 2700 MHz Catalogues 95
4.9 Strong Sources Not Catalogued in 4C 104

CHAPTER 5 122
THE SPECTRA OF SOURCES IN THE PARKES 2700 MHZ SURVEYS
II. SPECTRAL STATISTICS

5.1 The Forms of Radio Source Spectra 122
5.2 The Spectral Content 128
5.3 Prediction of Spectral Content 133
5.4 Variable Sources 140
5.5 The Spectra of Radio Galaxies and QSO's 143
5.6 The Unidentified Sources 148

CHAPTER 6 159
THE NUMBER - FLUX DENSITY RELATION AT 2700 MHZ

6.1 The 2700 MHz Source Counts 160
6.2 Corrections to the Source Counts; the Number - Flux Density Relation 161
6.3 Other Forms of the Number - Flux Density Relation 168
6.4 Comparison with Counts at 178 MHz and 408 MHz; Answers to Criticisms 173
6.5 Comparison with Number - Flux Density Relations at Other Frequencies 179
6.6 The Difference between the Number - Flux Density Relations at 2700 and 178 MHz 183
6.7 The Dependence of Spectrum on Flux Density 189
6.8 Source Counts for QSO's and Radio Galaxies 193

CHAPTER 7 199
INTERPRETATION OF THE NUMBER - FLUX DENSITY RELATION

7.1 Previous Investigations of the Significance of Source Counts 199

7.2 The Computational Technique; S - z Diagrams 201
7.3 Luminosity Functions for Radio Galaxies 204
7.4 Luminosity Functions for QSO's 221
7.5 The Computed Number - Flux Density Relations 229
7.6 The Dependence of Spectrum on Flux Density 238
7.7 Conclusions from the Present Analysis 247

CHAPTER 8 251
CONCLUSION

8.1 Results of the Present Investigation 251
8.2 Lines of Further Investigation 254

REFERENCES 259

APPENDIX I A1
CONFUSION EFFECTS AT 2700 MHZ

APPENDIX II A11
THE CATALOGUES

APPENDIX III A64
DATA ON THE OPTICAL IDENTIFICATIONS FROM THE 2700 MHZ SURVEY OF THE SELECTED REGIONS AND THE $\pm 4^{\circ}$ DECLINATION ZONE

AIII.1 Galaxy Identifications A64
AIII.2 QSO Identifications A73

APPENDIX IV A82
SPECTRAL DATA FOR SOURCES CATALOGUED AT 2700 MHZ

CHAPTER 1

INTRODUCTION

Virtually all conclusions on the physics of extragalactic radio sources have been derived from studies of those catalogued in sky surveys at or below the frequency of 408 MHz. Profound cosmological conclusions have also been drawn from studies of the source populations obtained in low frequency surveys.

This thesis presents the results of extragalactic source surveys at the comparatively high frequency of 2700 MHz, carried out over about 0.8 sr. with the 210 - foot telescope of the ANRAO at Parkes, N.S.W. The surveys are the first parts of the Parkes 2700 MHz survey which will extend eventually over the entire sky between declination -90° and declination $+27^{\circ}$, the northernmost limit of observation for the Parkes telescope.

For all sources catalogued in the present surveys, subsequent observational programmes at 2700 MHz have been carried out to measure accurate positions and flux densities at this frequency. The accurate positions have been used to derive complete statistics on the optical identification of sources in the catalogues. Statistics on the spectra of a large sample of these sources have been obtained in programmes of flux density measurements at Parkes, supplemented by low frequency data from other observatories.

It is the overall aim of this thesis to examine

whether the results of these programmes suggest amplification or modification of the general conclusions, both astrophysical and cosmological, previously derived from the lower frequency surveys.

1.1 Extragalactic Source Surveys

Sources found from surveys at or below 408 MHz illustrate a variety of radio spectra which show some correlation with class of optical identification. This is particularly apparent from comparison of the identification content of the Cambridge 178 MHz catalogues with the Parkes 408 MHz catalogue. The latter contains a larger fraction of quasi-stellar objects (QSO's) than the former, and the difference is due to the inclusion in the Parkes catalogue of a number of sources with "flat" radio spectra, most of which are identified as QSO's. On this basis, surveys at higher frequencies might be expected to detect still greater numbers of flat spectrum sources and increased proportions of QSO's as a consequence. These suppositions are borne out by the present investigation.

There is a considerable literature on the implications of the "log N - log S curve", the cumulative count of radio sources to specific levels of flux density which comprises the classic cosmological test of radio astronomy. This literature is concerned generally with counts from surveys at or below 408 MHz. The preceding discussion indicates that the proportions of the classes of optical identification present in a

radio source catalogue depend on survey frequency, and furthermore that these classes exhibit spectral distinctions which must result in different radio "K - corrections". It is hence quite possible that the form of the number - flux density relation will depend on frequency, and evidence for this is provided by the results of the present work.

The rewards of obtaining comprehensive sky surveys throughout the radio range consequently are not insignificant. The Parkes 2700 MHz survey was commenced at a time when the only published extragalactic source catalogues for frequencies higher than 1000 MHz were those from the limited areas surveyed by Price and Milne (1965) at 1410 MHz, and by Kellermann and Read (1965) at 1421 MHz. Other surveys at frequencies of 1400 to 1420 MHz, most notably those of the OSU (Scheer and Kraus 1967; Dixon and Kraus 1968; Fitch, Dixon, and Kraus 1969) were in progress. At still higher frequencies, the only survey for extragalactic sources known to be in progress was that of the University of Michigan at 8 GHz (G. Brandie and F. Haddock, personal communication to J. G. Bolton).

Table 1.1 contains data on the sky surveys from which the radio source catalogues in current usage have been compiled. Early surveys which have been superceded (e.g. the Cambridge 2C, and the first Ohio State University surveys) are omitted. Furthermore, many of those listed have been superceded by others in the table; the data given makes such cases self-evident. The table contains data on surveys rather than

TABLE 1.1

EXTRAGALACTIC SOURCE SURVEYS

(1) Frequency (MHz)	(2) Instrument	(3) Beam	(4) Area Surveyed	(5) No. of Sources Catalogued	(6) Flux Limit (f.u.)	(7) Source Density Limit (N/sr.)	(8) Corresponding Beam Areas per Source	(9) Ref.	(10) Remarks
38	Cambridge pencil beam synthesis	$45'$(r.a.) x $45'$sec(ZA)	$\delta \geq -10^\circ$ 7.4 sr.	1069	18	150	50	1	Estimated limiting flux density depends on galactic latitude
81.5	Cambridge pencil beam synthesis	$10'$ x $10'$	$\delta \geq +70^\circ$ 0.38 sr.	560	1.0	2500	60	2	Estimated limiting flux density depends on declination
85	Mills Cross, C.S.I.R.O.	$50'$ x $50'$	$+10^\circ \geq \delta \geq -80^\circ$ 7.3 sr.	2270	20	350	17	3,4,5	MSH
159	Cambridge 4 - element interferometer	$1^\circ.2$(r.a.) x $7^\circ.7$ Fringe sep. $11'$ (r.a.)	$+71^\circ \geq \delta \geq -22^\circ$ 8.3 sr.	471	8	80	6	6	3C; many spurious sources
178	Cambridge interferometer	$13'.6$(r.a.) x $4^\circ.6$; fringe sep. $7'.5$ (r.a.)	$\delta \geq -05^\circ$ 6.9 sr.	326	9	40	100	7	3CR; based on 3C, positions and flux densities remeasured
	Cambridge fan beam telescope	$13'.6$(r.a.) x $4^\circ.6$							
178	Cambridge aperture synthesis	$23'$(r.a.) x $31'$sec(ZA) Fringe sep. $7'.5$ (r.a.)	$+80^\circ \geq \delta \geq -07^\circ$ 7.9 sr.	4843	2.0	800	26	8,9	4C
178	Cambridge aperture synthesis	$4'.5$ x $4'.5$	$\delta > 86^\circ$ .015 sr.	87	0.25	11000	70	10	
408	A.N.R.A.O. 210 - foot paraboloid	$48'$ x $48'$	$+20^\circ > \delta > -90^\circ$ 7.5 sr.	1780	4.0	80	80	11	PKS: complete to 2.5 f.u. in some areas
408	Northern Cross (Bologna)	$3'$(r.a.) x $10'$	$07^h40^m < \alpha < 18^h20^m$ $35^\circ > \delta > 34^\circ$ .040 sr.	328	0.25	700	70	12	
			$34^\circ > \delta > 29^\circ$ 0.44 sr.	3235	0.20	8000	60	13	B2
408	E-W arm, Northern Cross	$4'$(r.a.) x $1^\circ.8$	$13^h > \alpha > 3^h$ $-20^\circ > \delta > -30^\circ$ 0.41 sr.	654	1.0	1000	35	14	B1

TABLE 1.1 continued

(1)	(2)	(3)	(4)	(5)	(6)	(7)	(8)	(9)	(10)
408	Cambridge one - mile telescope	80"(r.a.) x 100"	$\alpha\ 09^h40^m$ $\delta +50^\circ$ .003 sr.	106	0.025	50000	140	15	5C1
408	Cambridge one - mile telescope	2°.5(r.a.) x 100"	$00^h < \alpha < 15^h30^m$ $\delta +50^\circ$ 0.15 sr.	198	0.5	2000	30	16	Fan beam operation
408	Cambridge one - mile telescope	80"(r.a.) x 100"	$\alpha\ 11^h00^m$ $\delta +50^\circ$ .004 sr.	207	0.012	10^5	70	17	5C2
408	Cambridge one - mile telescope	80"(r.a.) x 100"	$\alpha\ 00^h40^m$ $\delta +41^\circ$ .004 sr.	213	0.012	10^5	70	18	5C3: centered on M31
610.5	V.R.O. 400 - foot telescope	16'(r.a.) x 20'	$+44^\circ > \alpha > +40^\circ$ $+22^\circ > \delta > +15^\circ$ 1.0 sr.	964	0.8	1000	110	19,20	
635	A.N.R.A.O. 210 - foot paraboloid	30'.6 x 30'.6	$+27^\circ > \delta > +20^\circ$ 0.70 sr.	397	1.5	300	55	21	PKS
750	N.R.A.O. 300 - foot paraboloid	18'.8 x 18'.8	$+20^\circ > \delta > -18^\circ$ 0.28 sr.	458	0.5	1000	45	22	Simultaneous survey at 1410 MHz
1410	A.N.R.A.O. 210 - foot paraboloid	14' x 14'	$-75^\circ > \delta > -90^\circ$ 0.22 sr.	135	0.5	700	110	23	Part of PKS
1415	O.S.U. 260 x 70 - foot telescope	10'(r.a.) x 40'	$+38^\circ > \delta > +25^\circ$ $+37^\circ > \delta > +19^\circ$ $+20^\circ > \delta > +0^\circ$ 2.2 sr.	3560	0.3	1000	35	24,25,26	Right ascension coverage in each zone is not complete
1417	Dwingeloo 25 - metre telescope	36' x 37'	$\delta \geq -20^\circ$ 3.7 sr.	188	2.3	35	150	27	DW; catalogue intentionally excludes many sources of ordinary spectrum
1420	D.A.O. 85 - foot telescope	36' x 36'	$+70^\circ > \delta > -5^\circ$ 6.0 sr.	615	2.0	55	200	28	DAO
1421	Caltech 2 x 90 - foot interferometer	Primary 33' x 33' Fringe sep. 12' (r.a.)	$+30^\circ > \delta > +24^\circ$ 0.68 sr.	143	1.15	120	115	29	CTD

TABLE 1.1 concluded

(1)	(2)	(3)	(4)	(5)	(6)	(7)	(8)	(9)	(10)
2700	A.N.R.A.O. 210 - foot paraboloid	7'.9 x 7'.9	6 selected regions .075 sr.	310	0.10	2500	50		PKS 2700 MHz: present survey
			$+4^{\circ} > \delta > -4^{\circ}$ 0.77 sr.	500	0.35	500			PKS 2700 MHz: present survey
5000	N.R.A.O. 140 - foot paraboloid	6' x 6'	2 selected regions .029 sr.	27	0.2	500	400	30	
5000	N.R.A.O. 140 - foot paraboloid	6' x 6'	5C1 .003 sr.	12	0.1	2700	80	31	
			2 selected regions 0.28 sr.	57	0.5	150			

References for Table 1.1

(1) Williams, P.J.S., Kenderdine, S., and Baldwin, J.E. (1966) - Mem. R. astr. Soc. 70, 53

(2) Branson, N.J.B.A. (1967) - Mon. Not. R. astr. Soc. 135, 149

(3) Mills, B.Y., Slee, O.B., and Hill, E.R. (1958) - Aust. J. Phys. 11, 360

(4) Mills, B.Y., Slee, O.B., and Hill, E.R. (1960) - Aust. J. Phys. 13, 676

(5) Mills, B.Y., Slee, O.B., and Hill, E.R. (1961) - Aust. J. Phys. 14, 497

(6) Edge, D.O., Shakeshaft, J.R., McAdam, W.B., Baldwin, J.E., and Archer, S. (1959) - Mem. R. astr. Soc. 68, 37

(7) Bennett, A.S. (1962) - Mem. R. astr. Soc. 68, 163

(8) Pilkington, J.D.H., and Scott, P.F. (1965) - Mem. R. astr. Soc. 69, 183

(9) Gower, J.F.R., Scott, P.F., and Wills, D. (1967) - Mem. R. astr. Soc. 71, 49

(10) Ryle, M., and Neville, Ann C. (1962) - Mon. Not. R. astr. Soc. 125, 39

(11) Ekers, Jennifer A. (ed.) and Staff of the Division of Radiophysics, C.S.I.R.O. (1969) - Aust. J. Phys. Astrophys. Supp. 7

(12) Grueff, G., and Vigotti, M. (1968) - Astrophys. Lett. 2, 113

(13) Roub, Gruppo (1969) - Contributions from Laboratorio Nationale di Radioastronomia, Università degli Studi, Bologna 55

(14) Braccessi, A., Ceccarelli, M., Fanti, R., Gelato, G., Giovanni, C., Harris, D., Rosatelli, C., Sinigaglia, G., and Volders, L. (1965) - Nuovo Cim. 40B, 267

(15) Kenderdine, S., Ryle, Sir Martin, and Pooley, G.G. (1966) - Mon. Not. R. astr. Soc. 134, 189

(16) Bailey, J.A., and Pooley, G.G. (1968) - Mon. Not. R. astr. Soc. 138, 51

(17) Pooley, G.G., and Kenderdine, S. (1968) - Mon. Not. R. astr. Soc. 139, 529

(18) Pooley, G.G. (1969) - Mon. Not. R. astr. Soc. 144, 101

(19) MacLeod, J.M., Swenson, G.W.,Jr., Yang, K.S., and Dickel, J.A. (1965) - Astron. J. 70, 756

(20) Dickel, J.R., Yang, K.S., McVittie, G.C., Swenson, G.W.,Jr. (1967) - Astron. J. 72, 757

(21) Shimmins, A.J., and Day, G.A. (1968) - Aust. J. Phys. 21, 377

(22) Hoglund, Bertil (1967) - Astrophys. J. Supp. 15, 61

(23) Price, R.M., and Milne, D.K. (1965) - Aust. J. Phys. 18, 329

(24) Scheer, D.J., and Kraus, J.D. (1967) - Astron. J. 72, 536

(25) Dixon, R.S., and Kraus, J.D. (1968) - Astron. J. 73, 381

(26) Fitch, L.I., Dixon, R.S., and Kraus, J.D. (1969) - Astron. J. 74, 612

(27) Davis, M.M. (1967) - Bull. astr. Insts Netherlands 19, 201

(28) Galt, J.A., and Kennedy, J.E.D. (1968) - Astron. J. 73, 135

(29) Kellermann, K.I., and Read, R.B. (1965) - Pub. Owens Valley Obs. 1,2

(30) Blum, E.J., and Davis, M.M. (1968) - Astrophys. Lett. 2, 41

(31) Kellermann, K.I., Pauliny-Toth, I.I.K., and Davis, M.M. (1968) - Astrophys. Lett. 2, 105

on catalogues, and as a consequence the widely consulted source lists of Howard and Maran (1965) and Pauliny-Toth, Wade, and Heeschen (1966) are not included.

The primary object of Table 1.1 is to indicate the status of extragalactic source surveys. A secondary object is to give brief descriptions of the first two parts of the Parkes 2700 MHz survey in context with descriptions of those surveys it is designed to complement. Beginning with the first two parts of the 2700 MHz survey, the observational programmes carried out in the course of this investigation are now briefly described.

1.2 Observational Programmes in the Present Investigation

1.2 (i) 2700 MHz Surveys

The basic observations for the thesis consist of 2700 MHz surveys with the 210 - foot telescope of the following areas (§2.2):

(1) Six selected regions, each of about 40 square degrees, which are covered by two-colour (blue - ultraviolet) plates taken by J. G. Bolton with the 48 - inch Schmidt telescope at Palomar. Five of the 6 regions are centered near declination 0°, while the sixth is at a declination of -18°.

(2) The zone between declinations $+4^{\circ}$ and -4°, excluding right ascensions $06^{h}00^{m}$ to $07^{h}21^{m}$ and $18^{h}00^{m}$ to $19^{h}40^{m}$ which are at low galactic latitudes.

The selected region catalogue is believed to be

complete to 0.10 f.u.* at 2700 MHz, and contains 310 sources. The catalogue for the ±4° declination zone is believed to be complete to 0.35 f.u. (except for the right ascensions 05^h to 06^h; see §2.10) and contains 500 sources.

1.2 (ii) 2700 MHz Positions/Flux Densities

Accurate positions and flux densities have been measured at 2700 MHz (§2.3) for all sources estimated from the survey records to be above the nominal flux density limits for each survey. These limits were taken as 0.08 f.u. for the selected regions and 0.35 f.u. for ±4° declination zone. The observations showed that a number of sources selected in this manner were weaker than the nominal flux density limits; these sources have been retained in the catalogues. Standard errors in the measured coordinates are about 15 arc seconds, and in flux densities about 0.012 f.u. for the weaker sources, increasing to 3% of the flux density for the stronger sources.

1.2 (iii) Spectral Measurements

Flux densities at several frequencies have been obtained for all sources in the ±4° declination zone catalogue for which $S_{2700} \geq 0.40$ f.u., and for many weaker sources in the zone. The flux density measurements have been made as follows:

---

* 1 f.u. ≡ 1 flux unit ≡ 10^{-26} w. m.$^{-2}$ hz^{-1}

5009 MHz: The flux densities of about 350 sources were measured with the 210 - foot telescope using a cooled parametric receiver on loan from the NRAO (§4.1). The standard error in these measurements is about 0.01 f.u. rising to 2% of the flux density for stronger sources.

1403 MHz, 468 MHz: The Parkes interferometer, operating simultaneously at the two frequencies, was used to measure the flux densities of some 300 sources (§4.3). The standard error in these measurements is about 5% of the flux density at each frequency for the stronger sources, and about 0.4 f.u. and 0.1 f.u. for the weaker sources at 468 and 1403 MHz respectively. Several of the 468 MHz flux densities were rejected because of confusion due to neighbouring sources.

635 MHz: The $\pm 4^{\circ}$ declination zone was surveyed with the 210 - foot telescope and a 635 MHz parametric receiver. Regions of low galactic latitude, right ascensions $06^{h}00^{m}$ to $07^{h}40^{m}$ and $18^{h}00^{m}$ to $19^{h}40^{m}$, were omitted. The survey is believed to be complete to $S_{635} = 0.8$ f.u., and flux densities for about 400 sources in the 2700 MHz catalogues were estimated from the survey records. Standard error in these estimates is about 0.4 f.u. rising to 8% of the flux density for the stronger sources.

The spectral data resulting from these observational programmes has been augmented by the results of other observers. For sources appearing in the 3C or 4C catalogues, 178 MHz flux densities have been taken from papers published

by the Cambridge group. Additional flux densities, or upper limits at this frequency, have been kindly communicated by Dr. Derek Wills from an examination of the 4C maps at positions of some of the sources in the 2700 MHz catalogue. Some accurate flux densities at 403 MHz have been published from the fan beam operation of the Molonglo Cross of the University of Sydney. Several of the stronger sources in the $\pm 4^{\circ}$ declination zone have been observed at Parkes at frequencies of 468, 635, and 1403 MHz by Dr. Beverley Harris in a programme of accurate flux density measurements. These have kindly been made available before publication. A few other flux densities at various frequencies have been taken from references acknowledged in the tabulation of the spectral data (Appendix IV).

1.3 A Summary of the Investigation

A summary of each chapter is presented in this section. The aim is to show how the data provided by observations described above have been used, and to illustrate briefly the results of the investigation.

In Chapter 2 the basic surveys and the subsequent position and flux density measurements at 2700 MHz are described. These observations occupied some 60 nights of observing time on the 210 - foot telescope over a period of two years. Partly because of the magnitude of the task involved, and partly because of interests in diverse aspects

of the anticipated results, the observations were made with the cooperation of J. G. Bolton, Miss Jeannette K. Merkelijn, and A. J. Shimmins (who is continuing the survey over large sections of the southern hemisphere).*

The results of the identification work are presented in Chapter 3. The positions of the catalogued sources were examined on both the Palomar Sky Survey prints, and for part of the area on two-colour 48 - inch Schmidt plates obtained at Palomar by J. G. Bolton. The examinations were made jointly with Miss Merkelijn and J. G. Bolton, and the results given in Chapter 3 are basically those of two papers with these authors which are presently in press. The identifications of galaxies are being used by Miss Merkelijn in a new derivation of the radio luminosity function. The redshifts of a number of the newly discovered QSO's have been determined by Leonard Searle and J. G. Bolton, and J. G. Bolton and T. D. Kinman (Searle and Bolton 1968; Bolton, Kinman, and Wall 1968).

In Chapter 4 the flux density measurements made to obtain spectra of the sources are described. The spectra which deviate from power laws are illustrated, and brief

---

* I analysed all the 2700 MHz observations, both for the surveys and the positions/flux densities, with the exception of the original survey records for three of the selected regions. Independent analysis was carried out by one of J.K.M., A.J.S., or J.G.B. for about half of the $\pm 4^{\circ}$ zone survey records and about one third of the position/flux density records.

discussions of many of the interesting cases are presented.

A statistical analysis of the source spectra is carried out in Chapter 5. At least 50% of the sources in the 2700 MHz catalogues have spectra which do not obey power laws between 178 and 5009 MHz. As classes the radio galaxies and QSO's are clearly distinguishable by their spectral characteristics. This distinction permits a fairly accurate estimate to be made of the fraction of unidentified sources (presumably beyond the plate limit of the Palomar Sky Survey) which belong to each class. It is suggested that at flux density levels above 0.40 f.u. at 2700 MHz, about 25% of the unidentified sources belong to the QSO category, while the remainder are distant radio galaxies.

Chapter 6 contains the 2700 MHz source counts, a discussion of the effects of experimental errors on these counts, and the subsequent derivation of a 2700 MHz number - flux density relation. The slope of this relation for source densities in the range 50 to 2500/sr. is about -1.45. The result is discussed in relation to source counts at other frequencies. It is suggested that the major difference between number - flux density relations at different frequencies is that at the lower frequencies the initial steep slope extends to a higher source density; at the higher frequencies, the initial steep slope is present, but in ranges of source densities where statistical uncertainties dominate. The effect can almost certainly be attributed to the influence of one

population - the QSO's.

In Chapter 7 a simple numerical approach to investigate the significance of number - flux density relations is described. The technique enables computation of the relation at a given frequency with the incorporation of any geometry, radio luminosity function, type of evolution, or radio spectrum. Moreover, it illustrates directly the manner in which successive volume shells contribute to the source count. In the preliminary computations carried out in Chapter 7, two uniform models for the universe have been considered (a Friedmann model with $\Lambda = 0$, $q_o = +1$, and the steady-state model), and a cosmological interpretation of the QSO redshifts has been assumed. Radio luminosity functions have been derived at 2700 MHz for the QSO's and radio galaxies in the catalogues, and the counts computed at 2700 MHz and at 178 MHz by combining different spectral types of each identification class in the proportions indicated by the results of Chapters 4 and 5. With no evolution in these models, the results are similar to those found in earlier investigations of low frequency source counts: (1) the computations indicate flatter number - flux density relations than those observed, and (2) the geometrical effects generally dominate the spectral effects ("K - corrections") in determining the form of these relations. If these preliminary results are accepted as indicating evolution, then (1) it is suggested that both radio galaxies and QSO's partake in that evolution, and (2) it is emphasized that types

of evolution which may be proposed must satisfy the additional constraints imposed by the present series of observations.

Chapter 8 contains a summary of the principal results of the investigation, and concludes the thesis with suggestions for further investigations.

CHAPTER 2

THE PARKES 2700 MHZ SURVEY: SELECTED REGIONS, AND THE ±4° DECLINATION ZONE

The observational programmes resulting in catalogues of radio sources found in 2700 MHz surveys of 6 selected regions and of the ±4° declination zone are described in this chapter. The catalogues contain the basic data for the thesis, and the accuracy of this data is discussed.

2.1 Telescope and Receiver

At the frequency of 2700 MHz, the 210-foot paraboloidal reflector of the ANRAO at Parkes, N.S.W., has an aperture efficiency of about 50% (Minnett and Yabsley 1966; personal communication, D. Yabsley, 1969). In April of 1967 a new 2700 MHz receiver (Batchelor, Brooks, and Cooper 1968) was completed and tested on the telescope. The receiver is of the dual channel correlation type, with a hybrid junction at the input. Each channel has two stages of degenerate parametric amplification of 400 MHz bandwidth followed by mixer and zero - frequency IF system of 200 MHz bandwidth. Several feed systems of the hybrid mode type (Minnett and Thomas 1966) have been constructed to permit operation of the receiver in different configurations. These include correlation of main beam and cold load inputs, and main beam and off-axis beam inputs. The feed system for the latter configuration produces a main (or on-axis) beam 7.9 arc minutes to half-power points, and

a secondary beam slightly broader than this and displaced 18.5 arc minutes off axis. With the receiver operating in this dual beam mode, the system noise temperature of 100°K. and the overall bandwidth of 200 MHz result in peak-to-peak output deflections of 0.04°K. (0.07 f.u.) for a 2 second output time constant. The preliminary tests of April 1967 indicated that a source of 0.05 f.u. could be reliably detected with a single scan.

The receiver was used in the dual beam configuration in the observational programmes described below. In this mode, the system temperature is smallest, and the effects of variable atmospheric extinction are minimized. However, standard errors in measured intensities and coordinates due to confusion are increased by a factor of $\sqrt{2}$.

2.2 The Survey Observations

2.2 (i) The Selected Regions

In the period 1966 to 1968 J.G. Bolton took a series of two-colour (blue - ultraviolet) plates with the 48" Schmidt telescope of Mount Palomar Observatory. In the first part of the Parkes 2700 MHz survey, 6 of these plate areas, selected as being free from galactic absorption, were scanned in surveys designed to be complete to $S_{2700} = 0.10$ f.u. The coordinates of the centres of each area are given in Table 2.1. The total area of the 6 selected regions is 247 square degrees or .0753 sr.

TABLE 2.1

CENTRES OF SELECTED REGIONS

48" Schmidt Plate Number	1950.0 Coordinates r.a.	dec.
PS 1112	$00^h04^m51^s$	$+00^\circ 32'$
PS 891	00 52 55	+00 31
PS 1114	02 32 31	+00 25
PS 1777	12 04 50	-00 31
PS 1778	13 40 48	-00 29
PS 896	22 03 26	-18 50

The survey technique was to cover each area with a grid of scans in right ascension and declination. The spacing between adjacent scans in either coordinate was 4 arc minutes. Survey time was halved by using the receiver in the dual beam configuration; sources in the main beam appeared as positive deflections, and those in the off-axis beam as negative deflections. Because of the alt-az mounting of the telescope, a control system was used to keep the feed platform oriented so that the off-axis beam effected a scan displaced 18.5 arc minutes from that of the main beam. A scan rate of 1° per minute was used together with an effective output time constant* of about 2 seconds. Calibration was carried out at

---

* The phrase "effective output time constant" refers to the use of a low pass output filter of the active second order type. Quoted time constants describe the filter bandpass in

half hour intervals by the injection of $1^{\circ}K$ of noise power ($\sim$1.8 f.u.) at the receiver input. The receiver output was recorded on chart running at 80 mm/minute; a sample record is shown in Figure 2.1(a).

The reduction procedure consisted of listing all positions and amplitudes of source-like deflections on the scans and plotting these on charts of the six selected areas. The coordinates of all sources which appeared from these charts to have $S_{2700} \geq 0.06$ f.u. were then listed for re-observation to determine accurate positions and flux densities (§2.3). These lists comprised some 70 sources for each region, about 50 of which appear in the final catalogue.

2.2 (ii) The Equatorial Zone Survey

The second part of the survey consisted of covering most of the zone between declinations $+4^{\circ}$ to -4° with a series of scans in declination. Regions of low galactic latitude, right ascensions $06^{h}00^{m}$ to $07^{h}21^{m}$ and $18^{h}00^{m}$ to $19^{h}40^{m}$, were omitted. The total area covered was 2400 square degrees or 0.730 sr. The survey was designed to be complete to $S_{2700} = 0.35$ f.u.

---

terms of a passive RC filter having the same half power point. In both parts of the survey, scan rates were such as to give 4 effective time constants between half power points for small diameter sources encountered in the scans. The RC filter network effects an 11% reduction in source amplitude at this scan rate; the observed reduction was 3%.

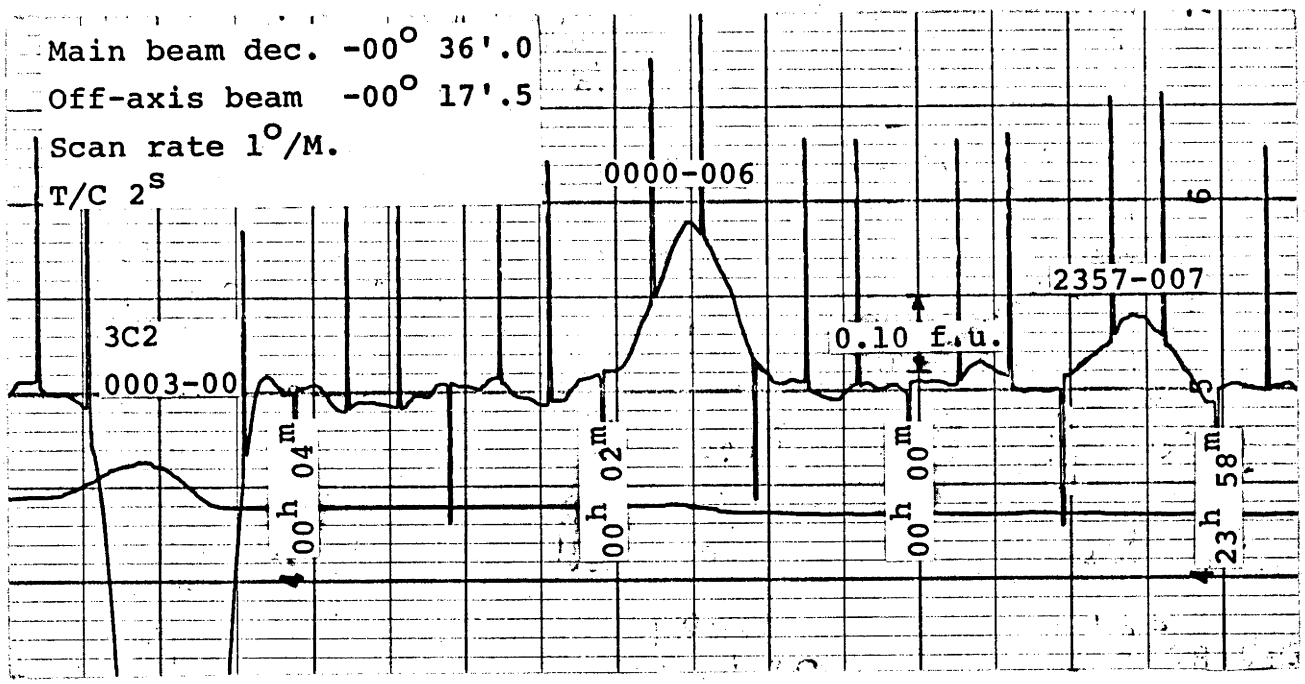

Figure 2.1(a). A portion of a scan in the survey of selected region PS 1112.

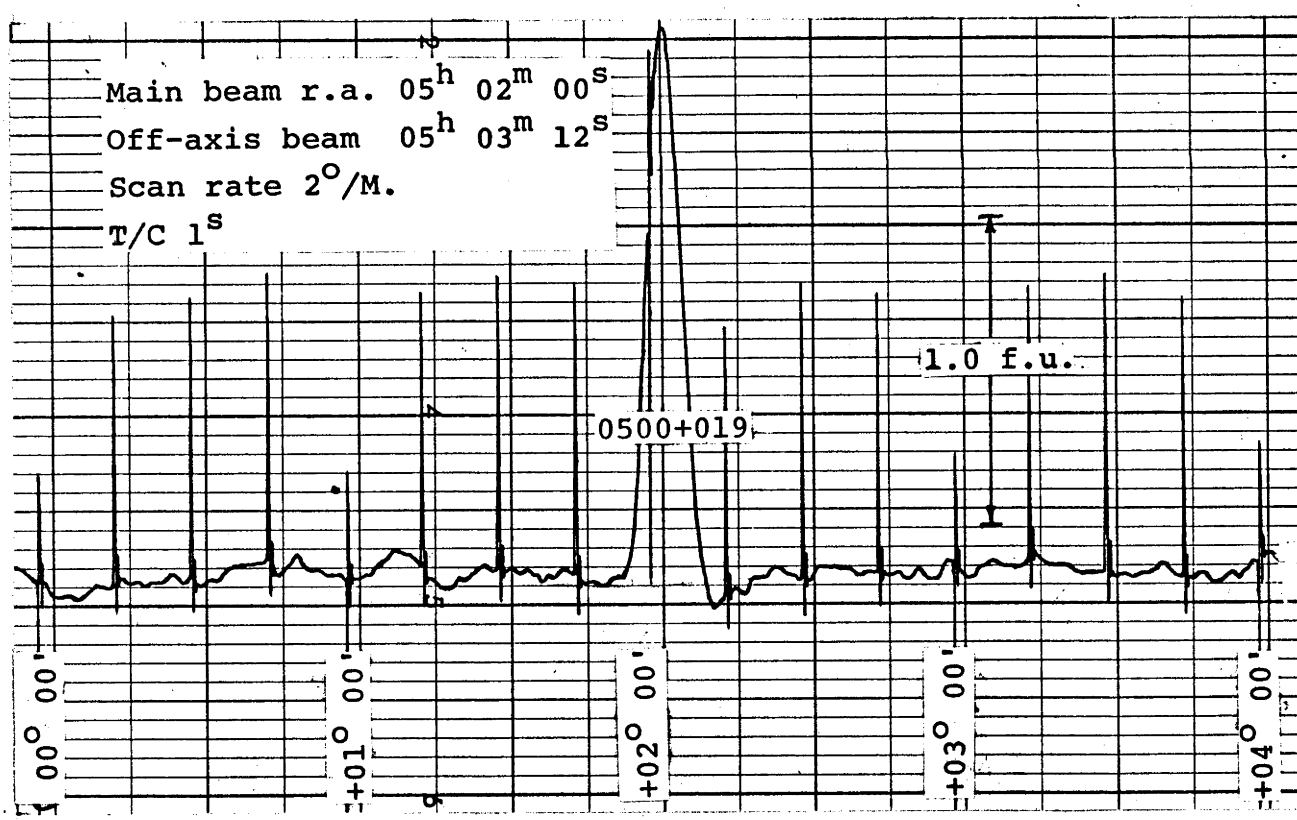

Figure 2.1(b). A portion of a scan in the survey of the ±4° declination zone; the scan illustrates the discovery of source 0500+019.

Scans were spaced every 6 arc minutes, and the dual beam system was used with feed rotation control as in §2.2(i). The scan rate was 2° per minute with an effective output time constant of about 1 second. Calibration signals of 1°K. were added after every three scans. The receiver output was again recorded on chart running at 80 mm/minute; a sample record is shown in Figure 2.1(b).

The reduction procedure consisted of estimating and listing the positions of all sources which appeared from the scans to be stronger than 0.25 f.u. Sources in the list were re-observed in the position/flux density programme described below. About 25 sources were listed in each hour of right ascension.

2.3 The Source Position/Flux Density Observations

All observations at 2700 MHz, both survey and measuremen of positions and flux densities, were carried out in 11 observing sessions between June 1967 and June 1969. Generally both types of observation were performed in any observing session. This procedure enabled preliminary results of the source counts to be obtained (Shimmins, Bolton, and Wall 1968), and the identification programme (Chapter 3) to be carried on concurrently. The dates of each observing session together with the type of observation carried out are given in Table 2.2.

The source positions and flux densities were obtained

TABLE 2.2

2700 MHZ OBSERVING SESSIONS

Observing Session	Dates	Type of Observation*	Approx. No. of P/F	σ_{run} - Standard Error, Flux Calibration (%)
1	1967.48 June 23-28	SS P/F	70	1.84
2	1967.63 Aug. 17-21	SS P/F	60	1.70
3	1967.67 Aug. 29-Sept. 8	SS, SZ P/F	200	1.77
4	1967.80 Oct. 18-21	SZ	-	3.0
5	1967.88 Nov. 14-23	SZ	225	1.52
6	1968.04 Jan. 16-19	SZ P/F	25	2.10
7	1968.24 Mar. 28-Apr. 1	SS, SZ P/F	105	1.75
8	1968.28 Apr. 9-14	SZ P/F	420	1.47
9	1968.92 Nov. 30-Dec.5	P/F	240	1.40
10	1969.06 Jan. 20 and 26	SZ P/F	20	1.70
11	1969.43 June 7-9	P/F	150	1.96

* SS - Survey, selected regions
SZ - Survey, declination zero zone
P/F- Measurement of source positions and flux densities

by scans through the source positions listed from the survey records. The number of scans in each coordinate generally was sufficient to ensure that errors due to noise were less than those of calibration in measuring the positions, and less than those due to confusion or calibration in measuring the flux densities. For the stronger sources ($S_{2700} \geq 0.5$ f.u.) at least 2 scans were made in each coordinate; weaker sources were scanned up to 6 times in each coordinate. A scan rate of $\frac{1}{2}^{o}$ per minute was used with an effective output time constant of about 2 seconds. The receiver output was recorded on chart running at 80 mm/minute, and markers were added to the record to indicate the apparent position of the main beam of the telescope during the scans. A calibration signal of 1^{o}K. noise power was injected at least once during the observation of every source. Most sources were observed within 1½ hours either side of transit. Sample records are shown in Figure 2.2.

In observing sessions 1 to 8, each source was observed at only one (linear) polarization, the position angle of the feed being chosen so that the off-axis beam did not encounter the source during scans in either coordinate. Where scans through a source indicated the presence of a confusing source in the off-axis beam, the position angle was changed. For position/flux density observations of sources in the selected areas (§2.2(i)), the plotted charts of the regions were consulted to choose orientations of the feed for minimal

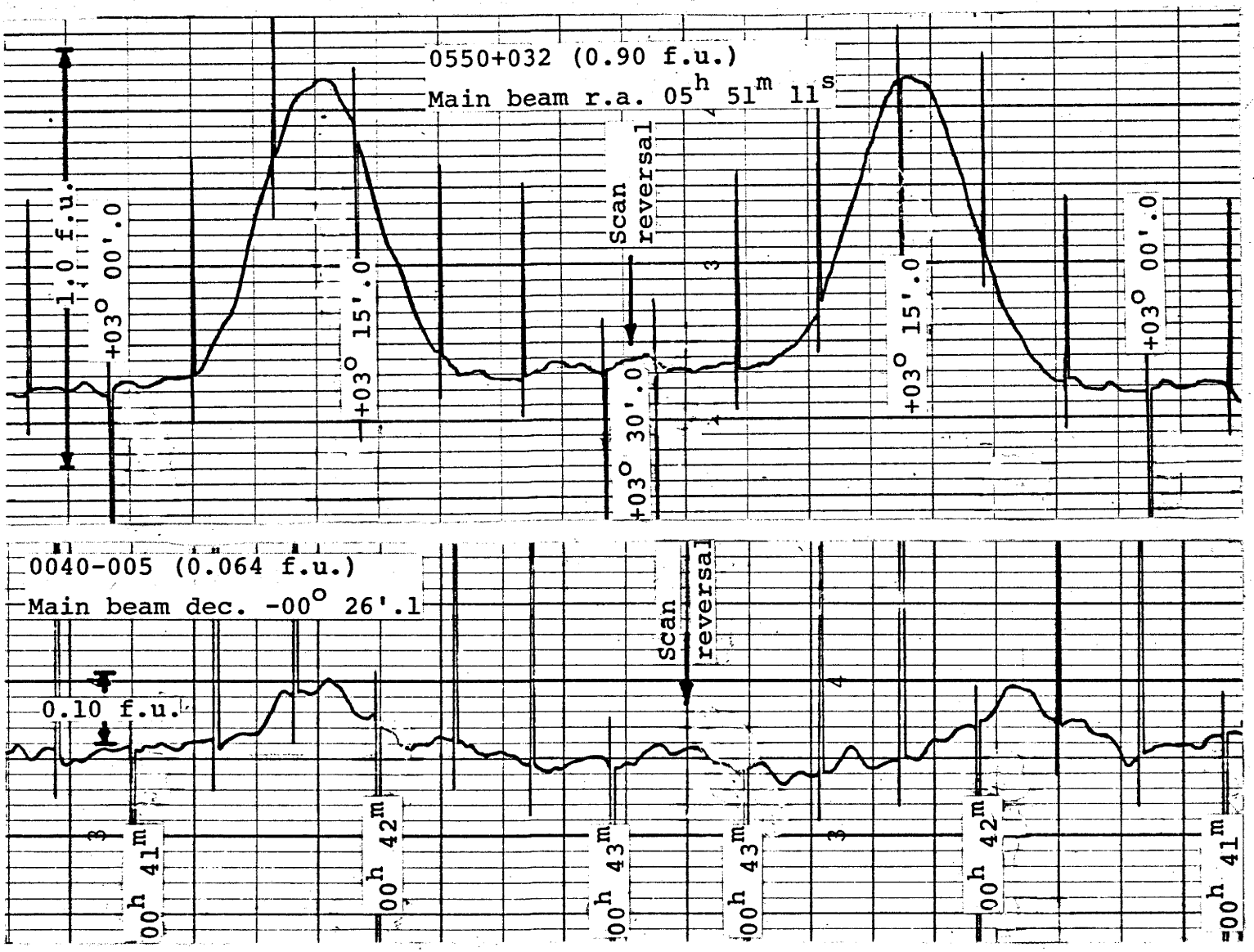

Figure 2.2. Scans through two sources in the 2700 MHz position/flux density programme.

confusion effects. In sessions 9 to 11, each source was measured at orthogonal polarizations, again chosen so that the off-axis beam did not encounter the source during scans in either coordinate.

Details of the observations and reduction procedures relevant to the source positions (§2.4) and the flux densities (§2.6) are now described, together with the corresponding error analyses (§2.5, §2.7).

2.4 The Source Positions

The original Parkes accurate positions were obtained by transit observations (Shimmins, Clarke, and Ekers 1966). It has been shown that a more extensive grid of position calibrators now permits determination of positions to 15 arc seconds or better with observations away from transit (Merkelijn 1968, 1969). The position calibrators are relatively strong radio sources for which optical identifications are well established. The calibration grid used in the present observations is comprised of the accurately measured positions of the optical objects and is presented in Table 2.3. All QSO's in the list of calibrators have been confirmed by photometry or spectroscopy. The radio galaxies are generally fainter then $m_{pg} = 16$ in order to minimize differences between optical positions and centroids of radio emission.

By observing sources from the calibration grid during a positioning programme, the systematic pointing corrections

TABLE 2.3

THE CALIBRATION GRID USED IN THE POSITION MEASUREMENTS

Source	1950 Coordinates r.a.	dec.	S_{2700} (f.u.)	Identification	Ref.	Other catalogue number
0003-00	$00^h03^m48^s.70$	$-00^\circ 21' 06''.6$	2.41	$19^m.5$ QSO	8	3C 2
0034-01	00 34 30.52	-01 25 44.3	2.56	17.1 E	10	3C 15
0035-02	00 35 46.79	-02 24 10.2	4.04	19.6 E	10	3C 17
0056-00	00 56 31.70	-00 09 16	(1.80)	17.3 QSO	4	4C-00.6
0106+01	01 06 04.39	+01 19 01.9	(1.88)	18 QSO	1	4C+01.3
0118+03	01 18 26.15	+03 28 29.3	0.51	18 QSO	1	4C+03.2
0119-04	01 19 55.91	-04 37 07.0	0.98	17 QSO	1	4C-04.4
0122-00	01 22 55.5	-00 21 34	1.43	17.0 QSO	4	
0218-02	02 18 21.90	-02 10 33.0	1.68	19.1 E	10	3C 63
0232-04	02 32 36.60	-04 15 11.0	0.91	16 QSO	7	4C-04.6
0240-00	02 40 07.00	-00 13 31.1	3.12	9.7 Sc	1	3C 71
0305+03	03 05 49.03	+03 55 12.7	[5.33]	14.4 D	1	3C 78
0336-01	03 36 59.2	-01 56 19	(2.23)	18.4 QSO	7	CTA 26
0340+04	03 40 51.47	+04 48 21.6	1.55	18.1 QSO	9	3C 93
0350-07	03 50 04.1	-07 19 55	1.41	16 QSO	4	3C 94
0420-01	04 20 43.1	-01 27 29	(1.92)	18 QSO	6	
0430+05	04 30 31.46	+05 15 01.0	(8.4)	15 S	1	3C 120
0440-00	04 40 05.4	-00 23 22	(3.53)	18.5 QSO	6	NRAO 190

TABLE 2.3 Cont'd.

Source	1950 Coordinates r.a.	dec.	S_{2700} (f.u.)	Identification	Ref.	Other catalogue number
0458-02	$04^h58^m41^s.4$	$-02^o\ 03'\ 36''$	(1.99)	20^m N?	6	
0530+04	05 30 25.29	+04 03 49.8	1.19	19 D	1	4C+04.18
0736+01	07 36 42.4	+01 43 57	(2.42)	18 QSO	3	
0812+02	08 12 47.20	+02 04 11	1.18	18.5 QSO	4	4C+02.23
0812-02	08 12 57.32	-02 59 13.9	0.95	18.9 D	10	3C 196.1
0957+00	09 57 43.84	+00 19 50.0	0.51	17.6 QSO	2	4C+00.34
1055+01	10 55 55.5	+01 50 03	(3.02)	18 QSO	4	4C+01.28
1148-00	11 48 10.23	-00 07 13.1	2.56	17.5 QSO	1	4C-00.47
1229-02	12 29 25.9	-02 07 31	1.33	17.2 QSO	3	4C-02.55
1253-05	12 53 35.94	-05 31 08.0	(13.1)	18.0 QSO	8	3C 279
1335-06	13 35 31.34	-06 11 57.4	1.82	17.7 QSO	8	MSH 13-011
1340+05	13 40 12.96	+05 19 39.0	1.16	17.8 N	6	4C+05.47
1454-06	14 54 02.7	-06 05 45	0.82	18.6 QSO	3	MSH 14-018
1518+04.7	15 18 46.15	+04 40 45.5	2.43	18 g	1	4C+04.51
1559+02*	15 59 55.67	+02 06 12.3	[5.04]	16.5 D	5	3C 327
1603+00	16 03 39.02	+00 08 29.3	1.50	16.5 E4	1	4C+00.58
1648+05	16 48 39.98	+05 04 35.0	[23.4]	19.0 D	10	3C 348
1949+02	19 49 44.57	+02 22 37.1	[3.68]	16.4 SO	10	3C 403
1949-01*	19 49 55.20	-01 25 07.2	[0.79]	17.5:E	10	3C 403.1

* Not recommended for further use as calibrator; significant beam broadening at 2700 MHz.

TABLE 2.3 Concluded

Source	1950 Coordinates r.a.	dec.	S_{2700} (f.u.)	Identification	Ref.	Other catalogue number
2045+06	$20^h45^m44.^s40$	$+06^\circ\ 50'\ 10.''2$	1.28	$18.^m4$ E	10	3C 424
2144-17	21 44 17.62	-17 54 05.6	0.6	19.5 QSO	1	MSH 21-118
2145+06	21 45 35.9	+06 43 43	3.62	16 QSO	7	4C+06.69
2159+04	21 59 28.63	+04 20 40.8	0.94	19.5 E	1	4C+04.76
2203-18	22 03 25.8	-18 50 16	5.20	19 QSO	7	MSH 22-11
2216-03	22 16 16.3	-03 50 43	1.04	16.4 QSO	4	4C-03.79
2223-05	22 23 11.05	-05 12 17.0	(5.1)	18.4 QSO	9	3C 446
2313+03	23 14 02.30	+03 48 56.0	2.38	18.7 N	10	3C 459
2322-05	23 22 44.72	-05 14 33.6	0.73	18.5 N	1	4C-05.96
2324-02	23 24 19.40	-02 18 43.7	[1.56]	18 E	1	MSH 23-011
2349-01	23 49 22.30	-01 25 54.2	1.01	17.5 N	1	4C-01.60

REFERENCES FOR TABLE 2.3

(1) Bolton, J.G. (1968) - Pub. astr. Soc. Pacific 80, 5

(2) Bolton, J.G., Clarke, Margaret E., Sandage, Allan, and Véron, P. (1965) - Astrophys. J. 142, 1289

(3) Bolton, J.G., and Kinman, T.D. (1966) - Astrophys. J. 145, 951

(4) Bolton, J.G., Shimmins, A.J., Ekers, Jennifer A., Kinman, T.D., Lamla, E., and Wirtanen, C.A. (1966) - Astrophys. J. 144, 1229

(5) Griffin, Roger F. (1963) - Astron. J. 68, 421

(6) Kinman, T.D. - personal communication to J.G. Bolton

(7) Kinman, T.D., Bolton, J.G., Clarke, R.W., and Sandage, A.R. (1967) - Astrophys. J. 147, 848

(8) Sandage, Allan, Véron, Philippe , and Wyndham, John D. (1965) - Astrophys. J. 142, 1307

(9) Véron, P. (1965) - Astrophys. J. 141, 332

(10) Véron, P. (1966) - Astrophys. J. 144, 861

and the short term variations which occur in these corrections can be established. In the present programme, calibration observations were made such that every programme source could be referred to one or more calibrator sources satisfying both of the following conditions:- (1) programme and calibrator source less than 15^{o} apart, and (2) programme and calibrator source observed within one hour of time. QSO's were generally used as calibrators in preference to radio galaxies because of (i) the greater reliability of the identifications, (ii) the generally smaller optical - radio position differences, and (iii) the greater accuracy of measurement of the optical position. The observational technique of §2.4 was used for both programme and calibrator sources. For each, apparent coordinates were determined from the records by measuring the position of the centroids of all scans. These were averaged for each coordinate; forward - reverse pairs of scans in both right ascension and declination removed the effect of the output time constant. Pointing corrections were established from the calibrator sources by determining differences between the apparent coordinates and those listed for the optical object precessed to the epoch of observation. The true position for each programme source was then determined from the apparent position with the corrections found from the calibrator to which it could be referred. If the source could be referred to two calibrators, the pointing corrections applied

were determined by interpolation. Corrected positions were precessed back to epoch 1950.0.

The calibration procedure differs from that of Merkelijn (1968, 1969) in that systematic corrections as a function of hour angle were not established and applied. The consequent error is discussed in the analysis below.

The positions of all sources measured in the programme appear in Appendix II, Tables AII.1 and AII.2, the catalogues for the selected regions and $\pm 4^{\circ}$ declination zone surveys respectively.

2.5 The Accuracy of the Catalogue Positions

There are three sources of error in the catalogue positions:

(1) Confusion and receiver noise affect the determination of apparent coordinates for both calibrator and programme sources.

(2) The systematic dependence of the pointing corrections on hour angle has not been considered.

(3) The calibration system cannot remove the effects of random changes in aerial pointing which take place on time scales shorter than the mean period between calibrator observations.

The effect of receiver noise on the position measurements was examined by determining differences between the measured position of the centroid of individual scans and the mean of

scans in one coordinate for a given source. The shift produced by the output time constant was evaluated by observing the displacement produced in scans on sources of high signal/noise ratio, and was removed from each of these differences. The differences were calculated for large numbers of sources in different ranges of flux density. The resulting standard errors for single scans are plotted as a function of flux density in Figure 2.3(a). As expected at a level of 50 beam areas per source (S_{2700} = 0.10 f.u.), the measurement of source coordinates rarely showed evidence of confusion effects. The curve in Figure 2.3 thus represents errors in the coordinates due to factor 1 above.

Errors from factor 2 were evaluated by plotting pointing corrections for both declination and right ascension against hour angle for observing session 11. A systematic dependence similar to that found by Merkelijn (1968) was obtained. Most sources were observed at hour angles differing by less than 45 minutes from the calibrator source to which they were referred. Applying this $\Delta r.a.$ to the above plots indicated that the standard error in the pointing correction (factor 2) is about 10 arc seconds in either coordinate.

Errors from factor 3 were obtained from the scatter among pointing corrections determined from calibrators measured at similar hour angles and within two hours of time. The scatter is about 6 arc seconds, similar to that found in

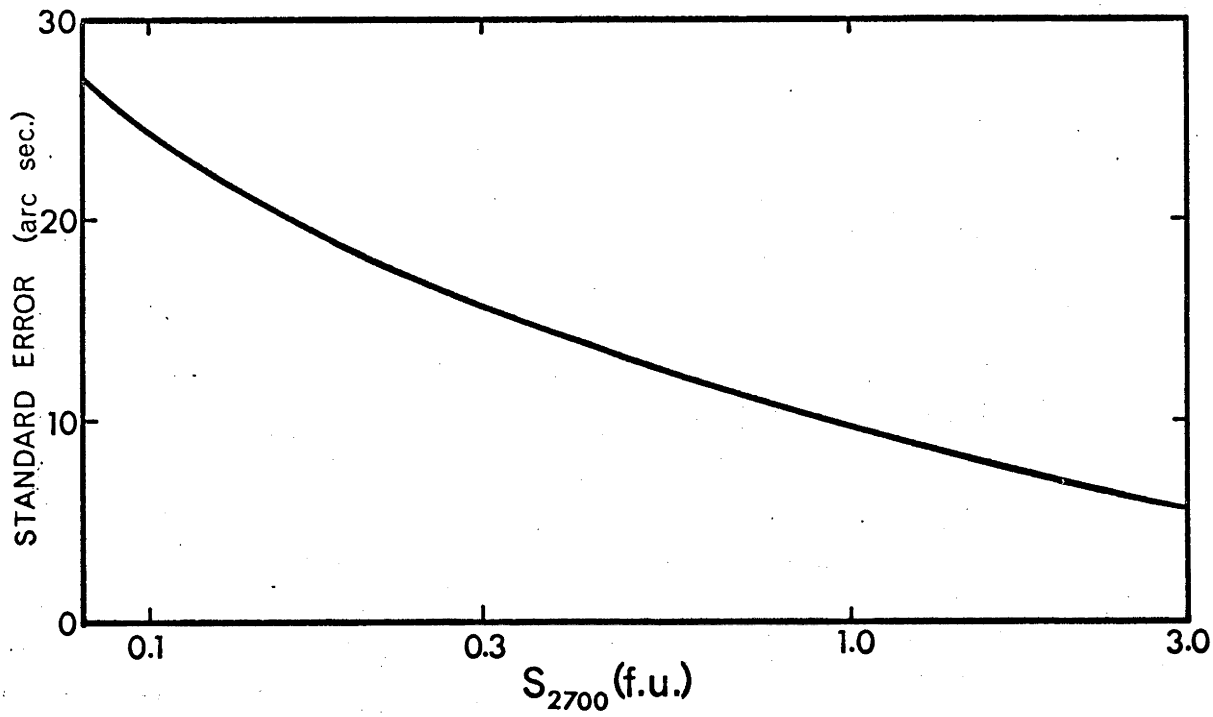

Figure 2.3(a). Standard error in coordinate measurement from a single scan.

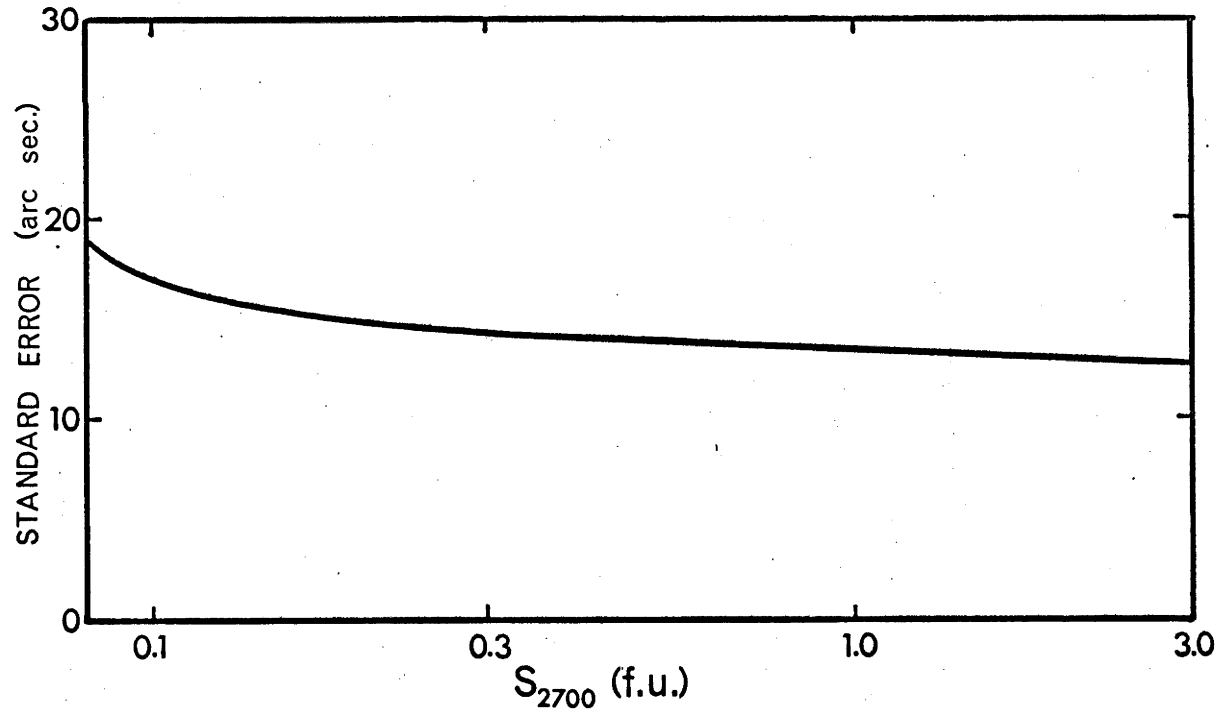

Figure 2.3(b). Estimated average standard error in the measurement of either source coordinate.

previous series of position measurements at Parkes.

Factors 2 and 3 thus produce a calibration error of 11.7 arc seconds. The total standard error in either coordinate of a source is then $\sqrt{(\sigma_1^2/n) + (11.7)^2}$ arc seconds, where σ_1 is the error for a single scan as read from Figure 2.3(a), and n is the number of scans. The estimated total error in either coordinate is shown in Figure 2.3(b). The curve has been calculated from the above expression with n as the mean number of scans per coordinate made for sources in each range of flux density.

2.6 Comparison with Other Observations

The right ascensions in the 4C catalogue (Pilkington and Scott 1965; Gower, Scott, and Wills 1967) are of similar accuracy to those of the Parkes 2700 MHz catalogue. The histograms of Figure 2.4 present the results of a comparison of the right ascensions of sources common to both catalogues. Sources for which the 2700 MHz observation indicated a lobe shift or possible confusion in the 4C observation have been excluded from the sample. The histograms show the numbers of differences (r.a.PKS - r.a.4C) for three ranges of 2700 MHz flux density. The mean difference for the 246 sources in the three ranges is +0.15 seconds in right ascension (2.3 arc seconds), and is of little significance. The results of Figure 2.4 are summarized in Table 2.4. The expected standard deviations of each histogram are the

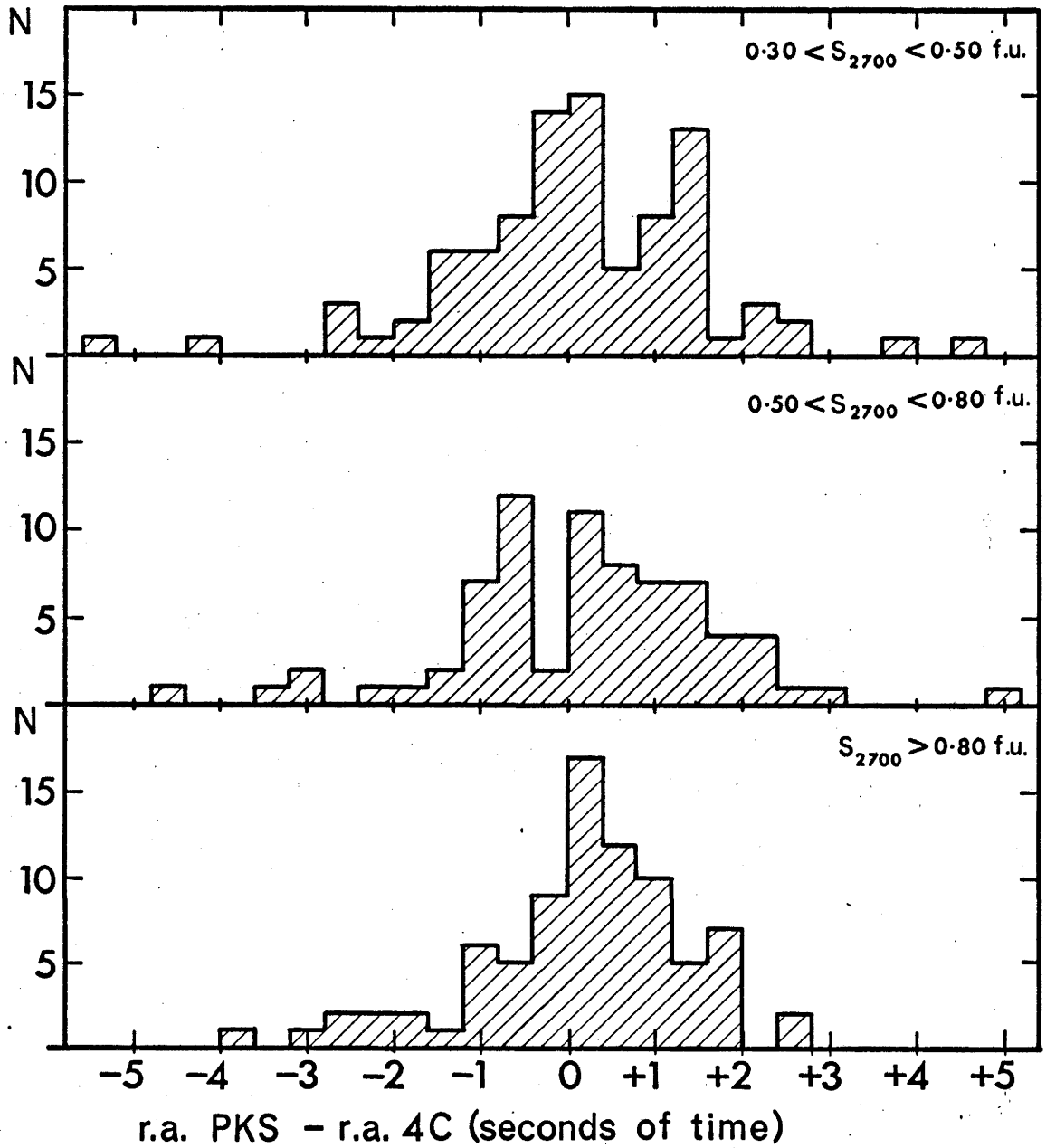

Figure 2.4. A comparison of the right ascensions obtained in the present work with those of the 4C catalogue.

estimated mean standard deviations of the Parkes and 4C samples added in quadrature. The observed standard deviations are slightly less; this is undoubtedly due to the exclusion of sources which are lobe shifted or confused in 4C.

TABLE 2.4

RIGHT ASCENSION DIFFERENCES, PARKES - 4C

S_{2700} (f.u.)	Sample size	$\bar{S}_{2700}$ (f.u.)	$\bar{S}_{178}$ (f.u.)	Standard Deviation Expected	Observed
0.30 - 0.50	91	0.38	3.52	$1^s.70$	$1^s.49$
0.50 - 0.80	73	0.63	4.86	1.56	1.53
>0.80	82	1.37	7.69	1.39	1.23

Eight percent of all sources common to the two catalogues were found to be lobe shifted in the 4C catalogue. No declination comparison has been made because the estimated errors in the 4C declinations are an order of magnitude larger than those of the present observations.

The work of Clarke and Munro (1968) indicates indirectly that there is no systematic discrepancy between right ascensions in the Parkes 2700 MHz catalogue and those determined with the fan beam of the Molonglo Cross. They compared right ascensions from the fan beam survey with 4C, and in the declination zone $+4^\circ$ to -4° they found a mean difference of about 0.05 seconds in right ascension. The result is not significant; however, it is in the same sense

as the mean discrepancy between Parkes 2700 MHz and 4C found above, and indicates good agreement between the right ascensions of the Molonglo fan beam survey and the Parkes 2700 MHz catalogue. Hunstead (1969) has compared Molonglo Cross positions with Parkes transit positions (Shimmins et al. 1966, Shimmins 1968a; again no systematic error is apparent in either right ascension or declination for the $+4^{\circ}$ to -4° declination zone. The calibration grid used in the present position observations is an expanded version of that used in the transit observations, and hence no systematic discrepancy between the source positions in Tables AII.1 and AII.2 and Molonglo Cross positions is anticipated.

The comparisons indicate that (1) error estimates for both the Parkes 2700 MHz catalogue source positions and the 4C right ascensions in the $+4^{\circ}$ to -4° declination range are satisfactory, and (2) in this declination zone no systematic discrepancies in coordinates exist between 4C, Molonglo, and Parkes 2700 MHz catalogue positions.

2.7 The 2700 MHz Flux Densities

The peak flux density was obtained for each source by measuring the amplitudes of the smoothed scans. Corrections for telescope setting errors were applied to the computed averages of the right ascension and declination scan amplitudes. These corrections were determined from the known shape of the telescope beam and from the differences between the apparent

(measured) coordinates and the coordinates to which the telescope was set for either scan series. The average of the two estimates of scan amplitude thus obtained was then multiplied by a factor of the order of 1% which corrected for changes in atmospheric attenuation and dish efficiency with zenith angle. The correction curve used was kindly supplied by Drs. J. A. Roberts and Beverley Harris, and is shown in Figure 2.5. The peak flux density was finally obtained by relating the corrected source amplitude to the deflection produced by the (nominal) 1°K. noise calibration signal which was recorded at least once during the measurement of each source.

The precise value of the noise calibration signal in flux units was determined for each observing session as follows. The flux density scale adopted is based on the assumption of $S_{2700} \equiv 23.5$ f.u. for the peak flux density of PKS 0915-11 (Hydra A). The scale is believed to be within 5% of absolute, and is the same as that of Harris (1969), which is in turn very close to the scale of Kellermann (1964). In session 9, the noise calibration signal was carefully measured against Hydra A, and in order to provide a uniform scale for all sessions, a large number of the stronger sources ($S_{2700} \geq 1.0$ f.u.) in the $\pm 4^{\circ}$ declination zone were also observed. These were used as a system of sub-calibrators for each of the other 10 sessions. The estimated standard

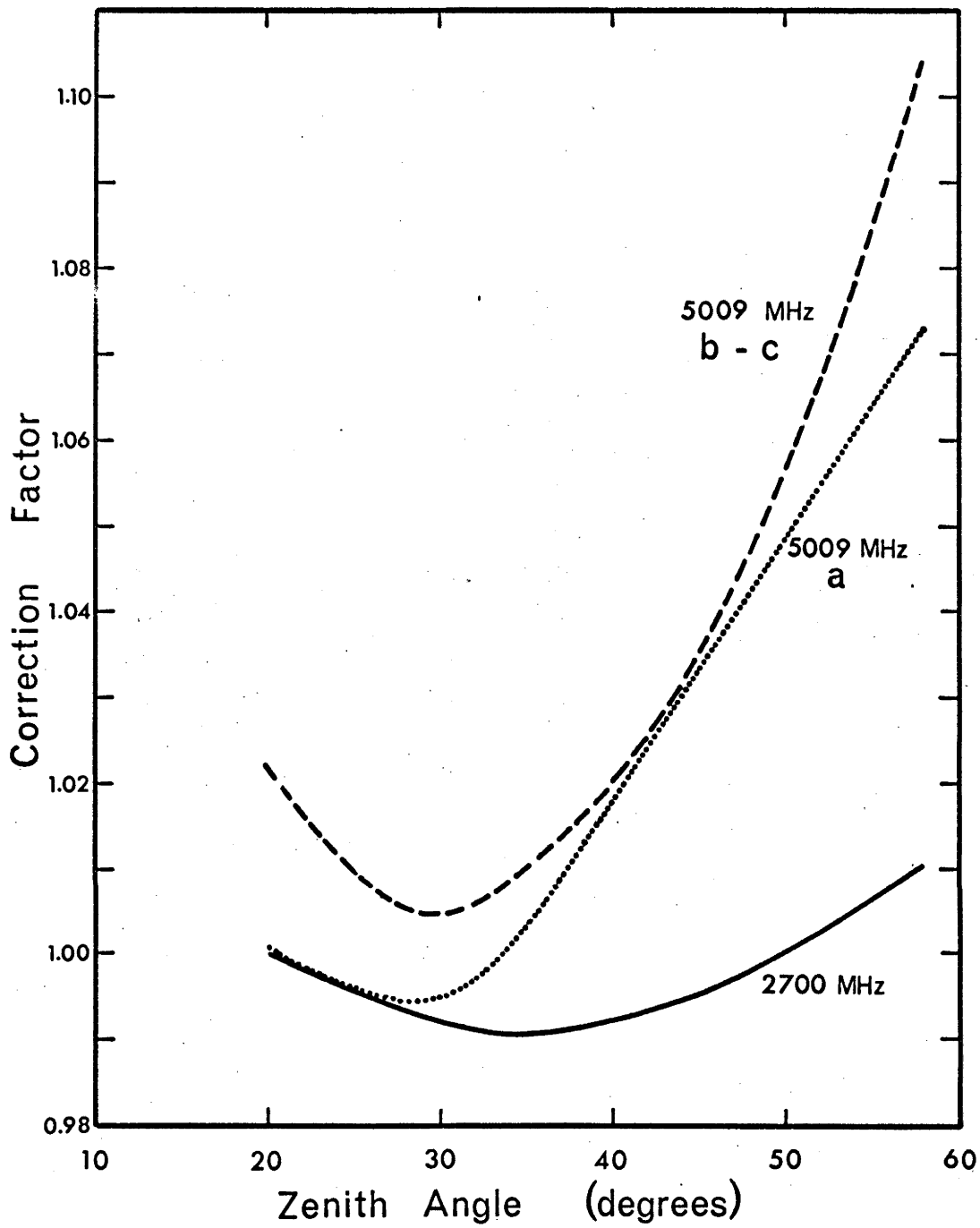

Figure 2.5. The 2700 MHz curve indicates the correction applied to flux densities for the effects of atmospheric attenuation and aperture efficiency. The 5009 MHz curve used for session (a) indicates the correction applied for the same factors with the telescope focus optimized for each observation. The curve for sessions (b) - (c) compensates in addition for fixed focus.

error in assigning a value to the noise calibration in this manner is listed for each session in Table 2.2. No significant changes in the value have been found during the course of any observing session at 2700 MHz (A.J. Shimmins, personal communication).

When the flux density of a source was measured at only one position angle, correction was made for linear polarization if the data were available (Gardner, Morris, and Whiteoak 1969 and personal communication).

Many of the stronger sources have angular dimensions sufficiently large to produce a significant difference between the peak flux density and the integrated or true flux density. Most such sources were observed at 5009 MHz (§4.1) with the Parkes telescope which has a half power beamwidth of 4.0 arc minutes at this frequency. The factors by which peak flux densities at 5009 MHz were multiplied to obtain integrated flux densities (the "size factors") were computed or obtained as described in §4.1. The size factors appropriate to the 2700 MHz beamwidth were obtained from the 5009 MHz size factors by

$$S.F.(2700\ \text{MHz}) = 1.00 + .257\left[S.F.(5009\ \text{MHz}) - 1.000\right] \quad (2.1)$$

The factor 0.257 is the ratio of the beam volumes. For the few sources not observed at 5009 MHz and for which beam broadening was evident at 2700 MHz, size factors were computed in the conventional manner.

Peak flux densities and estimated errors, together with the size factors, integrated flux densities, and position angles of observation where relevant, are listed for the catalogue sources in Tables AII.1 and AII.2.

2.8 Errors in the Flux Densities

2.8 (i) Confusion

Confusion effects are basically of two types - "masking" due to the presence of sources stronger than those being catalogued, and background irregularities caused by the integration of the underlying sources into a continuum by the antenna beam. The first bears directly on the completeness of the catalogue and is considered in §2.8. The second affects both measured positions and intensities, and the magnitude of the errors produced is set by the size of the fluctuations in the integrated background. Calculations to determine the error in flux densities have been carried out and are presented in Appendix I, from where the following results are drawn:

(i) With the receiver operating in the dual beam configuration, the standard error in flux densities due to background irregularities is $0.010\ ^{+.010}_{-.005}$ f.u. at 2700 MHz.

(ii) This quantity is principally determined by the number - flux density relation for the population of sources having intensities between 0.010 and 0.001 f.u.

An integrated series of 10 scans shown in Appendix I

offers very limited statistical support of the confusion error estimate.

2.8 (ii) Receiver Output Fluctuations

Fluctuations in the receiver output due to noise and short term instabilities were very similar in all observing sessions. A formal evaluation of the standard error produced by receiver output fluctuations was made from a large sample of sources in session 9. The error in estimating flux density from a single scan was found to be 0.014 f.u. Weak sources for which receiver noise was significant were measured with 8 or more scans, the error consequently being reduced to about 0.005 f.u.

2.8 (iii) Polarization

To evaluate standard errors in flux densities resulting from measuring source intensities in only one linear polarization, a sample of 80 sources was chosen from those observed in session 9. The selection criteria were (i) $0.16 \leq S_{2700} \leq 0.42$ f.u. and (ii) no previous attempts at optical identification. In session 9, each source was observed with 8 scans, 2 in each coordinate at a position angle of $+45^{\circ}$, and 2 in each coordinate at a position angle of -45°. In the polarization error analysis, the four scan amplitudes at each polarization, corrected for setting errors, were taken to give estimates of the flux densities

in the two polarizations for each source in the sample. The percentage half differences between these two flux densities were calculated, and the results for all sources in the sample were plotted in a histogram. The latter had standard deviation $\sigma = \sqrt{\sigma_{pol}^2 + \sigma_n^2}$ where σ_{pol} is the standard error in flux density due to measurement in one polarization only, and σ_n is the standard error due to receiver noise and errors in the setting corrections. To evaluate σ_n, the averages of the 4 scan amplitudes in both declination and right ascension, corrected for setting errors, were taken to give two independent estimates of the flux density. The half differences, calculated as a percentage of the mean flux density, were plotted in a histogram for all sources in the sample. The standard deviation of this histogram was σ_n, and σ_{pol} was then directly calculated to be 2.9%.

In consequence, all flux densities measured in only one polarization have been assigned an additional standard error of 2.9%. Flux densities so measured, and corrected to the mean of two orthogonal polarizations where data was available, have been assigned an additional error of 1%. This is representative of the accuracy of the polarization data (Gardner, Morris and Whiteoak 1969).

2.8 (iv) Calibration

The standard errors in the values assigned to the injected noise calibration have been calculated for each

observing session and are listed in Table 2.2. The errors have been calculated from (1) the scatter among several measurements made on the same sub-calibrators in each session, and (2) the estimated total standard error in the flux densities of the sub-calibrators measured in session 9.

Further calibration error results from short term gain fluctuations, and in measurement of the individual deflections produced by the calibration signal. The combined effect of these errors was estimated by plotting calibration signal deflections against sidereal time. The scatter indicated a combined standard error of 1.3% for a single noise calibration signal.

Total calibration error for each source is then $\sqrt{(\sigma_{run})^2 + (1.3/n)^2}$ %, where n is the number of noise calibrations during the observation, and σ_{run} is from Table 2.2.

2.8 (v) Setting Corrections

Errors in the setting corrections depend on the accuracy to which the apparent coordinates may be measured, and the magnitude of the discrepancy between the set and measured coordinates. A mean discrepancy between set and measured coordinates of 50 arc seconds was found for a large sample of sources whose coordinates were originally estimated from survey records. With 9 arc seconds as an estimate of the standard error in measuring apparent

coordinates (§2.5), the mean error in setting corrections is about 1.0%. For many sources in the catalogue, accurate positions had been obtained prior to measurement in the position/flux density programme. The standard errors in setting corrections were estimated as 0.2% for these sources, the error being greatly reduced because of the smaller differences between measured and set coordinates.

2.8 (vi) Zenith Angle Factor

The error in the zenith angle factor was estimated as 0.5% for all zenith angles.

2.8 (vii) Receiver Non-Linearity

For sources stronger than 6 f.u. at 2700 MHz, intensity measurements were made with on-source calibration as well as the standard off-source calibration. The means of on- and off-source calibration deflections were used for the subsequent calculation of flux densities. The mean discrepancy between deflections was about 10% for Hydra A (peak $S_{2700} \equiv 23.5$ f.u.). For sources stronger than 6 f.u., a 1% standard error was assumed in correcting for non-linearity as above.

2.8 (viii) Total Flux Density Errors

The errors shown in the catalogue, Table AII.1 and AII.2, are the square roots of the sums of the squares of the independent errors of §2.8(i) to §2.8(vii). Averaging the

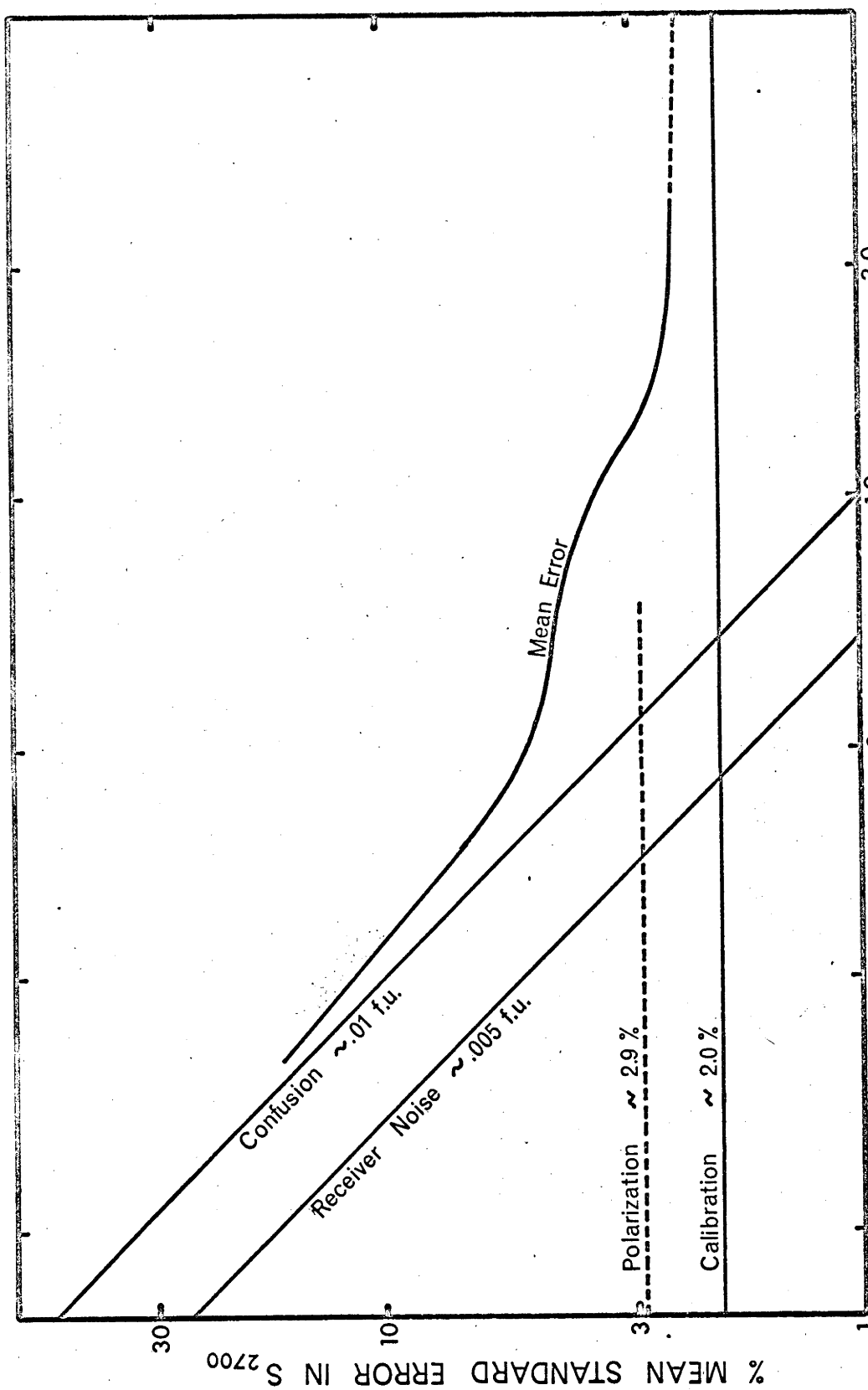

Figure 2.6. The percentage mean error in flux density at 2700 MHz as a function of flux density.

errors of all sources in all ranges of flux density produces the curve of mean error versus flux density shown in Figure 2.6. The dominant source of error for sources having $0.10 \leq S_{2700} \leq 0.40$ f.u. is confusion (§2.8(i)), and for sources $S_{2700} \geq 0.40$ f.u., polarization (§2.8(iii)). Where the polarization data was available, or the flux density measured at orthogonal position angles, calibration (§2.8(iv)) is the dominant source of error in the stronger sources. Receiver output fluctuations are not the dominant source of error at any flux density.

2.9 Comparison with Other Observations

Kellermann, Pauliny-Toth, and Tyler (1968) have published an accurate series of flux densities at 2695 MHz for 638 radio sources. The measurements were carried out with the NRAO 140-foot telescope. Quoted errors are about 1% for the stronger sources and 0.04 f.u. for the weaker sources. In Figure 2.7, the Parkes 2700 MHz flux densities have been plotted against the Green Bank 2695 MHz flux densities. The circled points are sources for which relatively large size factors are necessary to obtain integrated flux densities from peak flux densities. The mean ratio S_{2700}/S_{2695} is 1.035 ± .007 (solid line, Figure 2.7) indicating the Parkes flux density scale to about 3.7% higher than that of Kellermann et al. The scatter is in good agreement with error estimates.

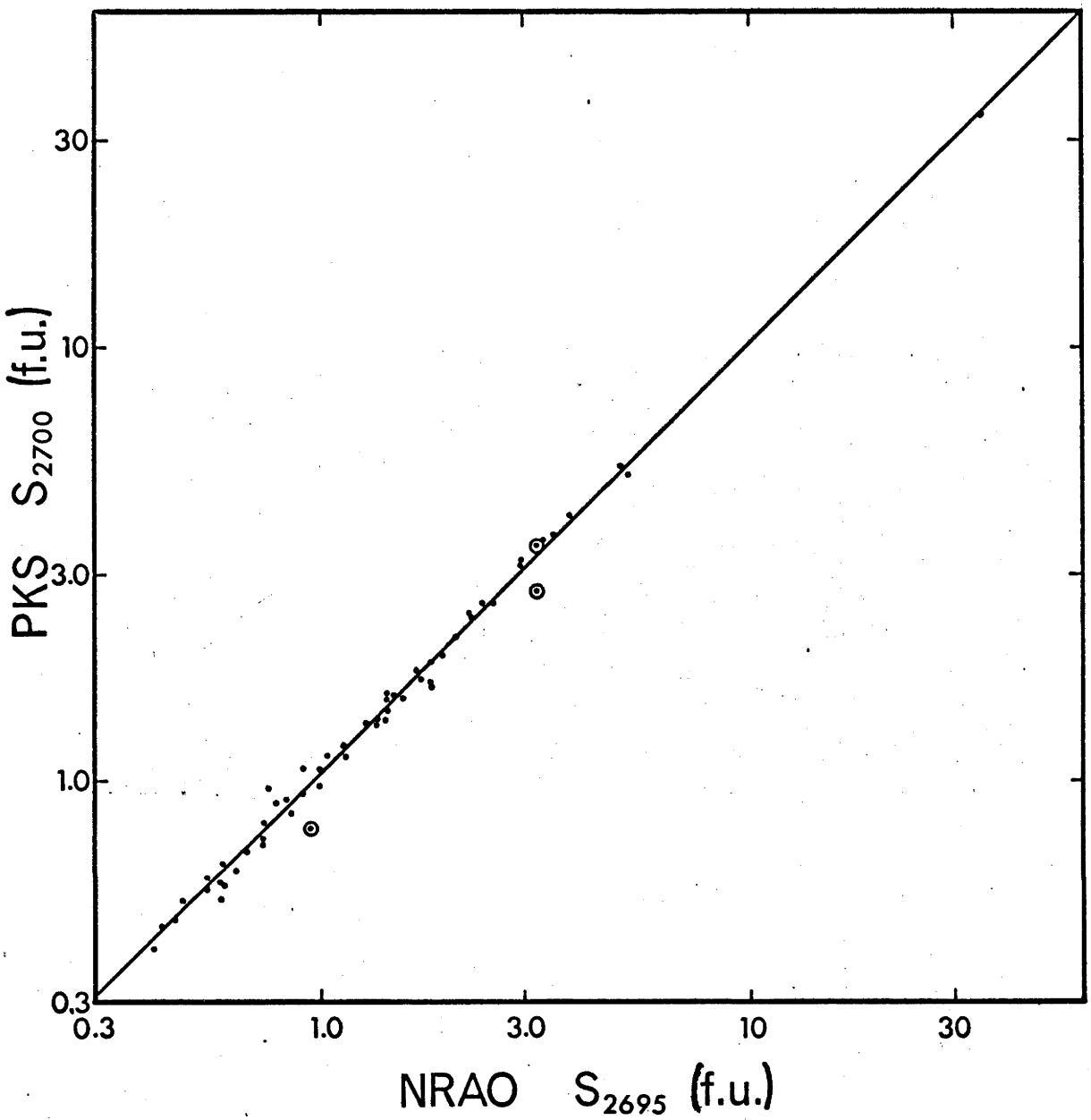

Figure 2.7. A comparison of the flux densities of the first parts of the PKS 2700 MHz catalogue with those measured at the NRAO. The sources for which the points are circled show considerable resolution in the PKS observations at 2700 MHz. The best fit line shown indicates a ratio of 1.035 (PKS to NRAO) and the scales thus disagree by a little over 3.5%.

Many of the 2700 MHz flux densities have been compared with those obtained at Parkes by Miss Harris (1969 and personal communication). The scatter again agrees with error estimates.

2.10 Reliability and Completeness

To describe the quality of catalogues of discrete radio sources obtained from sky surveys, Dixon and Kraus (1968) have defined four quantities: incremental and total reliabilities, and incremental and total completenesses. The reliabilities describe the probability of the sources in question being real. The completenesses describe the ratio of sources in the catalogue to those which should appear in the catalogue by virtue of their true flux density. "Incremental" and "total" refer respectively to the sources having flux densities in the range S to S+ΔS, and to all sources of flux density >S. As pointed out by Dixon and Kraus, the quantities can be accurately evaluated only if a survey at the same frequency and of higher angular resolution has been carried out to a lower limiting flux density over the same area of sky, or at least over a significant fraction of it. However, indirect estimates of the quantities may be made, and these represent the best evaluation of surveys of discrete sources.

2.10 (i) Reliabilities

The procedure of following the survey with position/flux density observations has ensured that no spurious sources were added to the catalogue by interference or by receiver noise. Hence the only factor affecting the reliability is the confusion effect of "blends", in which several weak sources of small angular separation are integrated by the beam to appear as a single small diameter source. The number of blends accepted as sources above the nominal limit of the selected region catalogues (S_{2700} = 0.10 f.u.) is negligible, as shown in the following considerations.

(1) Confusion effects were apparent on the position/flux density records for less than 10% of all sources stronger than 0.10 f.u. Of this fraction, the number showing beam broadening which might indicate blending was so small as to be insignificant. The confusion effects generally took the form of sloping baselines indicating the presence of weak neighbouring sources at separations greater than a beamwidth.

(2) In a comparison of the OSU 1415 MHz survey with the 4C survey, Dixon and Kraus (1968) found a lower limit to the total reliability for the latter of 98%. The result is in agreement with a comparison of the 4C catalogue with the selected region surveys. Out of 43 4C sources in the selected regions, only one (4C-02.1) does not appear on the

survey records; it may have a very steep spectrum. At the lower limit to 4C (S_{178}=2 f.u.) the source density is one per 28 primary beam areas, while for the selected regions, at S_{2700} = 0.10 f.u. the source density is one per 50 beam areas. On this criterion then, the total reliabilities for sources in the selected regions and the ±4° declination zone catalogues are estimated to approach 100%.

2.10 (ii) Completeness

The completeness of a survey is affected by two factors: (1) the failure to catalogue sources stronger than the nominal survey limit because of receiver noise and background irregularities, and (2) the masking of sources relatively near the catalogue limit by stronger sources.

For the selected region surveys, the considerations of §2.2(i), 2.8(ii), and 2.10(i) indicate that factor 1 is not significant. The effect of 2 has been estimated by a simple experiment. An area of sky corresponding in size to the selected regions was simulated by random placement of sources obeying a number - flux density relation $N = 104\ S_{2700}^{-1.4}$ (Shimmins et al. 1968), and plotted on the same scale as the original maps of the regions. The fraction of sources in each range of flux density which were masked by stronger sources was found by laying the simulated region over each of the selected region maps. The smoothed results are shown in Table 2.5. Total completeness is estimated to 98% at

S_{2700} = 0.10 f.u. It will be somewhat less than the 97% indicated at S_{2700} = 0.08 f.u. as factor 1 becomes significant.

TABLE 2.5

COMPLETENESS OF SURVEY

S_{2700} (f.u.)	Completeness Total (%)	Incremental (%)
.082	97.0	
		94.5
.105	98.0	
		96.0
.148	99.0	
		97.0
.218	99.5	
		98.0
.302	100.0	
		100.0
.594	100.0	

The source density in the $+4^{o}$ to -4^{o} declination zone survey is such that completeness was originally estimated directly as S_{2700} = 0.35 f.u. for all right ascensions surveyed except 05^{h} to 06^{h}. In this region the survey has been estimated as complete to 0.50 f.u., the higher value being due to the presence of several weak, extended HII regions. The estimate of 0.35 f.u. over most of the survey region is supported by two considerations. Firstly about 150 4C sources which did not appear in the $\pm 4^{o}$ zone catalogue have been observed at 2700 MHz (Wall and Shimmins, unpublished data.) Out of these, only two were found to be stronger than 0.35 f.u., and were consequently added to the catalogue. Secondly, there is excellent agreement between

the source densities found for S_{2700} = 0.35 f.u. from the selected region surveys and from the $\pm 4^{o}$ zone survey.

(The use of source counts in estimating completeness can be misleading. For example Dixon and Kraus have estimated completeness for the OSU survey by considering deviation of the low flux density numbers from a best fit line of -1.5 in their log N - log S diagram. The counts deviate from this line at about 1000 sources per steradian. The counts of Gower (1966) and Pooley and Ryle (1968) both show decreasing slope at this source density, and the fact that this completeness estimate agrees with two others made by Dixon and Kraus provides little justification for the procedure).

Time variations in the high frequency flux densities of some sources indicate that to be formally correct, the epoch should be included in descriptions of completeness for high frequency surveys. The observations of Chapter 4 show that the number of sources likely to be variable at 2700 MHz is small enough that the point does not require further consideration.

CHAPTER 3

OPTICAL IDENTIFICATIONS

Presented in this chapter are the results of the optical identification programme for the sources discovered in the surveys of Chapter 2. The chapter consists essentially of two papers, the first by Miss J.K. Merkelijn and Wall on the galaxy identifications, and the second by J.G. Bolton and Wall on the quasi-stellar object identifications. The former appears as §3.1 in a form very similar to that submitted for publication. The latter appears in §3.2; the introduction has been reduced as some of the content is in Chapter 2 and §3.1. Furthermore, the brief discussion of relations between various QSO parameters has been omitted, and appears where relevant in Chapters 5, 6, and 7.

3.1 Galaxy Identifications from the Parkes 2700 MHz Survey: the Selected Regions, and the ±4° Declination Zone

By Jeannette K. Merkelijn* and J.V. Wall

3.1 (i) Introduction

The coordinates of all sources in the catalogues resulting from the first two parts of the Parkes 2700 MHz survey (Wall, Shimmins, and Merkelijn, in preparation) have been measured accurately in order to obtain complete

* Division of Radiophysics, C.S.I.R.O. Sydney, N.S.W., Australia. Now at The Observatory, Leiden, The Netherlands.

identification statistics. In this paper we present the galaxy identifications; the quasi-stellar object identifications will be presented in a companion paper (Bolton and Wall, in preparation).

3.1 (ii) The Position Measurements and Identification Procedure

The positions of all the survey sources have been measured with the Parkes 210-foot telescope and the 2700 MHz broad-band correlation receiver (Batchelor, Brooks, and Cooper 1968) equipped with a dual beam feed system. The feed system produces on- and off-axis beams separated by 18.5 arc minutes and the difference between the signals at the two feeds is recorded. The main beam is approximately Gaussian with a width of 7.9 arc minutes to half-power points. The position of each source was measured by scanning the main beam through the source several times in both right ascension and declination. The resulting apparent positions were corrected for hour angle and diurnal pointing errors by observing sources from the Parkes grid of pointing calibrators. The position measurements are described in detail in the presentation of the 2700 MHz catalogue; similar observations have been described by Merkelijn (1968, 1969). The standard error in the position measurements averages 12 arc seconds in both coordinates for sources stronger than S_{2700} = 1.5 f.u., 16 arc seconds for sources of S_{2700} = 0.15 f.u., and increases rapidly for sources of

still lower flux densities.

The prints of the Palomar Sky Surveys were searched at the measured source positions with the aid of computer-drawn transparent overlays. On these overlays a 2 arc minute square field, centered on the source position, is plotted together with the positions of ten nearby stars from the Smithsonian catalogue. The technique has been described in detail in previous Parkes identification papers.

3.1 (iii) The Identifications

The first part of the 2700 MHz catalogue consists of all sources with $S_{2700} \geq 0.10$ f.u. in six selected regions of 41 square degrees each. Many sources for which $S_{2700} < 0.10$ f.u. are also tabulated. The regions correspond to areas covered by six two-colour (blue - ultraviolet) plates taken by J.G. Bolton with the 48-inch Schmidt telescope at Palomar. The centres of the plate areas are listed in Table 2.1. In Table AIII.1, 42 sources in these regions for which galaxies are considered as identifications are listed. The upper limit to the differences permitted between radio and optical coordinates was 1 arc minute; the criterion was varied according to optical apparent magnitude and estimated error in the radio position. Of the 42 sources, 6 had been previously identified (see references for Table AIII.1).

The second part of the 2700 MHz catalogue consists

of sources found in a survey of the declination zone $+4^{\circ}$ to -4°. Right ascensions $06^{h}00^{m}$ to $07^{h}21^{m}$ and $18^{h}00^{m}$ to $19^{h}40^{m}$, regions which are heavily obscured on the Sky Survey prints, were excluded from the survey. The catalogue is believed to be complete to 0.35 f.u. at 2700 MHz, and includes many weaker sources. In Table AIII.2 94 sources for which galaxies are considered as identifications are listed. The upper limit to coordinate discrepancies permitted was 0.5 arc minutes, the criterion varying as above. Of the 94 sources, 45 had been identified in previous programmes (see references for Table AIII.2). For completeness, 9 sources from Table AIII.1 have been included in Table AIII.2.

Appendix III contains a description of the data presented in Tables AIII.1 and AIII.2.

3.1 (iv) Finding Charts

Finding charts for the 80 new identifications of Tables AIII.1 and AIII.2 have been prepared from [E] Palomar Sky Survey prints. The scale is approximately 5mm = 1 arc minute, and contrast has been increased over that of the originals. The finding charts have not been bound into the thesis.

3.1 (v) Conclusions

The two-colour plates which define the selected areas were taken in regions of negligible obscuration.

Consequently, Table AIII.1 is believed to contain all galaxies in the selected regions with $S_{2700} \geq 0.10$ f.u. and with $m_{pg} \leq 20^m.5$, the plate limit. In the $\pm 4^o$ declination zone, heavy obscuration is evident on the Palomar Sky Survey for right ascensions 05^h to 07^h20^m and 18^h to 19^h40^m, and there may be significant obscuration up to 20^h30^m. Outside these areas, Table AIII.2 is thought to be complete to the limiting m_{pg} of $20^m.5$ and to $S_{2700} = 0.35$ f.u.

The present observations confirm most galaxy identifications previously suggested for the $\pm 4^o$ declination zone. The identifications of galaxies with the following sources appear to be in error on the basis of the present observations:

Bolton and Ekers (1967)	0118-00, 0131-00, 0300-00 0747-00, 1159-02
Bolton and Ekers (1967) Merkelijn (1969)	1307-00.7
Clarke, Bolton, and Shimmins (1966)	0029+01, 0031+01, 0505+03, 0932+02, 1354+01
Wyndham (1966)	0358+00

In addition further position measurements on 0439+01 and 1523+03 are necessary. The present observations indicate differences of about 30 arc seconds between the radio positions and the positions of the suggested galaxy identifications (Bolton and Ekers 1966a). Finally we note that Gent et al. (1969) show the identification suggested for 0949+00 (Bolton and Ekers 1966a) to be

incorrect.

The sources 0239+002, 1103+002, and 1157-008 are identified with the bright spiral galaxies NGC 1055, 3521, and 4030. These galaxies are "normal" in the radio sense; it is evident that surveys to fainter flux limits such as the present one will detect increasing numbers of such objects. "Finding charts" for these three objects have been included with the others to illustrate the morphological characteristics.

The results of this investigation will be statistically examined elsewhere. In particular, one of us (J.K.M.) is using them in conjunction with other observations to derive an accurate luminosity function for radio galaxies.

3.1 (vi) Acknowledgements

We thank Mr. J.G. Bolton for his participation in the observations, and for his examination of source fields in conjunction with us. We also wish to thank Mr. A.J. Shimmins and Dr. R.N. Manchester for participation in the observing programme. Wall wishes to acknowledge a Research Scholarship from the Australian National University during the course of this work.

3.2 Quasi-Stellar Objects in the Parkes 2700 MHz Survey: the Selected Regions, and the ±4° Declination Zone

by J.G. Bolton* and J.V. Wall

3.2 (i) Introduction

The first two parts of the Parkes 2700 MHz survey and the subsequent position measurements have been described in Chapter 2.

In order to aid in the positive identification of QSO's in the Parkes 2700 MHz surveys, a series of two-colour plates were taken with the 48-inch Schmidt telescope at Palomar in 1966 and 1968 by Bolton. Kodak 103a-0 plates were used and an exposure of 8 minutes was made behind a GG-13 (minus UV) filter followed by an exposure of 60 minutes behind a UG-1 (UV) filter. The telescope was displaced by 12 arc seconds in right ascension between the two exposures. On most of these plates a stellar object with an ultraviolet excess greater than (U-B) = -0.4 has an ultraviolet image brighter than the blue image. Plates which were taken under conditions of good seeing have a limit in the blue which is about half a magnitude brighter than the standard blue Sky Survey plates. Unfortunately it was not possible to secure plates covering the entire ±4° declination zone; no plates were obtained between right ascensions 14^h and 17^h,

* Division of Radiophysics, C.S.I.R.O., N.S.W., Australia

and the plates cover $6^{o}\ 40'$ in declination compared to the 8^{o} in declination for the equatorial zone survey. The areas covered by the photographic and radio surveys are shown in Figure 3.1. The six plates chosen for the selected region surveys were amongst a number which were taken in 1966 under conditions of good seeing in regions free from galactic obscuration. Five of these are in the $\pm 4^{o}$ survey zone, and one is at a declination of -18^{o}. The plate centres are listed in Table 2.1.

3.2 (ii) Identification of QSO's

The Palomar Sky Survey prints and the two-colour plates, where available, were examined at the positions of the 310 sources in the selected area catalogues and the 500 sources in the $\pm 4^{o}$ zone catalogue. The examination was made with the aid of the computer-drawn overlays described in §3.1(ii). Radio galaxies found in this examination have been discussed by Merkelijn and Wall (§3.1).

In most cases where two-colour plates were available a positive identification of a radio source as a QSO could be made from the close positional agreement between the source and a stellar object with obvious ultraviolet excess. In the identification tables (Tables AIII.3 and III.4) such objects are denoted by 'UVX' in the comments column (13). Identifications for which the ultraviolet excess is less certain are indicated by 'UVX?'. In some

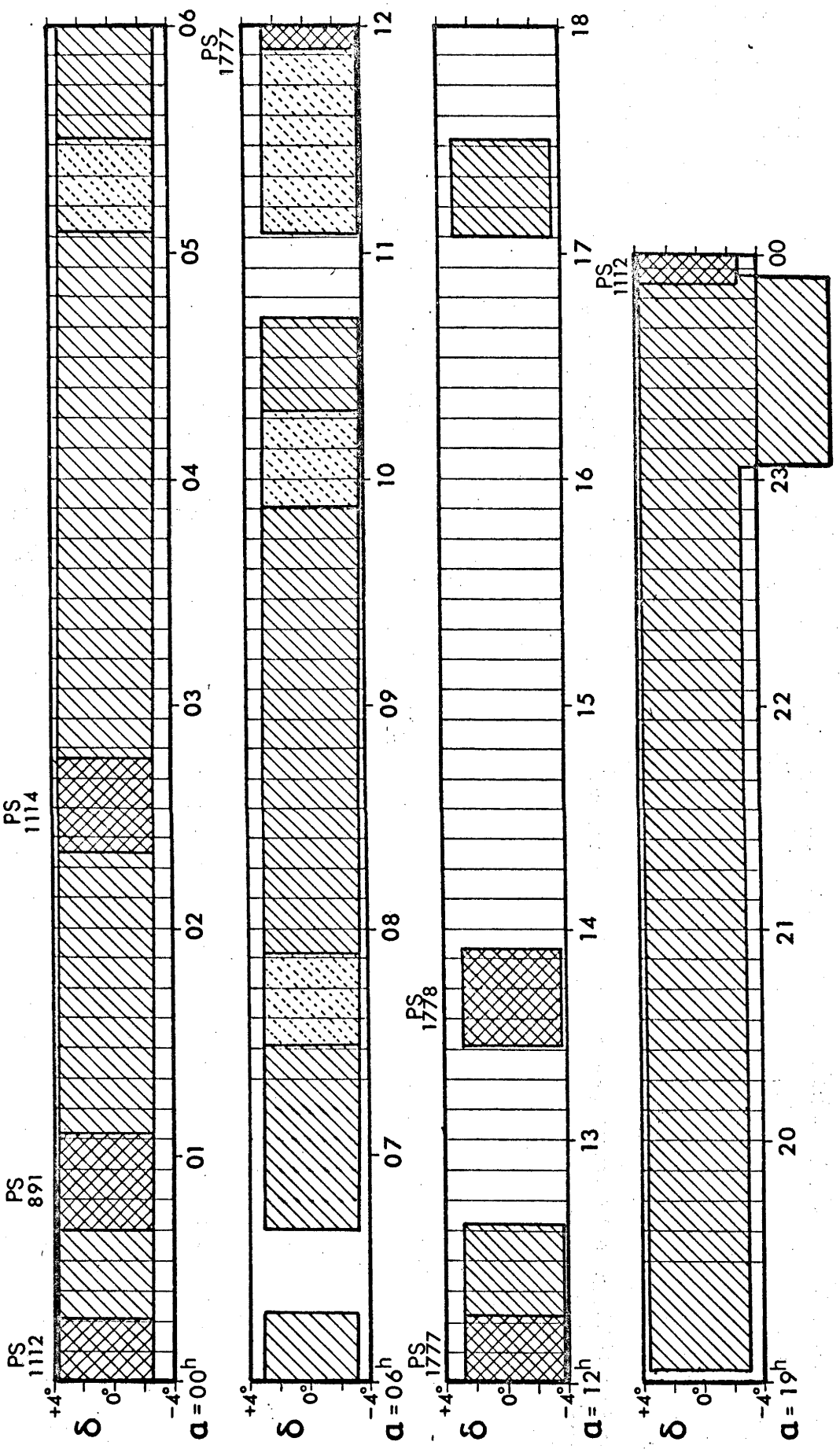

Figure 3.1. The areas covered by photographic and radio (2700 MHz) surveys in the ±4° declination zone. The 45° lines indicate the area covered by two-colour (blue - ultraviolet) Schmidt plates taken by Bolton. Where these lines are dashed, the plates are of inferior quality. The area covered in the 2700 MHz survey is indicated by vertical lines, and the five regions in the ±4° zone selected for the deep surveys are distinguished by cross-hatching.

cases these are objects which are noticeably brighter on the blue Sky Survey print than on the red but have almost equal images on the two-colour plate. These may be QSO's having UV excess close to the known lower limit of ~ -0.4, due perhaps to a strong emission line in the blue region of the spectrum. In other cases where the plate was taken under conditions of poor seeing, the ultraviolet images are degraded and the colour balance of the place upset. However, UV excess is suggested from a comparison of the relative image intensities of the object in question and other objects of the same blue intensity within a radius of 20 arc minutes.

In the region not covered by two-colour plates identifications are suggested on the basis of coincidence in position between the source and an object which is relatively brighter on the blue than on the red Sky Survey print. Many such coincidences were found in regions which were subsequently covered in the 1968 series of two-colour plates. The existence of ultraviolet excess confirmed about two thirds of these as QSO's.

Of the sources catalogued in the $\pm 4^{\circ}$ zone, 103 were found to be QSO's or possible QSO's. Identifications for 36 of these have been published, 11 of which resulted from the present work. The two-colour plates yielded confirmation for 36, and redshifts for 6 of these have been obtained. A further 31 identifications are suggested but

not confirmed. In the selected regions, an additional 29 QSO's were found, all confirmed by their ultraviolet excess.

Details of the identifications and suggested identifications are given in Appendix III, Tables AIII.3 and AIII.4.

3.2 (iii) Finding Charts

The finding charts have been prepared from the blue Sky Survey prints, in the same fashion as those for the radio galaxies (§3.1(iv)). They have not been bound into the thesis.

3.2 (iv) Retraction of Previously Suggested Identifications

A number of possible identifications of Parkes catalogue sources in the $\pm 4^{\circ}$ zone suggested by Bolton and Ekers (1966b and 1967) can be retracted on the basis of the present work. These are PKS 0013-00, 0047-02, 0458-02, 0854-03, 2121-01, and 2154-18. More precise radio positions eliminate PKS 0047-02 and 0854-03, and the absence of ultraviolet excess eliminates the remainder. Positional agreement in the case of PKS 0458-02 is very good; it may be an N-galaxy. The identification for PKS 0300-00 originally suggested as a galaxy by Bolton and Ekers (1967) has been changed to a nearby QSO, as has the identification for PKS 0505+03 (Clarke, Bolton, and Shimmins 1966).

3.2 (v) Additional Redshifts

Redshifts for six of the QSO's in Table AIII.4 were obtained by Bolton with the image-tube spectrograph at the prime focus of the 120-inch telescope at Lick Observatory. The sources are PKS 0038-020 (z = 1.176), 0118+03 (z = .673), 0226-038 (z = .695), 0336-01 (z = .852), 0420-01 (z = .915), and 0421+019 (z = .689).

3.2 (vi) Relationships between Various QSO Parameters

The version of this paper submitted for publication contained brief examination of four relationships for QSO's in the present sample. These are (a) radio spectra and flux density, (b) redshift and flux density, (c) flux density and visual magnitude, and (d) the log N - log S curve. Relations (a) and (c) are discussed in the context of both Chapters 5 and 6, (d) in Chapter 6, and (b) in Chapter 7.

3.2 (vii) Acknowledgements

We would like to thank Miss J.K. Merkelijn for assistance in examining the Sky Survey prints. Bolton wishes to thank Dr. Horace Babcock for permission to use the 48-inch Schmidt telescope to obtain the two-colour plates and Dr. Robert Kraft for permission to use the 120-inch telescope to obtain spectra of some of the QSO's. Wall acknowledges receipt of an A.N.U. Research Scholarship during this work.

CHAPTER 4

THE SPECTRA OF SOURCES IN THE PARKES 2700 MHZ SURVEYS
I. THE OBSERVATIONS, AND SPECTRA OF INDIVIDUAL SOURCES

Spectral data for most sources in the 2700 MHz catalogues for which $S_{2700} \geq 0.30$ f.u. have been compiled in Table AIV.1 of Appendix IV. Flux densities at 468, 635, 1403, 2700, and 5009 MHz have been measured at Parkes. Those at 178, 408, and 1415 MHz are from other observatories, and carry references in the table. Particulars of the observations are summarized in Table 4.1, and are discussed in the following sections. The source spectra which do not follow power laws are illustrated. The chapter concludes with brief discussions of some of these, and of the stronger sources in the 2700 MHz catalogues which do not appear in the 4C catalogue.

4.1 Flux Densities at 5009 MHz (λ = 6.0 cm.)

During the loan of the NRAO 5009 MHz receiver to CSIRO, the flux densities of 1100 extragalactic radio sources were measured. About 750 of these flux densities have been published (Shimmins, Manchester, and Harris 1969, hereinafter referred to as SMH); the remainder are presented here.

Of the 344 sources catalogued in the $\pm 4^{\circ}$ declination zone with $S_{2700} \geq 0.35$ f.u., the flux densities of all but 24 were measured at 5009 MHz. Flux densities at this frequency were also obtained for many sources weaker than 0.35 f.u. at 2700 MHz. The principal objectives of the

TABLE 4.1

FLUX DENSITIES FOR SOURCES IN THE 2700 MHZ CATALOGUES

Frequency (MHz)	Reference, Table AIV.1	Instrument	Beam	Scale Factor	Typical Errors in Flux Density	No. of Sources
178	1	Cambridge pencil beam synthesis	23'(α) × 18'sec z	1.08	0.5 f.u. or 6%	61
178	2	Cambridge total power fan beam	13!6(α) × 4°.6	1.10	10%	18
178	3,4,5	Cambridge 4C Interferometer	23'(α) × 31'sec z Fringe sep. 7!5(α)	1.08	0.6 f.u. or 15%	218,74,4
408	6	E-W arm, Molonglo Cross	1!9(E-W) × 4°.2	0.91	0.4 f.u. or 5%	31
408	7	E-W arm, Molonglo Cross	1!9(E-W) × 4°.2	0.95	0.3 f.u. or 5%	9
468	-	Parkes Interferometer	Primary 54' × 54' Fringe sep. 25'(δ)	-	0.4 f.u. or 4%	284
468	8	Parkes Interferometer	Primary 54' × 54' Fringe sep. 25'(δ)	-	0.8 f.u.	27
635	-	Parkes 210' Paraboloid	30' × 30'	-	0.3 f.u. or 8%	457
635	8	Parkes 210' Paraboloid	30' × 30'	-	0.2 f.u.	39

TABLE 4.1 concluded

Frequency (MHz)	Reference, Table AIV.1	Instrument	Beam	Scale Factor	Typical Errors in Flux Density	No. of Sources
1400	10	Green Bank 300' Paraboloid	10' × 10'	1.00	-	1
1403	-	Parkes Interferometer	Primary 18' × 18' Fringe sep. 8'(δ)	-	0.1 f.u. or 5%	313
1410	8	Parkes 210' Paraboloid	14' × 14'	-	0.1 f.u.	34
1415	9	Ohio 260' × 70' Mirror	10'(α) × 40'	1.00	0.15 f.u. or 25%	46
1425	11	Caltech E-W Interferometer	Primary 33' × 33' Variable fringe sep. 1!3 - 11!9	1.00	-	1
2700	-	Parkes 210' Paraboloid	7!9 × 7!9	-	0.01 f.u. or 2.5%	532
5009	-	Parkes 210' Paraboloid	4!0 × 4!0	-	0.01 f.u. or 2.5%	370

programme were to determine the high frequency spectra for a statistically significant sample of the sources in the 2700 MHz catalogue, and, by virtue of the smaller beamwidth, to provide corrections for partial resolution at 2700 MHz (the "size factors" of §2.7). These are essential in deriving the correct number - flux density relation at 2700 MHz, as discussed in Chapter 6.

4.1 (i) Observations, Calibration, Reduction

The observations were carried out in 3 observing sessions, the dates of which are listed in Table 4.2. Twelve of the 5009 MHz flux densities listed in Table AIV.1 are from SMH, and the corresponding sessions and dates are also in Table 4.2.

TABLE 4.2

5009 MHZ OBSERVING SESSIONS

Session	SMH Session	Dates	Epoch	Number of Sources
a		May 30 - June 4, 1968	1968.42	125
b		Aug. 1 - 3, 1968	1968.59	145
c		Aug. 8 - 12, 1968	1968.61	85
d	2	May 4 - 5, 1968	1968.34	4
e	3	June 4 - 8, 1968	1968.51	2
f	4	July 12 - 16, 1968	1968.53	3
g	5	Aug. 4 - 7, 1968	1968.60	3

The NRAO receiver, switched between on- and off-axis feeds for the present observations, produced a main beam 4.0 arc minutes to half power points, and r.m.s. receiver output fluctuations of 0.03 f.u. for a 1 second time constant. Receiver properties have been briefly described in SMH; in performance, the excellent short term stability should be mentioned.

In session (a), flux densities were measured by scanning through each source position as obtained from the 2700 MHz programmes (§2.4) approximately 8 times. Half of these scans were made in either coordinate, and orthogonal feed angles were used for each scan series. The scans were made at a rate of $0^{\circ}.25$/minute with an output time constant of 1 second. Telescope focus is important at this wavelength, and a curve of optimum position of the feed platform versus zenith angle was kindly supplied by D. Yabsley. The focus was reset for the observation of each source. The deflection produced by a noise calibration signal of about 3 f.u., injected at the receiver input, was recorded during the observation of each source. The receiver output was recorded on chart running at 80mm/minute. A sample pair of scans is shown in Figure 4.1(a).

For sessions (b) and (c) the procedure was refined slightly. Eight scans were again made for each source, but with pairs of scans at orthogonal feed angles in either coordinate. Two noise calibrations were made during the

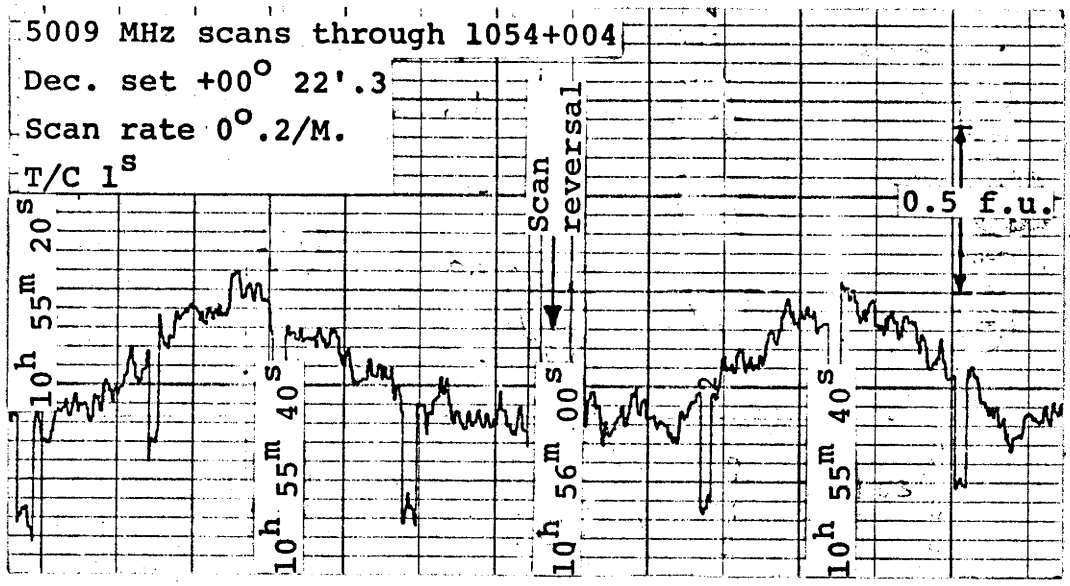

Figure 4.1(a). A pair of scans at 5009 MHz through the source 1054+004. Half-power beamwidth is 4.0 arc minutes.

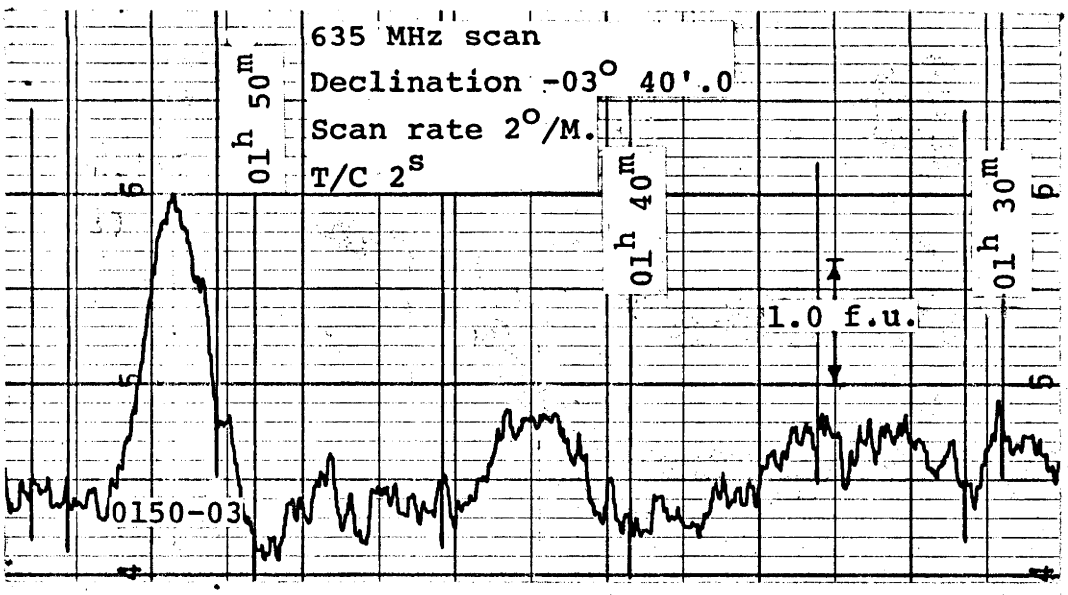

Figure 4.1(b). A portion of a scan in the 635 MHz survey of the ±4° declination zone. Half-power beamwidth is 30.5 arc minutes.

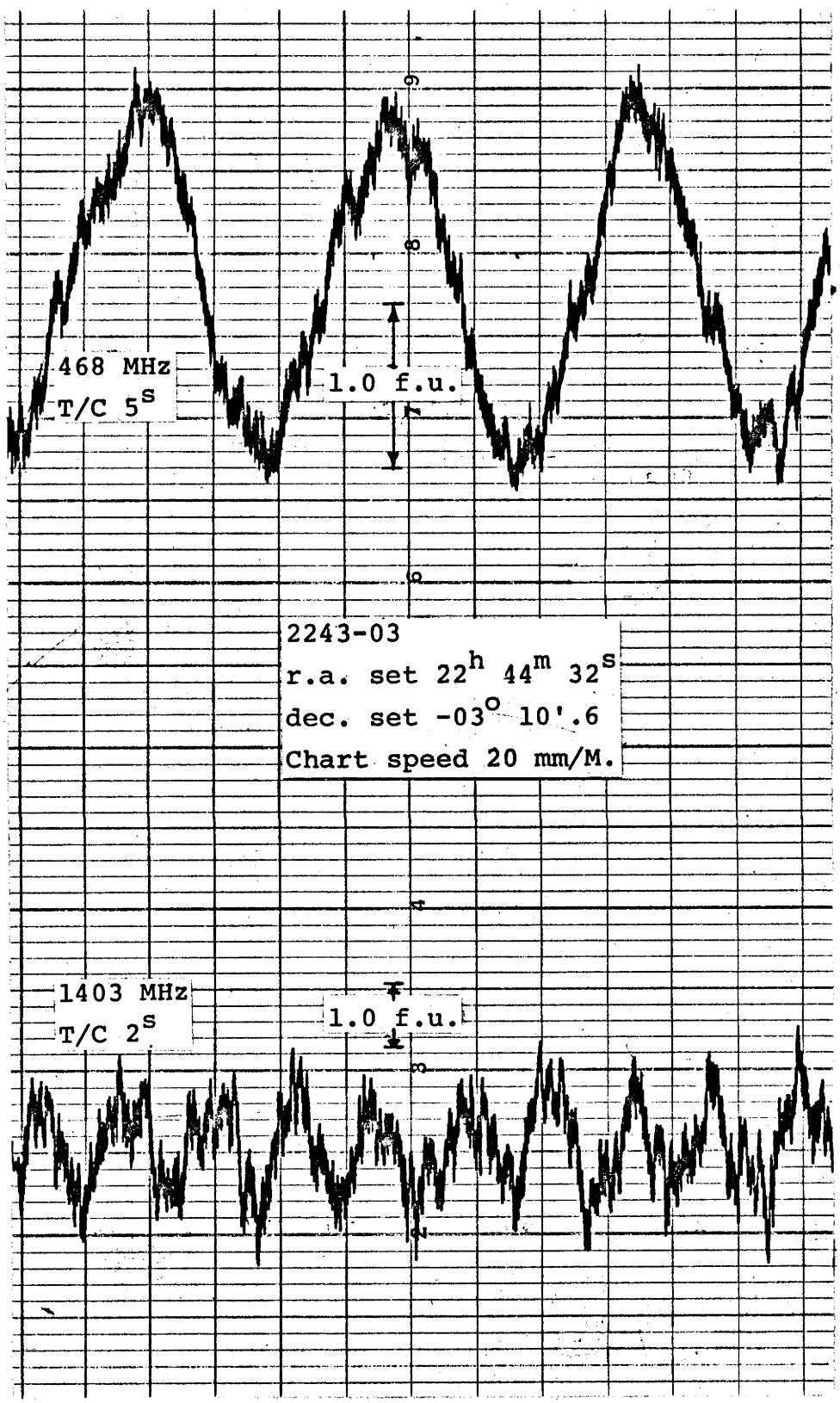

Figure 4.1(c). A sample record of the observations with the Parkes interferometer from which flux densities at 468 MHz and 1403 MHz were obtained.

observation of each source. The telescope focus was kept constant in order to save observing time, and source amplitudes were corrected for the consequent small reduction in telescope gain (see Figure 2.5). A lower scan rate of $0^{\circ}.2$/minute was used.

For sources stronger than $\sim$.8 f.u. at 5009 MHz, generally only 4 scans were made. The scans for several of the weakest sources (S_{5009} $\sim$0.15 f.u.) were augmented by a series of on - off observations, and for a few of these the flux density was obtained in only one (linear) polarization as indicated in Table AIV.1.

The determination of flux densities from the scans followed the procedure for the 2700 MHz flux densities (§2.6). The effects of receiver non-linearity again were removed by taking the mean of calibration deflections from noise injection both on and off the strong sources. The curves of zenith angle correction factors are shown in Figure 2.5. Curve (a) indicates the compensation for changes in atmospheric extinction and aperture efficiency with zenith angle. It was kindly supplied by D. Yabsley who obtained it by observation of sources over a large range in zenith angle with the telescope focus optimized. Curve (b)-(c), taken from SMH, compensates in addition for the effect of fixed focus, and was obtained from the observations of PKS 0915-11 (Hydra A) over a wide range in zenith angle by SMH and Wall, supplemented by data on the same source kindly supplied by

Dr. Miller Goss.

Following SMH, the flux density scale was based on the assumption of $S_{5009} \equiv 13.5$ f.u. for PKS 0915-11. The size factor of 1.034 for the 4 arc minute beam (Miss Harris, personal communication) indicates a corresponding peak flux density of 13.05 f.u. In sessions (b) and (c), the value of the noise calibration signal was determined directly from several observations of 0915-11. As for the 2700 MHz sessions 1 to 8, the value of the calibration signal in session (a) was determined by using several of the stronger sources observed in (a) as sub-calibrators, and re-observing these sources in (b) and (c). Repeated observations indicated no change in the value of the calibration signal during any observing session.

4.1 (ii) Errors in Peak Flux Densities

The sources of error in the peak flux densities are identical to those in the 2700 MHz flux densities (§2.8). However, there are changes in the relative importance of the factors.

The standard error due to background irregularities was estimated by a similar analysis to that for 2700 MHz (Appendix I), and the result is 0.003 f.u. Confusion error is consequently negligible for the weakest sources measured in this programme.

Errors due to receiver output fluctuations were directly estimated as in §2.8(ii) for each observing session.

The standard errors in estimating the flux densities from a single scan were found to be 0.030, 0.018, and 0.024 f.u. for sessions (a), (b), and (c) respectively. The differences are attributed to weather conditions; considerable heavy cloud in session (a) in particular produced many unstable baselines. For all sessions, however, 8 scans reduced the standard error due to receiver output fluctuations to 0.01 f.u. or less.

For the few sources indicated in Table AIV.1 to be measured in only one polarization, an additional error of $\sim$5% should be added in quadrature to the quoted error. No formal evaluation of this error has been carried out as was done for the 2700 MHz flux densities (§2.8(iii)).

Standard errors in the value of the noise calibration were calculated for each session as described in §2.8(iv). The calibration deflections were again plotted against sidereal time to obtain the scatter due to measurement and short term gain fluctuations. Adding these two sources of error in quadrature resulted in the standard errors of calibration 1.4%, 1.0%, and 1.2% for runs (a), (b), and (c) respectively.

The principal difference between the error analyses for the 2700 MHz and the 5009 MHz peak flux densities is in the evaluation of the errors for the setting corrections. Inaccuracy in measuring the apparent coordinates from the scans causes considerably larger errors in the setting

corrections at 5009 MHz because of the smaller beamwidth. By considering (1) the individual differences between the set and apparent coordinates as determined from the scan centroids, and (2) the accuracy to which the apparent coordinates could be measured, the standard errors in setting corrections were evaluated separately for each source. For many sources, errors in the setting corrections were found to be the dominant errors in the peak flux densities.

The standard errors in the zenith angle correction factor were taken as 1.0% for zenith angles 20° to 40°, 1.5% for the zenith angles 40° to 50°, and 2.0% for zenith angles 50° to 60°. These errors were estimated from the scatter in the observations used in the determination of the factor.

For sources stronger than 4.0 f.u. at 5009 MHz, a standard error of 0.5% was assumed in the procedure of removing non-linearity effects with on-source off-source calibration.

The final standard errors in the 5009 MHz peak flux densities are the square roots of the sums of the squares of the independent errors discussed above. In Figure 4.2, the mean error in each range of peak flux density has been plotted against flux density. Receiver output fluctuations dominate below 0.30 f.u.; for the stronger sources, calibration errors, and errors in setting corrections and in zenith angle factors are all significant.

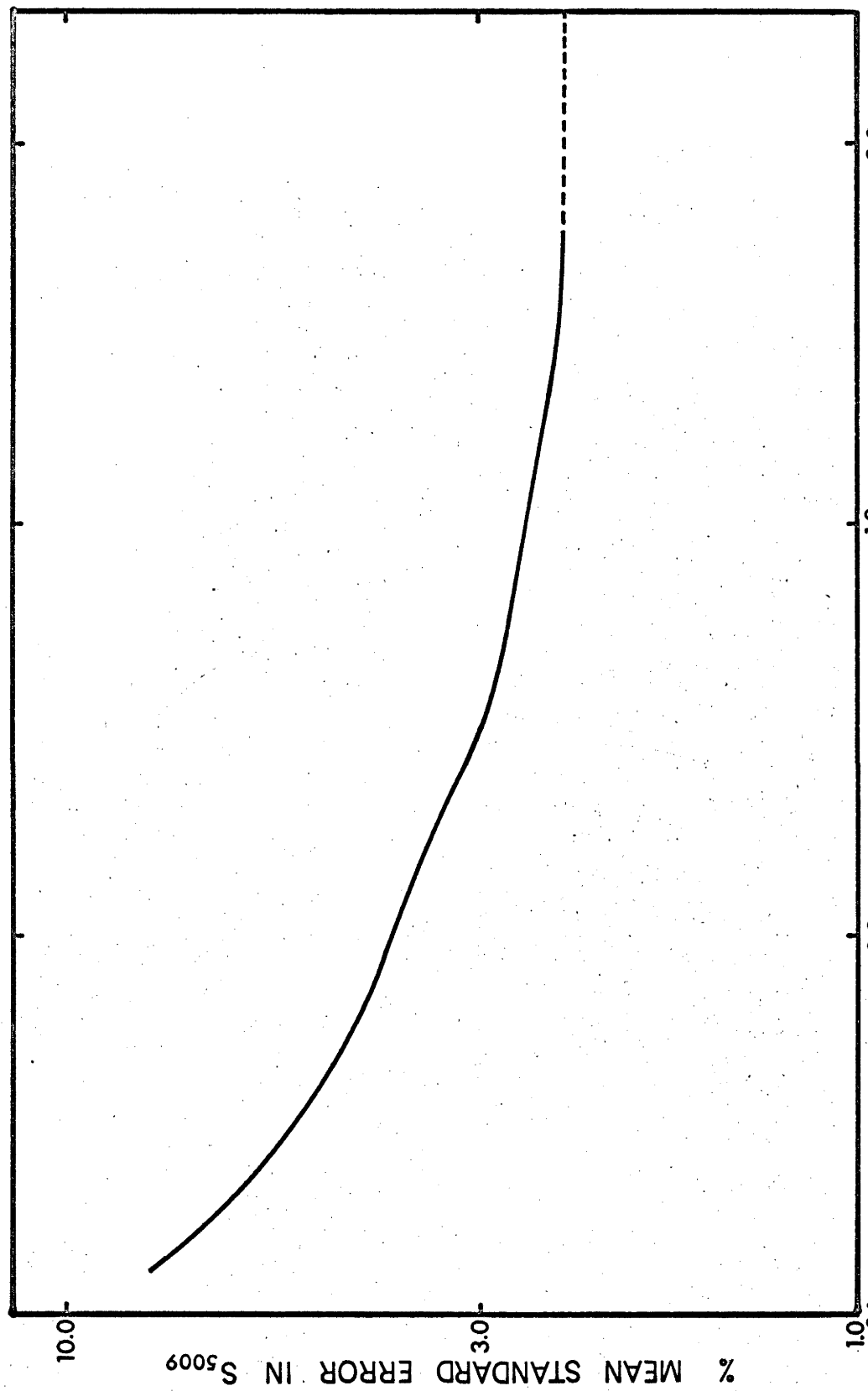

Figure 4.2. The percentage mean error in flux density at 5009 MHz as a function of flux density.

4.1 (iii) The Angular Extent of the Sources

With a 4.0 arc minute beam, many of the stronger sources are partially resolved, and careful determination of size factors is necessary to obtain accurate flux densities. The point has been emphasized by SMH.

Available data on angular structure for the present sample of sources is collected in Table 4.3. All source records obtained in the 5009 MHz programme have been examined for beam broadening by means of transparent overlays, and information on the angular extent of partially resolved sources thus obtained has also been entered in Table 4.3. Size factors have been computed in the conventional manner; formulae are given in SMH. As stated in SMH, strong sources extended east-west or north-south by 1' show detectable beam broadening and the resultant size factor is 1.05. The size factors (and consequently the flux densities) will be underestimated if the extension is along position angles 45^{o} or 135^{o}. Fortunately, structural data is available for most of the apparently bright sources. For sources having peak flux densities < 0.5 f.u., beam broadening becomes increasingly difficult to detect. However, such sources are generally more distant and the likelihood of partial resolution diminishes with flux density. For instance, Wall, Cole, and Milne (1968 and unpublished Parkes interferometer results) find that only 35% of all sources with $S_{2700} \geq 1.0$ f.u. have angular dimensions ≥ 0.2 arc minutes. For this sample of

TABLE 4.3

DATA ON SOURCE STRUCTURE FOR SIZE FACTOR CALCULATIONS

Source	Data on Structure	References	Size Factor	
			5009 MHz	2700 MHz
0003-00	<30" x 3"	1,4,8	1.000	1.000
0010+00	<0'.7 x <0'.3	4,8	1.000	1.000
0025-007	Double, sep. 2'.8	3	1.230	1.059
0034-01	Triple, sep. 18" NS; components 2"	7	1.011	1.003
0035-02	Core + halo, halo 20"	10	1.000	1.000
0036+03	1'.8(EW) x <0'.5 (5009 MHz)		1.095	1.024
0051-03	<0'.4 x <0'.25	2,4	1.000	1.000
0053-016	1'.3 EW } PKS 0053-01, sep. 7'.9 EW	4	1.105	1.027
0053-015	1'.3 EW }		1.105	1.027
0055-01	2'.5(NS) x 1'.1	4	1.180	1.046
0122-00	<0'.3 NS	2	1.000	1.000
0123-01	Double, sep. 5'.7 NW; components 1'.6, 2'.6 EW. But see contour map, Figure 4.3, which disagrees with interpretation of the interferometry. Size factors from map.	4,8	1.848	1.218
0128+03	Double, sep. 3'.0 EW; components <0'.3 EW. Observation at 5009 MHz indicates that source is 1'.5(NS) x <0'.7. A weak source (~.1 f.u.) appears 6' S on the declination scans. 2700 MHz observation indicates confusion with this weaker source, as half-power widths are 11'.2(NS) x 8'.6 (HPBW 7'.9), and the position at 2700 MHz (centroid of scans) is 2' S of that obtained at 5009 MHz.	4	1.071	1.018
0218-02	<0'.7(NS) x <0'.25	4,8	1.000	1.000
0240-00	<0'.5(NS) x <0'.2	2,4,8	1.000	1.000
0305+03	Double, sep. 0'.3 NS; components 1'.0 x 1'.5, <0'.5	2,4,8	1.080	1.021
0325+02	Double, sep. 2'.3 EW; components 1'.4, 0'.7 EW	2,4,8	1.289	1.074
0331-01	Double, sep. 0'.8 EW: components <0'.6 EW	4	1.031	1.008
0336-01	Double, sep. 2'.3 NS; components <0'.3 EW	4,8	1.000	1.000
0404+03	Triple, sep. 3'.4 EW; components <0'.3, 0'.2, 0'.2	4	1.295	1.076
0409-01	<0'.4 EW	2	1.000	1.000
0416-03	1'.6(EW) x <0'.5 (5009 MHz)		1.080	1.021
0440-00	<0".05, <1".5 EW	9,1	1.000	1.000
0511+00	Double, sep. 2'.9 EW; components <0'.5, 1'.3 E; weaker source 6' W.	4	1.085	1.022
0550+032	0'.5(NS) x 1'.1 (5009 MHz). Spectrum inverted, and 2700 MHz flux density is variable. Possibly high and low frequency components are widely separated, or a confusing source is present.		1.042	1.000
0724-01	0'.45 EW	4	1.050	1.013
0736+01	<0'.25 EW	4	1.000	1.000
0742+02	Double, sep. 1'.9 NS; components <0'.5 EW	4,8	1.155	1.040
0812+02	<0'.3 EW	4	1.000	1.000
0812-02	<0'.4(NS) x <0'.25	4,8	1.000	1.000
0833-01	1'.5(NS) x 2'.2 (5009 MHz)		1.222	1.057
0949+00	1'.0(NS) x <0'.3	4,8	1.023	1.006

TABLE 4.3 concluded

Source	Data on Structure	References	Size Factor	
			5009 MHz	2700 MHz
1008-01	2.4(NS) x <0.5 (5009 MHz)		1.165	1.042
1039+02	<0.25 EW	4	1.000	1.000
1055+01	<30"(NS) x <.05"	5,9	1.000	1.000
1059-01	Double, sep. 7" EW	1	1.000	1.000
1105+037	<0.5(NS) x 3.1 (5009 MHz)		1.262	1.067
1116-02	<1."5 EW	1	1.000	1.000
1118+000	<0.5(NS) x 1.4 (5009 MHz)		1.062	1.016
1138+01	Double, sep. 7."3	1	1.000	1.000
1146-037	<0.5(NS) x 2.2		1.142	1.036
1148-00	<24"(NS) x <."05	2,9	1.000	1.000
1215+03	Triple, total sep. 2.9 EW; components all <0.4	4,5	1.277	1.071
1226+02	Double, sep. 19"	6	1.000	1.000
1229-02	<0.4 x <0.4	2	1.000	1.000
1330+02	Double, sep. 1.2 EW; components <0.3, 2.1	4	1.195	1.050
1354+01	0.3 EW	4	1.000	1.000
1425-01	<0.25 EW	4	1.000	1.000
1434+03	<1'(NS) x <0.25	4,8	1.000	1.000
1446+00	<0.25 EW	4	1.000	1.000
1509+01	<0.25 EW	4	1.000	1.000
1514+00	Triple,total sep. 3.0 EW; components 0.7, 1.1, 0.7	4	1.225	1.058
1523+03	<0.25 EW	4	1.000	1.000
1559+02	Double, sep. 3.5 EW; components 1.2, 2.2	4	1.530	1.136
1602+01	Double, sep. 8"	1	1.000	1.000
1603+00	<0.25 EW	4	1.000	1.000
1701+024	1.8(NS) x <0.5 (5009 MHz)		1.102	1.027
1708+00	<0.5 EW	2	1.000	1.000
1712-03	<0.5 EW	2	1.000	1.000
1717-00	Double, sep. 2.5 EW; components 1.4	4,8	1.245	1.063
1722-02	1.7(NS) x <0.5		1.090	1.023
1741-03	<0.5 EW	2	1.000	1.000
1949+02	Double, sep. 1.3 EW; components 0.6 EN	4,8	1.089	1.023
1949-01	1.3(NS) x 3.2 (5009 MHz)		1.345	1.089
2044-02	<0.25 EW	4	1.000	1.000
2210+01	<0.25 EW	4	1.000	1.000
2221-02	Double, sep. 3.8 NS; components 0.7 EW. But see 5009 MHz contour map, Figure 4.3, which disagrees with interpretation of the interferometry. Size factors from map.	4,8	2.52	1.40
2313+03	Double, sep. 6" EW	1	1.000	1.000
2324-02	1.2(NS) x 1.2	2	1.085	1.022
2347-02	<0.4 EW	2	1.000	1.000

References for Table 4.3

(1) Bash, F.N. (1968) - Astrophys. J. Supp. 16, 373

(2) Cole, D.J., Milne, D.K., and Wall, J.V. - Unpublished data, Parkes Interferometer

(3) Collins, R.A., and Scott, P.F. (1969) - Mon. Not. R. astr. Soc. 142, 317

(4) Fomalont, E.B. (1968) - Astrophys. J. Supp. 15, 203

(5) Harris, Beverley J. - Unpublished data, Parkes Interferometer

(6) Hazard, C., Mackey, M.B., and Shimmins, A.J. (1963) - Nature 197, 1037

(7) Hazard, C., Mackey, M.B., and Nicholson, W. (1964) - Nature 202, 227

(8) Maltby, P., and Moffet, Alan T. (1962) - Astrophys. J. Supp. 7, 141

(9) Palmer, H.P., Rowson, B., Anderson, B., Donaldson, W., Miley, G.K., Gent, H., Adgie, R.L., Slee, O.B., and Crowther, J.H. (1967) - Nature 213, 789

(10) Taylor, J.H., Jr. (1966) - Astrophys. J. 146, 646

sources taken from the Parkes 408 MHz catalogue, 1.0 f.u. at 2700 MHz translates to approximately 0.6 f.u. at 5009 MHz. Furthermore, the present sample, selected from the 2700 MHz survey has an appreciably greater fraction of flat spectrum sources which in general will be of smaller angular size for a given flux density. It appears that the difficulty of detecting beam broadening for the weak sources will not lead to serious underestimation of their flux densities at 5009 MHz.

The sources PKS 0123-01 and 2221-02 were of sufficient angular extent to be mapped at 5009 MHz. The contour maps are shown in Figure 4.3; in each case size factors were determined from volume integration of these maps. The apparent structure of both sources is in disagreement with that deduced from interferometry by Maltby and Moffet (1962) and Fomalont (1967). In the case of 0123-01 the discrepancy cannot be explained by a change in angular structure with frequency.

The improved resolution at 5009 MHz was used to obtain accurate positions for the sources 0053-016 and 0053-015, both of which were subsequently identified as galaxies (Chapter 3). These two sources, separated by 8 arc minutes, were previously catalogued together as PKS 0053-01. The interpretation of interferometry by Fomalont (1967) is in reasonable agreement with the 5009 MHz observations.

For sources with size factors $\geq$1.030, the principal errors in the 5009 MHz flux densities lie in the corrections

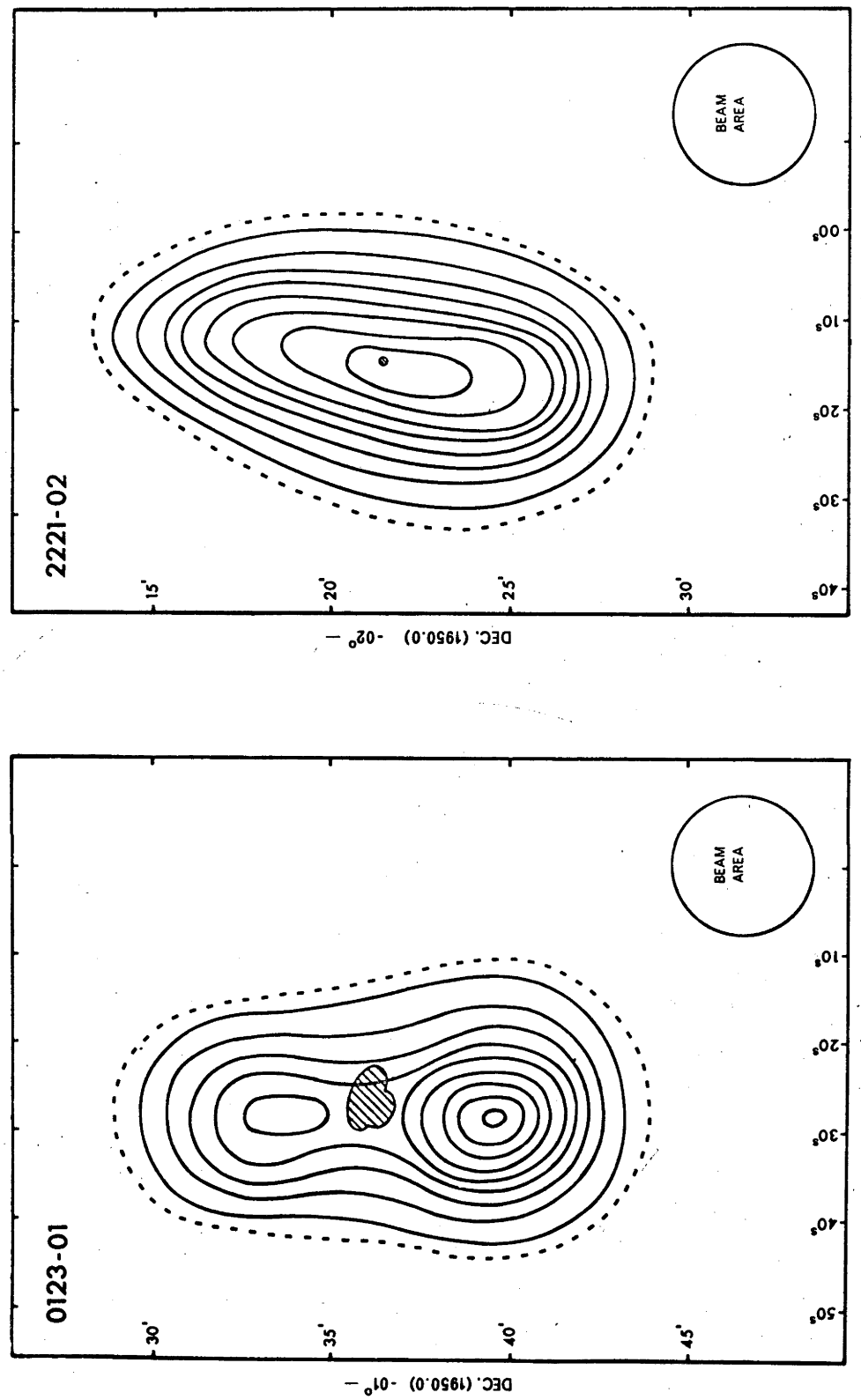

Figure 4.3. The structure of PKS 0123-01 and 2221-02 at 5009 MHz.

for partial resolution, and are difficult to estimate.

4.1 (iv) The 5009 MHz Flux Densities

The 5009 MHz flux densities obtained are presented in Table AIV.1, column 8. Sources known or suspected to be variable at this frequency have the flux density in round brackets. Flux densities corrected for partial resolution are in square brackets, and the size factors are in Table 4.3. Quoted errors are the standard errors in peak flux density only.

4.2 Flux Densities at 2700 MHz (λ = 11.1 cm.)

The observations and error analysis for the 2700 MHz flux densities have been described in Chapter 2. If multiple observations of a source at this frequency do not indicate time variation, the flux density listed in column 7 of Table AIV.1 is the weighted mean of the entries in the catalogue (Table AII.1 or AII.2). The entries are in round brackets if the source is known or suspected to be variable, and such entries represent the best estimate of the 2700 MHz flux density at epoch 1968.5. This epoch has been chosen as it is close to that of the majority of the 5009 MHz observations. Square brackets again indicate partial resolution; size factors are listed in the catalogue (Tables AII.1 and AII.2), and in Table 4.3. Quoted errors are the errors in peak flux densities from the analysis of §2.8.

4.3 Flux Densities at 1403 MHz (λ = 21.4 cm.) and 468 MHz (λ = 64 cm.)

Flux densities of over 300 sources from the 2700 MHz catalogues have been measured at frequencies of 468 and 1403 MHz with the Parkes interferometer. The instrument comprises the 210-foot paraboloid and a moveable 60-foot paraboloid which operates on tracks extending 1400 feet both due north and due west of the main telescope (Ekers 1967, Cole 1967). Observations can be made simultaneously at both frequencies. For the present measurements a fixed north-south baseline of 460 feet was used, corresponding to 218λ and 654λ at 468 and 1403 MHz respectively.

4.3 (i) Observations, Calibration, Reduction

All observations were made in two observing sessions of three days each: January 10-12, 1968 (1968.03) and January 12-14, 1969 (1969.04).

The performance of the interferometer has been described by Ekers (1967). The characteristics of the instrument relevant to the present observations are summarized below:

Frequency (MHz)	Primary Beam (arc min.)	Element Spacing	Fringe Sep.* (arc min.)	Fluctuation in Correlated Output (f.u. peak-to-peak)†
468	54 x 54	218λ N-S	25	0.10
1403	18 x 18	654λ N-S	8	0.05

* Declination 0° at transit.

† Time constants 5 seconds (468 MHz) and 2 seconds (1403 MHz).

The observational procedure was simply to set the interferometer to the current position of each source, and to record several fringes on each frequency. The output time constants were generally 2 and 5 seconds at 1403 and 468 MHz respectively, and the lobe rotator was set to give corresponding fringe periods of about 30 seconds and 1.5 minutes. The fringes were recorded on chart running at 20 mm/minute; a sample record appears in Figure 4.1(c). In this fashion the flux densities at the two frequencies could be determined for about 7 sources per hour of observing time. Most sources were observed within 1½ hours either side of transit.

Calibration was carried out without recourse to a secondary noise standard. Several of the stronger small diameter sources in the $\pm 4^{\circ}$ declination zone were used, together with a few others with well established flux

densities and structural information at the interferometer frequencies: PKS 0316+16 (CTA 21), 0624-05 (3C 161), 0915-11 (Hydra A), 1648+05 (Herc A), and 2230+11 (CTA 102). The flux densities of all these sources at the interferometer frequencies were kindly supplied before publication by Miss Harris. They ensure that the present flux scales are the same as the self-consistent scales that she derived (Harris 1969). Calibration sources were observed about every 1½ hours.

Reduction of the records was carried out by a visual smoothing of the fringes followed by measurement of the amplitude of each fringe. The averaged fringe amplitudes were corrected for the effect of the output time constant, and finally converted to flux densities from the calibration curves. The calibration curves for each frequency were formed by plotting the flux densities of the calibrator sources against their averaged fringe amplitudes, measured and corrected as described above.

4.3 (ii) Errors in the Interferometer Flux Densities

The scatter in the individual points about the mean calibration curve was generally about 5%, reflecting good agreement with the flux densities of Miss Harris and satisfactory gain stabilities of the receivers. This scatter has been taken as the estimate of the standard error in calibration. On one night of the 1968 observations,

gain instabilities at 1403 MHz were evident in the calibration, and the error estimate for this night consequently has been increased to 12%.

At 468 MHz receiver noise is insignificant, and the dominant source of error is confusion due to the extent of the primary beam. Ekers (1967) calculated that the source density becomes about one per primary beam area at a level of S_{468} = 0.35 f.u., and found that observation of random points in the sky produced a distribution of fringe amplitudes with a standard deviation of 0.6 f.u. The standard confusion error in the present observations will be less than 0.6 f.u. because affected sources can be recognized from the proximity of other sources listed in 4C or PKS 2700 MHz catalogues. A standard error due to confusion of 0.4 f.u. has accordingly been adopted. Measured 468 MHz flux densities of about 30 sources were rejected because of the presence of other catalogued sources within the primary beam. Errors greater than 0.4 f.u. have been assigned to the flux densities of a few sources possibly affected by the proximity of other sources.

At 1403 MHz, receiver noise is the dominant source of error. An estimate from the scatter among the amplitudes of fringes for a large sample of sources indicated a standard error of about 0.09 f.u. due to receiver fluctuation. Assuming an error of 0.04 f.u. for confusion, the

resultant standard error due to noise and confusion is 0.10 f.u.

The 1403 MHz flux densities of sources of angular extent 0.5 arc minutes in declination will be underestimated by $\sim$ 5% because of resolution. The 468 MHz flux densities will be similarly affected if this dimension exceeds 1.5 arc minutes. The angular size data of Table 4.3, available for most of the sources likely to be resolved, have been used to decide whether the flux densities have been so affected. Such flux densities have been omitted from Table AIV.1; however in these cases, 1410 MHz pencil beam observations by Miss Harris were generally available, and were kindly communicated before publication. For weaker sources the arguments of §4.1(iii) indicate that resolution is unlikely, and no error has been assigned for such effects.

The linearity of the receivers has been shown to be excellent (Ekers 1967). Errors due to telescope setting, and to measurement of flux densities in one linear polarization are negligible compared to those of calibration, receiver fluctuation, and confusion. The zenith angle dependent effects of atmospheric attenuation and aperture efficiency are negligible at frequencies below 2000 MHz.

4.3 (iii) The 468 and 1403 MHz Densities

The results of the interferometer observations are listed in columns 4 and 6 of Table AIV.1. The errors are

the square roots of the sums of the squares of the independent errors discussed above. The 468 MHz flux densities obtained by Miss Harris have generally been entered in preference to those obtained here because of a more accurate calibration.

From the collected data of Table AIV.1 and the spectral plots of Figure 4.4, the 468 MHz flux density is anomalously high in the following sources: 0320+015, 0358+031, 0454+039, 0808+019, 0912+029, 1351+021, 1351-018, 1402-012, 2047+039, 2215-027. For several of these the result must be due to confusion, although care has been taken to reject the 468 MHz measurement in sources which might be so affected (see §4.3(ii)).

4.4 Other Flux Densities between 1400 and 1425 MHz

For 34 of the strongest sources in the $\pm 4^{o}$ declination zone, Miss Harris has measured flux densities at 1410 MHz with the 210-foot telescope (Table 4.1). These pencil beam observations have been adopted in preference to the interferometer observations of the sources because of possible resolution (§4.3(ii)). Flux density scales are identical. The 1410 MHz flux densities are entered in column 6 of Table AIV.1.

The 1415 MHz flux densities obtained in the OSU survey (Fitch, Dixon, and Kraus 1969) have quoted errors larger than those of the 1403 MHz interferometer flux densities; the latter have hence been retained in preference.

However, 46 flux densities (Table 4.1) were taken from the OSU catalogue for weaker sources not observed with the interferometer, and are entered in column 6 of Table AIV.1. A comparison of flux densities of the strongest sources common to both catalogues indicated that the intensity scales agree to within 2%.

Flux densities at 1425 MHz for the two components of PKS 0053-01, considered to be two individual sources, (see §4.1(iii)) were taken from Fomalont (1967). A flux density at 1400 MHz for PKS 0723-008 (DW 0723-00) was taken from Davis (1967). These are also entered in column 6, Table AIV.1.

4.5 Flux Densities at 635 MHz (λ = 47 cm.)

To obtain flux densities at 635 MHz, the $\pm 4^{\circ}$ declination zone was surveyed with the 210-foot telescope and the 635 MHz parametric receiver. Regions of low galactic latitude, right ascensions 06^{h} to $07^{h}40^{m}$ and 18^{h} to $19^{h}40^{m}$, were omitted.

4.5 (i) Observations, Calibration, Reduction

The observations were carried out in three sessions: 6-8 May 1967, 21-25 October 1967, and 2-3 January 1969. The zone was surveyed with 2°/minute right ascension scans, each being one hour of right ascension in length. A receiver output time constant of 2 seconds was used, for which r.m.s. output fluctuations were about 0.05 f.u. The

half power beamwidth of the telescope is 30.5 arc minutes at this frequency; scans were spaced every 20 arc minutes from declinations $+04^{\circ}\ 20'$ to $-04^{\circ}\ 20'$. The deflection produced by a noise calibration signal of about 10°K. ($\sim$ 15 f.u.), injected at the receiver input, was recorded every three scans. The output was recorded on chart running at 40 mm/minute, and a sample record is shown in Figure 4.1(b).

The value of the calibration signal was established by comparing the calibration deflection to the amplitude of scans through the source PKS 2211-17 (3C 444) in each observing session. The adopted flux density was $S_{635} \equiv 20.0$ f.u., as obtained by Miss Harris (1969).

About 500 flux densities, or upper limits to flux densities, were obtained from the survey by measuring deflections at the catalogued source positions from baselines hand fitted to the scans. Many sources appeared on two or more adjacent scans, and all deflections produced by a source were used in deriving the corresponding source amplitudes. These amplitudes were converted into flux densities by relating them to adjacent deflections produced by the calibration signal.

4.5 (ii) Errors in the 635 MHz Flux Densities

Because of (1) the great variation in background structure at this frequency, and (2) some variation in receiver performance, errors due to confusion and noise

were estimated individually from the records for each source. Most estimates of the combined standard error due to noise and confusion were about 0.4 f.u. Miss Harris measured flux densities at 635 MHz for 39 of the strong sources (Table 4.1) in the $\pm 4^{\circ}$ zone by scans through the source positions with careful calibration. The flux densities obtained from the survey were compared with these results; the expected agreement in scales was found, together with an r.m.s. error of 8% for the individual flux densities. This 8% is believed to be the inherent inaccuracy in the estimation of the flux densities from the survey records, since confusion, noise, and calibration errors were all much smaller for the sources in the comparison sample. Accordingly, standard errors in the 635 MHz flux densities were obtained from $\sqrt{\sigma_{cn}^2 + (.08S_{635})^2}$ f.u. where σ_{cn} is the estimated error due to confusion and noise.

4.5 (iii) The 635 MHz Flux Densities

The results appear in column 5 of Table AIV.1, together with standard errors as described above. The 39 flux densities obtained at this frequency by Miss Harris and kindly communicated to me have been used in preference to the survey estimates.

4.6 Flux Densities at 408 MHz

The flux densities of about 40 sources in the $\pm 4^{\circ}$

declination zone have been measured at 408 MHz with the east - west arm of the Molonglo Cross of the University of Sydney (Murdoch and Large 1968; Wyllie 1969). These flux densities have been scaled by factors (Table 4.1) suggested by Miss Harris (1969), and are entered in Table AIV.1. The standard errors are those published by the authors.

4.7 Flux Densities at 178 MHz

For 375 of the sources catalogued at 2700 MHz, estimates of the flux densities at 178 MHz are available from observations at Cambridge (Table 4.1). Preference has been given to synthesized pencil beam and to fan beam measurements in an attempt to avoid the effects of resolution. About 75 of the entries in column 2 of Table AIV.1 are due to examination of the 4C maps at the positions of sources in the 2700 MHz catalogues by Dr. Derek Wills. He has generously communicated these results to me.

The 178 MHz flux densities entered in column 2 of Table AIV.1 have been scaled by factors (Table 4.1) suggested by Miss Harris (1969). The standard errors are those published by the authors.

4.8 The Spectra of Individual Sources in the 2700 MHz Catalogues

The data of Table AIV.1 indicate that the spectra of many of the sources do not obey single power laws with

indices between 0.4 and 1.5 over the frequency range 178 to 5009 MHz. In Figure 4.4,* the data have been plotted for sources whose spectra show any of the following characteristics: (1) $\alpha \leq .3$ (where $S = K\nu^{-\alpha}$),† (2) the possible existence of multiple components, and (3) the possible existence of self-absorption. The spectra are for epoch 1968.5. In Figure 4.5, the recent 2700 MHz data have been plotted for sources indicating possible variation at this frequency. Brief comments on some of the sources follow.

0013-00: Two observations at 2700 MHz (1967.63 and 1968.92) are in agreement, and consequently provide no evidence for variability at this frequency.

0019-00: Low frequency spectrum somewhat dependent on identification with 4C+00.2, suggested by Wills (private communication). Two observations at 2700 MHz (1967.88 and 1968.92) are in agreement.

0038-020: Identified as a QSO. Low frequency observations confused by 0038-019.

0056-00: A QSO, z = .717. Not plotted in Figure 4.4 because the spectrum obeys a power law, $\alpha = 0.45$. Nevertheless there is evidence of variability at 2700 MHz (Figure 4.5).

0106+01: A well known case of a QSO showing high frequency enhancement and variability (Kellermann and Pauliny-Toth 1968a). Analysed by Miss Harris (1969) who finds that the time of origin of the expanding component was 1963.1 ± .5, and that the assumption of magnetic fields of 10^{-4} and 1 gauss lead respectively to expansion velocities of 0.52c

* Figures 4.4 and 4.5 have been placed at the end of the chapter because of their length.

† This definition of spectral index is used hereinafter.

and .85c, and to dimensions of 0.52 and 5.2 pc assuming the redshift of 2.107 to be cosmological. The 1968.5 spectrum is shown in Figure 4.4; other illustrations of the spectrum are in Harris (1969) and Kellermann and Pauliny-Toth (1969). Recent observations at 2700 MHz appear in Figure 4.5, and suggest that the source may now be optically thin at this frequency.

0111+021: A flat low frequency spectrum with enhancement at the high frequencies. The source has been identified with an E galaxy ($m_{pg} = 16^{m}.3$); such spectra are exceedingly rare for radio galaxies (§5.3). An observation at 1969.60, kindly obtained by Miss Harris, is in agreement with the catalogue observation of 1968.92. The radio spectrum is very similar to that of the bright galaxy NGC1052 (Heeschen 1968) but the luminosity at 2700 MHz is at least two orders of magnitude greater, and appears to be typical for a radio galaxy.

0122-00: A QSO, z = 1.070. The source does not appear in the 4C catalogue but the 178 MHz data must be confused by the proximity of 0122-005 (4C-00.10?) The apparent low frequency cut-off is thus probably not real. Two observations at 2700 MHz (1968.28 and 1968.92) are in agreement.

0217+01: An E galaxy showing low frequency self-absorption. Two observations at 2700 MHz (1967.67 and 1968.92) are in agreement.

0237-027: Identified as a QSO. Three observations at 2700 MHz (1967.88, 1968.28, 1968.92) are in agreement.

0310+013: A peculiar spectrum which possibly is due to low and high frequency components both showing self-absorption.

0336-01: CTA 26, a QSO with z = 0.852. A well known variable in both radio (Kellermann and Pauliny-Toth 1968a) and optical spectral regions. The epoch 1968.5 spectrum is shown in Figure 4.4; illustrations of the spectrum at other epochs are shown in Harris (1969). The analysis of Miss Harris has indicated the presence of two expanding components, originating at 1944 and 1964.5. Her assumptions of magnetic fields of 10^{-4} gauss and 1 gauss led to expansion velocities of .29c and .95c, and to dimensions of 1.2 and 12 pc respectively for the recent component.

0358+031: Definite variation at 2700 MHz (see Figure 4.5). Due to confusion the low frequency observations are not reliable. Some optical obscuration is present in this region.

0420-01: A QSO, z = .915. A known variable at frequencies above 1400 MHz (Kellermann, Pauliny-Toth, and Tyler 1968). The spectrum is difficult to interpret in terms of components; further monitoring at several frequencies is required. The recent 2700 MHz observations are shown in Figure 4.5.

0421+019: A QSO, z = .689. Two measurements at 2700 MHz (1967.88 and 1969.43) are in agreement.

0422+00: Possible variation at 2700 MHz; see Figure 4.5. The spectrum indicates synchrotron self-absorption for both low and high frequency components.

0432+03: The high frequency spectrum is extremely steep and further measurements are required at centimeter

wavelengths. The spectrum is so steep that a truncation of the high energy end of the electron distribution may be necessary to explain it. Note the change in ordinate scale, Figure 4.4.

0440-00: NRAO 190, a QSO and well known radio variable (Pauliny-Toth and Kellermann 1966). Harris (1969) discusses the observations at several frequencies and finds a time of origin for the expanding component of about 1949. The recent observations at 2700 MHz are shown in Figure 4.5, and the epoch 1968.5 spectrum in Figure 4.4. Other illustrations of the spectrum appear in Kellermann and Pauliny-Toth 1966, ibid 1969, and Harris 1969.

0457+024: The source, identified as a QSO?, has a low frequency cut-off which appears to be at least as sharp as 1934-63 (Bolton, Gardner, and Mackey 1963, Kellermann 1966). Three observations at 2700 MHz (1967.88, 1968.92, 1969.43) are in agreement.

0458-02: Tentative identification as an N galaxy; the BSO on position does not have UV excess. Definite evidence for variation in the 2700 MHz flux density (Figure 4.5). The components forming the spectrum cannot be separated on the basis of present observations.

0500+019: Two observations at 2700 MHz (1968.04 and 1969.43) are in agreement.

0550+032: Definite variability in the 2700 MHz flux density (Figure 4.5).

0736+01: A QSO, z = 0.191, and a well studied radio variable (Kellermann, Pauliny-Toth, and Tyler 1968; Harris

1969, Locke, Andrew and Medd 1969). The latter consider that the source has undergone three recent outbursts; at the maxima of the first two (1968.6 and 1969.2), flux densities at 6.5 and 10.7 GHz reached peaks at the same time, in clear violation of the uniformly expanding cloud theory. They point out that such rapid variables might be expected to violate the theory as the injection of particles must take a finite amount of time. The recent 2700 MHz observations appear in Figure 4.5, together with the observations of Locke et al. Although the time lag is not apparent between the higher frequencies, the 2700 MHz maxima are indeed displaced. The 1968.5 spectrum appears in Figure 4.4.

0743-006: Identified as a QSO? Three observations at 2700 MHz (1968.24, 1968.92, 1969.43) are in agreement.

0808+019: Figure 4.5 shows evidence for variability at 2700 MHz. If the 2700 MHz flux density is due solely to an optically thick expanding component, then a time of origin (t_o, observer's rest frame) of 1947±5 is derived for the event from the simple estimate $(1/S)(dS/dt) = 3/(t - t_o)$ (see e.g. van der Laan 1966).

0823+033: Figure 4.5 indicates evidence for variability at 2700 MHz. More spectral information is necessary before the components of the source can be delineated.

0906+01: Identified as a QSO. Three observations at 2700 MHz (1967.88, 1968.92, 1969.43) show little evidence of variability.

0922+005: Identified as a QSO, z = 1.72. Marginal evidence for variability at 2700 MHz from observations at 1967.88 and 1969.43.

1004-018: Identified as a QSO. Two observations at 2700 MHz (1967.88 and 1969.43) are in reasonable agreement.

1055+01: A QSO, and well known radio variable (Kellermann, Pauliny-Toth, and Tyler 1968; Harris 1969). Miss Harris has distinguished three expanding components, and states that they must all be of similar intensity and expansion velocity. The 1968.5 spectrum appears in Figure 4.4, and the recent 2700 MHz observations in Figure 4.5.

1146-037: Identified as a QSO?. The source evidently has a high frequency component (Figure 4.4) which does not appear to vary at 2700 MHz (observations at 1968.28 and 1968.92). The 5009 MHz observations indicate some beam broadening, and investigation by a higher resolution instrument is clearly desirable.

1148-00: A QSO, z = 1.982. Kellermann and Pauliny-Toth (1968a) suggest the source to be variable at 1400 MHz. The collected data of Miss Harris, and the present observations, indicate no significant variation at 2700 MHz over the last five years.

1217+02: A QSO, z = .240. Three observations at 2700 MHz (1967.88, 1968.92, 1969.43) are in agreement.

1222+037: Identified as a QSO?. Two observations at 2700 MHz (1967.88, 1969.43) are in agreement.

1226+02: 3C 273, a QSO, z = .158. The first extragalactic source discovered to be variable (Dent 1965). Observations and analysis by many authors (e.g. Pauliny-Toth and Kellermann 1966; Dent 1968;

Schorn et al. 1968; Harris 1969). The 1968.5 spectrum appears in Figure 4.4.

1229-02: A QSO, z = .388. Three observations at 2700 MHz (1967.88, 1968.92, 1969.43) are in agreement.

1317+019: Two observations at 2700 MHz (1967.88, 1969.43) are in agreement.

1337-033: Two observations at 2700 MHz (1967.48 and 1967.63) are in agreement.

1349+027: An apparent case of self-absorption, which is incompatible with the source being resolved in 4C (Wills 1968). Possibly the source has a component which is of very steep spectrum. The flux density at 2700 MHz shows evidence of a slow decrease (Figure 4.5) and there may hence be a third component involved.

1351+021: Three observations at 2700 MHz (1967.63, 1968.28, 1969.43) are in agreement.

1351-018: Four observations at 2700 MHz (1967.63, 1968.28, 1968.92, 1969.43) are in agreement.

1352+00: Identified as a QSO?. Possible variation at 2700 MHz (Figure 4.5).

1502+036: Identified as a QSO?. Two observations at 2700 MHz (1968.28, 1969.43) are in agreement.

1535+004: Two observations at 2700 MHz (1968.28, 1969.43) are in reasonable agreement.

1543+005: Identified as a QSO?. Two observations at 2700 MHz (1968.28, 1968.92) are in agreement.

1546+027: Identified as a QSO?. Definite decrease at 2700 MHz (Figure 4.5), but the 1968.5 spectrum indicates that the expanding component is probably

optically thick at this frequency, and the flux density, on the expanding cloud model, would be expected to be increasing.

1555+001: Very marginal evidence for variability from two observations at 2700 MHz (1968.28, 1968.92). Davis (1967) suggested variability for the source at 1400 MHz on the basis of observations of S_{1400} = 2.2 f.u. and 1.4 f.u. for 1966.2 and 1967.2 respectively. The 1968.5 flux density at 1403 MHz was measured as 1.46±.12 f.u. In a survey by Galt and Kennedy (1968), the flux density was measured as S_{1420} = 1.5 f.u. sometime between 1963 and 1967. The original estimate of Davis is hence suspect.

1602-00.2: Identified as a QSO?. Figure 4.5 indicates possible variation at 2700 MHz.

1705+018: Two observations at 2700 MHz (1968.28 and 1969.43) are in agreement.

1741-03: Spectacular high frequency enhancement, first noted in 2650 MHz transit measurements by Shimmins (1968). Variability at 2700 MHz shown in Figure 4.5.

2001-022: Two observations at 2700 MHz (1968.92, 1969.43) are in agreement.

2022+031: Two observations at 2700 MHz (1968.92, 1969.43) are in agreement.

2131-021: A QSO. Two observations at 2700 MHz (1967.88, 1969.43) are in reasonable agreement.

2134+004: PHL 61, a QSO, z = 1.94. Spectrum fully described by Shimmins et al. (1968). Two observations at 2700 MHz (1968.92, 1969.43) are in agreement with

all previous observations by Shimmins and indicate no variability at this frequency.

2203-18: A QSO; not included in the spectral observation programme. Three observations at 2700 MHz (1967.67, 1967.80, 1969.43) together with collected data of Miss Harris show no evidence for variability at this frequency over the past four years.

2210+01: Two observations at 2700 MHz (1968.24, 1968.92) are in agreement.

2216-03: A QSO, z = .901. Four observations at 2700 MHz (1968.24, 1968.28, 1968.92, 1969.43) are all in agreement. The collected data of Miss Harris shows no evidence for variability at this frequency over the past four years.

4.9 Strong Sources Not Catalogued in 4C

A histogram of effective spectral indices*, 178 to 2700 MHz, from the data of Kellermann, Pauliny-Toth, and Williams (1969) is shown in Figure 5.2(a). About 4% of the spectral indices are less than 0.4, and with this spectral index, the lower limit of the 4C catalogue translates to 0.74 f.u. at 2700 MHz. Accordingly, in Table 4.4, all sources in the $\pm 4^{o}$ zone with $S_{2700} \geq .74$ f.u. and which are not in 4C have been listed. Of the 30 sources, only 6 do not appear in the 4C catalogue because of the effects of confusion or resolution. One (2324-02) is in a region not covered by 4C. The remainder do not appear because of their spectral characteristics, and hence do not violate complete-

*indices defined by flux densities at two frequencies.

ness claims for the 4C catalogue. Of these, 14 are QSO's or QSO?'s and the remaining 9 are unidentified. The absence of any sources identified as galaxies is a clear indication of the spectral differences among the identification classes, as discussed in the following chapters.

TABLE 4.4

SOURCES NOT IN 4C FOR WHICH $S_{2700} \geq 0.73$

SOURCE	S_{2700} (f.u.)	$\sim S_{178}$ (f.u.)	IDENTIFICATION	REASON FOR 4C OMISSION
0112-017	1.38	1.2	QSO	Spectrum
0122-00	1.43	5	QSO	Confusion (0122-005)
0336-01	(2.23)	<2.2	QSO	Confusion (0336-017) and/or spectrum
0420-01	(1.92)	1.8	QSO	Spectrum
0421+019	.76	<.7	QSO	Spectrum
0422+00	(1.29)	~1.5	III	Spectrum
0440-00	(3.53)	<1	QSO	Spectrum
0457+024	1.63	<.4	QSO?	Spectrum
0500+019	2.47	<.7	III	Spectrum
0550+032	(.90)	<.7	III	Spectrum
0723-008	3.01	2.2	III	Not listed because of proximity to 3C 180
0736+01	(2.42)	1.1	QSO	Spectrum
0743-006	1.40	<1	QSO?	Spectrum
0808+019	(.71)	<.5	QSO	Spectrum
0823+033	(.87)	.8	III	Spectrum
0922+005	.74	<.5	QSO	Spectrum
1021-00	.95	<.8	QSO?	Spectrum
1349+027	(.76)	2.5	III	Resolved (Wills 1968)
1351-018	.98	<.6	III	Spectrum
1355+01	1.01	~4	III	Confused (4C+01.39) (4C+01.40)
1532+01	1.08	<.8	III	Spectrum
1535+004	1.01	<.5	III	Spectrum
1543+005	1.30	1.0	QSO?	Spectrum
1546+027	(1.27)	$\leq$.7	QSO?	Spectrum
1555+001	2.01	~.4	III	Spectrum

TABLE 4.4 Concluded

SOURCE	S_{2700} (f.u.)	$\sim S_{178}$ (f.u.)	IDENTIFICATION	REASON FOR 4C OMISSION
1615+029	.74	.8	QSO?	Spectrum
1716+006	1.30	~10	III	Confused (3C 353)
1741-03	(2.96)	0.9	III	Spectrum
2134+004	7.59	<1	QSO	Spectrum
2324-02	[1.56]	-	E gal	Omitted region (Cas A transit)

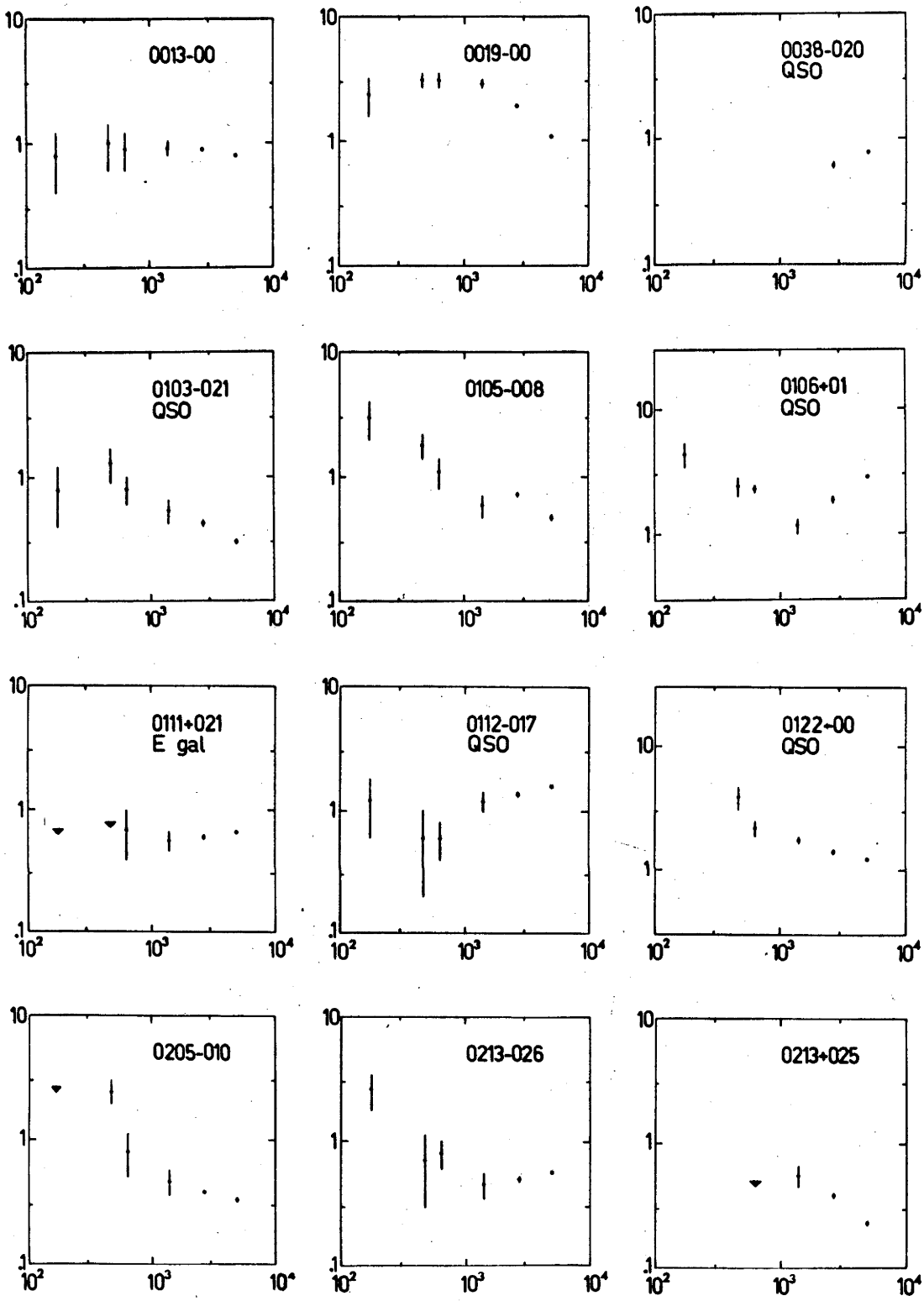

Figure 4.4. Spectra of sources in the ±4° declination zone of the 2700 MHz catalogue which do not obey power laws. Each graph is a logarithmic plot of intensity (f.u.) versus frequency (MHz).

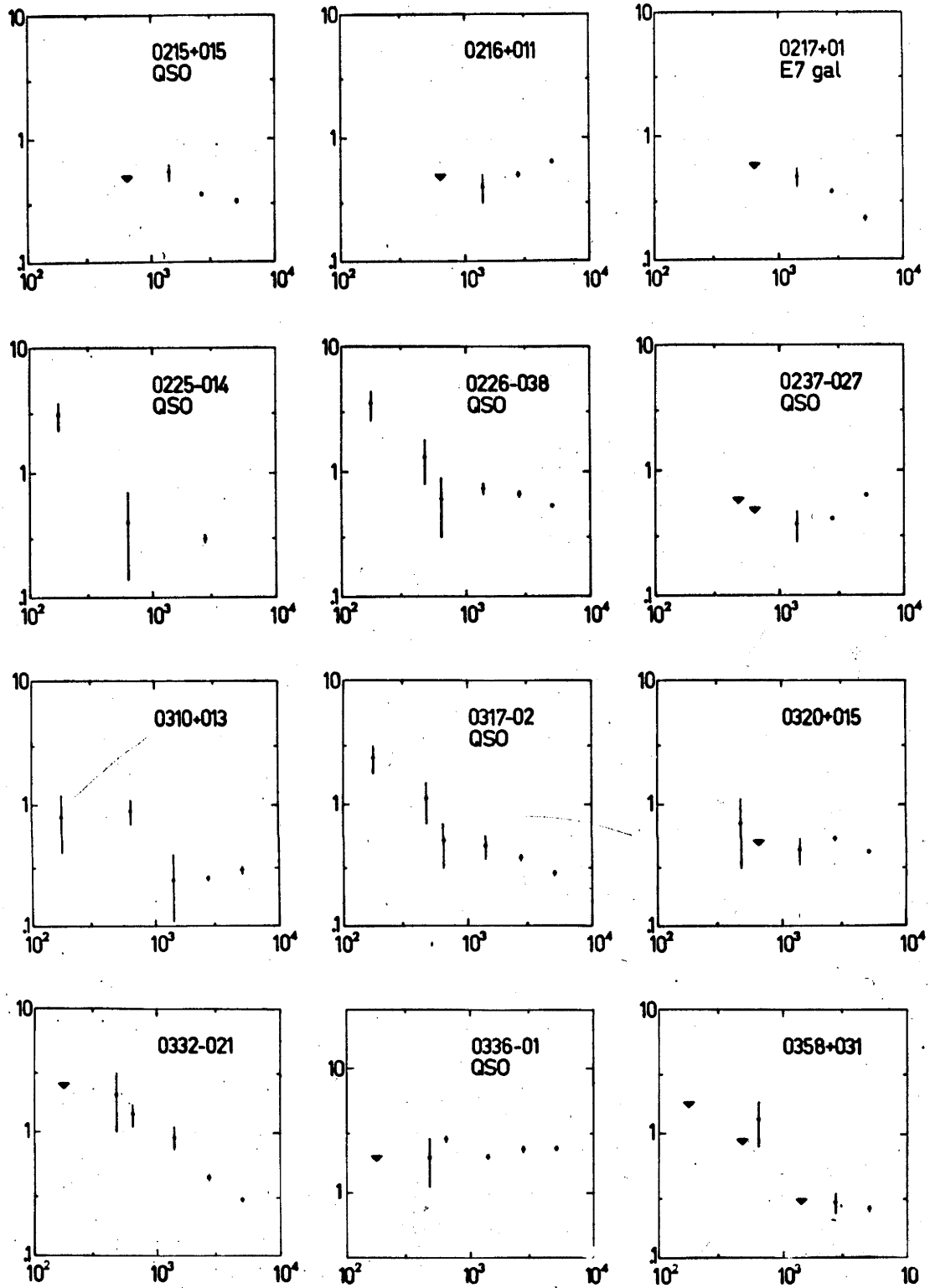

Figure 4.4 continued

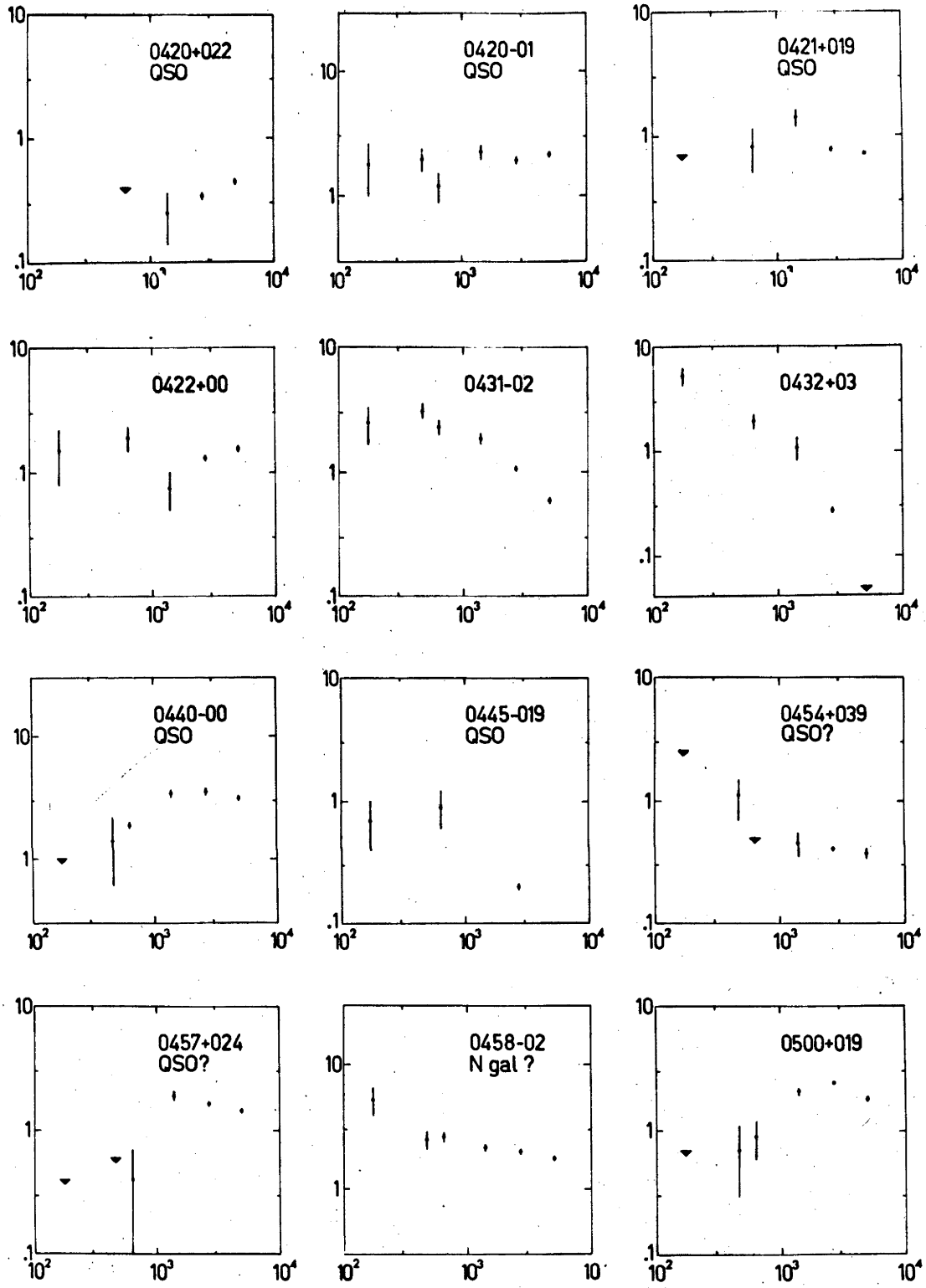

Figure 4.4 continued

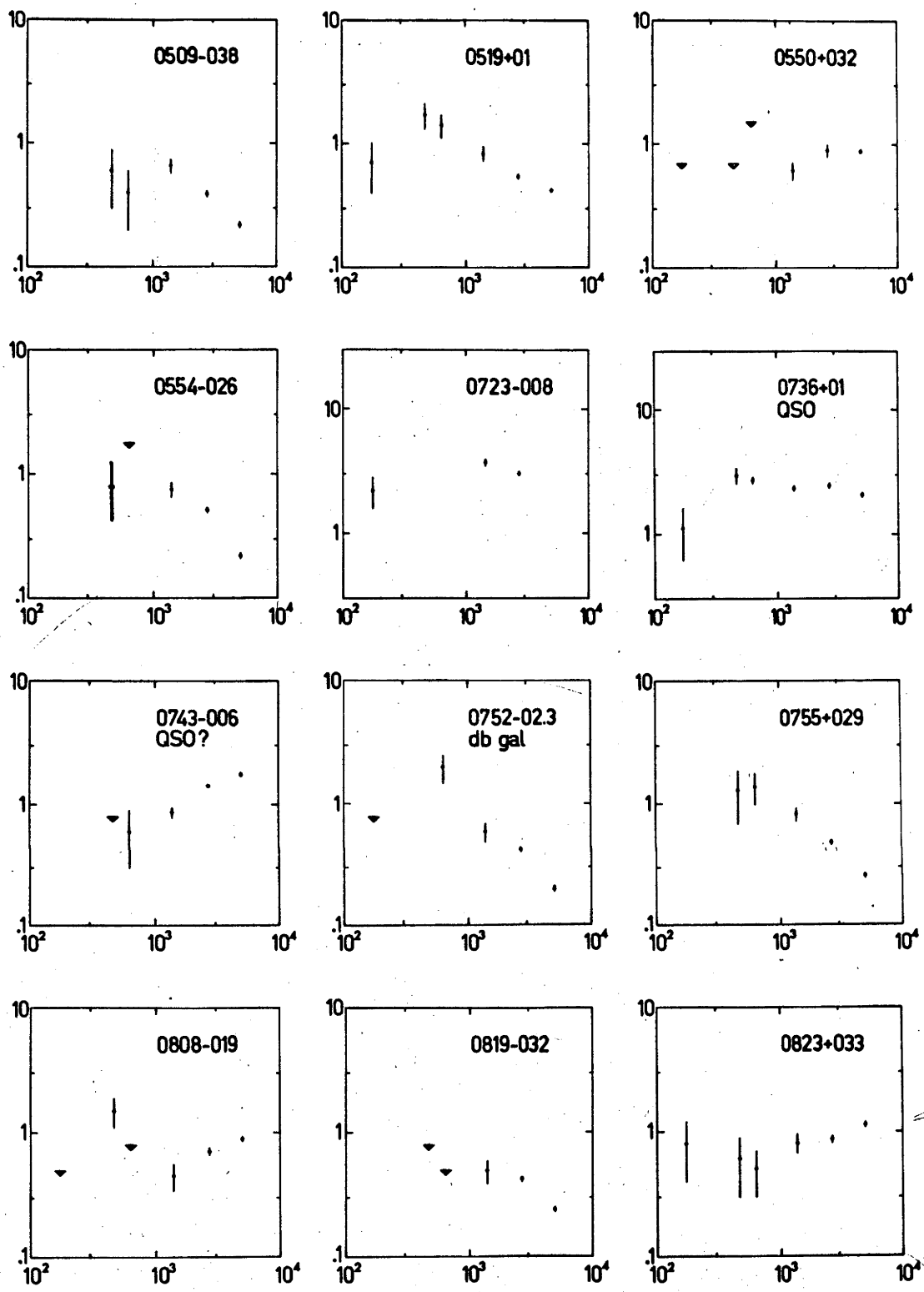

Figure 4.4 continued

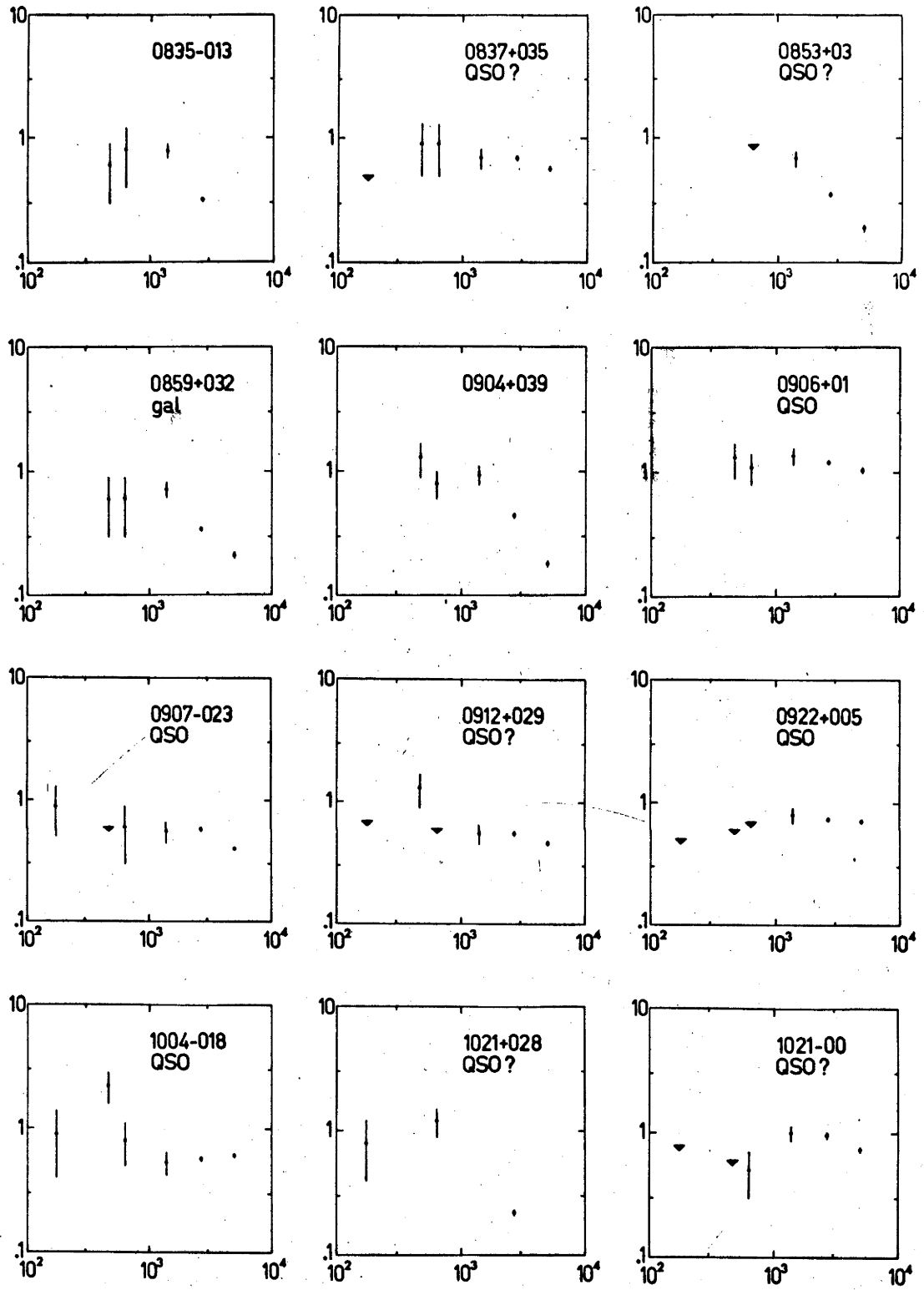

Figure 4.4 continued

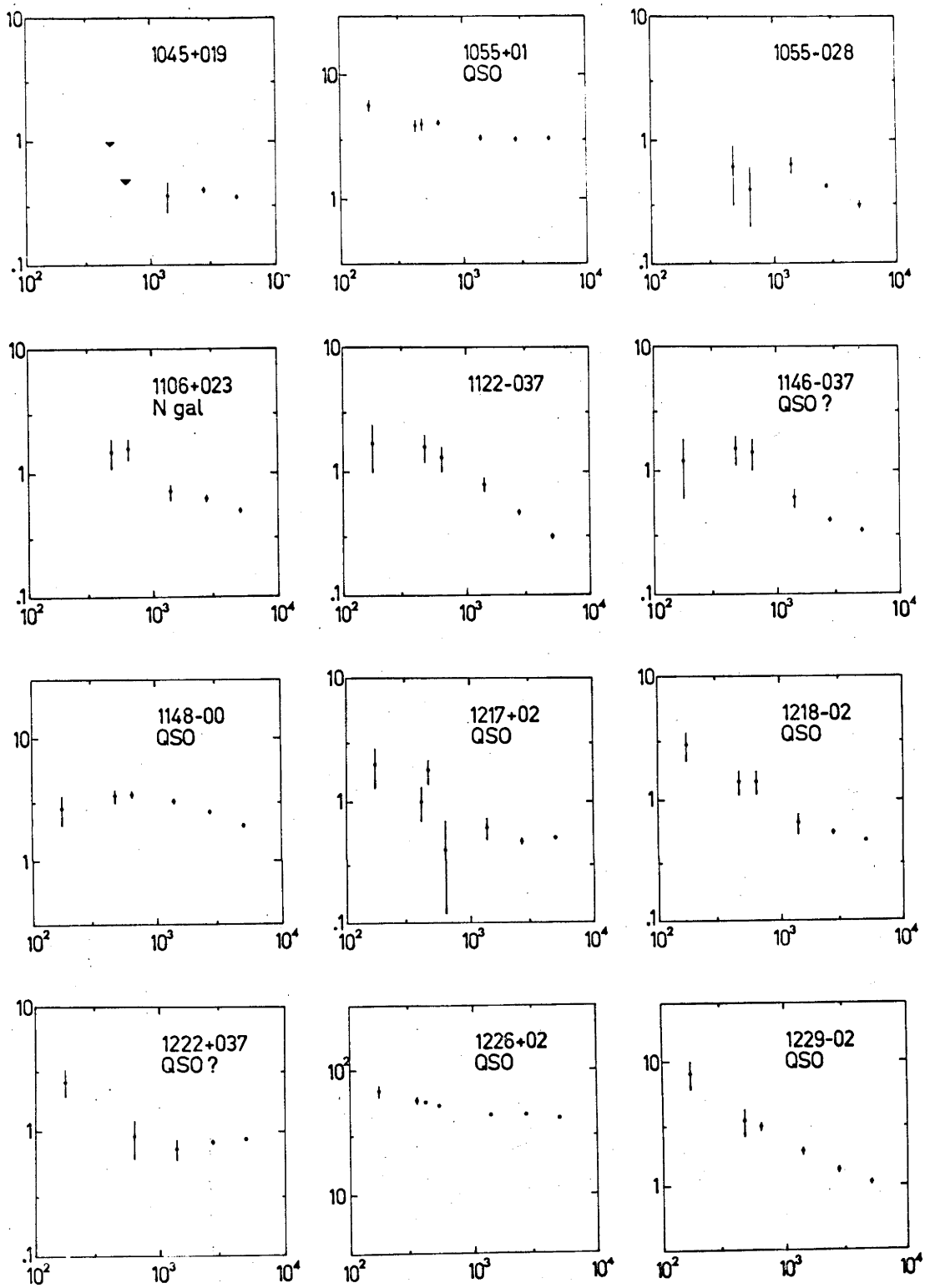

Figure 4.4 continued

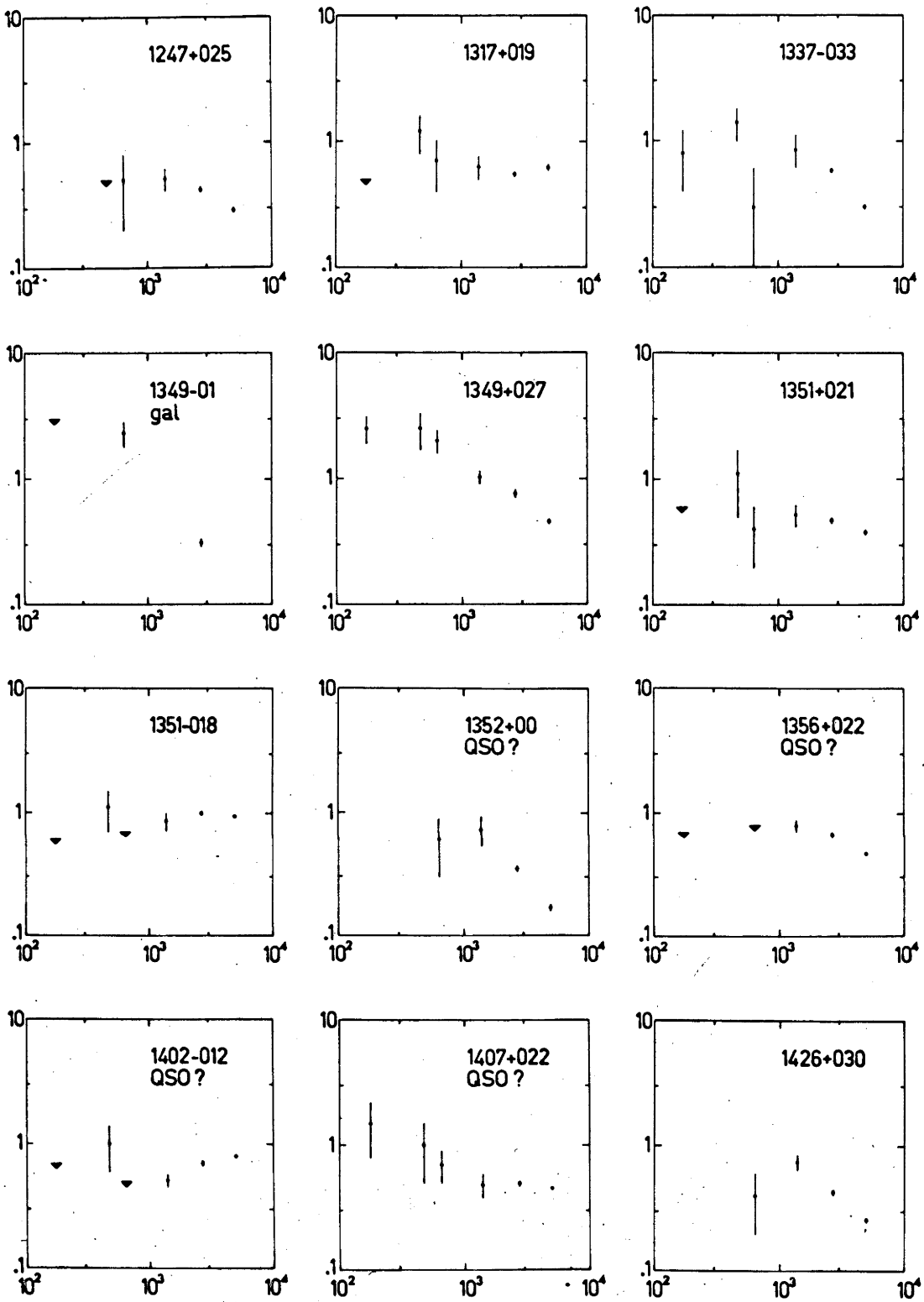

Figure 4.4 continued

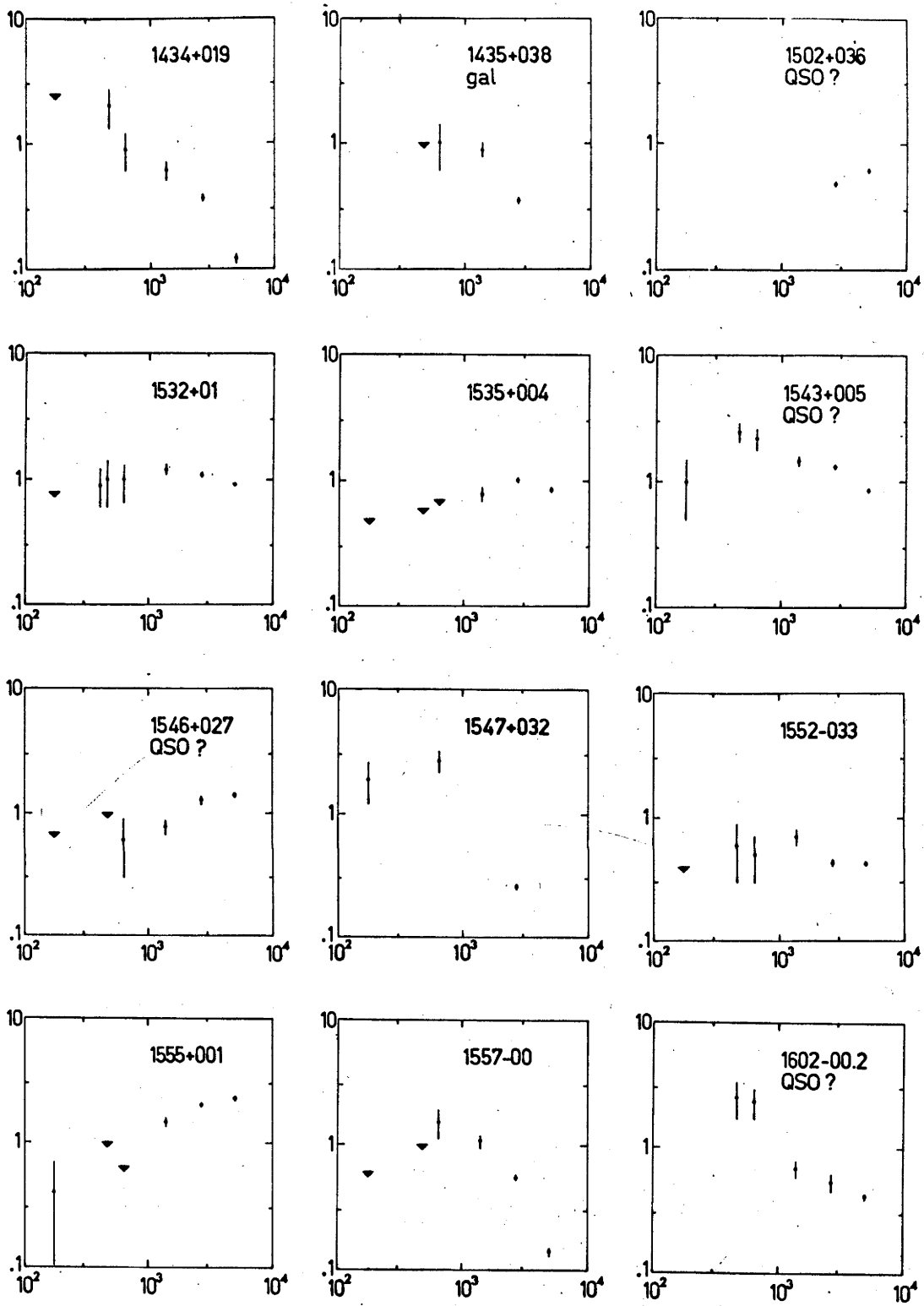

Figure 4.4 continued

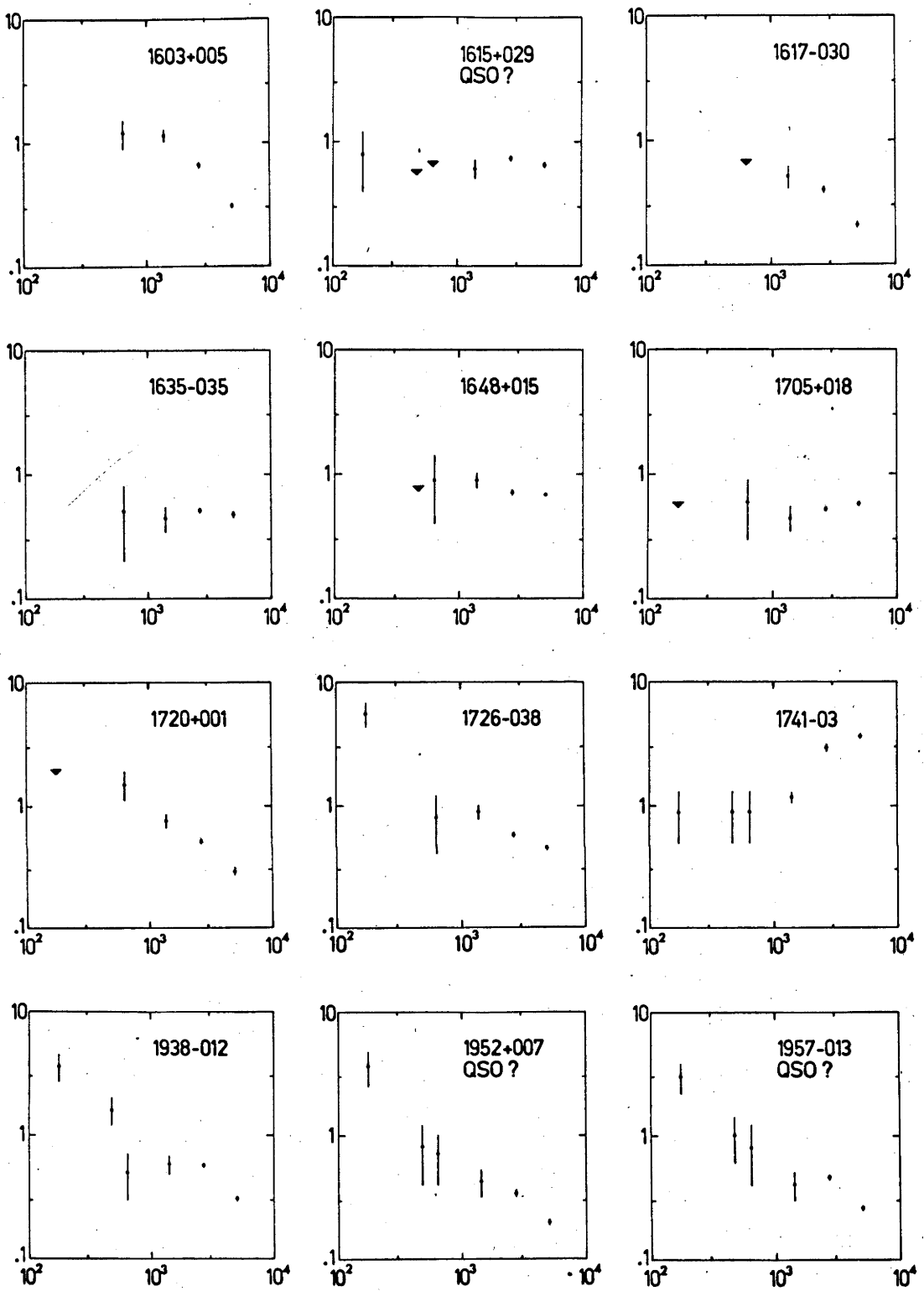

Figure 4.4 continued

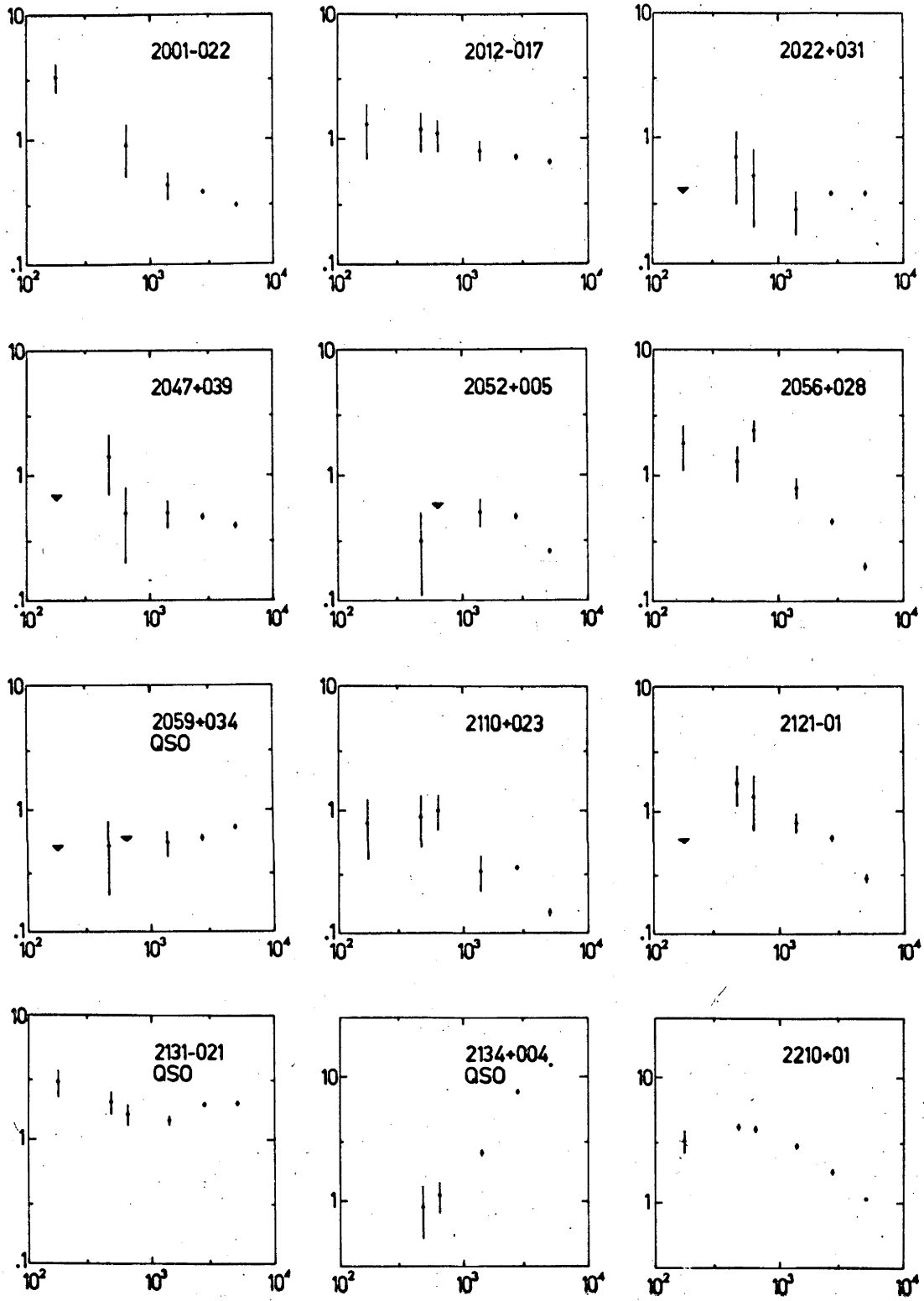

Figure 4.4 continued

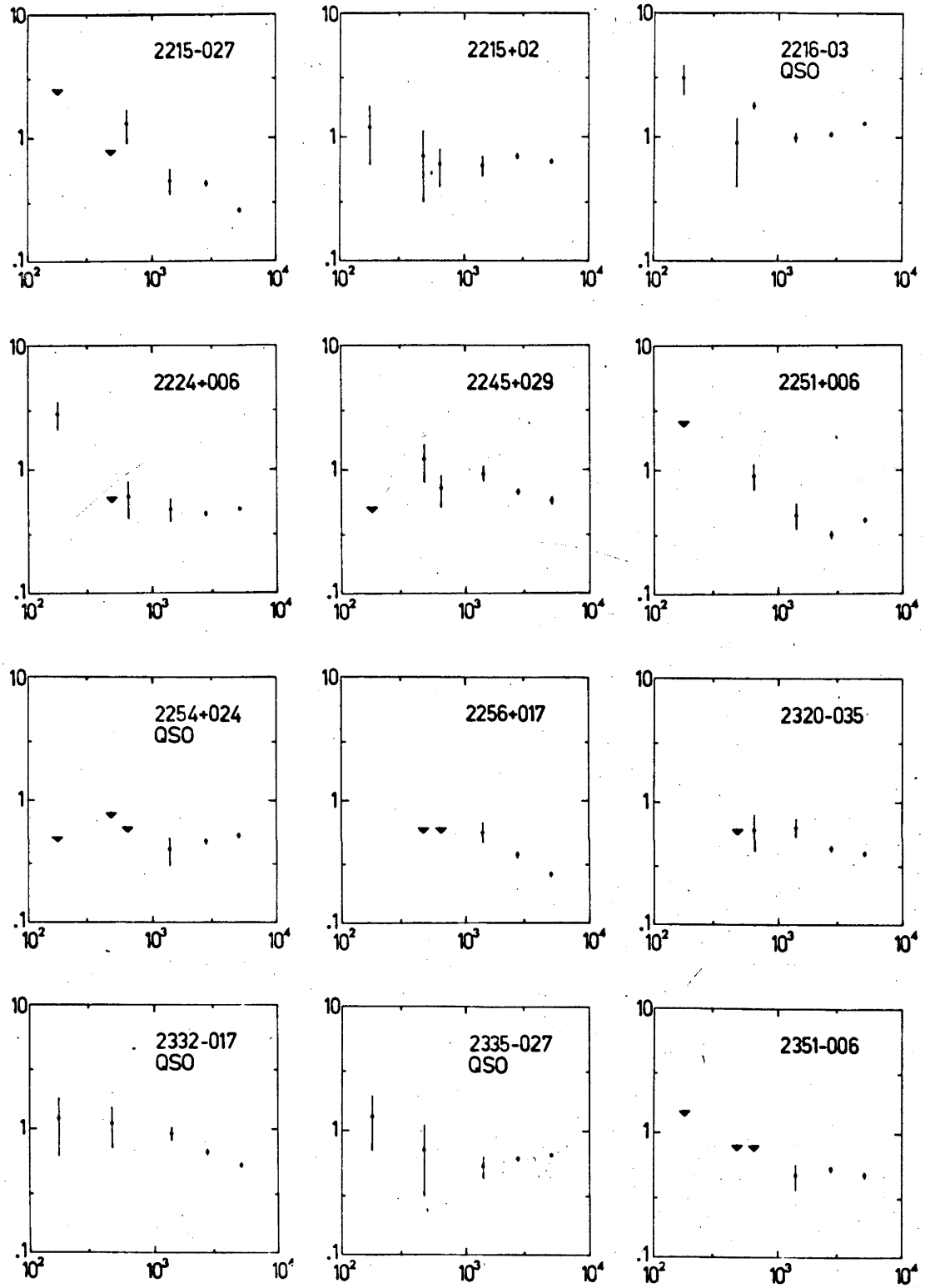

Figure 4.4 concluded

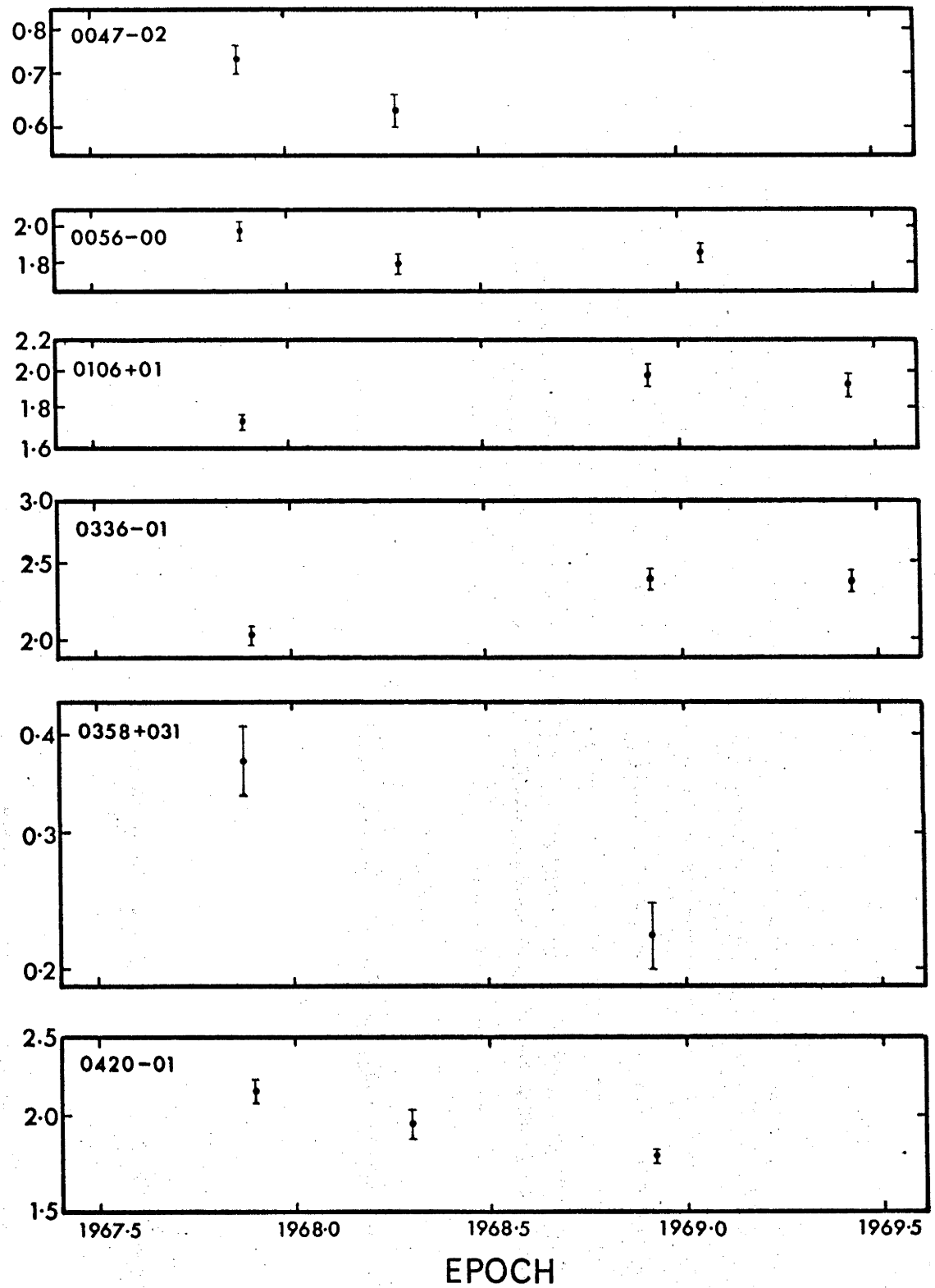

Figure 4.5. The present series of 2700 MHz flux densities (f.u.) versus epoch for sources known or suspected to be variable at this frequency.

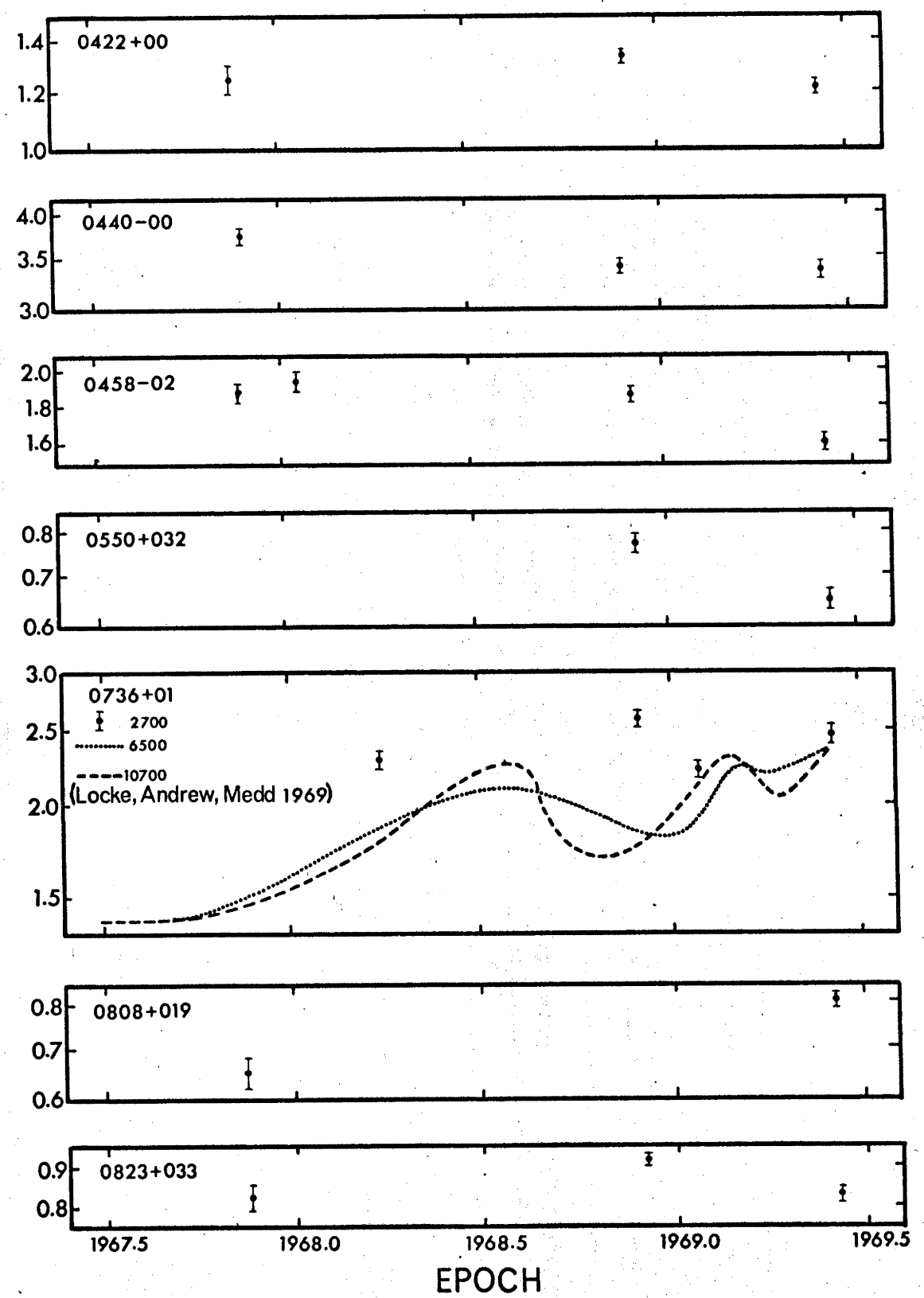

Figure 4.5 continued.

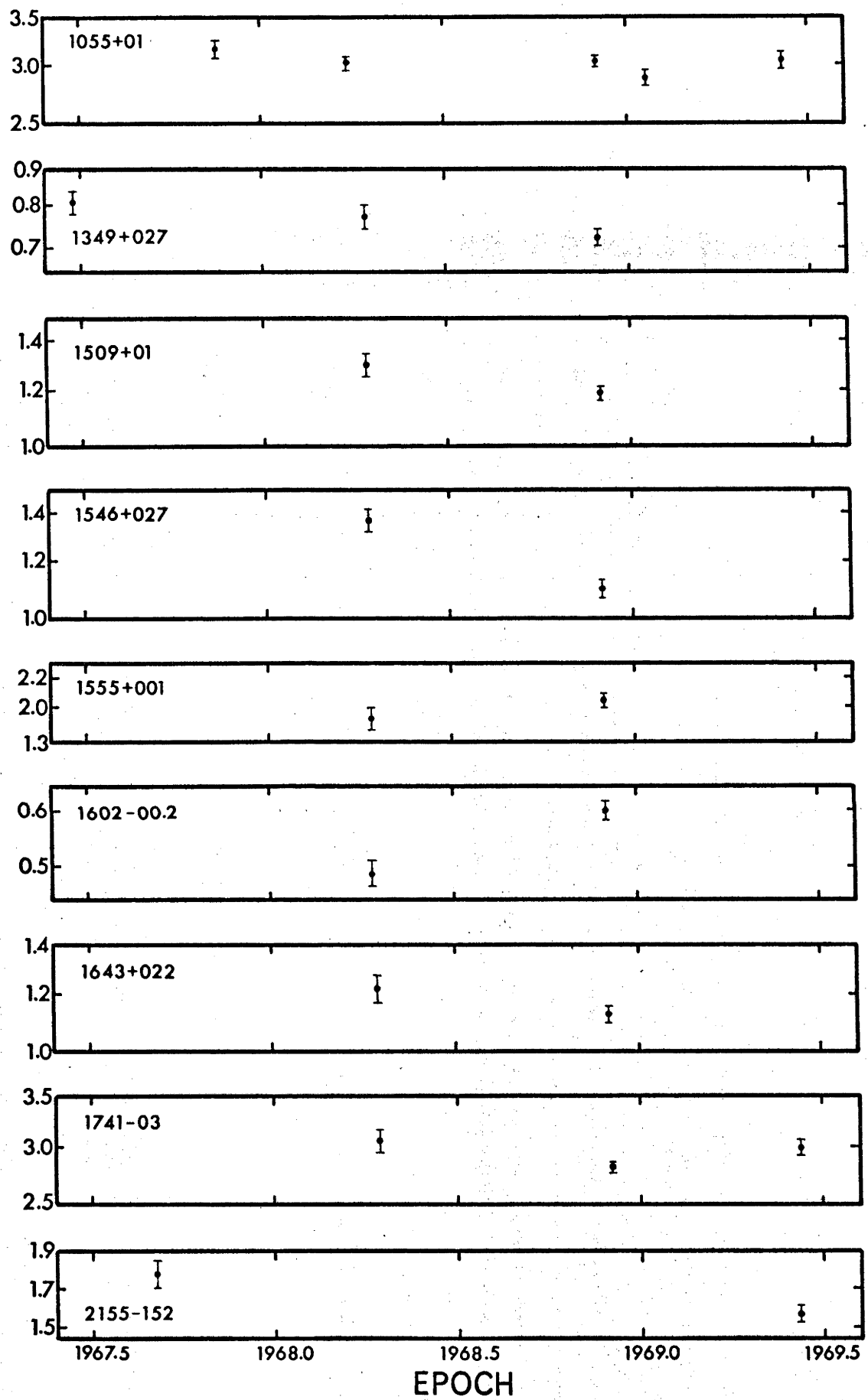

Figure 4.5 concluded.

CHAPTER 5

THE SPECTRA OF SOURCES IN THE PARKES 2700 MHZ SURVEYS
II. SPECTRAL STATISTICS

The statistics from the spectral observations just described are examined in this chapter.

5.1 The Forms of Radio Source Spectra

5.1 (i) Results of Previous Investigations

The spectra of radio sources detected in extragalactic source surveys have been measured at frequencies between 10 and 10^5 MHz. In this frequency range the following features have been observed:

(1) A power law spectrum, resulting in a straight line in the conventional log(flux density) versus log(frequency) diagram. The form of such a spectrum is described by the single parameter α, where α is the spectral index as defined previously. For sources with this type of spectrum the spectral index distribution has upper and lower limits of $\sim$1.4 and $\sim$0.3 respectively, and shows a strong concentration to a value of $\sim$0.8.

(2) A steepening of the spectrum with frequency, described in the literature as "convex curvature" or "negative curvature". The spectra of such sources may be frequently defined by two power laws meeting at a "break" frequency which is generally between 400 and 1400 MHz. In other sources the steepening takes place in a downward curvature over a large frequency

range.

(3) A steepening of the spectrum at the lowest frequencies (<200 MHz).

(4) A cut-off at the lower frequencies which may be gradual or dramatic in nature, and which results in a peak in the spectrum at some frequency above 100 MHz. At frequencies higher than that corresponding to maximum flux density, the spectrum is often power law in nature.

(5) An upward curvature of the spectrum to the high frequencies which has been described as "concave curvature", "positive curvature", or "high frequency enhancement". The spectra of such sources may show a peak at the highest frequencies within the range measured, and at frequencies above that at which the upward curvature becomes apparent the flux densities usually vary with time.

The physical conditions indicated by these features are generally believed to be these:

(1) The common power law spectrum of index α indicates the presence of relativistic electrons with energy distribution $N(E)dE = KE^{-(2\alpha+1)}$, radiating by the synchrotron mechanism in a uniform magnetic field.

(2) The steepening of the spectrum with increasing frequency shown by many sources is due to the lack of continuous replenishment of the higher energy electrons for which time scales of the operating loss processes (e.g. synchrotron radiation, inverse Compton effect) are shorter.

(3) The steepening of the spectrum at the lowest frequencies exhibited by a few sources is due to the superposition of the spectra of two components, one of which has a very steep spectrum and is relatively large in angular extent.

(4) The cut-off towards the lower frequencies observed for some sources is indicative of synchrotron self-absorption due to a very high surface brightness. For some sources it is difficult to decide whether the downward curvature of the spectrum to the higher frequencies is the result of self-absorption at lower frequencies or the simple steepening of 2 above.

(5) The spectrum showing "high frequency enhancement" is the result of a superposition of two spectra, one of which is due to a component with the relatively common power law form, and the other of which is that of a compact component showing self-absorption at a relatively high frequency. The variability at the frequencies where the spectrum of the compact component is dominant is believed to be the result of rapid expansion of this component. In some such sources, the spectrum of the "power law" component may be modified by self-absorption at the lower frequencies.

The observations and theoretical work which have led to this general picture have been reviewed by Scheuer and Williams (1968). They emphasize the paradox of being able to understand the deviations of spectra from power laws without being able to account for the apparently fundamental power law

itself.

The flux density measurements of Chapter 4 indicate that the spectral characteristics discussed above are adequate to describe all features of spectra found in the sample of sources catalogued at 2700 MHz. Of particular interest in the present context are those sources exhibiting features 4 and 5; Figure 4.4 illustrates that 2700 MHz surveys detect them in considerable numbers. The work of many authors has indicated that detailed studies of such sources can yield estimates of magnetic field strengths, linear dimensions, and brightness temperatures, and for those that show time variation, approximate time scales of the outbursts, and estimates of expansion velocities (see, e.g. Slish 1963, Williams 1963, Shklovsky 1965, van der Laan 1966, Pauliny-Toth and Kellermann 1966, Pauliny-Toth and Kellermann 1968, Kellermann and Pauliny-Toth 1969; also the reviews by Scheuer and Williams 1968, and Kellermann and Pauliny-Toth 1968b). The spectra of many of the sources illustrated in Figure 4.4 were briefly discussed in the preceding chapter with reference to these results. A primary object of the first parts of the 2700 MHz survey (and the subsequent flux density observations of Chapter 4) was to catalogue such objects for further studies. These studies, and the determination of the relative numbers of such sources appear essential in that they may lead to some understanding of the direction and manner in which the evolution of individual

sources proceeds.

5.1 (ii) Analysis of the Present Results

A statistical analysis of the spectra requires that they be described by the minimum number of parameters. The spectral index is just such a parameter for the sources whose spectra are power law in nature. For sources detected in surveys at or below 408 MHz, ∿80% of those having spectra which deviate from a power law in the frequency range 178 to 5000 MHz show a simple steepening of the spectrum with increasing frequency, described above as spectral feature 2 (Shimmins 1968, and personal communication; Harris 1969; Kellermann, Pauliny-Toth and Williams 1969, hereinafter referred to as KPW). Examination of the data of Chapter 4 for many of the sources catalogued at 2700 MHz indicated that the same is true of about half the sources in the present sample which have spectra deviating from single power laws over this frequency range. For such sources, with the choice of an appropriate "break" frequency, the high and low frequency portions of the spectrum may be described with reasonable accuracy by separate spectral indices. Accordingly for statistical analysis (and following KPW), the spectral data for each source in the present sample have been fitted by two power laws meeting at a "break" point near the (logarithmic) middle of the frequency range considered. For the ∿25% of sources in the present sample whose spectra indicate self-absorption to the

lower frequencies or the presence of compact components at the high frequencies (features 4 and 5 above), description of the spectrum by two power law sections is quite reasonable in many cases, and is generally of sufficient accuracy for statistical purposes.

The frequency of 1403 MHz was chosen as the "break" frequency on the basis of an approximately equal division of the data, and the flux densities obtained at this frequency were used in determining both the high and the low frequency spectral indices. KPW used 750 MHz as their "break" frequency, and Shimmins (1968b) found the steepening of the spectrum (if it occurs in a particular source) to take place between 400 and 1000 MHz. However, it is believed that the quantitative results have not been affected by the choice of a higher "break" frequency.

The power law fits were effected by a computer programme which used the method of least squares, weighting each observation according to the reciprocal of the square of the estimated error. The programme derived a spectral index α for the entire frequency range considered, 178 to 5009 MHz, as well as α_{LF} and α_{HF}, indices for the low frequency (178 - 1403 MHz) and high frequency (1403 - 5009 MHz) flux densities as mentioned above. In the derivation of α, the programme indicated that the spectrum could not be described by a single power law over the frequency range when any observation deviated by more than 2 standard errors from the best fit line.

For such sources, the computed value of α has not been retained, and the spectral data have been plotted to determine if the derived values of α_{LF} and α_{HF} provide reasonable descriptions of the spectrum over the low and the high frequency ranges. Where such is not the case, the values of α_{LF} and/or α_{HF} similarly have not been retained. With the exception of such cases, the values computed for α, α_{LF}, and α_{HF} have been entered in columns 9, 10, and 11 of Table AIV.1. The spectra of sources in the present sample which deviate from power laws in the range 178 to 5009 MHz have been shown in Figure 4.4 (with the exception of those for which the deviation is due to a simple steepening of the spectrum with increasing frequency).

The following section uses the results of this programme to describe the spectral content of the present surveys.

5.2 The Spectral Content

Table 5.1 is an attempt to describe the spectral content of the catalogue in broad terms. The results have been derived from the power law fitting programme, and from visual inspection of plots of more than half the spectra. Sources weaker than 0.40 f.u. at 2700 MHz have been discarded from this and further analyses of the chapter, the spectral observations being both incomplete and of diminishing accuracy. Prototypes of each spectral class have been included in the table. The fraction of the identification classes in each category is

TABLE 5.1

SPECTRAL CONTENT, ±4° DECLINATION ZONE OF THE 2700 MHZ CATALOGUE

Description of Spectrum	Percentage of Sample*		KPW Class	KPW (3CR)	Prototype	Identification Percentage QSO + QSO?	Gal.	III
Power law, $0.3 < \alpha < 1.5$, 178 - 5009 MHz	49±4		S	42	0003+00	22	40	62
Single component, self-absorption	17±4		C-		2134+004	34	2	19
178 MHz < f_{max} < 1403 MHz		9						
1403 MHz < f_{max} < 5009 MHz		5						
f_{max} > 5009 MHz		3						
		17		7				
Multiple components, one or more with high frequency self-absorption	11±2		C+, Cpx		2216+03	34	0	3
Steepening with increasing frequency	23±3		C-	51	0218-02	10	58	16
	100			100		100	100	100

* The errors represent the uncertainties in classifying the present sample; they are not indicative of the uncertainties in predicting the classification of all sources detected at 2700 MHz.

entered in the final columns and discussed in §5.5. The KPW spectral classification also has been entered, but note that it suffers from a serious defect when applied to the present sample; sources showing self-absorption (e.g. 2134+004) or a steepening of the high frequency spectrum (e.g. 0218-02) both belong to KPW class C-.

The data of KPW indicate that 93% of sources in the 3CR catalogue ($|b^{II}| > 20^{o}$) may be classified as spectral types S or C- (excluding self-absorption objects). In the present sample, for which the spectra have been examined over a somewhat smaller frequency range, 72% fall into these categories. Kellermann and Pauliny-Toth (1969) have stated "...contrary to some published statements (Shimmins et al. 1968; MacLeod and Andrew 1968), opaque radio sources with positive spectral indices* are not rare or unusual but comprise more than half of all sources observable at centimeter wavelengths (Kellermann, Pauliny-Toth, and Davis 1968)". The statement is evidently incorrect; only about 17% of all sources having $S_{2700} \geq .40$ f.u. can be so described. A further 11%, (KPW class Cpx) may show such spectral indices over limited regions of the spectrum.

A further result, apparent from Table 5.1 and Figure 4.4, is that the present sample contains no sources having power law spectra with indices <0.3. Such indices

---

* These indices are defined in the sense opposite to that of the present work.

correspond to electron energy distributions of power law form with an exponent of -1.6. Instances of source components with apparently flatter electron energy distributions are known (e.g. 3C 120, Pauliny-Toth and Kellermann 1968), but in all such cases, self-absorption is apparent. The result is consistent with the association of flat electron energy distributions with compact components of high surface brightness.

In Figure 5.1, histograms of α_{LF} and α_{HF} are plotted for the $\pm 4^{\circ}$ declination zone sources with $S_{2700} \geq .40$ f.u. A few sources for which these spectral indices have no significance (see §5.1(ii)) have been omitted from either histogram. The enormous dispersion and skewed nature of these histograms is in contrast to those obtained for sources in low frequency catalogues (see, e.g. KPW; Long et al. 1966). Two further points of interest are the relative displacement of the main peaks of the histograms, and the tail in the α_{HF} distribution at the steep spectrum end which has not been noted previously. In the following section it is shown that the skewed nature and increased dispersion are qualitatively predictable from the results of spectral observations on sources catalogued at the lower frequencies. In §5.5, the spectra of the various identification classes are discussed and the objects responsible for the main features of Figures 5.1(a) and (b) are delineated.

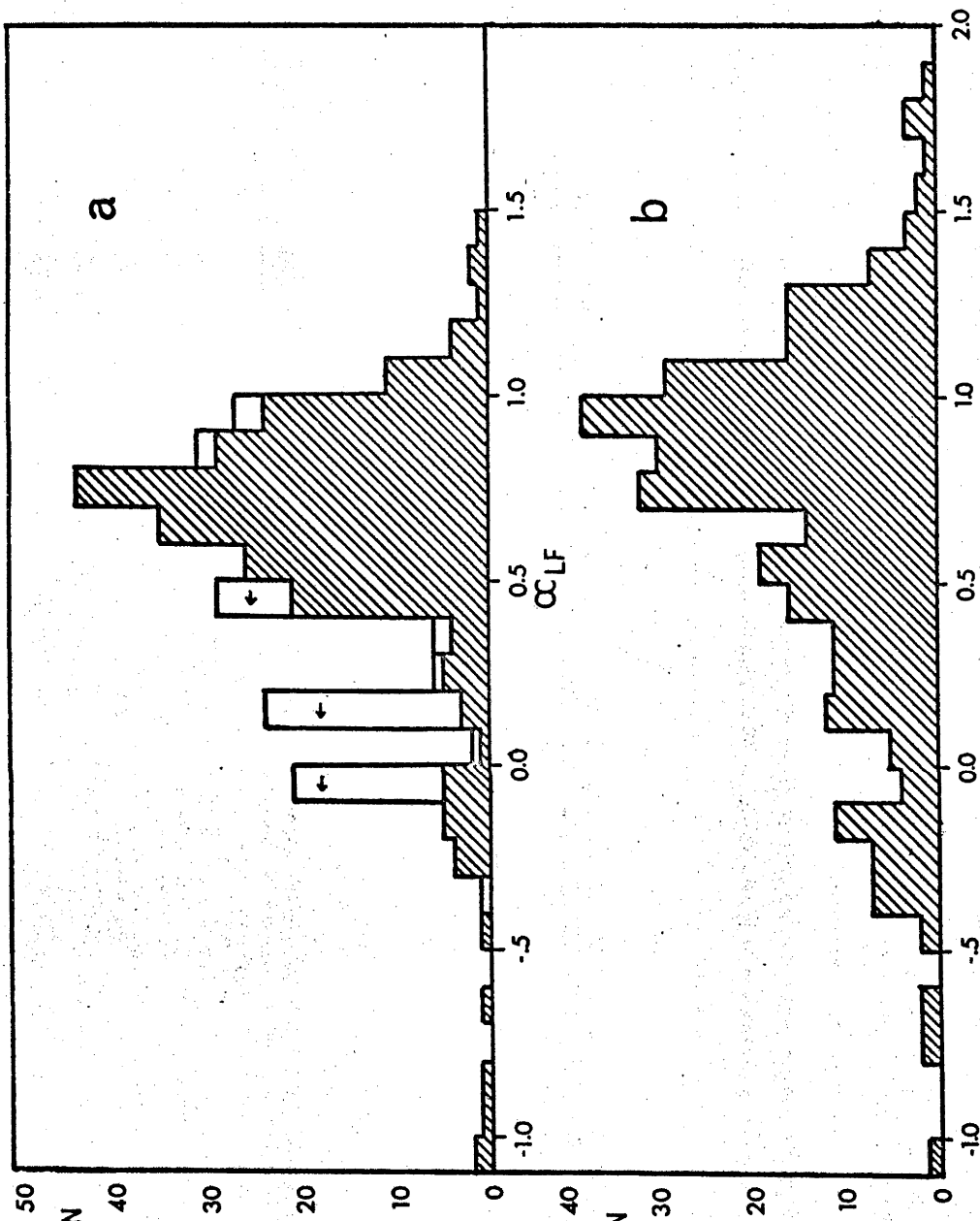

Figure 5.1. The distributions in low and high frequency spectral indices (as defined in §5.1(ii)) for sources catalogued at 2700 MHz with $S_{2700} \geq 0.40$ f.u. Unshaded areas represent upper limits to the spectral indices of those sources for which flux densities at low frequencies are not available.

5.3 Prediction of Spectral Content

Kellermann (1964) and Kellermann, Pauliny-Toth, and Davis (1968; hereinafter called KPD) indicate how for a survey at frequency ν_2, the distribution in effective spectral index $\alpha_{\nu_1-\nu_2}$ (as defined previously) may be predicted when flux densities at ν_1 and ν_2 are available for a large sample of sources catalogued in a survey at ν_1. In KPD the distribution in $\alpha_{\nu_1-\nu_2}$ has been computed for ν_2, where ν_1 and ν_2 are 178 and 5000 MHz respectively, and the flux densities at 178 and 5000 MHz have been taken from KPW. The computation has been made for purposes of comparison with the distribution of effective spectral indices found for a very limited sample of sources from a survey at 5000 MHz (see Table 1.1). In this section the calculation of KPD is repeated and is shown to result in a prediction of very limited significance. Bearing the limitations in mind, the calculation is then made for the frequency of 2700 MHz using the data of KPW for sources catalogued at 178 MHz, and compared with the observations.

From KPD,

$$Q(\alpha) = \frac{N[(\nu_2/\nu_1)^{+\alpha}S_2, \nu_1] \cdot P(\alpha)}{N(S_2, \nu_2)} \qquad - \quad (5.1)$$

where $Q(\alpha)$ is the distribution in effective spectral index ($\alpha_{\nu_1-\nu_2}$) for a sample of sources stronger than S_2 from a survey at ν_2,

$P(\alpha)$ is the distribution in effective spectral index ($\alpha_{\nu_1-\nu_2}$) for a sample of sources from a survey at ν_1, and is assumed to be independent of flux density,

$N(S,\nu)$ is the number of sources at frequency ν of flux density greater than S_ν (i.e. the conventional number - flux density relation).

$P(\alpha)$ has been derived from the flux densities measured by KPW, and is shown in Figure 5.2(a) for sources with $|b^{II}| \geq 10^\circ$ and with $|b^{II}| \geq 20^\circ$. Although not stated explicitly, it appears that in making the calculation KPD assumed the number - flux density relation at 5000 MHz to be of the same form as that derived by Gower at 178 MHz (1966) save for a translation in the log N - log S plane. $N(S_2,\nu_2)$ may then be taken as a constant giving the required normalization for comparison with the sample obtained. The results of the calculation (normalized to a sample size of 1000) are illustrated in Figure 5.2(b). The enormous influence of the two sources with negative effective spectral indices in the $P(\alpha)$ distribution is evident. One of these sources (3C 147.1 in the $|b^{II}| \geq 10^\circ$ sample) is an HII region which becomes optically thick by 178 MHz. It has been retained in the calculation to illustrate the effect produced by <u>one source</u> of such a spectrum on the result at 5000 MHz. In Figure 5.2(b) the calculated distribution of KPD is also illustrated, and its description by the authors as "smoothed" is obviously well justified. It is pointed out that the computed distribution is ill-defined in this region because of the samll numbers of flat spectrum objects; however, the authors have evidently chosen to neglect the troublesome QSO 3C 454.3 which has a negative effective index. The validity of

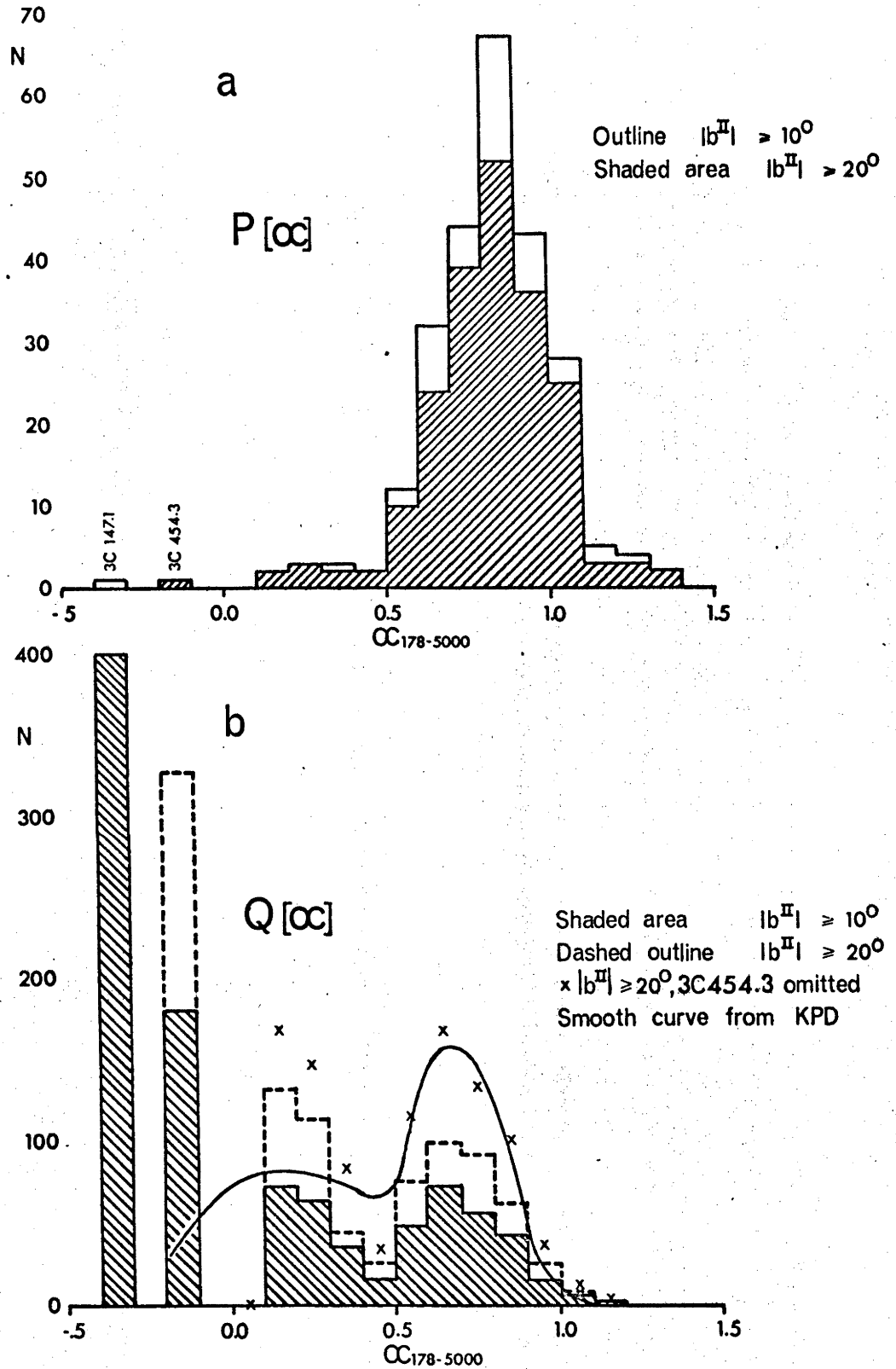

Figure 5.2. The P(α) and Q(α) distributions (see text) for the prediction of the distribution of 178 - 5000 MHz effective indices for sources found in a 5000 MHz survey.

this is questioned, but in any case it is certain that unless samples of thousands of effective spectral indices are available from a catalogue at one frequency, attempts at prediction of spectral content over such a wide frequency range can serve as order of magnitude estimates only.

In Figure 5.3(a), $P(\alpha)$, the distribution in effective spectral index for the frequency range 178 - 2695 MHz is shown for all sources with $|b^{II}| \geq 20^{o}$ and which have the requisite flux densities in KPW. This histogram shows no source with a negative effective spectral index; 3C 454.3 has, at the epoch of the KPW measurement, $S_{2695} < S_{178} < S_{5000}$. (The source is variable (Pauliny-Toth and Kellermann 1966), and because of its considerable influence in the calculation, one is faced with the curious phenomenon of the predicted histograms being sensitive to epoch of observation of one source). The $Q(\alpha)$ distribution has been calculated using the counts of Gower at 178 MHz and the 2700 MHz counts of §6.2. The results are shown in Figures 5.3(b),(c), and (d) for sources stronger than 1.01 f.u., .64 f.u., and .40 f.u. at 2700 MHz. The predicted distributions now show a slight dependence on flux density because of the apparent difference in the form of number - flux density relations at the two frequencies. They have been normalized to the sample sizes available for comparison, and the observed distributions in $\alpha_{178-2700}$ are also shown in Figure 5.3. The calculations have been described in some detail because they have a bearing on the apparent differences in the form of the

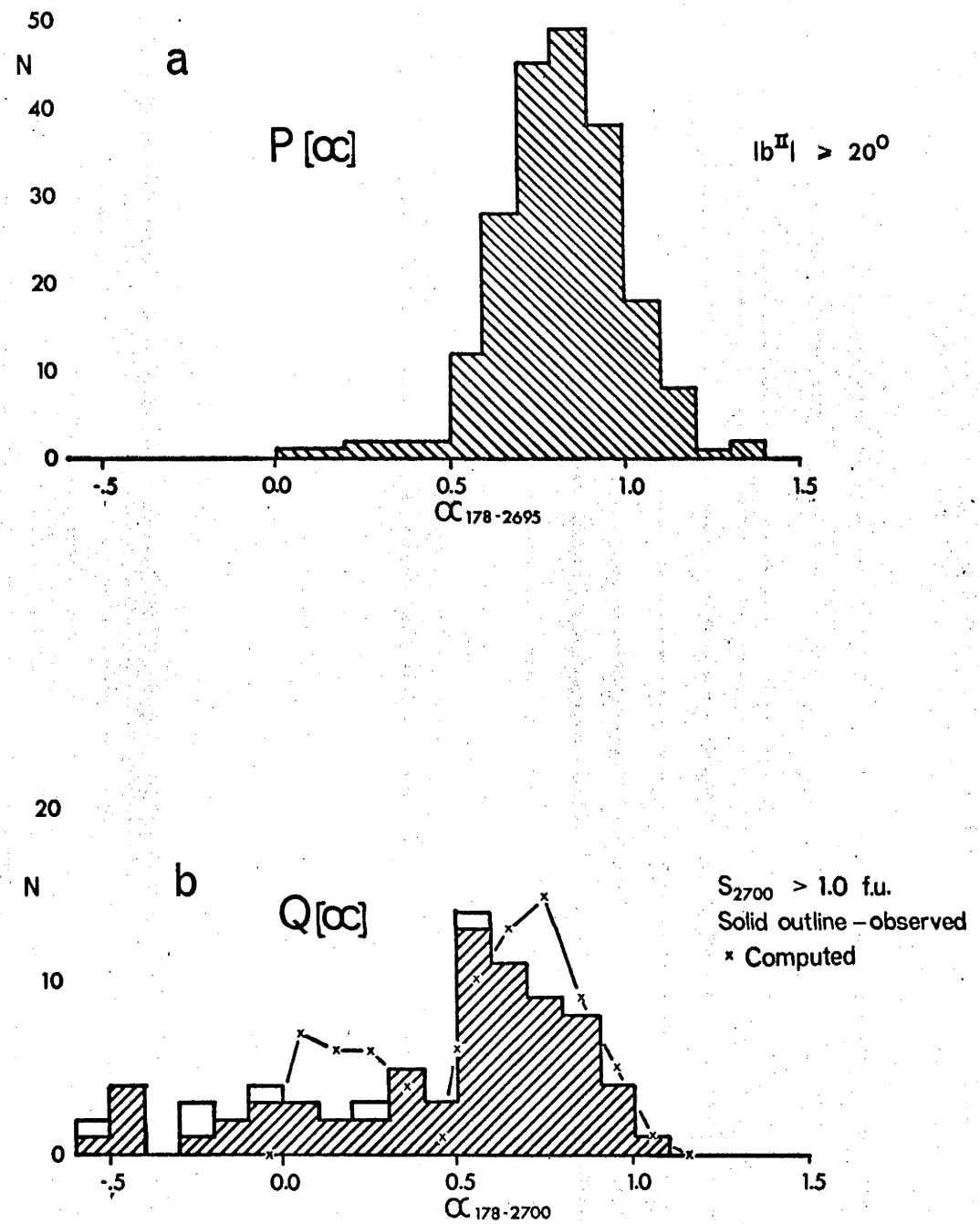

Figure 5.3. The P(α) and Q(α) distributions for the prediction of 178 - 2700 MHz effective indices for sources found in a survey at 2700 MHz. The three computed Q(α) distributions, Figures 5.3(b), (c), and (d), have been normalized to the sizes of the samples of sources available for comparison from the 2700 MHz survey of the $\pm 4^{\circ}$ declination zone. Unshaded areas in the distributions shown for these samples represent sources for which the estimated effective index has been obtained from an unreliable estimate of the 178 MHz flux density.

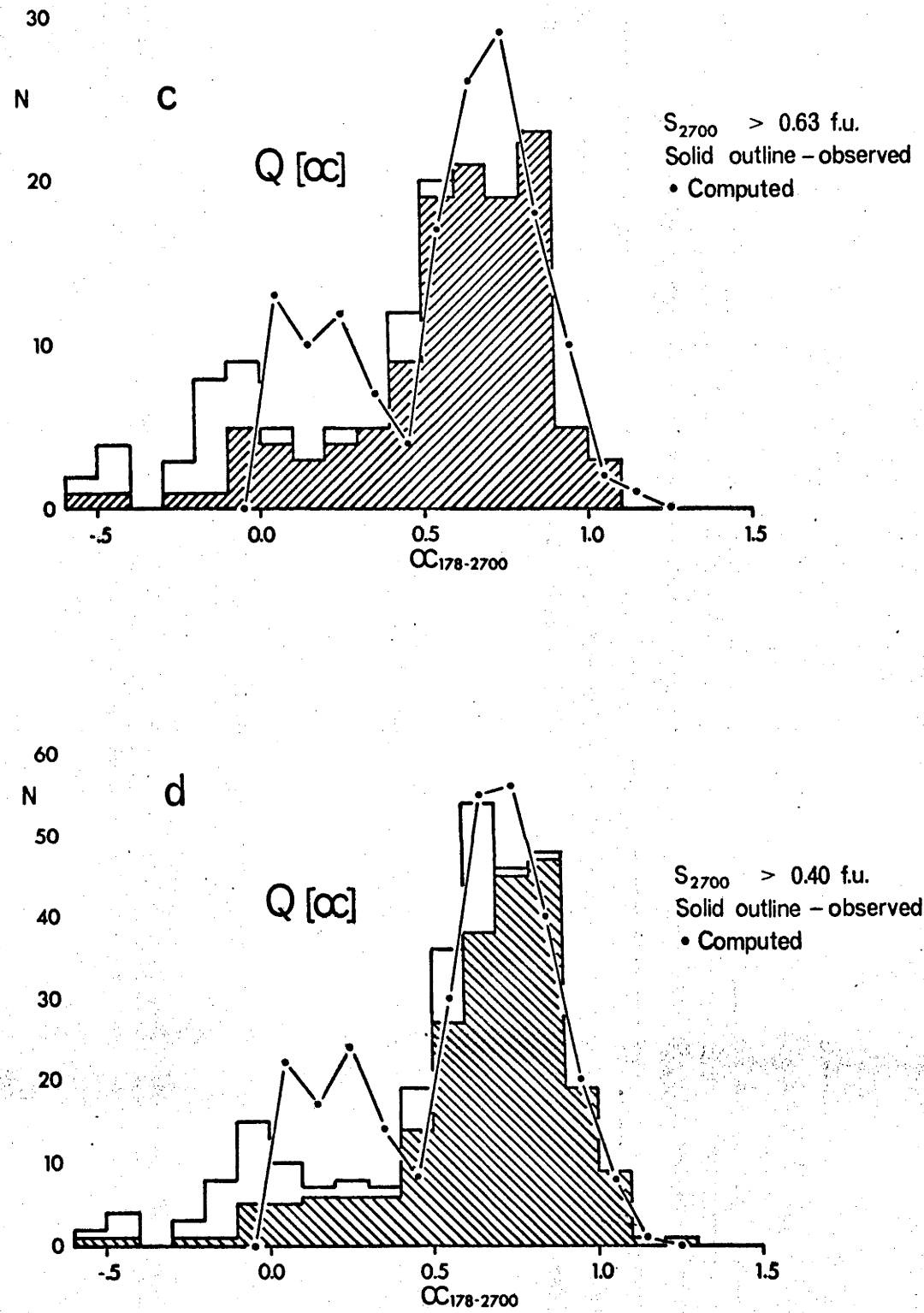

Figure 5.3 concluded.

number - flux density relations at high and low frequencies; the comparisons between observed and predicted distributions are further discussed in Chapter 6. In the present context, it is apparent that the predictions and observations are in good agreement for effective spectral indices ≥ 0.4. The tail for the lower values is once again ill-defined but not to the same extent as for the doubled frequency range treated in KPD. The calculated distributions appear to indicate the existence of two spectral populations, "flat" and "normal" with the division in effective spectral index at about 0.40. Blum and Davis (1968) and KPD both proposed just such a division from their limited sky surveys at 5000 MHz. The observed histograms in the present sample show no division at this value, and consequently differ markedly in form from the calculated towards the lower spectral indices. However, if the proportion of effective indices below 0.4 is considered rather than the form of the distribution for such indices, the results of Table 5.2 are derived, and good agreement is apparent between prediction and observation. The uncertainties indicated in the observed numbers lie in deciding on the effective indices of

TABLE 5.2

PROPORTION OF EFFECTIVE SPECTRAL INDICES ($\alpha_{178-2700}$) <0.4

$S_{2700} \geq$ (f.u.)	Sample Size	Effective Indices <0.4			
		Predicted		Observed	
		No.	%	No.	%
1.01	73	23	29.5	28	36
.64	148	42	28.5	46±2	31±1.5
.40	297	77	26.0	75±10	25±3.5

those sources for which only upper limits to the flux density at 178 MHz are available.

The calculations thus provide excellent estimates over this frequency range for the form of the effective spectral index distribution above 0.4, and good quantitative estimates of the relative proportions above and below this value. This is a significant result in view of the fact that there are very few sources with power law spectra over the range 178 to 5000 MHz having indices <0.4 (§5.2). For values less than 0.4 the effective index is in general determined by modification of the spectrum by self-absorption or by the presence of additional compact components, and becomes a function of ν_1 and ν_2. The calculations indicate that reasonably good estimates of the relative numbers of such sources can be made from the data on sources in the low frequency catalogues. Furthermore, because of this change in the physical significance of the effective index, it is not surprising that the forms of observed and predicted distributions are in poor agreement for values below 0.4.

5.4 Variable Sources

Systematic observations to detect time variations at centimeter wavelengths have not been carried out for sources in the present sample, and an accurate estimate of the proportion which exhibit this phenomenon is thus not possible. The observations of Kellermann and co-workers, Miss Harris, and

Shimmins (personal communication) have shown that almost every source in which the spectrum indicates the presence of a second component exhibiting self-absorption at relatively high frequencies shows variation at centimeter wavelengths. Several sources in the present sample with this spectral feature were measured a number of times at 2700 MHz. Some of these were previously known or suspected (Miss Harris, personal communication) to be variable at this frequency. The results of this very incomplete programme are in Table 5.3. The 2700 MHz flux densities for all sources showing definite or probable time variations are plotted in Figure 4.5. Six sources showing definite variations were previously known variables (PKS 0106+01, 0336-01 (CTA 26), 0440-00 (NRAO 190), 0736+01, 1055+01, and 1226+02 (3C 273)). Nine other sources are almost certainly variables, and four of these have not been previously catalogued.

Several sources showing simple self-absorption cut-offs at relatively high frequencies and no evidence of conventional power law components were also observed more than once at 2700 MHz. No variations were detected in such sources. Shimmins et al. (1968) and Kellermann and Pauliny-Toth (1969) both comment on this phenomenon. The sources 0440-00 and 1148-00 are similar in spectra (Figure 4.4) and each possibly has a weak steep spectrum component because of the gradual nature of the low frequency cut-off. The former is variable at 2700 MHz on a time scale of months, while the latter does not

TABLE 5.3

SOURCES VARIABLE AT 2700 MHZ

Definite Variables Deviations > 2σ			Probable Variables Deviations $\sim 2\sigma$		Possible Variables Deviations > σ	
0106+01	QSO	(2)	0047-02	III	0422+00	III
0336-01	QSO	(2)	0056-00	QSO	0823+033	III
0358+031	III		1349+027	III	1509+01	III
0420-01	QSO				1555+001	III
0440-00	QSO	(4)			1643+022	E
0458-02	N?					
0550+032	III					
0736+01	QSO	(3)				
0808+019	QSO					
1055+01	QSO	(3)				
1226+02	QSO	(1)				
1546+027	QSO?					
1602-00.2	QSO?					
1741-03	III					
2155-152	III					

References for Table 5.3

(1) Dent, W.A. (1965) - Science 148, 1458

(2) Kellermann, K.I., and Pauliny-Toth, I.I.K. (1968a) - Astrophys. J. 152, 639

(3) Kellermann, K.I., Pauliny-Toth, I.I.K., and Tyler, W.C. (1968) - Astron. J. 73, 298

(4) Pauliny-Toth, I.I.K., and Kellermann, K.I. (1966) - Astrophys. J. 146, 634

appear to vary over a time scale of 5 years; it seems that such objects are intermediate between the simple self-absorption sources and the sources with two components, one "conventional" and the other compact. The central question is why the one type should vary while the other remains stable. It seems likely that in the latter type of source, the lack of confinement of the plasma produces leakage resulting in the formation of the conventional power law component apparent at the lower frequencies (J. G. Bolton, A. J. Shimmins, personal communication).

An examination of the results of Table 5.1 indicates that 15±5% of sources found in 2700 MHz surveys should prove to be variable. The predominance of QSO's and QSO?'s among the variables is evident in Table 5.3 and from an examination of the spectra of Figure 4.4. Only two sources with suggested galaxy identifications appear in Table 5.3. Of these, 0458-02 may not be correctly identified (see §3.2, §4.8) and the 2700 MHz observations of 1643+022 show a difference of very marginal significance. Spectral differences between the radio galaxies and QSO's are now discussed.

5.5 The Spectra of Radio Galaxies and QSO's

In Figure 5.4, the distributions of α_{LF} and α_{HF} for radio galaxies and for QSO's are presented.

For radio galaxies, the distributions appear to be approximately Gaussian; the single source with a negative spectral index in the α_{LF} histogram is 0752-02.3, and in the

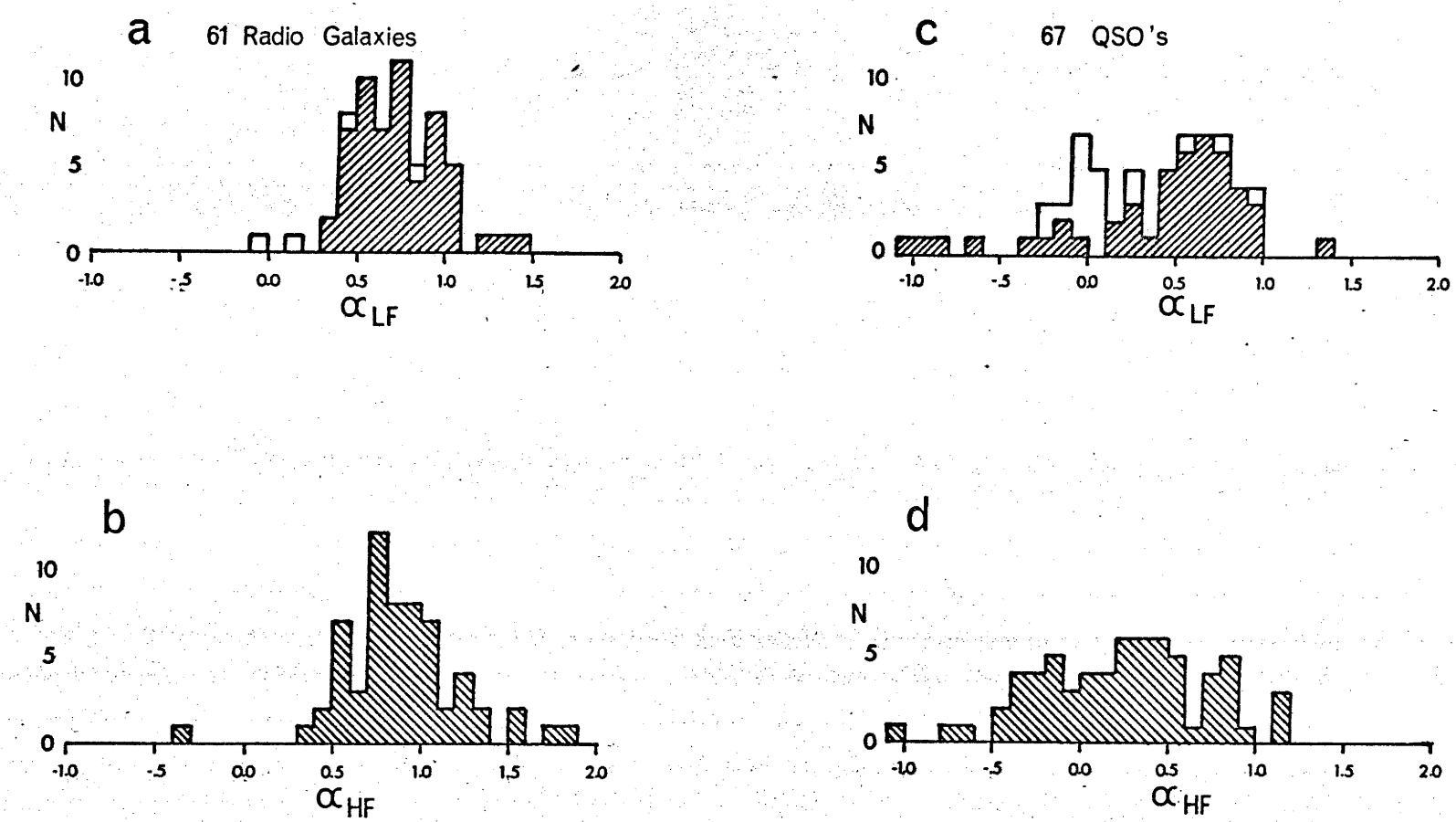

Figure 5.4. Distributions in low and high frequency spectral indices for optical identifications from the 2700 MHz survey of the $\pm 4^{\circ}$ declination zone. Unshaded areas represent upper limits to the low frequency indices.

Figures 5.4(a) and (b): Radio Galaxies.

Figures 5.4(c) and (d): QSO's.

α_{HF} histogram 0111+021. In Table 5.4 the parameters describing these histograms are shown together with those derived by other authors for the radio galaxies. The dispersions were estimated from $\sigma = \sqrt{\sigma^2_{obs} - \sigma^2_n}$, where σ_{obs} is from the histograms of Figures 5.4(a) and (b) (68% within $\pm\sigma_{obs}$ of the mean), and σ_n is the estimated error due to inaccuracy of measurement of the flux densities. The present results indicate that samples of radio galaxies selected at different frequencies show very little difference in their spectral properties. In particular, as the high frequency survey tends to favour the detection of objects with flat high frequency spectra, the fact that the majority of radio galaxies do show steepening of the spectra in the present sample implies that the spectra of most radio galaxies must steepen at the higher frequencies. Because of the relatively shorter time scales for the processes of energy loss affecting the spectra at the higher frequencies (see §5.1(i)), a dispersion in ages for the sources may explain the fact that the dispersion for the α_{HF} distribution appears to be larger than that for the α_{LF} distribution.

In contrast to the case of the radio galaxies, no low frequency survey has produced a sample of QSO's having distributions in spectral indices which resemble those of Figures 5.4(c) and (d). Both of these show a large dispersion, and unlike Figures 5.4(a) and (b), bear a close resemblance. Just over half of the objects in the α_{LF} histogram lie between 0.5 and 1.0, and it is this population of "normal" spectrum QSO's

TABLE 5.4

SPECTRAL INDEX DISTRIBUTIONS, RADIO GALAXIES

Reference	Catalogue for Sample	Sample Size	Index*	Dispersion	Comment
KPW (1969)	3CR (178 MHz)	132	0.753±0.013	0.15±0.01	Median, 38-750 MHz
			0.851±0.018	0.20±0.01	Median, 750-5000 MHz
Shimmins (1968)	PKS (408 MHz)	82	0.71	0.13	$\bar{\alpha}_{300}$
			0.90	0.17	$\bar{\alpha}_{3000}$
Harris (1969)	PKS (408 MHz)	120	0.72±0.02	0.23	$\bar{\alpha}_{1000}$
			0.85±0.03	0.32	$\bar{\alpha}_{4000}$
Present work	PKS (2700 MHz)	61	0.72±0.05	0.22±0.05	$\bar{\alpha}_{LF}$ (178-1403 MHz)
			0.89±0.05	0.26±0.03	$\bar{\alpha}_{HF}$ (1403-5009 MHz)

* See Comment column.

which generally has been detected in low frequency surveys. This led to controversy as to whether there are significant differences between the spectra of QSO's and radio galaxies (see, e.g. Williams and Collins 1967, Shimmins 1968b). Figure 5.4 puts the issue beyond question for the present sample.

Table 5.1 indicates that only 22% of the QSO's in the present sample have spectra which can be represented by a single power law between 178 and 5009 MHz. Of the remainder, 34% show evidence of simple self-absorption above 178 MHz, 34% exhibit an increase in flux density to the higher frequencies implying the presence of an additional compact component, and 10% show a steepening of the spectrum at higher frequencies. In comparison the sample of Shimmins (1968b), taken from the 408 MHz Parkes catalogue, shows 53% with power law spectra, 38% with enhancement at high frequencies, and 9% with synchrotron self-absorption above 100 MHz. The 2700 MHz survey thus favours the detection of the QSO's with simple self-absorption and with evidence of high frequency compact components at the expense of those exhibiting power law spectra.

The means and dispersions of Figures 5.4(c) and (d) are not physically significant since they generally represent the combined effects of electron energy distribution and surface brightness.

If Figure 5.4 is compared with the histograms of Figures 5.1(a) and (b) which represent the entire sample, the

following points are apparent:

(1) The "flat spectrum" tails in both Figures 5.1(a) and (b) are generally due to the QSO's which have spectra exhibiting self-absorption in the low and/or the high frequency regions of the spectrum.

(2) The steep spectrum tail in Figure 5.1(b) is due to the radio galaxies and unidentified sources. (Distributions of α_{LF} and α_{HF} for the latter appear in Figure 5.5.)

(3) The main peak in both Figures 5.1(a) and (b) is due to radio galaxies and power law spectrum QSO's.

(4) The shift of the peak in Figure 5.1(b) to spectra steeper than the peak in Figure 5.1(a) is due to the influence of the radio galaxies.

The differences in spectra between the identification classes, particularly evident at the high frequencies, suggest that it may be possible to "identify" the unidentified sources from their radio spectra. Bolton (1966) attempted such a separation, and a similar investigation is carried out for the present sample in the following section.

5.6 The Unidentified Sources

Four arguments have been presented by Bolton (1966, 1969) to support the view that the majority of sources which are in regions free of optical obscuration and which remain unidentified are radio galaxies beyond the plate limit of the Palomar Sky Survey. The arguments are based on (1) spectral

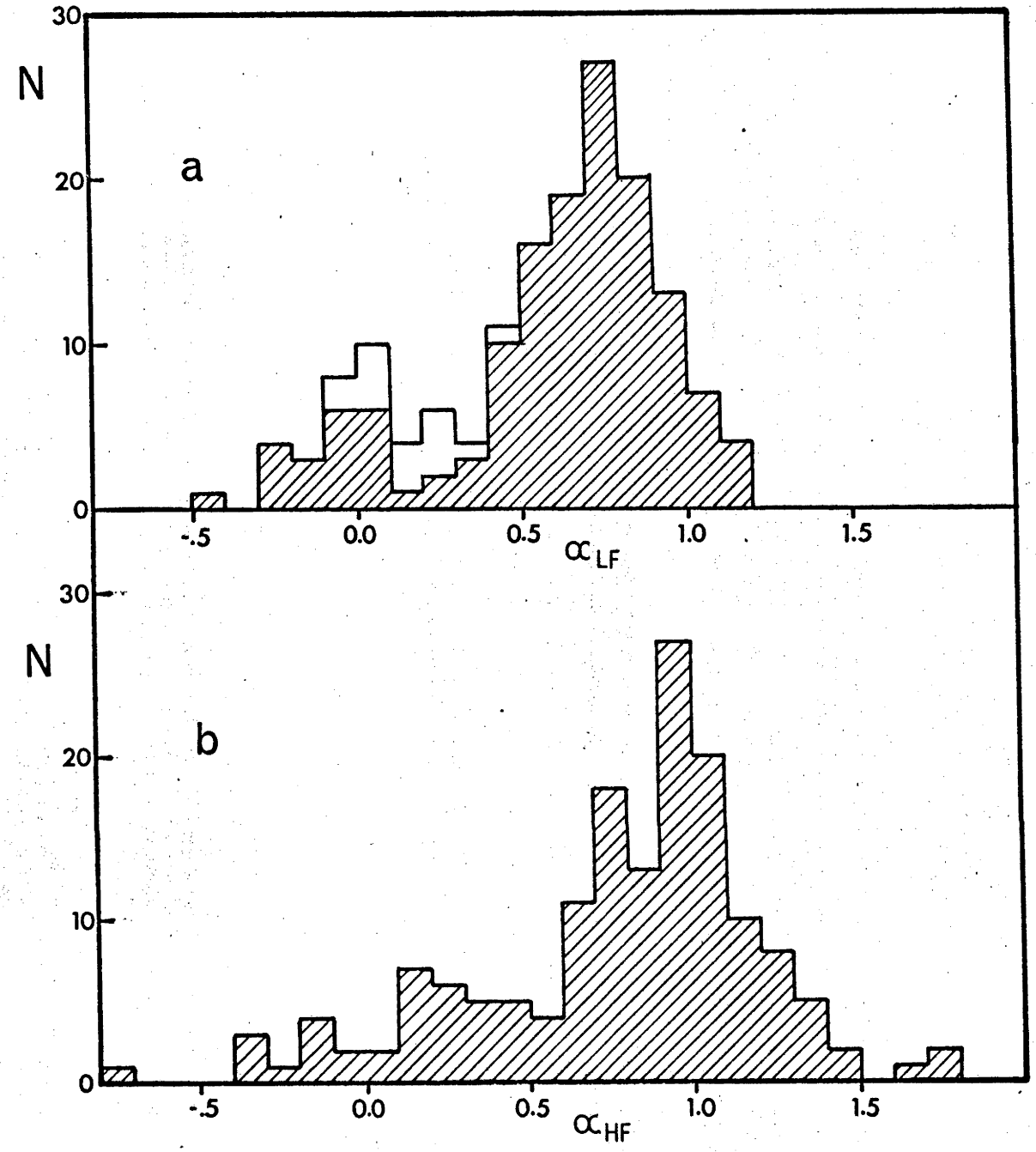

Figure 5.5. Distributions for low and high frequency spectral indices for sources from the 2700 MHz survey of the ±4° declination zone which have $S_{2700} \geq 0.40$ f.u.

differences between QSO's and radio galaxies at the higher frequencies, (2) the form of the optical apparent magnitude distributions, (3) the results of interplanetary scintillation observations, and (4) the results of polarization observations (which are also discussed by Gardner and Whiteoak (1969)). Véron reached the opposite conclusion (1966), but his evidence, based on a comparison of the source counts and apparent magnitude - redshift relations, appears to give equal weight to Bolton's hypothesis. In the following analysis, the high frequency spectral differences are shown to support Bolton's view and to serve to divide the present sample of unidentified sources into radio galaxies and QSO's to an accuracy of about 10%.

From Table 5.1, 78% of all the unidentified sources (referred to as III's hereinafter) have power law spectra or spectra which steepen with increasing frequency. Such spectral forms account for 98% of the radio galaxies and 32% of the QSO's. Most of the III's thus appear to have galaxy-like spectra. Examination of the α_{LF} and α_{HF} distributions for the III's (Figures 5.5(a) and (b)) leads to the same conclusion; the skew nature of the total sample distributions (Figures 5.1(a) and (b)) is still in evidence but to a lesser extent. A further point of interest is that for the indices in Figure 5.5 which correspond to the galaxy-like spectra, i.e. those with values between, say, 0.45 and 1.25, the peaks in the distributions are shifted to a slightly higher value than those

in the radio galaxy distributions (Figures 5.4(a) and (b)). The same result was found by KPW and by Harris (1969), and has been interpreted, in view of an apparent correlation between luminosity and spectrum (e.g. KPW 1969) as evidence of generally greater luminosities for the III's than for the radio galaxies. However, examination of the data on radio galaxies compiled by Miss Merkelijn indicates that only the objects of lowest luminosity have significantly flatter spectra, and casts some doubt on the apparent strength of the correlation between luminosity and spectrum obtained by KPW (personal communication, Miss J. K. Merkelijn, J. G. Bolton).

Because the 2700 and 5009 MHz flux densities have the smallest errors and indicate the largest spectral differences, they have been used to determine the QSO - radio galaxy ratio among the III's. Two-frequency diagrams for sources catalogued in the $\pm 4^{\circ}$ declination zone are shown in Figure 5.6 for the QSO's, QSO?'s, and radio galaxies, and in Figure 5.7 for the III's. In these diagrams, the 5009 MHz flux densities have been plotted against the 2700 MHz flux densities; the 45° lines represent constant spectral indices ($\alpha_{2700-5009}$). Figure 5.6 reflects the same results as Figure 5.4, namely that the QSO's exhibit generally flatter spectra with a broader dispersion than the galaxies, and that very few galaxies show high frequency spectral indices <0.4. There is, however, one important new feature. The QSO's appear to exhibit a dependence of spectrum on S_{2700} in the sense that the steeper spectrum objects are of

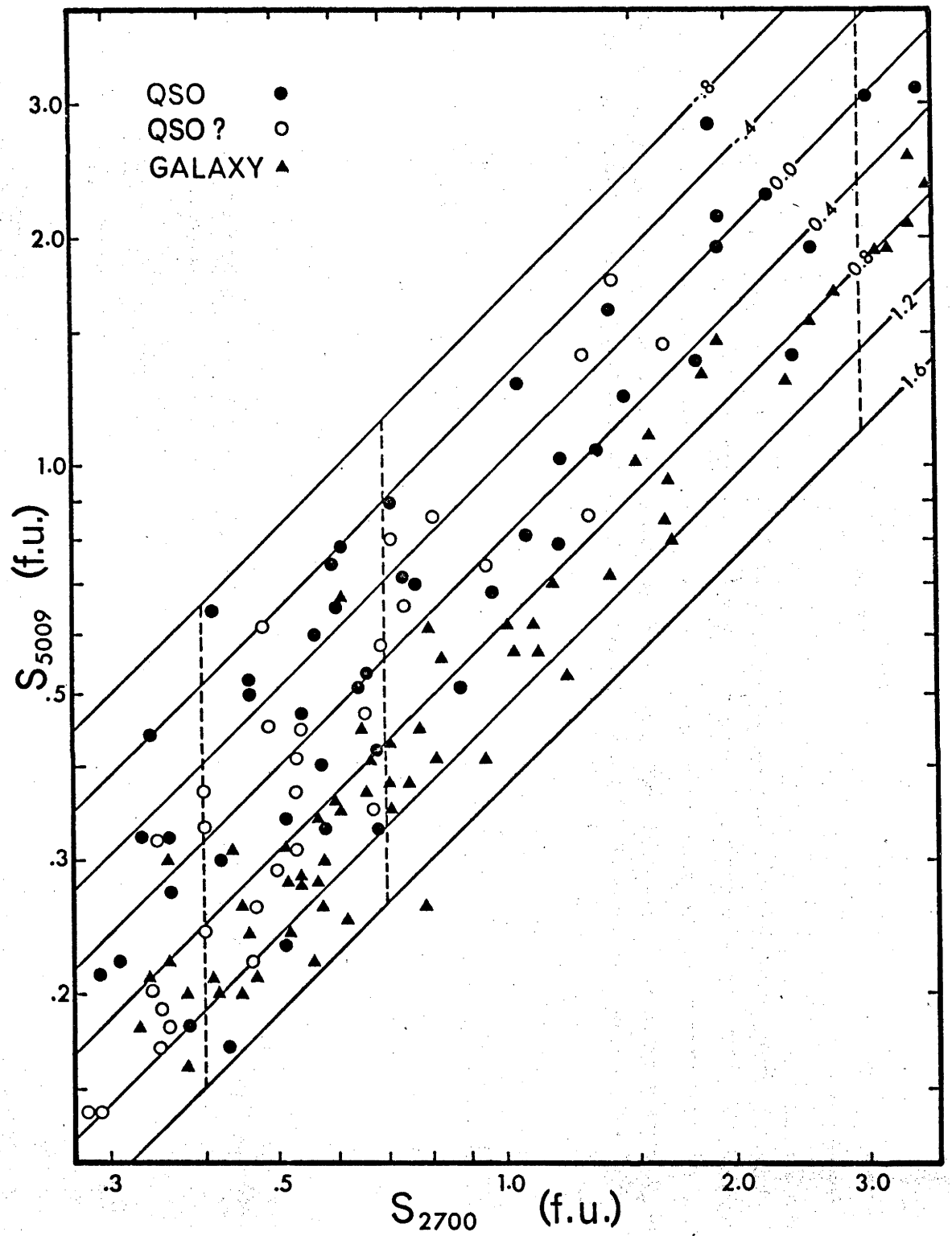

Figure 5.6. Two-frequency diagram for identified sources catalogued in the 2700 MHz survey of the ±4° declination zone. The 45° lines represent constant effective indices, 2700 - 5009 MHz.

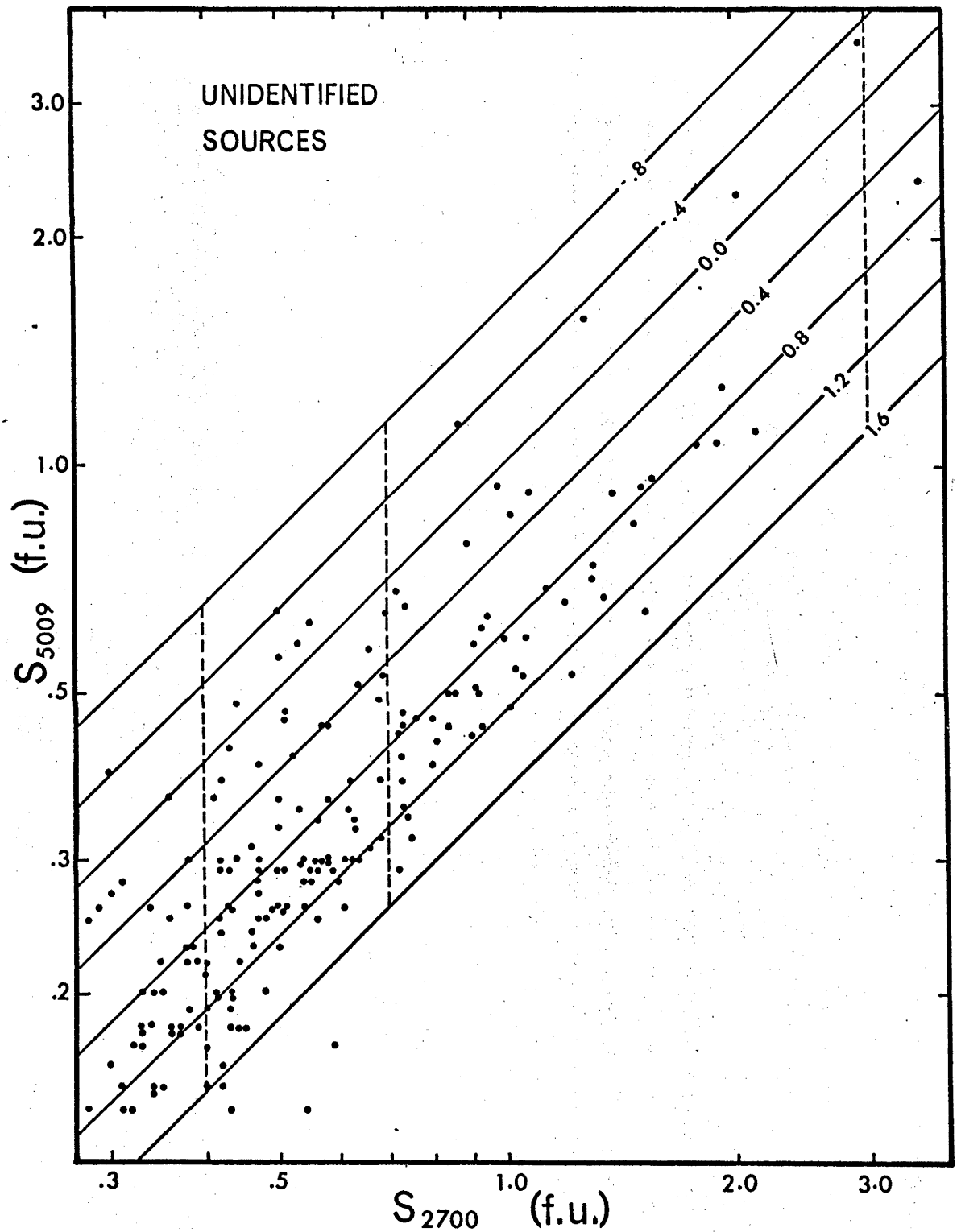

Figure 5.7. Two-frequency diagram for unidentified sources catalogued in the 2700 MHz survey of the ±4° declination zone.

fainter flux density. The effect is not immediately evident in Figure 5.6 because of the addition of the galaxies to the diagram. It is further discussed in Chapter 6; in passing it is noted that systematic overestimation of the flux densities for the weaker sources could result in a similar effect but in the opposite sense. In the present context, the result indicates that a spectral separation for the III's must be carried out for each range in flux density. The ranges chosen for the analysis were $0.4 < S_{2700} < 0.7$ f.u., and $0.7 < S_{2700} < 3.0$ f.u., as indicated by the vertical lines in Figures 5.6 and 5.7.

To obtain the spectral separation from Figures 5.6 and 5.7, the number of objects in each area bounded by lines of constant spectral index and flux density have been counted, and appear as histograms in Figure 5.8. The proportions of QSO's and radio galaxies have then been adjusted to give the best fit to the histograms for the III's, as shown in Figure 5.8. For this purpose, the QSO?'s have been treated by placing 50% of them in class III and 50% in class QSO. The results indicate that in the 2700 MHz flux density range 0.4 to 0.7 f.u., 35±10% of the III's are QSO's and 65±10% are radio galaxies; in the range 0.7 to 3.0 f.u., 30±10% are QSO's, and 70±10% are radio galaxies. Precise values and errors are not formally assessable because the distributions do not obey known probability distributions, and indeed there is every reason to expect that they should not.

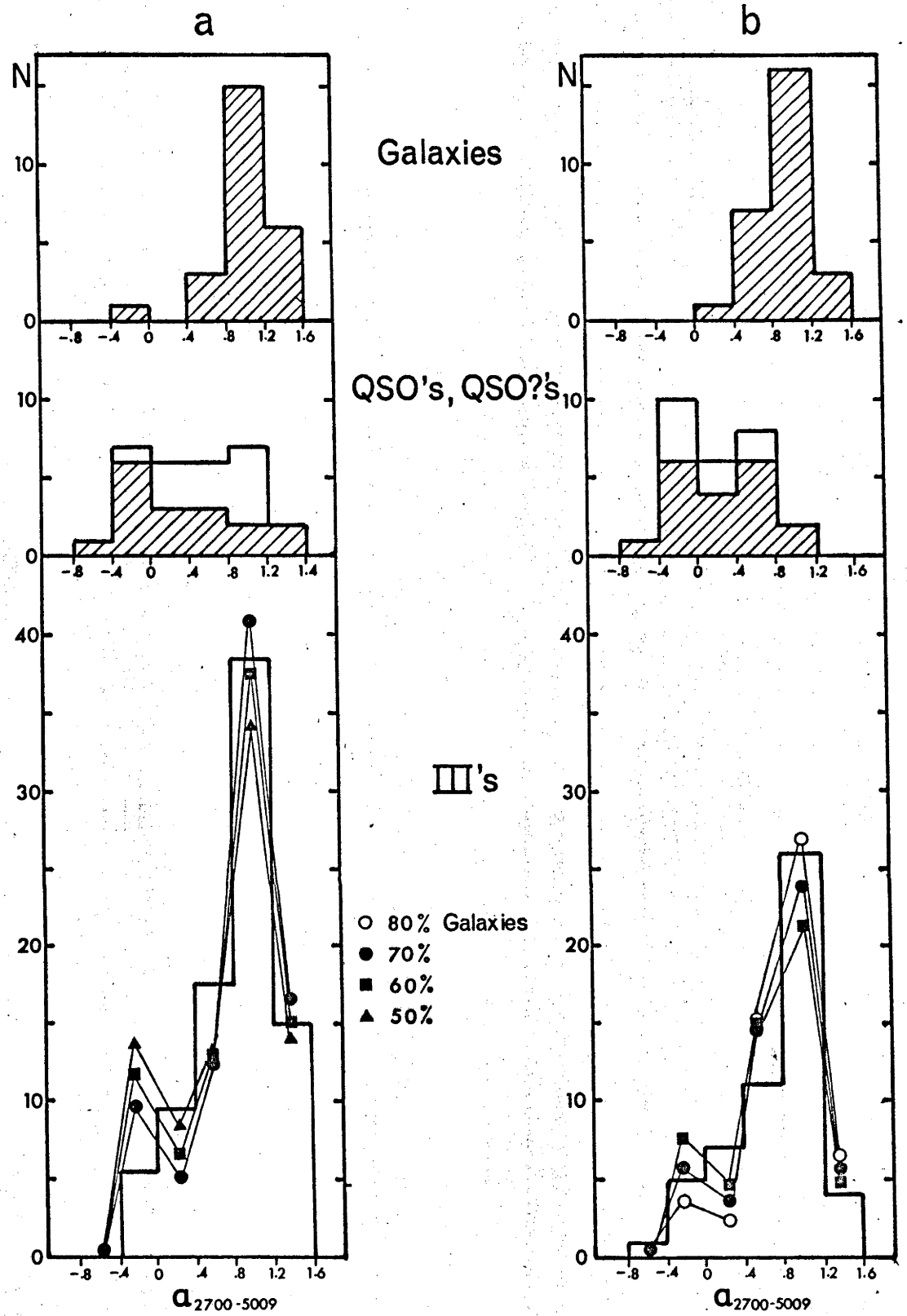

Figure 5.8. The distributions in high frequency effective indices for the classes of optical identification, as obtained from the two-frequency diagrams, and the combination of these distributions to estimate the proportion of unidentified sources belonging to each. The unshaded areas in the QSO distributions represent QSO?'s.

Figure 5.8(a)

$0.4 < S_{2700} < 0.7$ f.u.

Figure 5.8(b)

$0.7 < S_{2700} < 3.0$ f.u.

In the preceding analysis several regions of the ±4° declination zone in which certain or possible obscuration was present were included. An identical analysis has subsequently been carried out from which all such regions were excluded. The sample size was reduced by about one third in consequence, but the results are nevertheless considered to be more reliable. The analysis has also been repeated classifying all QSO?'s as QSO's. From the results obtained, the best estimate for the proportion of QSO's among the III's is 25±10% for the range in 2700 MHz flux density 0.7 to 3.0 f.u., with a possible increase to 30±10% for the range 0.4 to 0.7 f.u. When larger numbers of sources become available, the analysis may be refined and the results treated with greater confidence.

Bolton (1969) found the proportion of QSO's among the III's of the Parkes (408 MHz) catalogue to be ≤25%. If the proportion of QSO's among the III's in the 2700 MHz catalogue is significantly higher, two effects may be responsible. Firstly, the lower flux density limit of the ±4° zone survey might be expected to result in the detection of QSO's which in general are optically fainter. This effect has indeed been found by Bolton and Wall (§3.2), and is illustrated in Figure 5.9. The histograms of apparent magnitudes of QSO's for different ranges in flux density illustrate a shift to the fainter apparent magnitudes with decreasing flux density. These distributions indicate that the tails of the apparent magnitude distributions do indeed run through the plate limits

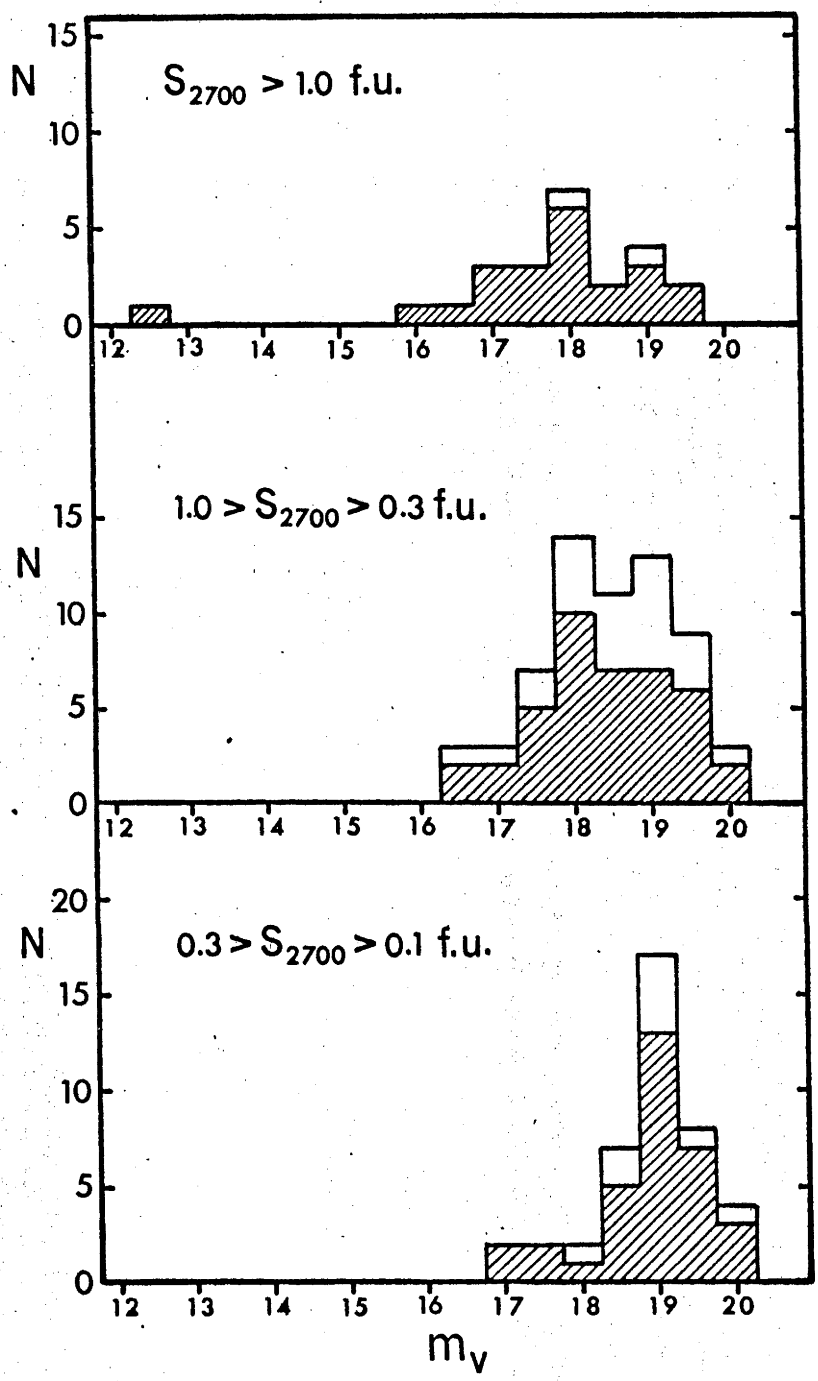

Figure 5.9. The distributions in apparent magnitude for QSO's from the first two parts of the Parkes 2700 MHz survey.

CHAPTER 6

THE NUMBER - FLUX DENSITY RELATION AT 2700 MHZ

Preliminary results on source counts from the first two parts of the 2700 MHz survey have been published (Shimmins, Bolton, and Wall 1968; hereinafter referred to as SBW). With the completion of the first two parts of the survey (Chapter 2), the sample size for source densities lower than 500/sr. ($S_{2700} \sim 0.35$ f.u.) is twice that available to SBW. In this chapter the corrections to the source counts for various experimental factors have been considered, and the number - flux density relation* derived from the complete sample and these appropriate corrections is presented. The result is compared with published number - flux density relations for other frequencies. The number - flux density relations for the different classes of optical identification have also been derived.

---

* A distinction is made between the "source counts" and the "number - flux density relation" in the present work. The former is taken to mean the counts of sources above specific flux density levels made directly from observation and plotted in the log N - log S plane; the latter is the "true" source count, and is derived from the former with the application of any corrections necessary for experimental factors.

6.1 The 2700 MHz Source Counts

In April of 1967 the new 2700 MHz receiver was tested for a period of 10 days on the Parkes telescope which was undergoing overhaul at the time. Transit scans were carried out at the Celestial Equator for a strip about $1\frac{1}{2}^{\circ}$ wide and about 12^{h} of right ascension long. Several sources with $S_{2700} \geq 0.5$ f.u. were observed which had not been previously catalogued, and the count for about 150 sources was found to have a slope of about -1.5. However, for a highly enlongated area, edge effects (particularly the tendency to include strong sources just outside the region) are difficult to estimate, as are errors in flux densities unless independent measurements are subsequently made. The results were of sufficient interest to provide added incentive for detailed large scale surveys at this frequency.

For the selected regions, edge effects were eliminated by surveying beyond each plate area by one or two beamwidths. The identification overlay obtained from the accurate position programme (§2.4) was used to determine whether the source lay within the plate area. Only those within the plate areas have been used in the source count; however, all sources which were accurately positioned are given in the selected region catalogue (Table AII.1). For the $\pm 4^{\circ}$ declination zone survey, scans were continued at least one beamwidth beyond declinations $+04^{\circ}00'$ and $-04^{\circ}00'$, and the positions of §2.4 (precessed to epoch 1950.0) were used to decide if the sources

lay within this declination range. Only sources within the $\pm 4^{\circ}$ zone were subsequently used in the source counts or included in the catalogue (Table AII.2).

The areas involved are $6 \times 41.20 = 247.2$ square degrees (0.0753 sr.) for the selected regions, and 2397 square degrees (0.730 sr.) for the $\pm 4^{\circ}$ declination zone. (The region between right ascensions $05^{h}00^{m}$ and $06^{h}00^{m}$ was excluded from the source count to avoid confusion with possible galactic sources). The selected region PS 896 (right ascension 22^{h}, declination -18°) has been included with the $\pm 4^{\circ}$ declination zone in making the counts above a level of $S_{2700} = 0.35$ f.u., and the total area is hence 2438 square degrees (0.742 sr.).

The counts for the selected regions are shown in Table 6.1, and for the $\pm 4^{\circ}$ declination zone + PS 896 in Table 6.2. The integral counts (the conventional log N - log S curve) are shown in Figure 6.1; corrections to these counts to derive the number - flux density relation are now considered.

6.2 Corrections to the Source Counts; the Number - Flux Density Relation

The discussion of §2.10 indicates that at a level of $S_{2700} = 0.10$ f.u., the source counts of the present survey should not be affected by blends of sources or by incompleteness. There are then four other sources of error which can produce significant differences between the source counts and

TABLE 6.1. SOURCE COUNTS FROM THE 2700 MHZ SURVEY
SELECTED REGIONS

S2700 F.U.	48-INCH SCHMIDT PLATE NO. 1112	891	1114	1777	1778	896	1 N	2 N/SR	3 (DN/DS)/SR
0.079	40	42	36	34	34	47	233	3095	
									2.90E+04
0.100	30	31	32	25	31	39	188	2497	
									2.20E+04
0.126	20	24	24	19	24	34	145	1926	
									1.91E+04
0.158	13	15	16	13	18	24	99	1315	
									6.64E+03
0.200	10	13	13	12	13	17	78	1036	
									6.25E+03
0.251	6	11	8	7	10	12	54	717	
									3.47E+03
0.316	4	9	5	4	8	7	37	491	
									1.08E+03
0.501	3	6	3	1	5	4	22	292	
									3.73E+02
1.000	1	2	1	0	1	3	8	106	

THE NUMBERS IN THE COLUMNS UNDER '48-INCH SCHMIDT PLATE NO.' ARE THE CUMULATIVE COUNTS IN EACH SELECTED REGION.
COLUMN 1 - TOTAL CUMULATIVE COUNT FOR THE SELECTED REGIONS
COLUMN 2 - THE INTEGRAL SOURCE COUNT
COLUMN 3 - THE DIFFERENTIAL SOURCE COUNT

TABLE 6.2. SOURCE COUNTS FROM THE 2700 MHZ SURVEY
+4 TO -4 DEGREE DECLINATION ZONE

S2700 F.U.	1 N	2 N/SR	3 (DN/DS)/SR
.316	385	519	
			1.43E+03
.398	298	401	
			1.02E+03
.501	220	296	
			7.15E+02
.631	151	203	
			3.63E+02
.794	107	144	
			1.63E+02
1.000	82	110	
			9.21E+01
1.585	42	57	
			2.39E+01
3.162	14	19	

COLUMN 1 - CUMULATIVE COUNT FOR THE +4 TO -4 DEG. DEC. ZONE
COLUMN 2 - THE INTEGRAL SOURCE COUNT
COLUMN 3 - THE DIFFERENTIAL SOURCE COUNT

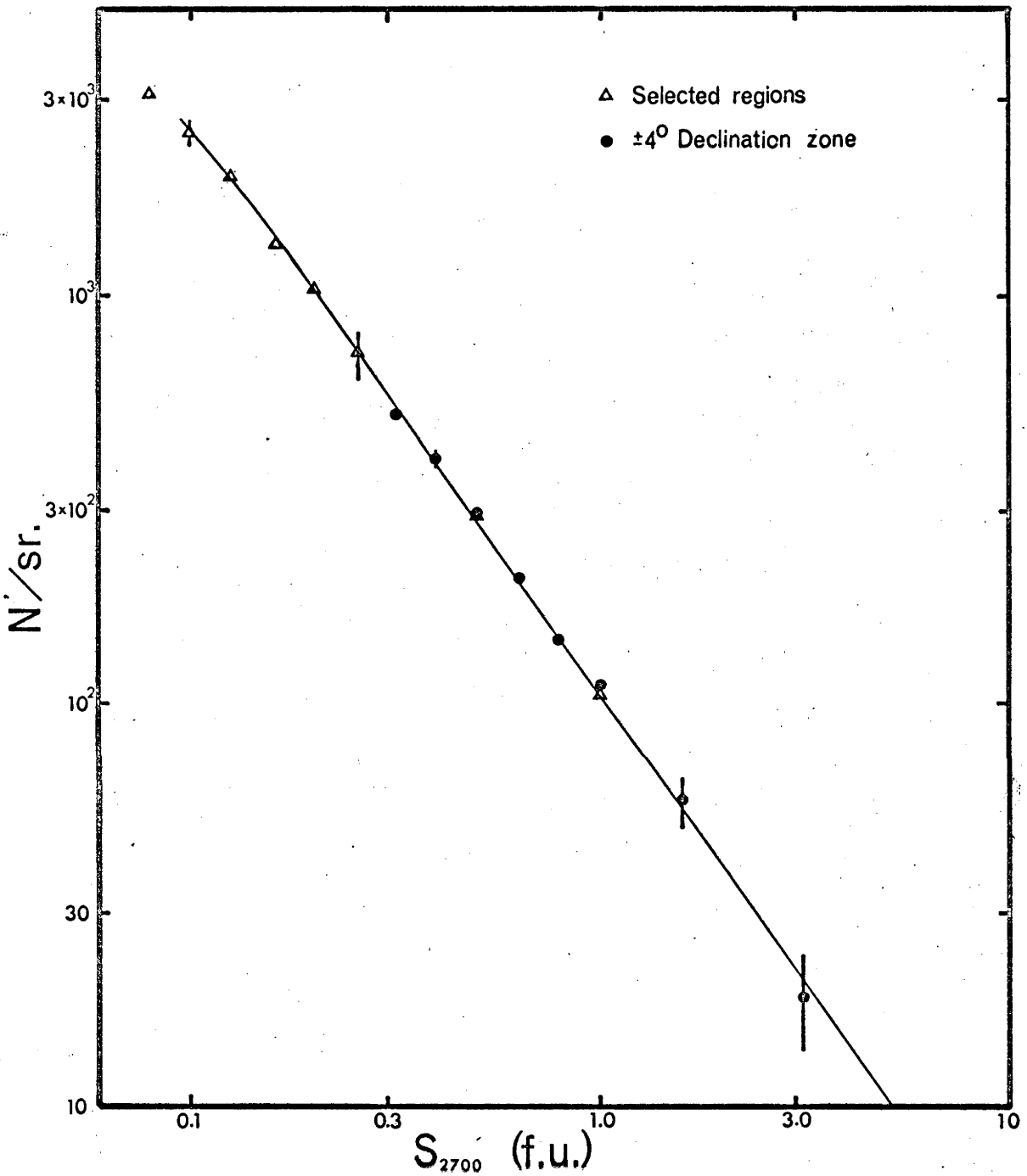

Figure 6.1. The integral source count (conventional log N - log S diagram) from the 2700 MHz surveys of the selected regions and the ±4.0° declination zone. The error bars are representative of the statistical ($\sqrt{N}$) uncertainties at different source densities. The straight line shown for source densities 10 to 10^3/sr. has a slope of -1.45.

the number - flux density relation:

(1) Random errors due to background irregularities and receiver output fluctuations which represent a greater fraction of the source flux density as the flux density level decreases. Such errors will always produce a source count steeper than the number - flux density relation. This is due to the basic form of the relation; there are more sources in an increment of flux density below a particular flux density than in the same increment above, and the imposition of a random dispersion thus transfers larger numbers of the weaker sources into the higher flux density range than vice versa. The effect has been directly observed in counts from the Parkes 408 MHz surveys.

(2) The systematic overestimation of flux densities for sources with signal - to - noise ratios below ∿5. The effect has been discussed by several authors and was first pointed out by Mills, Slee, and Hill (1960). It is present for any type of instrument and any form of record analysis, and results in a steepening of the source count.

(3) Undetected partial resolution of the stronger sources. The effect diminishes the number of sources with high flux densities, and again results in a steepening of the source count.

(4) The masking of weak sources by stronger sources. Despite surveys being apparently complete in the sense that no sources have been missed due to fluctuations in the

background or in receiver output, the effect must occur to some extent. Of the four effects, this is the only one which will reduce the slope of the source count.

For surveys in which the confusion limit (defined as in Appendix I) is approached, all these effects together with those of blending and incompleteness become interrelated. In such surveys, number - flux density relations may only be derived by properly conducted Monte Carlo analyses, comparison of the observations with computer simulation, or analyses similar to that of Scheuer's (1957) P(D) technique. In the present surveys, the corrections for factors 1, 2, and 4 were found to be small enough to render insignificant the order of evaluation and application.

The effect of factor 3 has been removed by observing all the stronger sources in the survey at 5009 MHz. The doubled resolution enabled accurate size factors to be obtained (§4.1(iii)) to derive correct integrated flux densities at 2700 MHz. The source counts made considering only peak flux densities at 2700 MHz appear markedly steeper at the low source densities than those of Figure 6.1.

The influence of factor 1 is strongly dependent on the form of the number - flux density relation, in a similar fashion to the calculation of the background fluctuations described in Appendix I. Provided that the error distribution in each interval of flux density is precisely known, and that corrections required for the other experimental factors have

been applied, the effect may be removed by successive approximations as follows. If the (true) number - flux density relation is divided up into differentials ΔN and ΔS, and if the flux densities in each ΔS are dispersed by the error distribution corresponding to that flux interval, the recombination of all the intervals and subsequent recounting will result in the (observed) source count. A computer programme was written to start from the observed source counts, and using the technique described above with the estimated distributions in errors for the 2700 MHz flux densities (§2.8, Figure 2.6), to derive the number - flux density relation from successive approximations. At the level of $S_{2700} = 0.10$ f.u., the difference between this relation and the source counts of Figure 6.1 was found to be less than 1%, well under the statistical uncertainty due to the number of sources involved in the counts. The calculations were repeated increasing the standard deviation of the background fluctuations. For a standard deviation of 0.03 f.u., three times that estimated in Appendix I, the results indicated that a significant steepening of the counts should be apparent at $S_{2700} \sim 0.10$ f.u. Such steepening does not appear in Figure 6.1; this is interpreted as indicating no serious underestimation of the standard errors in flux density due to fluctuations in the background or in receiver output.

Similar calculations have been carried out by Braccesi *et al.* (1965b) in a comparison of the Parkes 408 MHz

counts with observations at Bologna (Braccesi et al. 1965a). In addition they correct for overestimation of the flux densities of the weaker sources (factor 2), and find very good agreement between the Parkes 408 MHz counts and the preliminary Bologna results. Their analysis of the Parkes source count reduces the slope in the range 10 to 100 sources/sr. from $\sim$-1.35 to $\sim$-1.6.

Factor 2 has been shown by Murdoch and Jauncey (reported by Murdoch and Large 1968) to lead to a fractional overestimation of the flux density by $(\gamma + 1)/R^2$ where the (integral) number - flux density relation is of the form N (sources/sr.) $\propto S_\nu^{-\gamma}$, and R is the ratio of flux density to the r.m.s. value of the fluctuations in background and receiver output. At a level of $S_{2700} = 0.10$ f.u., the standard error of §2.8 indicates an overestimation of flux density by 3.3%, and this value diminishes rapidly to the larger flux densities. Factor 4, the masking of weak sources by strong sources, has been estimated in §2.10 with a random source experiment, and a correction of 2% to the integral count at 0.10 f.u. was obtained. The sense of these two corrections is opposite, and the modification subsequently indicated to derive the number - flux density relation from the source counts of Figure 6.1 is again far smaller than the statistical uncertainty.

The considerable amount of calculation described in this section indicates simply that in the source counts of

Tables 6.1 and 6.2 the correction required for the combination of experimental effects described is negligible compared with the statistical uncertainties set by the numbers of sources in the counts. These counts consequently represent the 2700 MHz number - flux density relation to within the statistical uncertainties involved.

6.3 Other Forms of the Number - Flux Density Relation

Jauncey (1967) has pointed out that the conventional log N - log S presentation of the number - flux density relation suffers from two defects. Firstly the statistical errors at each level of flux density are not independent because a sample at any level includes sources already counted at a higher intensity level. Formal fitting of a function describing the relation using these error bars is consequently erroneous and leads to a serious underestimation of the goodness of fit. Secondly, the integral counts smooth out fluctuations in the numbers of sources at each level to the extent that a change in the relation between source density and intensity may either go undetected or be detected at an intensity level significantly below that at which the change actually occurs. Jauncey proposes the use of the differential form of the relation, in which $\Delta N/\Delta S$ is plotted against S; in such a representation both defects are overcome.

The differential form of the present number - flux density relation is presented in Tables 6.1 and 6.2, and is shown in Figure 6.2. A comparison of Figures 6.1 and 6.2

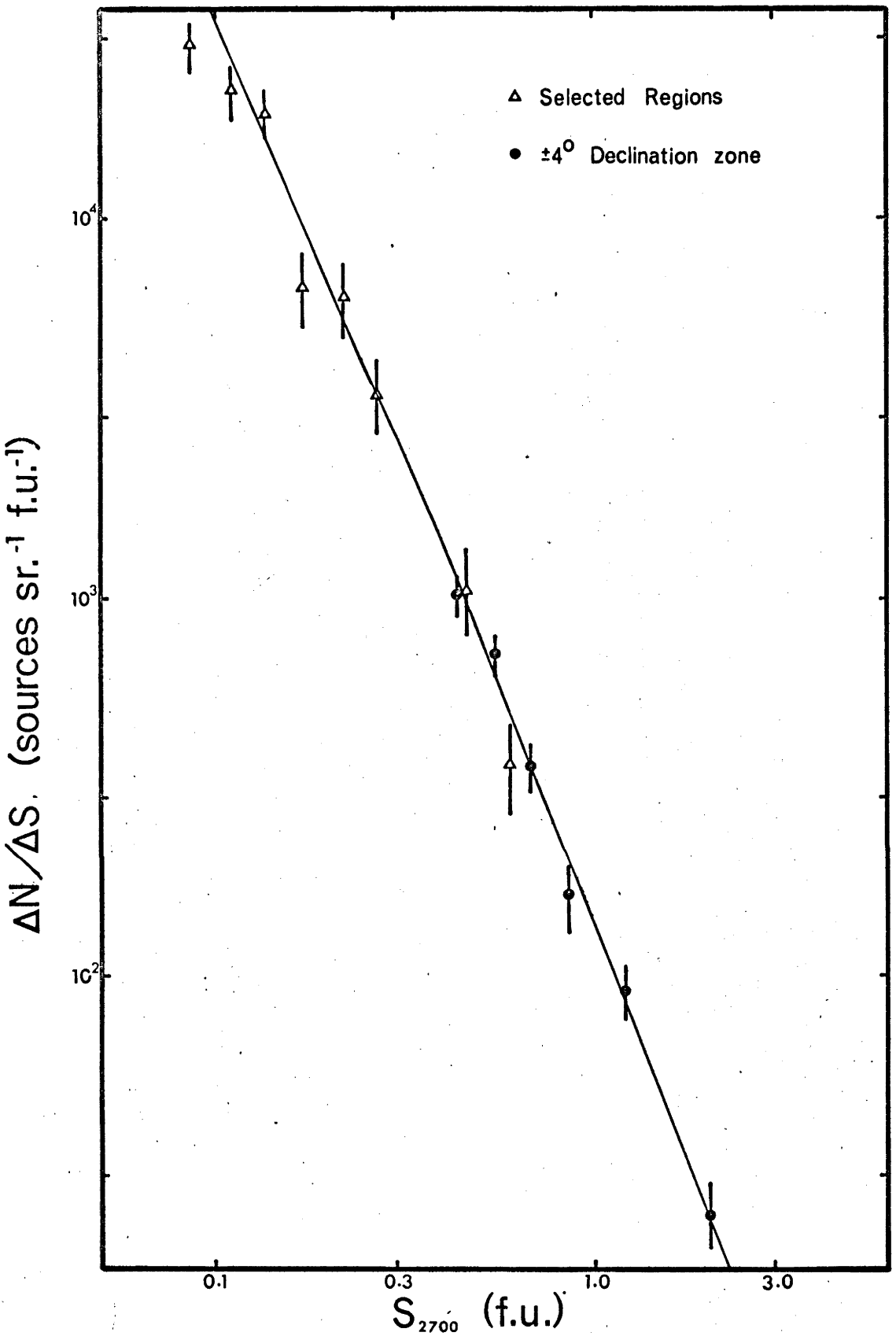

Figure 6.2. The differential source count for the 2700 MHz surveys of the selected regions and the ±4° declination zone. The statistical ($\sqrt{N}$) errors are shown. The line fitted through the high flux density portion has a slope of -2.55.

illustrates Jauncey's second point. The differential count may be fitted by a straight line which just passes through all error bars and which has a slope of -2.40. This is equivalent to a slope of -1.40 in the log N - log S plane (from $dN \propto S^{-(\gamma+1)}dS$) which provides a very good fit to the data in Figure 6.1. However, examination of Figure 6.2 indicates that a gradual decrease in slope of the number - flux density relation with source density is statistically more probable, and that the low source density portion (to, say, N = 200/sr.) is best fitted by a straight line of slope -2.55±.10.

(The survey is not believed to be complete at a level of S_{2700} = 0.085 f.u., and consequently no weight can be given to the point at this level in either diagram).

Refsdal (1969) has presented a simple technique for the formal evaluation of the error in fitting a straight line to any portion of the conventional log N - log S curve. He shows that $\Delta\gamma/\gamma$, the fractional error in the estimate of the slope γ, is given by $F(N_j/N_i)\cdot(N_i - N_j)^{-\frac{1}{2}}$ where N_i and N_j are the numbers of objects greater than S_i and $S_j (S_j > S_i)$. The simple function $F(N_j/N_i)$ tends to unity for $N_i >> N_j$. Figure 6.3 shows the result of this analysis for the 2700 MHz counts. The computed slopes have been plotted against source density, and the results obtained by Refsdal from reanalysis of Gower's (1966) 178 MHz data are also shown. The analysis and this presentation of the number - flux density relation suffer from a shortcoming in that there is no explicit

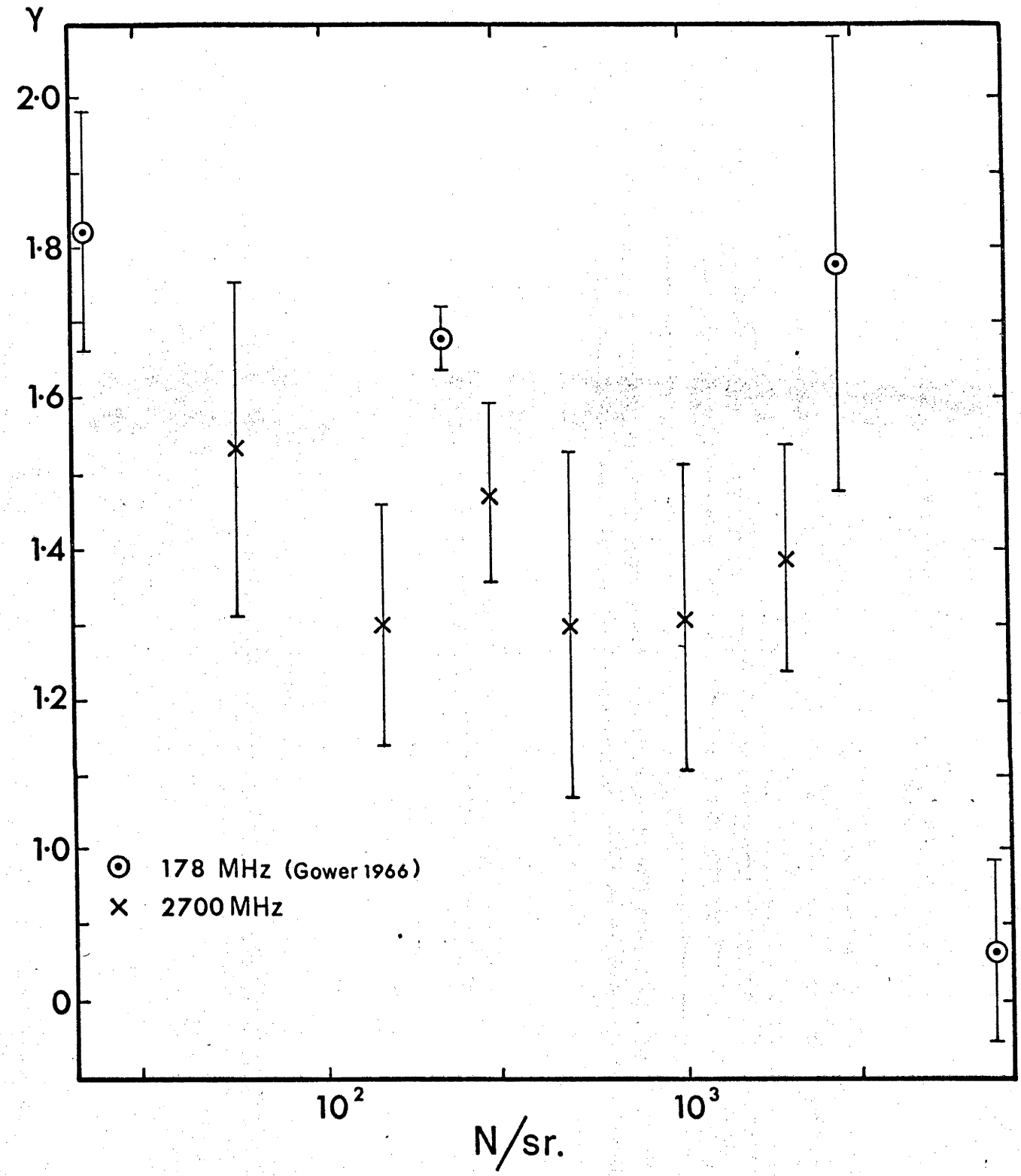

Figure 6.3. The slope (γ) of the integral number - flux density relations at 178 and 2700 MHz versus source density (from the analysis of Refsdal (1969)).

indication of where the derived value of γ should be plotted along the interval in N (or S) considered. In Figure 6.3, the average value for S_{2700} in each interval considered was computed and converted to a source density N_{2700} via Figure 6.1. The same procedure was used in plotting the results obtained by Refsdal from Gower's 178 MHz counts, Gower's conventional log N - log S curve being used to obtain the $\overline{S}_{178}$ - N_{178} translation. Examination of Refsdal's Figure 2 indicates that he used a different procedure which unfortunately is not discussed. A formal combination of the first three 2700 MHz points of Figure 6.3 gives $\gamma = 1.43 \pm .09$ for the interval 50 to 300 sources/sr., and of the remaining three points gives $\gamma = 1.35 \pm .11$ for the interval 300 to 2500 sources/sr.

All presentations of the number - flux density relation and all attempts at formal description of these presentations suffer from the same central problem: any formal description requires an a priori assumption on the form of the relation. In particular, the common assumption of straight lines in the log N - log S plane has only one justification - that of ease of description of the relation over a limited range in source density. The most obvious approach is strongly recommended; the data should be presented in tabular and/or the simplest of graphical forms (the integral (Figure 6.1) or differential (Figure 6.2) counts). Comparisons of theoretical computations with such presentations are

just as simple as if precise mathematical descriptions of number - flux density relations were somehow derived.

6.4 Comparison with Counts at 178 MHz and 408 MHz; Answers to Criticisms

The preliminary results of source counts from the 2700 MHz surveys were compared with Gower's 178 MHz counts in SBW. The new results support the conclusion of SBW; the 2700 MHz number - flux density relation indicates the presence of relatively greater numbers of sources at low source densities than does the 178 MHz relation. This result is illustrated in Figures 6.3 and 6.4. In the former, the Refsdal analysis for both frequencies indicates that the initial slope of the 178 MHz relation is significantly higher than that of the 2700 MHz counts. In Figure 6.4, the spectral data of Kellermann, Pauliny-Toth and Williams (1969; referred to as KPW) have been used to derive the distribution of effective spectral indices (178 - 2700 MHz) for the sources in the 3CR catalogue. Assuming no dependence of this distribution on S_{178} (see, e.g. Williams *et al.* 1968), Gower's counts, scaled in flux density by a factor of 1.08 (§4.7) have been convolved with the histogram to yield a prediction of the 2700 MHz number - flux density relation. The difference in initial slope is again apparent.

In Figure 6.4 the result of a similar convolution of the 408 MHz relation of Pooley and Ryle (1968) is also shown. The distribution in effective indices (408 - 2700 MHz) again

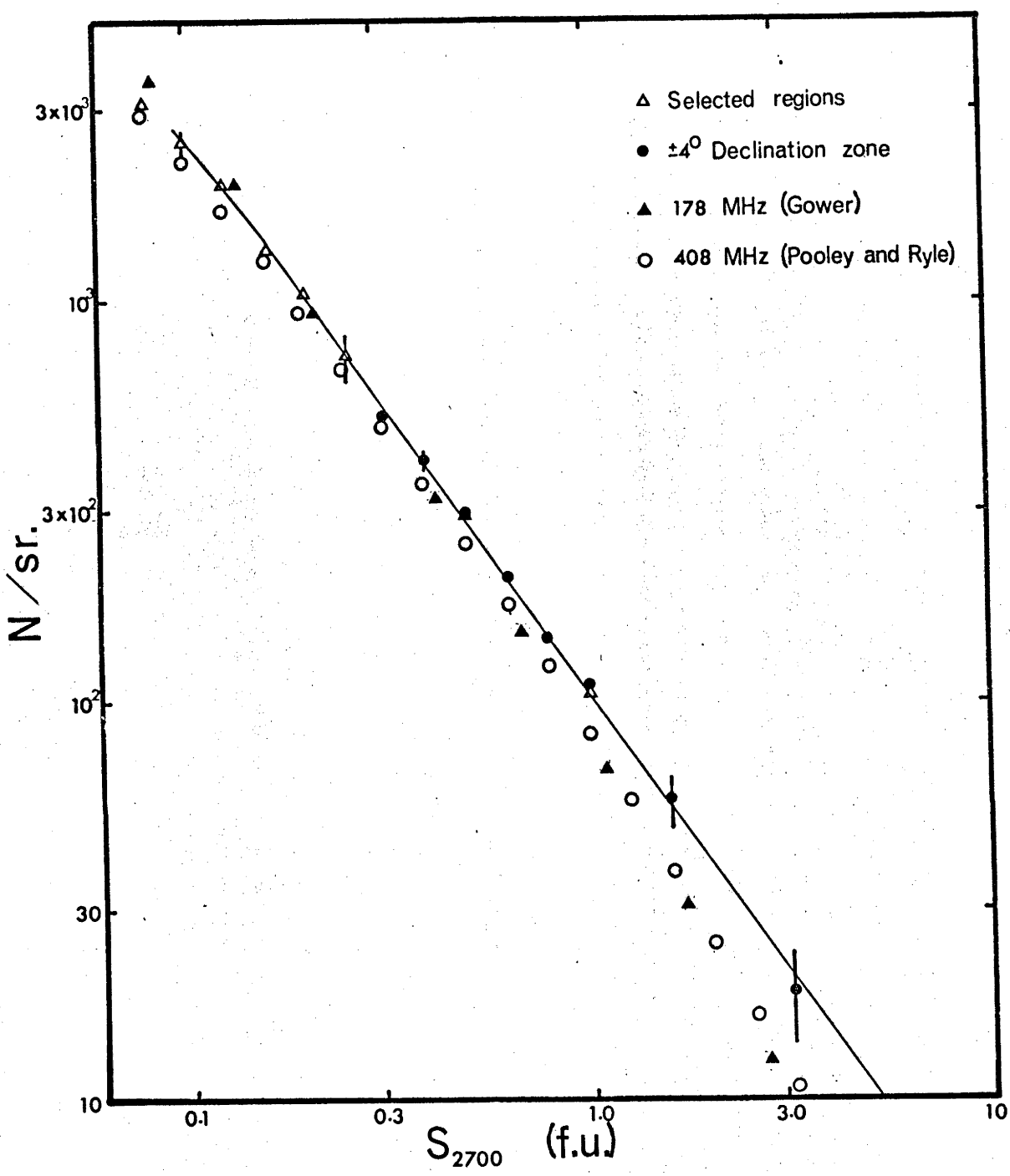

Figure 6.4. The 2700 MHz number - flux density relation of Figure 6.1 compared with the 178 MHz count of Gower (1966) and the 408 MHz count of Pooley and Ryle (1968), each convolved to 2700 MHz as described in the text.

has been derived from the data of KPW, by interpolating between the 178 and 750 MHz flux densities. The procedure is not strictly valid in that the sample of sources forming the effective index distribution is from a 178 MHz survey rather than a 408 MHz survey, and consequently contains too few sources of flat spectra. In Figure 6.4 this is apparent in the displacement of the computed 2700 MHz relation from that observed. The form of the predicted 2700 MHz relation is in better agreement with the 2700 MHz observations than that obtained from the 178 MHz counts; the difference may not lie outside the statistical uncertainties. Proper scaling of flux densities and use of the correct effective index distribution would help to settle the question.

After the difference between the 178 MHz and 2700 MHz number - flux density relations was noted and discussed by SBW, several criticisms were published (Pooley 1968a, 1968b; Kellermann, Pauliny-Toth, and Davis 1968; van der Laan 1969). These are now considered.

Pooley (1968a) pointed out that the best fit line through the Cambridge 408 MHz counts (which were not available to SBW) has the same slope as the 2700 MHz counts of SBW for the range of source densities 300 to 3000/sr. Figure 6.4 indicates that the point is not in dispute, and that the 408 MHz counts may be compatible with the 2700 MHz number - flux density relation at source densities well below 300/sr. Pooley further stated that the 408 and 178 MHz counts were

similar in form to within statistical uncertainties, and thus implied that the differences between the 178 and 2700 MHz counts were unimportant. As can be seen from Figures 6.3 and 6.4, this is not the case. Pooley also contended that the counts of SBW were in conflict with the counts from a 1420 MHz survey by Galt and Kennedy (1968). It is shown in the next section that the effects of large errors in flux density due to low signal - to - noise ratio have seriously affected these 1420 MHz counts, and that in consequence no such conclusion may be drawn. In attempting to disprove the existence of any dependence of spectrum on flux density, pointed out by SBW to be requisite if source counts at different frequencies were dissimilar in form, Pooley stated that observations of faint sources at 1407 MHz showed a similar distribution in spectral index to that found for 3C catalogue sources. This is to be expected: Pooley himself remarked on the similarity of the form of the number - flux density relations at the higher source densities. Because the divergence in the relations occurs at the lowest source densities, any dependence of spectrum on flux density will be most marked for the brighter sources, as discussed in §6.6. Pooley's final point that the "four or five sources with unusual spectra...cannot be held responsible for the (initial) slope of -1.8 found in other surveys" is not valid unless it is clear that a count at a particular frequency is of greater significance than counts at other frequencies. The conclusion of Pooley's communication,

in which he suggests that "it would be inappropriate to reinstate a steady-state model of the universe on the present evidence" is also not in contention; this suggestion was not made in SBW. The same points are raised in Pooley's second criticism (1968b), but now the rider is added: "It would, of course, be surprising if some differences (in the form of the source counts) were not found since some sources exhibit unusual spectra."

Kellermann, Pauliny-Toth and Davis (1968; referred to as KPD) have made limited surveys at 5000 MHz, and on the basis of these and other considerations, criticize all aspects of SBW. They claim to have discovered an excess of flat spectrum sources at the higher source densities, implying a dependence of spectrum on flux density in the sense opposite to that shown by SBW to be necessary if the 2700 MHz and 178 MHz counts differ in the manner apparent in Figures 6.3 and 6.4. Their result is based on observations of only 9 sources in a small survey area which was specifically chosen (for the Cambridge 5C1 survey) as being devoid of strong sources in the 3C and 4C catalogues. The procedure used by SBW to obtain a prediction of the 2700 MHz source count from the 178 MHz counts of Gower was criticized by KPD on two grounds. Firstly they pointed out that the counts of Gower do not extend to low enough flux levels. In the SBW computation, these counts were extrapolated by one order of magnitude in flux density. Little error was consequently introduced because the samples of

sources from low frequency catalogues contain few with flat spectra, and the result of the convolution is hence insensitive to the extrapolation assumed. Secondly KPD pointed out that the wrong spectral index distribution had been used for the convolution. This question was explicitly discussed in SBW. KPD claim to have carried out the convolution in precisely the manner described at the beginning of this section. It is difficult to see how they arrived at the conclusion that "above a flux density of 0.3 f.u. at 2700 MHz there is no significant deviation between the computed number - flux count and the observational data of SBW."

Van der Laan (1969) introduced a notation for discussing number - flux density relations and spectral index distributions at different frequencies. His subsequent analysis appears to be almost identical to unpublished calculations carried out by Wall prior to publication of SBW. Van der Laan concluded that the Parkes counts at 2700 MHz have been overestimated at source densities below 100/sr. because there is no supporting evidence in the literature for the spectral conditions which must be met for reconciliation with the 178 MHz counts. Both SBW and the present catalogues which give a sample size double that of SBW do provide such evidence. The difference in the form of the 2700 MHz number - flux density relation is due to the presence of sources which are strong at this frequency and apparently below the flux limits of the 178 MHz surveys. Further discussion of this

point is presented in §6.6.

6.5 Comparison with Number - Flux Density Relations at Other Frequencies

In Figure 6.5, the number - flux density relations at 178, 408, and 2700 MHz are shown together with three other such relations near 1400 MHz which are now discussed.

(1) The counts from a survey at 1420 MHz by Galt and Kennedy (1968) were invoked by Pooley (1968a) as evidence of overestimation of the 2700 MHz counts of SBW at low source densities. These counts (Galt and Kennedy Figure 3) indicated a slope of -1.88 in the log N - log S plane in the range of source densities 55/sr. to ∿3/sr. for sources well away from the galactic plane. The serious effect of errors in the flux densities on these counts does not appear to have been recognized, as no attempts to derive the requisite corrections have been described by Galt and Kennedy or by Pooley. The magnitude of the errors is such that the effects described in §6.2 become interrelated, and in addition the error distributions in flux density will no longer be Gaussian. A first approximation to the number - flux density relation has been derived using the programme described in §6.2, and assuming the errors quoted by the authors to be the standard errors of normal distributions. From the result shown in Figure 6.5, it is apparent that at source densities where the counts are free from the effects of flux density errors, statistical

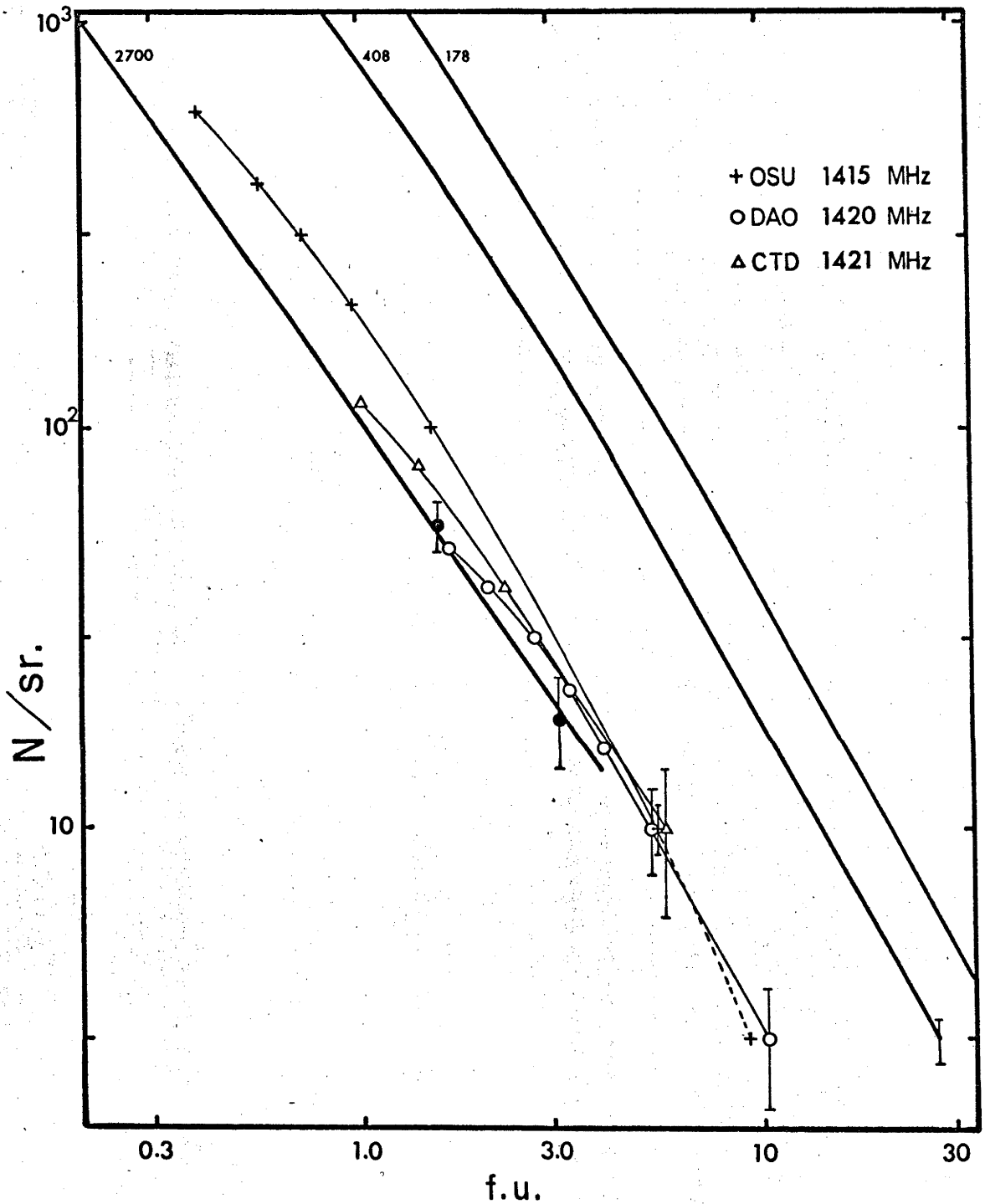

Figure 6.5. Number - flux density relations at several frequencies. The curves shown for 2700, 408, and 178 MHz are those of §6.2, Pooley and Ryle (1968), and Gower (1966) respectively. The relations at frequencies near 1400 MHz are those discussed in §6.5.

uncertainties are such that the form of the relation is indeterminate. Moreover, the rapid flattening of the relation at source densities above 30/sr. (when compared to the OSU 1415 MHz counts discussed below) indicates that the survey is probably complete to about half the source density of 0.55/sr. suggested by Galt and Kennedy. It is certain that there is no discrepancy between counts from the DAO survey and the 2700 MHz number - flux density relation of §6.2.

(2) The number - flux density relation from the CTD survey at 1421 MHz (Kellermann and Read 1965) has been estimated by means of the programme of §6.2, using the counts shown by Kellermann and Read in their Figure 1 and the flux density errors which they quote. The form of this relation when compared to the OSU count indicates that the survey is probably complete to a level of S_{1421} = 1.5 f.u. (∿75 sources/sr.) rather than to 1.15 f.u. as suggested by the authors. The counts are from a small sample (∿140 sources) and the derived number - flux density relation shows no marked difference in form when compared to the 2700 MHz relation.

(3) The OSU surveys at 1415 MHz (Scheer and Kraus 1967; Dixon and Kraus 1968; Fitch, Dixon, and Kraus 1969) provide the most significant counts of sources in this part of the radio spectrum. The number - flux density relation shown in Figure 6.5 has been derived from the counts presented by Dixon and Kraus (1968) and Fitch, Dixon, and Kraus (1969) in the manner described for the two surveys discussed above. This

relation is the only one derived at a frequency above 1000 MHz to show definite evidence of steepening to the lower flux densities. Some of this steepening may be due to undetected partial resolution of a fraction of the stronger sources, but the size of the beam (10 × 40 arc minutes) makes it doubtful that the relation could have been seriously affected.

The differences apparent between the three number - flux density relations derived near 1400 MHz appear to lie within uncertainties due to flux scaling and to the numbers of sources involved in the counts.

If one accepts the number - flux density relations of Figure 6.5 at face value, than at source densities of ∿200/sr. the slope of the relation is ∿-1.5 for all frequencies. It is suggested that below this source density, the relations at all frequencies steepen, but that the source density at which the onset of steepening occurs (and possibly the magnitude of this steepening) decreases as frequency increases. Significant steepening of the 2700 MHz relation may not occur before source densities as low as 30/sr.; in this regard a survey of an additional 0.8 sr. of the southern sky is nearing completion (A. J. Shimmins, personal communication), and the further doubling of the sample size anticipated for source densities above 500/sr. will be of considerable interest.

6.6 The Difference between the Number - Flux Density Relations at 2700 and 178 MHz

From a limited survey carried out simultaneously at frequencies of 750 and 1410 MHz, Hoglund (1968) obtained source counts which showed marked steepening at low source densities and which were identical in form to the 178 MHz (4C) counts for the same area. The results of a count of the 4C sources in the $\pm 4^{\circ}$ declination zone to a level of $S_{178} = 5$ f.u. (150 sources/sr.) is shown in Figure 6.6, together with the 2700 MHz counts for the same zone. (For sources stronger than $S_{178} = 5$ f.u. in the 4C catalogue, the 2700 MHz survey revealed only a few cases of confusion in this zone; e.g. 4C-01.4 ≡ PKS 0053-015 and 0053-016; 4C+01.24 ≡ PKS 0906+01 and 0906+011; 4C+03.31 ≡ PKS 1502+036 and 1502+039. The errors in this 4C count due to confusion and/or resolution are thus much smaller than statistical uncertainties due to the limited number of sources in the count.) The statistical probability of the two counts indicating number - flux density relations of the same slope is not negligible; however, the precise agreement in form found by Hoglund is most certainly not present.

SBW showed that if a change in form of the number - flux density relation between 178 and 2700 MHz was real, then it must be paralleled by a dependence of effective index $\alpha_{178-2700}$ on flux density. The calculations illustrated in Figures 5.3(b), (c), and (d) show the change in effective index

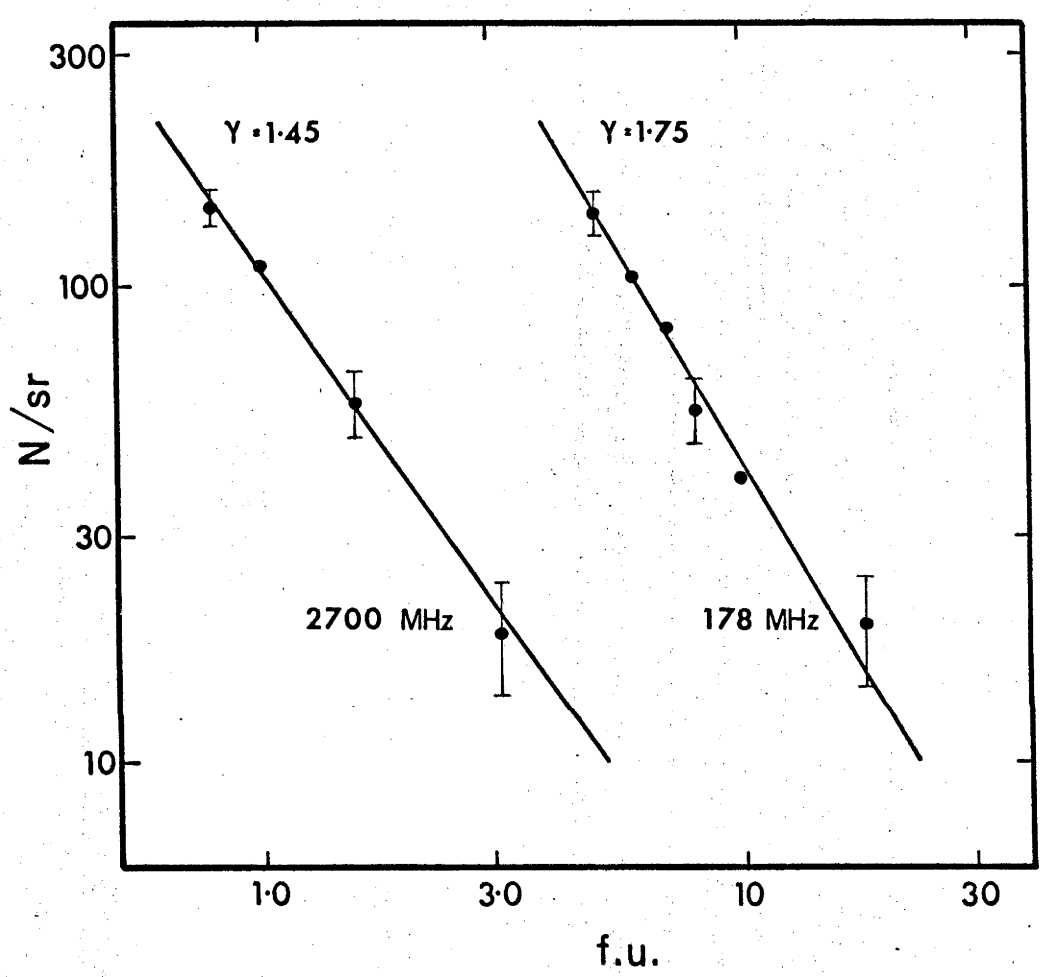

Figure 6.6. Source counts for the ±4° declination zone from the 4C catalogue (178 MHz) and the 2700 MHz survey.

distributions with 2700 MHz flux level expected if number - flux density relations at the two frequencies are as in Figure 6.5. Two difficulties are encountered in testing for the existence of this effect. Firstly, the forms of the number - flux density relations become similar at source densities >300/sr. and the relatively small numbers available for the lower source densities limit the significance of the result. Secondly, for many of the sources in the 2700 MHz catalogue, the 178 MHz flux densities are not available. Thus only the two ranges in 2700 MHz flux density, $0.64 \leq S_{2700} < 1.01$ f.u. and $S_{2700} \geq 1.01$ f.u. have been considered. Effective indices $\alpha_{178-2700}$ were obtained for all sources in the 2700 MHz catalogues for these ranges. (For several of the sources which are apparently below the limit of the 4C catalogue, flux densities at 178 MHz were estimated by extrapolating the higher frequency data.) Histograms for the sources in these two ranges of 2700 MHz flux density appear in Figure 6.7. There is a significant difference between them which is most apparent in considering the fraction of each sample below $\alpha_{178-2700} = 0.4$. This fraction is 0.38 for the sample of $S_{2700} \geq 1.01$ f.u., and 0.28 for the sample of $0.64 \leq S_{2700} < 1.01$ f.u. The median effective index for the former sample is 0.55, and for the latter 0.64. The difference between the samples is in the sense required by the observed difference in the number - flux density relations.

In Figure 6.7, the predicted distributions in

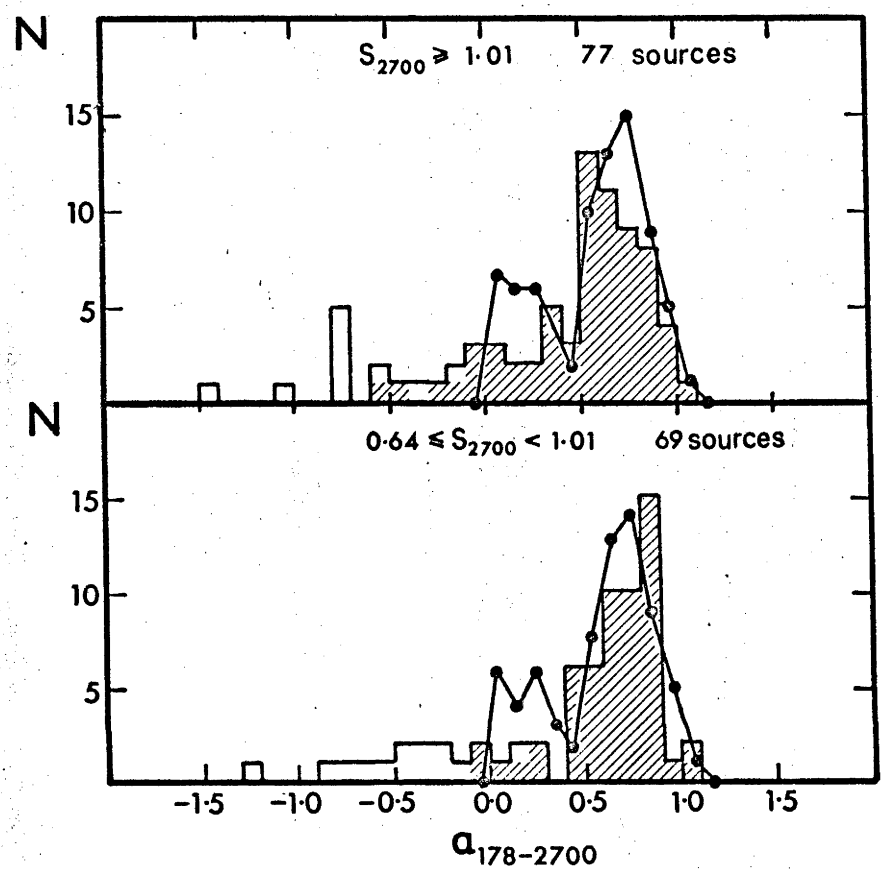

Figure 6.7. Histograms of effective indices 178 - 2700 MHz for sources catalogued in the 2700 MHz survey of the $\pm 4^{\circ}$ declination zone. The non-shaded areas represent sources for which the 178 MHz flux density has been estimated from extrapolation of the spectrum to the lower frequencies. The distributions represented by the dots are the predicted distributions calculated as described in §5.3.

effective index, calculated in the manner described in §5.3 for the number - flux density relations of Figure 6.5, are also shown. These distributions have been normalized to the sizes of the samples in the two flux density ranges. They show a somewhat smaller difference than the observed distributions.

The dependence of effective index on flux density indicated that differences might appear in the distributions of the low and high frequency spectral indices. The distributions for α_{LF} and α_{HF} ($\alpha_{LF} \simeq \alpha_{700}$; $\alpha_{HF} \simeq \alpha_{2700}$; see §5.1) in the two ranges of 2700 MHz flux density considered above are shown in Figure 6.8. The translation of the more intense sample to the flatter spectra is apparent for both the α_{LF} and α_{HF} distributions.

Observations indicating (1) different slopes of the number - flux density relation for sources counted in surveys of the same region of sky at widely separated frequencies, and (2) a dependence of distributions of effective indices at these two frequencies on flux density for these sources, are obviously not independent phenomena, and serve only as a measure of self-consistency in interpretation. The reality of the suggested difference in forms of the number - flux density relations depends on the accuracy to which the relations derived from the $\pm 4^{\circ}$ declination zone represent those obtained over much larger areas of sky.

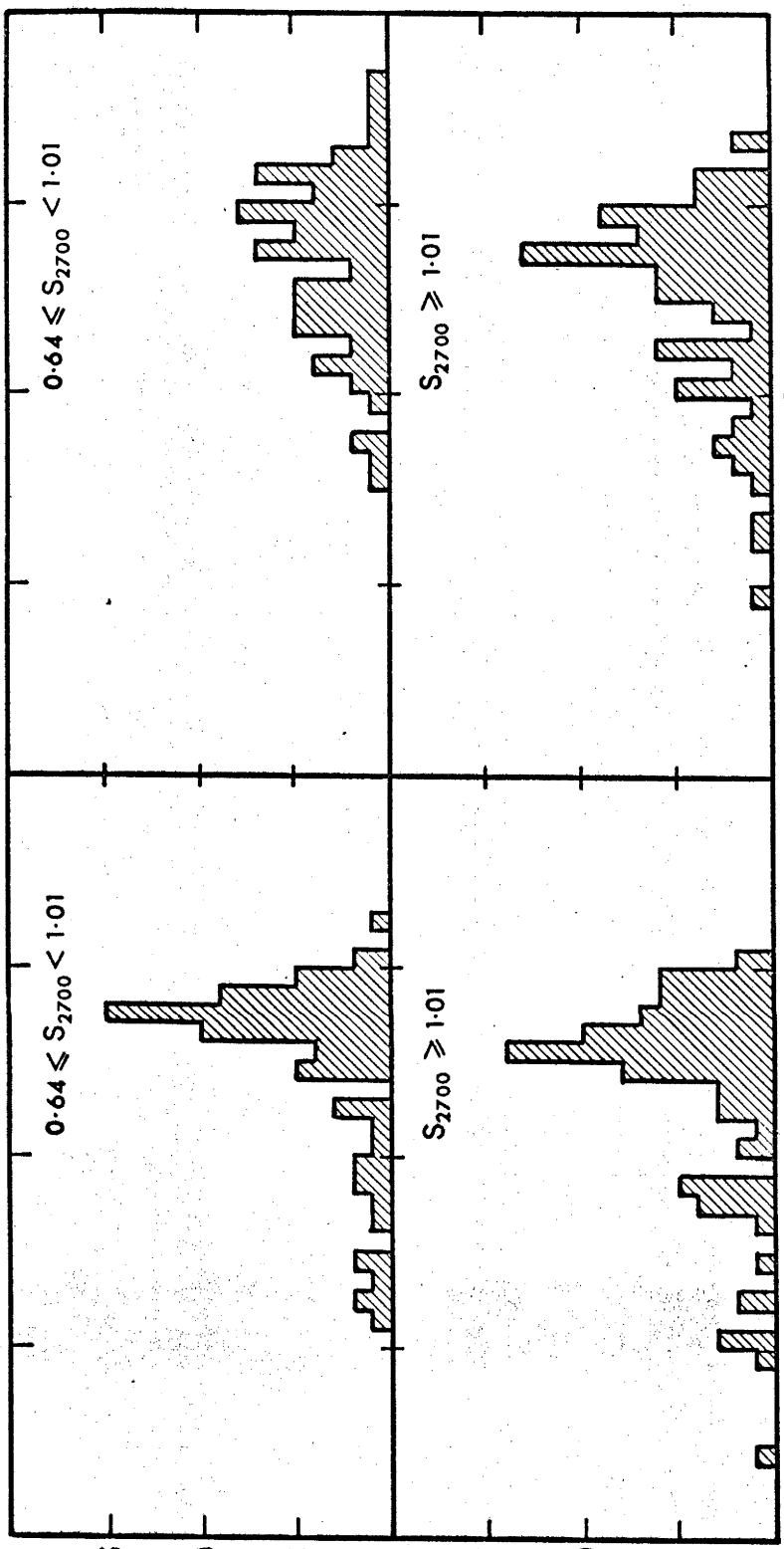

Figure 6.8. Distributions of the low and high frequency spectral indices (see §5.1) for the complete samples of sources catalogued at 2700 MHz in the two ranges of 2700 MHz flux density under consideration.

6.7 The Dependence of Spectrum on Flux Density

The dependence of spectrum on 2700 MHz flux density suggests the following:

(1) Suppose that the QSO's and radio galaxies have number - flux density relations with very different slopes at 2700 MHz. If the QSO relation is flatter than that of the radio galaxies, then samples of sources in decreasing intervals of flux density will contain decreasing proportions of QSO's. Because the QSO's as a class have flatter spectra than radio galaxies (§5.5), samples in different intensity ranges of sources catalogued at 2700 MHz will show a dependence on spectrum in the sense found in the previous section. Moreover, the spectral selection effect of survey frequency ensures that the majority of objects in catalogues of sources compiled at 178 MHz are radio galaxies. The result is that little dependence of spectrum on flux density for the sources from a survey at such a frequency would be expected if the foregoing should prove to be correct.

(2) As an alternative, suppose that the QSO's and radio galaxies have approximately the same form of number - flux density relation at 2700 MHz. One or both of these classes then must exhibit a dependence of spectrum on 2700 MHz flux density in the sense found for the samples of the preceding section. This possibility is now discussed; the former is considered in §6.8.

For the sources of the 4C catalogue (amongst which

radio galaxies predominate) little dependence of spectrum on flux density has been found (e.g. Long et al. 1966). It is therefore most likely that if one class of identification were to be responsible for the dependence of the spectra of sources catalogued at 2700 MHz on 2700 MHz flux density (and consequently for the change in initial slope of the number - flux density relation) then that class should be the QSO's.

Two - frequency diagrams provide a convenient method of studying the question. These are shown for 2700 MHz and 178 MHz in Figures 6.9 and 6.10 for the radio galaxies and the QSO's in the 2700 MHz catalogue of the $\pm 4^{\circ}$ declination zone. The diagram for galaxies shows a concentration to the effective spectral index line 0.8 and it is clear that surveys at either frequency reveal radio galaxies with a similar distribution in effective spectral index at any flux level within the ranges presently being considered. A similar grouping of sources to the effective index line 0.8 occurs in the QSO diagram, and from the point of view of a survey at 178 MHz, it dominates the effective index distribution at all flux levels to the limit of 4C. However, at 2700 MHz this group only becomes important towards the limiting flux density (S_{2700} = 0.35 f.u.) of the $\pm 4^{\circ}$ declination zone survey, and clearly shifts the median spectral index from a low value at the high flux density levels (where the distribution is dominated by flat and inverted spectrum sources) to a higher value at the survey limit.

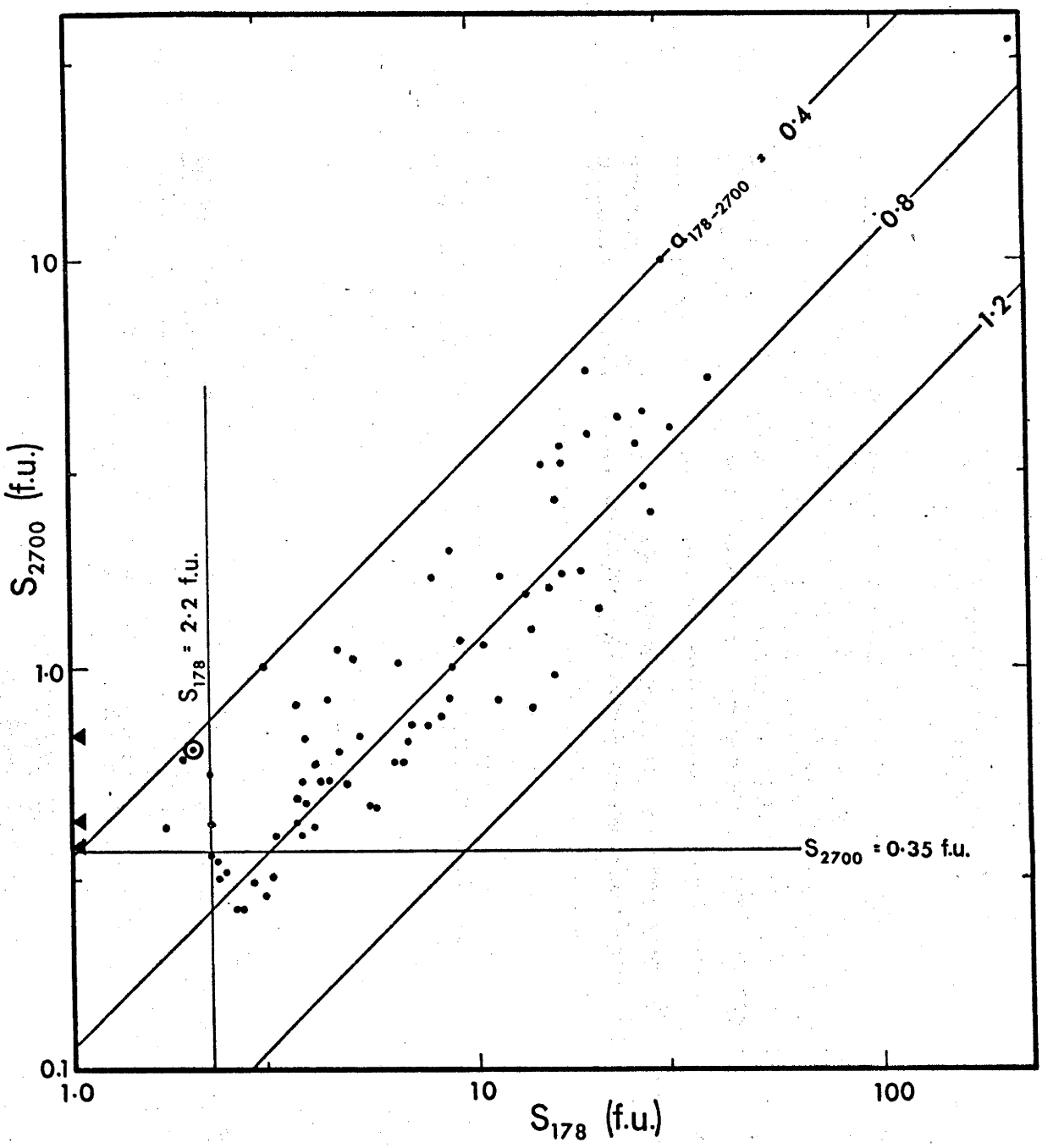

Figure 6.9. Two-frequency diagram for radio galaxy identifications in the ±4° declination zone of the 2700 MHz catalogue. Circled point indicates a source for which the estimate of the 178 MHz flux density is unreliable. Arrowheads indicate upper limits to flux densities at 178 MHz.

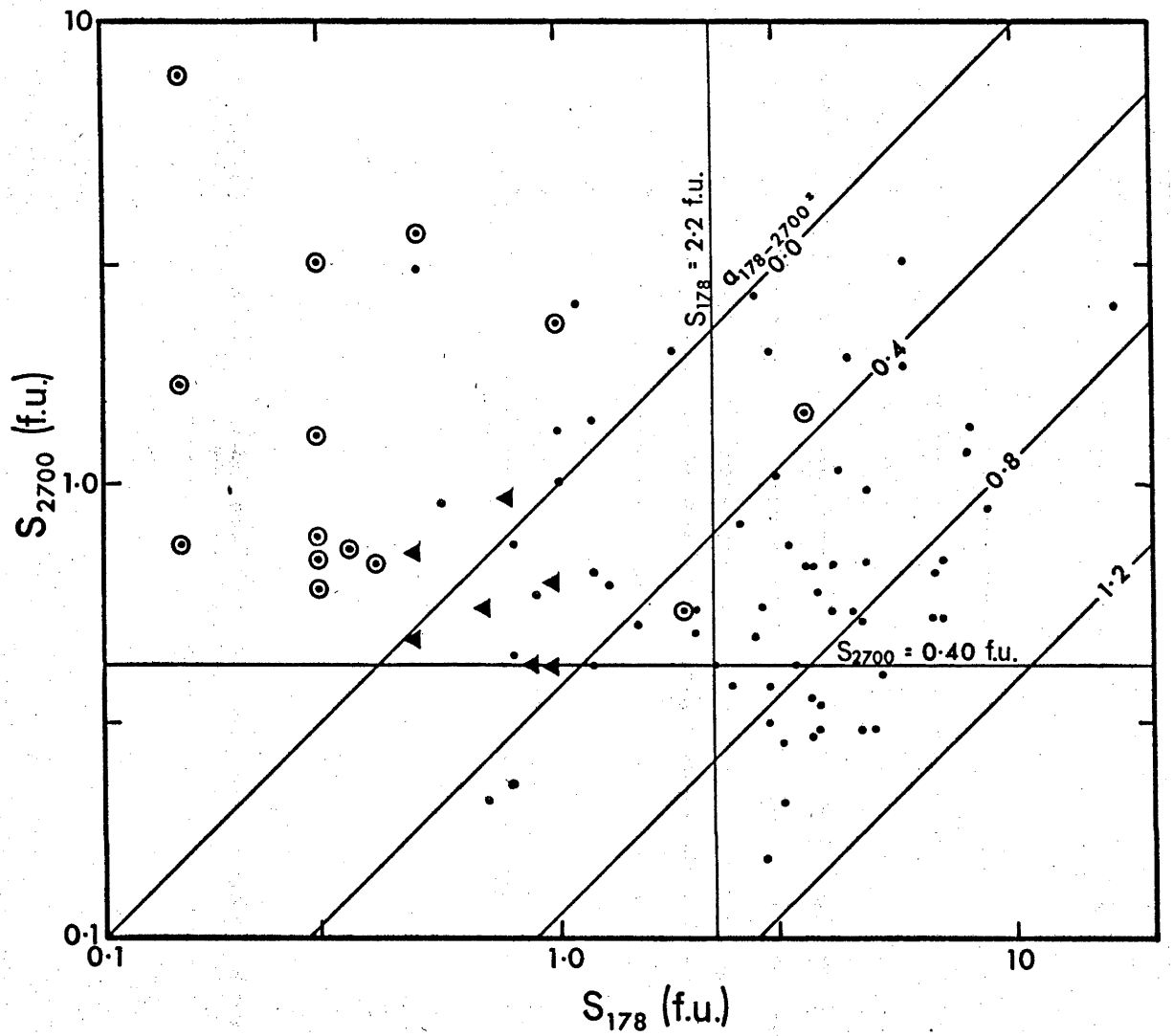

Figure 6.10. Two-frequency diagram for the QSO and QSO? identifications in the ±4° zone of the 2700 MHz catalogue. Circled points indicate sources for which the estimate of the 178 MHz flux densities are unreliable. Arrowheads indicate upper limits to flux densities at 178 MHz.

That the high frequency spectrum of QSO's found in the 2700 MHz survey also indicates a dependence on flux density at 2700 MHz has been mentioned in §5.6. To illustrate the effect with greater clarity, the two frequency diagram for 5009 MHz and 2700 MHz has been plotted in Figure 6.11 with the data from Figure 5.6 for the QSO's alone. A similar diagram has been plotted for the QSO's identified in the Parkes (408 MHz) catalogue, using 2650 MHz flux densities from Shimmins et al. (1966) and Shimmins (1968a), and 5009 MHz flux densities from Shimmins, Manchester, and Harris (1969). The same steepening of the high frequency spectrum with decreasing intensity level is apparent.

Further evidence that the QSO's are responsible for the dependence of spectrum on 2700 MHz flux density for sources catalogued at this frequency is provided by Figure 6.12. The distributions shown are those of Figure 6.8 save for the removal of the QSO's. It is apparent that all dependence of both high and low frequency spectral indices on flux density has been eliminated.

6.8 Source Counts for QSO's and Radio Galaxies

In Figure 6.13 the source counts for the radio galaxy and QSO identifications from the 2700 MHz catalogues for the selected regions and the $\pm 4^{\circ}$ declination zone are shown. When the unidentified sources are added to these counts such that 25% are assigned to the QSO's and the remainder to the radio

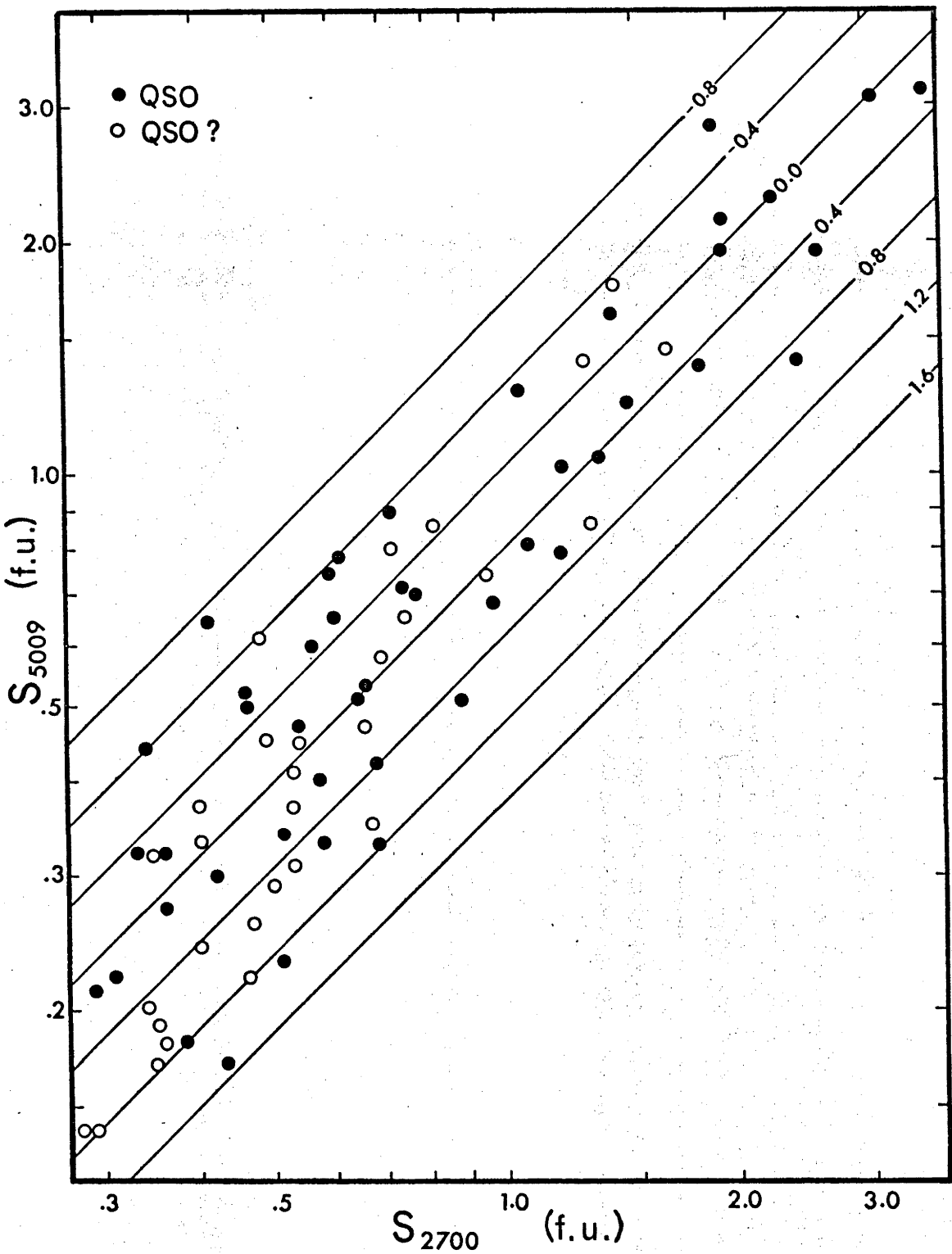

Figure 6.11. Two-frequency diagram for QSO's and QSO?'s in the ±4° declination zone of the 2700 MHz catalogue. The 45° lines indicate constant effective indices, 2700 - 5009 MHz.

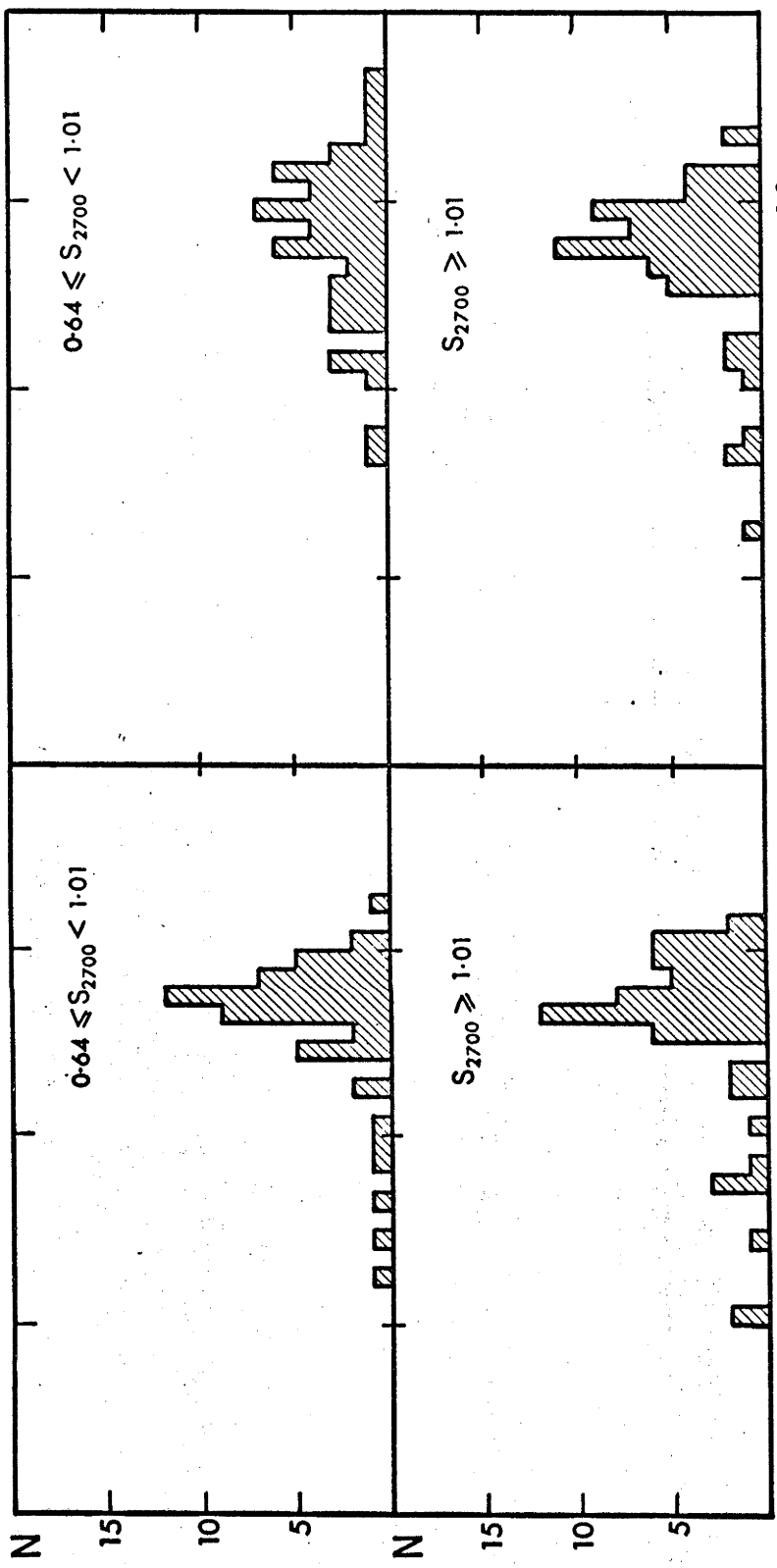

Figure 6.12. Distributions of the low and high frequency spectral indices for the samples of Figure 6.8 with the QSO's and QSO?'s removed.

galaxies (§5.6), both counts are appreciably steepened as shown in the diagram. There is then evidence that the number - flux density relation for the radio galaxies is of steeper slope than that for the QSO's. This result depends upon the classification of the unidentified sources; to equalize the slopes, more than 50% would have to be QSO's. The analysis of §5.6 indicates that this is highly unlikely, and a further argument in favour of the suggested division is given in §7.3. (The error bars shown are representative of the statistical uncertainty and do not include the ∿10% uncertainty in the classification of the unidentified sources.)

If the radio galaxies show no dependence of spectrum on flux density as the previous section has indicated, then the number - flux density relation for these objects must be of the same form as that found at lower frequencies. Bolton (personal communication) has recently re-analysed the identification data from the $+20^{\circ}$ to -20° declination zone of Parkes (408 MHz) catalogue, and has constructed a source count of radio galaxies + 75% of the unidentified sources. There is good agreement in form between this count and that of Figure 6.13.

On the other hand, the dependence of spectrum on 2700 MHz flux density for the QSO's found in the 2700 MHz surveys indicates that the number - flux density relation at this frequency must be flatter than that obtained from the low frequency surveys. At the same source densities, Bolton's

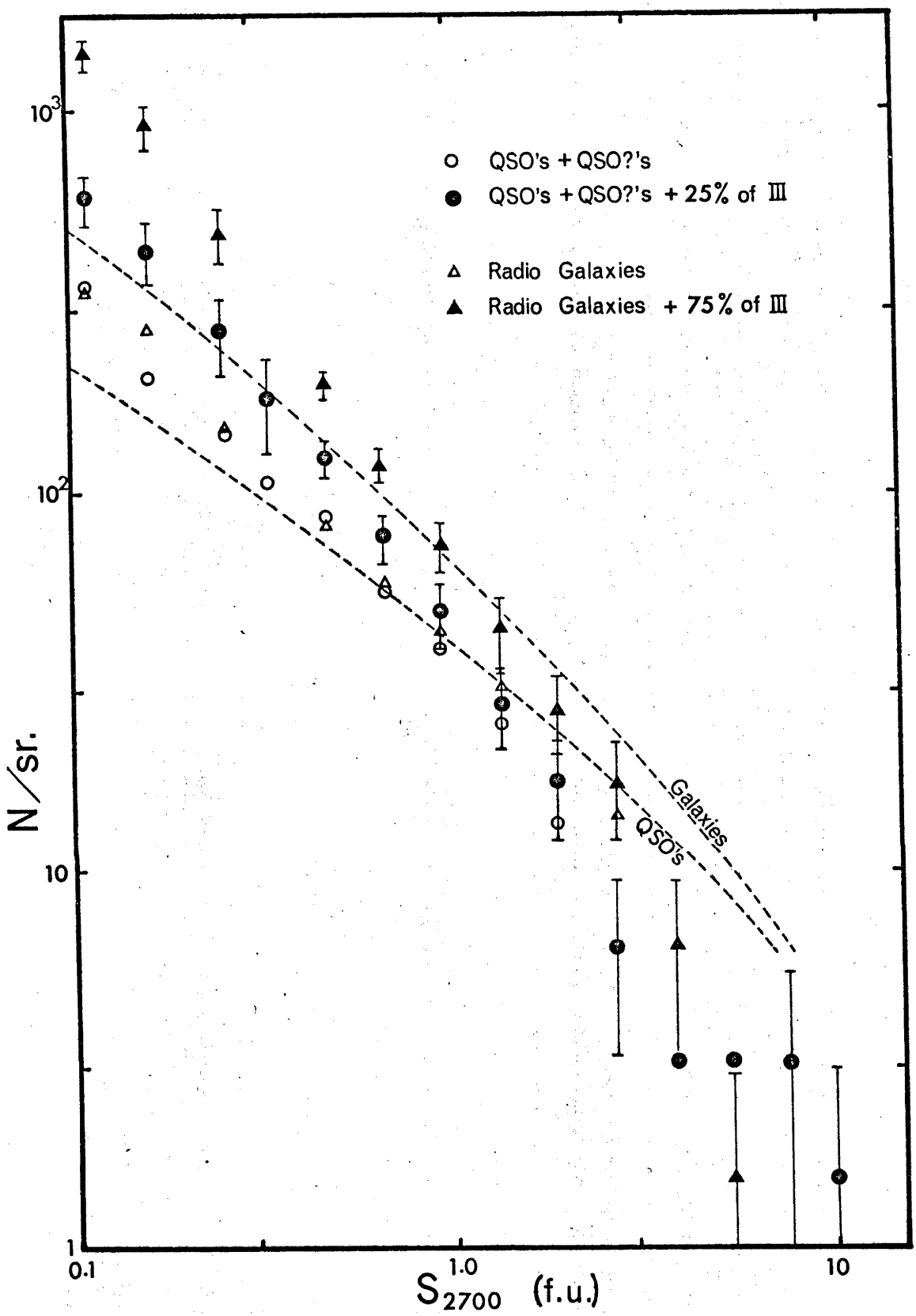

Figure 6.13. Source counts for the identifications from the 2700 MHz surveys of the $\pm 4^{\circ}$ declination zone and the selected regions. Some of the area of the $\pm 4^{\circ}$ zone has been excluded because of possible obscuration. The error bars shown represent the statistical uncertainties. The dotted curves are the number - flux density relations computed for a non-evolutionary Friedmann universe, as described in Chapter 7.

count for the QSO's + 25% of the unidentified sources is indeed considerably steeper than that of Figure 6.13.

From a consideration of surface brightnesses derived from 1425 MHz interferometry, Fomolont (1968) concluded that sources of high surface brightness (a high proportion of which are QSO's) had a source count at this frequency significantly steeper than that of sources of low surface brightness. The result is in direct conflict with that obtained in this section, and it appears that Fomalont's sample must suffer from serious incompleteness. Furthermore, he has overinterpreted integral source count data in precisely the manner pointed out to be erroneous by Jauncey (1967), although he refers to Jauncey's work in his introduction.

The results of the last two sections indicate that the change in form of the number - flux density relation with frequency, and the consequent dependence of spectrum on flux density, is in fact due to a combination of the two explanations suggested at the beginning of §6.7. Of the two possible effects, however, the dependence of spectrum on 2700 MHz flux density is dominant. The radio galaxies appear to show no change in form of the number - flux density relation with frequency, and no dependence of spectrum on flux density. The QSO's appear to have a steeper relation than the radio galaxies at the low frequencies, a slightly flatter relation than the radio galaxies at 2700 MHz, and a spectrum which is dependent on flux density at 2700 MHz. The implications are discussed in the following chapter.

CHAPTER 7

INTERPRETATION OF THE NUMBER - FLUX DENSITY RELATION

A simple numerical technique is presented in this chapter to derive luminosity functions and to investigate number - flux density relations at different frequencies. Computations have been carried out for two popular models of the universe (a Friedmann model with $\Lambda = 0$, $q_o = +1$; and the steady-state model) with the assumption of no evolution in power or density for the radio sources involved. The results are compared with the observations.

7.1 Previous Investigations of the Significance of Source Counts

There have been many attempts, both analytical and numerical, to examine the significance of experimentally determined number - flux density relations. Early work was carried out by McVittie (1957), Priester (1958), Davidson (1959), Mills (1960), Minkowski (1960), Hoyle and Narlikar (1961, 1962), and Ryle and Clarke (1961). Of the later investigations, the numerical approach of Longair (1966) appears to offer the greatest promise in that any form of the geometry, luminosity function, radio spectrum or evolution can be considered. Moreover these may be considered for different source populations which may then be combined. Longair's conclusions were that the form of the 178 MHz source counts indicated (i) evolution of a class of high luminosity sources

(which he tentatively identified as the QSO's), and (ii) a cut-off (source density zero) beyond $z \simeq 4$. The result is in essential agreement with those of previous investigations with the exception of that of Hoyle and Narlikar. The "hierarchal" model of the steady-state theory proposed by these authors is mentioned in §7.5.

Chapters 3, 4, 5, and 6 have shown that in comparison to low frequency catalogues, a sample of sources catalogued from a 2700 MHz survey exhibits a different initial slope for the number - flux density relation, a dependence of radio spectrum on flux density, a large proportion of sources whose spectra deviate dramatically from power laws, and a considerable increase in the ratio of identified QSO's to radio galaxies. It is clear that any theory suggested to explain the low frequency source counts must satisfy the conditions imposed by the present results. In none of the previous investigations have the results been transferred from one frequency to an another, although a few authors speculate briefly on the problem (e.g. McVittie 1965; Kellermann, Pauliny-Toth, and Davis 1968). Moreover, the influence of the form of the radio spectrum has rarely been considered.

In this chapter a simple numerical technique is described for the investigation of source counts at different frequencies. Any geometry, evolution, luminosity function, or radio spectrum may be incorporated. Development of the technique stems from a conversation with Dr. Allan Sandage, in

which he suggested that the radio counterpart of the classic "m - logπ diagram" might be useful in examining the spatial distribution of radio sources in a manner similar to that in which the diagram was used to examine the distributions of stars and absorbing material.

7.2 The Computational Technique; S - z Diagrams

The computations have been carried out in the form of S - z (flux density - redshift) diagrams. In these, each column i represents a range about S_i, the flux density at a particular frequency ($S_{i+1} < S_i$), and each row j represents a range in redshift about z_j ($z_1 \simeq 0$ and $z_{j+1} > z_j$). The ranges spanned by each column and row are narrow enough so that the area in every element (i,j) of the diagram may be approximated by (S_i, z_j). The analogy to the m - logπ diagram is evident, and exact save for the fact that the interpretation of stellar parallax evokes less controversy than that of QSO redshift. For a particular class of object, assumptions of a metric, a radio spectrum and a radio luminosity function (abbreviated hereinafter to RLF) enable computation of the number of radio sources in any element of the diagram as described below. The summation of the entries in column i to row j gives the number of sources between $S_i + \Delta S/2$ and $S_i - \Delta S/2$ at all redshifts $< z_j$; the summation of the entries in row j to any flux density S_i gives the number of sources at redshift z_j down to a level S_i. If the diagram extends to redshifts large enough that

entries in column i become zero, then the number - flux density relations down to S_i (in either differential or integral forms) are available from the summation of each column.

The approach is clearly similar to that of Longair's, and the same flexibility is present. However, the S - z diagram has the advantage over the P - z diagram which he computes in that it is a plot of observed quantities. The S - z diagram is a direct display of the manner in which the source counts build up by the contribution of each class of object from a particular volume (redshift) shell. Moreover, the technique avoids the use of the confusing term "luminosity distribution".

Sources appearing in element (S_i, z_j) of the S - z array must radiate (into 4π sr. and in their rest frame) a power at the frequency at which the array is being compiled given by

$$F_{i,j} = 4\pi \left[D(z_j)\right]^2 \cdot S_i \cdot (1 + z_j)^{\alpha_j - 1} \qquad - \quad (7.1)$$

where $D(z_j)$ is the luminosity distance for the cosmological model being considered,

and α_j is the effective spectral index (defined in the sense used previously) between the frequency of the S - z diagram and $(1 + z_j)$ times this frequency.

The factor $(1 + z_j)^{\alpha_j - 1}$ corrects for the effects of "K - dimming" and bandwidth expansion. In the absence of evolution, the number of sources appearing in element (S_i, z_j) is then

given by:

$$N_{i,j} = \psi(F_{i,j}) \cdot \Delta V_j \cdot \Delta F_{i,j} \qquad - \quad (7.2)$$

where $\psi(F_{i,j})$ is the RLF, i.e. the number of sources per unit volume with radio power outputs between $F_{i,j}$ and $F_{i,j} + dF_{i,j}$,
ΔV_j is the co-moving volume element, or shell, between redshifts $z_j + \Delta z/2$ and $z_j - \Delta z/2$,
and $\Delta F_{i,j}$ is the element in power corresponding to the finite width of element (i,j) in the S - z plane.

The calculations described herein must be regarded as preliminary. They were performed on the IBM 1620 computer at Mount Stromlo Observatory; the relatively small core storage (40K) did not provide a serious limitation on the size of the S - z array which could be examined. The luminosity functions and geometries used are both in the form of sub-programmes which may easily be altered for different populations, model universes, or evolutions. The radio galaxies have been divided into 7 different spectral classifications, and the QSO's into 16. Each spectral classification is described by 10 pairs of (S_ν, ν) entered as data from which the α_j's of equation 7.1 are computed. The final output is the S - z array for each class of object, with integral and differential counts computed for each level S_i in the array.

In the present computations, the Hubble constant H_o has been assumed as 75 km. $sec.^{-1}$ Mpc^{-1} (Sandage 1968a) and two models have been tried: $\Lambda = 0$, $q_o = +1$ (a closed universe

with positive curvature), and the steady-state model. The luminosity distances in these universes are given by (see e.g. McVittie 1965):

$$\begin{aligned} q_o &= +1 \qquad D = cz/H \\ q_o &= -1 \qquad D = cz(1 + z)/H \end{aligned} \qquad - \quad (7.3)$$

The volume elements were derived from Sandage (1961). Each entry in his Table 3 is $(\log V(z_j) - 6.131)$ for $H_o = 75$ km. $sec.^{-1}$ Mpc^{-1}.

The luminosity functions for each class of object, spectrum, and geometry have been derived at 2700 MHz and 178 MHz from comparison of the observed and computed S - z diagrams as is now described.

7.3 Luminosity Functions for Radio Galaxies

The determination of luminosity functions by comparison of computed and observed S - z arrays requires knowledge of redshifts for all radio galaxies and QSO's in samples complete to known flux density limits. Only 19 redshifts are known for the approximately 130 radio galaxy identifications of Chapter 3. However, the form of the optical luminosity function for radio galaxies suggests that it is possible to estimate redshifts for the remainder from their apparent magnitudes.

7.3 (i) Optical Luminosity Functions for Radio Galaxies

Sandage (1967) has shown that for radio galaxies, plots of log z versus apparent magnitude (corrected for aperture effect, K - dimming, and galactic absorption) show a dispersion of less than one magnitude about a line with a slope of 5. The relatively narrow optical luminosity function which this implies permits rough estimates of redshifts from apparent magnitudes alone.

Figure 7.1 is a diagram of log z versus $(m_{pg})_o$ for the 19 galaxies in the $\pm 4^\circ$ declination zone catalogue for which redshifts have been measured. The values of $(m_{pg})_o$ have been derived from Miss Merkelijn's estimates of m_{pg} with corrections for galactic absorption of $0^m.25 \mathrm{cosec}(b^{II})$. (The coefficient $0^m.25$ is intermediate between those suggested by Peterson (1969) and Shane and Wirtanen (1967).) The line

$$(m_{pg})_o = 22.0 + 5 \log z \qquad - \quad (7.4)$$

provides quite a good representation of this limited sample, and the scatter is similar to that found by Sandage (1967). If the correct absorption coefficient has been assumed, the relation implies $M_{pg} = -21.0 \pm 1.0$ for $H_o = 75$ km. sec.$^{-1}$ Mpc^{-1}. In using equation 7.4 to estimate the redshift, $(m_{pg})_o = 12^m$ gives $z = 0.010 \pm .006$, and $(m_{pg})_o = 20^m$ gives $z = 0.40 \pm .15$.

There is an additional uncertainty in the use of equation 7.4 to estimate redshifts for the 2700 MHz galaxy identifications; the 19 galaxies in the sample above are

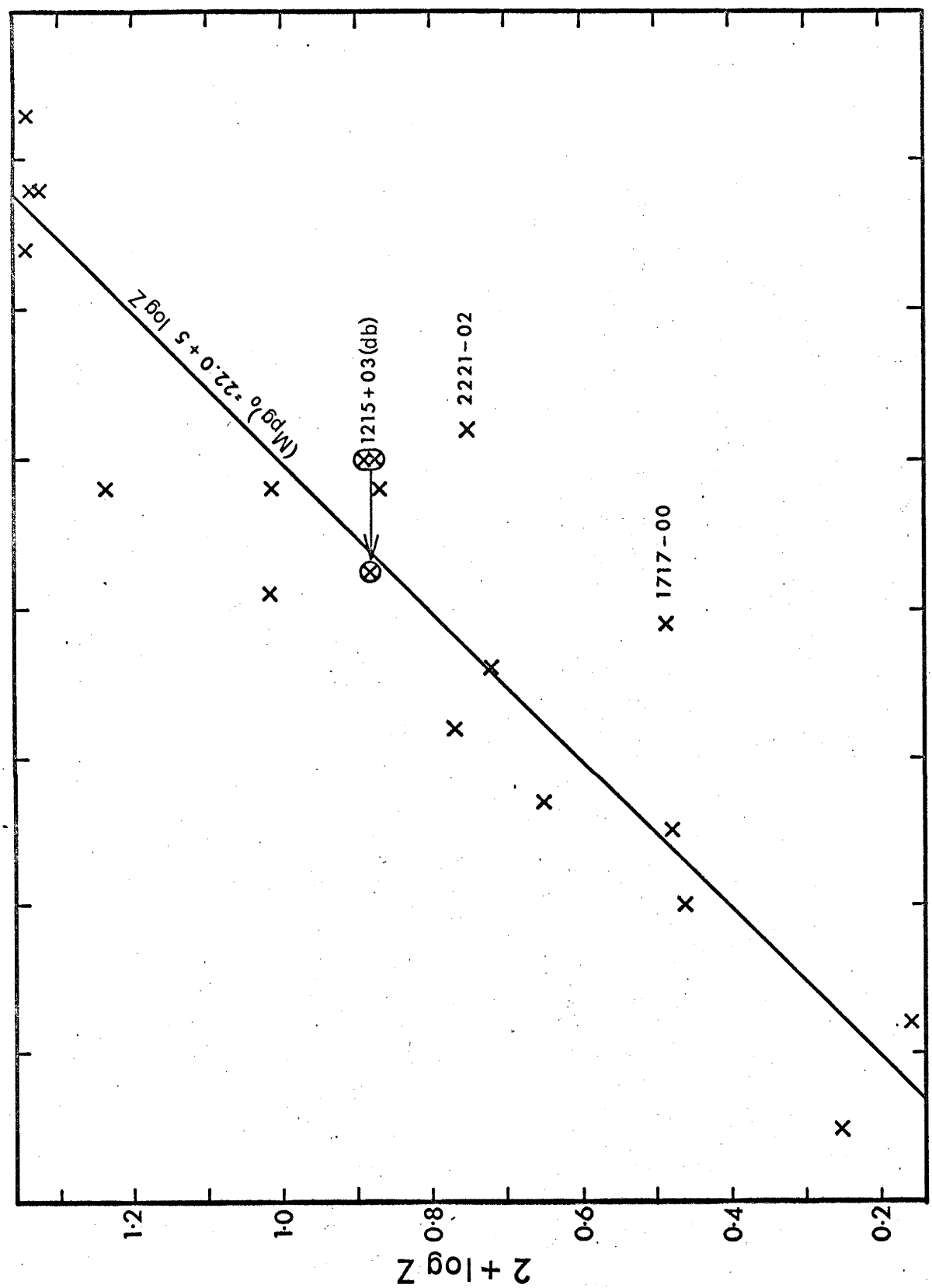

Figure 7.1. Redshift - apparent magnitude diagram for radio galaxies in the ±4° declination zone.

exclusively from low frequency surveys. In §3.1 there are several cases in which the galaxy identified as the radio source is fainter than neighbouring galaxies which are obviously members of the same cluster. Thus the optical luminosity function for the radio galaxies of the 2700 MHz survey possibly contains an increased proportion of galaxies having lower optical luminosities. An overestimation of several of the redshifts may have resulted.

Figure 7.2 is the S - z array for galaxy identifications in the first two parts of the 2700 MHz catalogue. Some areas in the $\pm 4^{\circ}$ declination zone have been excluded because of possible absorption. The redshifts have been estimated from equation 7.4 with corrections for galactic absorption applied as described above. The array shown has been prepared for the $\Lambda = 0$, $q_o = +1$ geometry; the appearance of the steady-state diagram is similar.

7.3 (ii) Radio Luminosity Functions for Radio Galaxies

In the region of Figure 7.2 for which $S_{2700} < 2$ f.u., the steady increase in population of the elements as redshift increases indicates that short of some universal miracle at the plate limit, considerable numbers of radio galaxies are required to populate the elements for redshifts greater than that corresponding to the plate cut-off. Moreover, if the unidentified sources in the flux density ranges corresponding to the columns of Figure 7.2 are considered, it is clear that

z \ S_{2700}	35.3	25.0	17.7	12.55	8.89	6.30	4.46	3.16	2.24	1.58	1.122	0.795	0.563	0.398	0.282	0.200	0.1415	0.1002
0.00068																		
0.00162																		
0.00256																		
0.00406								∘∘										
0.00643												∘∘ ∘∘	•	•				
0.01019														•				
0.01615								•			•							
0.0256						•		•			•			•	•			
0.0406								∘∘				•	∘∘	•	∘∘	∘∘		
0.0643							∘	•	•	••	•	∘		••	∘		∘	∘
0.1019							•			•	•		•	∘∘∘	••	∘∘	∘	
0.1615	x								x	•••	•••	•	•••	∘∘∘	∘∘	∘	∘∘	∘
0.256							•		••	••	•	∘∘∘	∘∘∘ x	∘∘∘	∘∘∘	∘		
0.406											xx		•	•••	∘∘∘	∘∘∘	∘	∘
0.562													•					x
0.707										x		xx x	xx		x			
0.891									x	x	xx							
1.121									x	x			x					
1.615					x							x				xx		
2.56									xx					x				
4.06																		
$\frac{3}{4}$ x III =	-	-	-	-	-	-	-	2	3	3	11	20	32	54	∘-10 •-54	23	34	40

Figure 7.2. The 2700 MHz S - z array for the $\Lambda = 0$, $q_o = +1$ model. The filled circles represent radio galaxies in the catalogue for the $\pm 4^o$ declination zone, some areas of which have been omitted from this analysis because of possible obscuration. The open circles represent radio galaxies in the selected region catalogues. QSO's with measured redshifts are shown as crosses. The heavy vertical line represents the completeness limit for the $\pm 4^o$ zone survey. The heavy horizontal line is at $(m_{pg})_o \doteq 19.4$ for radio galaxies, the approximate limit for completeness of optical identification set by the plate cutoff. The bottom row contains 75% of the unidentified sources in each range of flux density.

more than half of them must go to represent these distant radio galaxies for any reasonable RLF. There is thus strong support for the estimate of §5.6 which placed 75% of the unidentified sources in the radio galaxy category on the basis of spectral characteristics.

Figure 7.2 is evidently too sparsely populated in the region above the plate limit for any formal derivation of the 2700 MHz RLF for radio galaxies. S - z diagrams were hence computed for various assumed RLF's and compared with Figure 7.2. In making the comparisons, the following two simple criteria were found to provide the severest constraints in deriving an acceptable RLF.

(1) The numbers in the elements of Figure 7.2 increase quite slowly towards the plate limit, and this requires a relatively flat initial (low-power) portion for the RLF, as is illustrated below.

(2) Assuming that (i) $(m_{pg})_o = 19.4$ ($z = 0.314$) represents the apparent magnitude to which galaxy identifications are complete as set by the Sky Survey plate limit, and (ii) 75% of the unidentified sources are distant radio galaxies, then the ratio of radio galaxies at $z < 0.314$ to those at $z > 0.314$ may be estimated as a function of flux density from Figure 7.2. This ratio plotted against 2700 MHz flux density is shown in Figure 7.3 (for $\Lambda = 0$, $q_o = +1$). The error bars represent statistical uncertainties due to sample size, and do not include possible errors due to the above

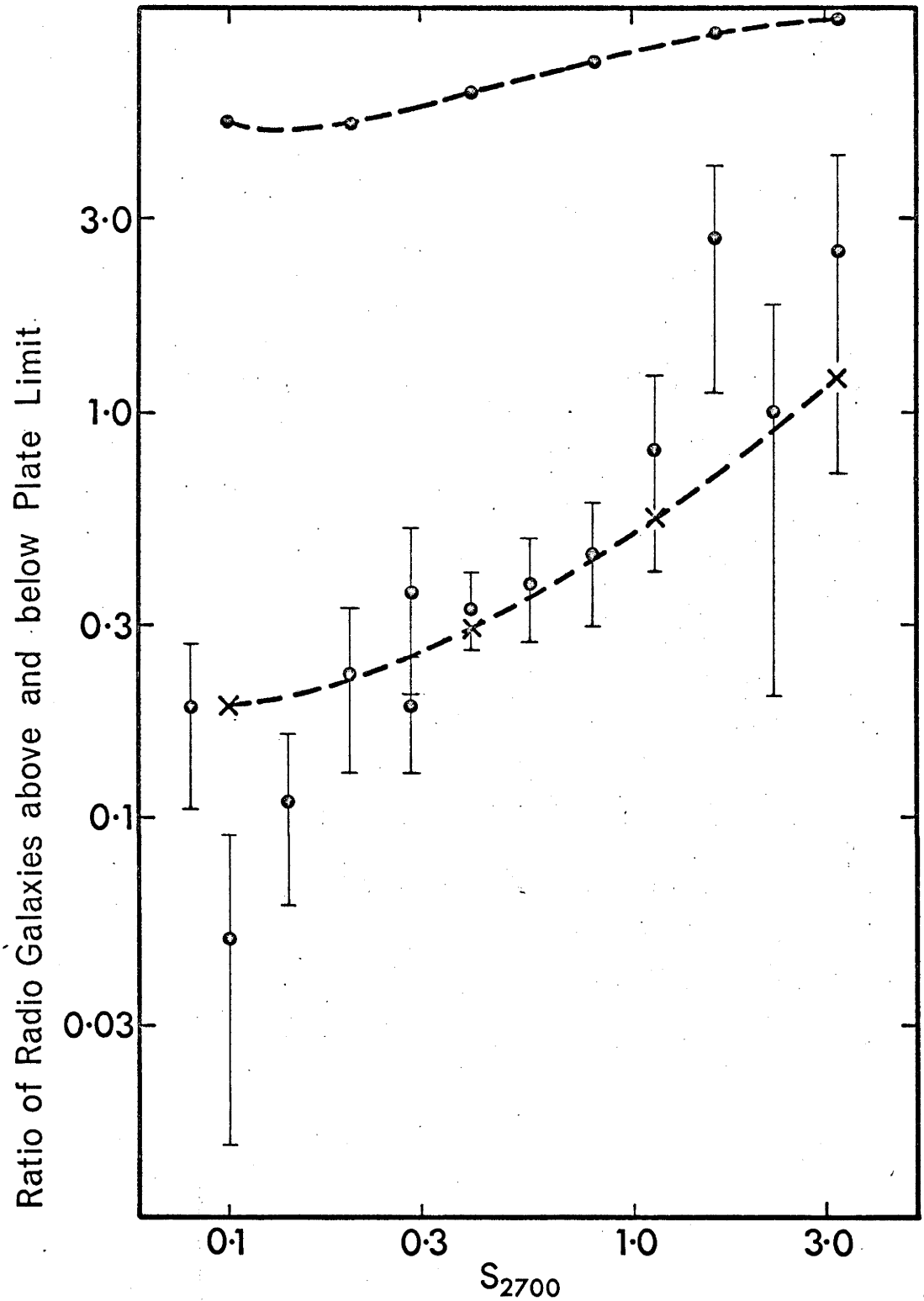

Figure 7.3. The ratio plotted against 2700 MHz flux density (f.u.) is described in detail in the text. The dots joined by the dashed line result from the S - z array computed using the RLF suggested by Petrosian for 178 MHz with translation to 2700 MHz. The crosses joined by the dashed lines result from the S - z array computed with the galaxy RLF of Figure 7.4. The diagram is for the Friedmann model ($\Lambda = 0$, $q_o = +1$).

assumptions. The form of this diagram indicates that the RLF must steepen for radio luminosities higher than those corresponding to the relatively flat initial portion required by criterion 1. Again this is illustrated in the following.

All trial computations to derive the 2700 MHz RLF for radio galaxies were carried out assuming a spectral index of 1.0. As is shown in §5.5, this is a close approximation to the spectral behaviour of these objects at frequencies above 2700 MHz. Moreover, if the 2700 MHz RLF for radio galaxies derived below is used with spectral indices in the range 0.6 to 1.4 in computing S - z diagrams, the differences in the forms of these diagrams are insignificant in relation to the statistical uncertainties in comparing these with Figure 7.2.

A first approximation to an RLF for the 2700 MHz radio galaxies in the ($\Lambda = 0$, $q_o = +1$) geometry was obtained from the work of Petrosian (1969). He computed luminosities at 178 MHz in this geometry for all 3C radio galaxies with measured redshifts. These were used to obtain a simple (178 MHz) RLF for these objects of the form

$$\psi(F) = -aF + K \qquad \log F_1 < \log F < \log F_2 \qquad - \quad (7.5)$$

where a and K are constants. This RLF was translated to 2700 MHz by using the effective spectral index $\bar{\alpha}_{178\text{-}2700} = 0.78$. A mean effective index very close to this value is obtained for radio galaxies from both the data of KPW and the data of Appendix IV. The values derived for the

constants in equation 7.5 for this first approximation were $a = 2.4$, $K = 28.18$, $\log F_1 = 23.08$, and $\log F_2 = 27.58$. A portion of the 2700 MHz S - z array computed with this RLF and geometry is shown in Table 7.1, and it is evident that neither criterion described above is satisfied. Furthermore, reducing the value of a to satisfy criterion 1 resulted in S - z arrays containing too many radio galaxies at large redshifts to satisfy criterion 2. Consequently it was necessary to abandon the simple form of equation 7.5 and to adopt RLF's which steepen with increasing luminosity.

Figure 7.4 indicates the result of a considerable amount of further such comparison procedure. The RLF shown for the $\Lambda = 0$, $q_o = +1$ geometry, meets both criteria quite well, and has been normalized so that the number - flux density relation computed from the S - z diagram passes through the point $N = 70.0$, $S_{2700} = 0.94$ for the galaxy source count of Figure 6.13. A portion of the resulting S - z array is shown in Table 7.2, and the dependence on flux density of the ratio described above as criterion 2 is shown in Figure 7.3. The cut-off at $F_{2700} = 10^{23}$ w. hz^{-1} is evidently only an approximation; galaxies "normal" or "intermediate" in radio power output, a few of which appear in Figure 7.2, are not represented by this RLF. The contribution of such objects to the source counts is insignificant and they are not considered further.

For the steady-state model an RLF very similar in form

TABLE 7.1 THE 2700 MHZ S-Z ARRAY FOR THE RADIO GALAXY RLF DERIVED BY PETROSIAN (FRIEDMANN MODEL, LAMBDA = 0, DECELERATION PARAMETER +1.0)

S(I) = / Z(J)	1.1218	0.7945	0.5627	0.3985	0.2822	0.1998	0.1415	0.1002
0.00068	0.000	0.000	0.000	0.000	0.000	0.000	0.000	0.000
0.00162	0.000	0.000	0.000	0.000	0.000	0.000	0.000	0.000
0.00256	0.000	0.000	0.000	0.000	0.000	0.000	0.000	0.000
0.00406	0.000	0.000	0.000	0.000	0.000	0.000	0.000	0.000
0.00643	0.000	0.000	0.000	0.000	0.000	0.000	0.000	0.000
0.01019	0.323	0.524	0.000	0.000	0.000	0.000	0.000	0.000
0.01615	0.344	0.557	0.904	1.465	2.375	0.000	0.000	0.000
0.02560	0.364	0.590	0.957	1.552	2.516	4.078	6.610	10.715
0.04057	0.377	0.611	0.991	1.607	2.605	4.223	6.846	11.097
0.06430	0.377	0.611	0.991	1.607	2.606	4.224	6.847	11.099
0.10190	0.359	0.583	0.945	1.532	2.484	4.026	6.527	10.580
0.16150	0.320	0.518	0.840	1.363	2.209	3.581	5.805	9.410
0.25600	0.258	0.418	0.678	1.100	1.783	2.890	4.685	7.594
0.40570	0.184	0.298	0.483	0.784	1.271	2.061	3.341	5.415
0.56200	0.067	0.108	0.176	0.285	0.463	0.751	1.217	1.974
0.70750	0.050	0.081	0.132	0.214	0.347	0.563	0.913	1.480
0.89060	0.036	0.059	0.096	0.155	0.252	0.409	0.663	1.075
1.12120	0.024	0.040	0.065	0.106	0.172	0.279	0.452	0.733
1.61500	0.000	0.000	0.064	0.104	0.170	0.275	0.446	0.724
2.56000	0.000	0.000	0.000	0.000	0.062	0.100	0.163	0.264
4.05700	0.000	0.000	0.000	0.000	0.000	0.000	0.000	0.083
6.43000	0.000	0.000	0.000	0.000	0.000	0.000	0.000	0.000
9.19100	0.000	0.000	0.000	0.000	0.000	0.000	0.000	0.000
15.15000	0.000	0.000	0.000	0.000	0.000	0.000	0.000	0.000
1	3.09	5.01	7.33	11.88	19.32	27.47	44.52	72.25
2	8.54	13.55	20.80	32.76	52.08	79.54	124.00	196.30
3	7.94	18.17	37.50	85.98	197.40	396.30	907.00	2078.00

ROW 1 - SUM (N/SR) OF THE CONTRIBUTIONS FROM ALL Z IN THE INTERVAL ABOUT S(I)
ROW 2 - INTEGRAL SOURCE COUNT (N/SR) DOWN TO LOWER LIMIT OF THE INTERVAL S(I)
ROW 3 - DIFFERENTIAL SOURCE COUNT (DN/DS) FOR EACH S(I)
THE LINES CORRESPOND TO THOSE DRAWN IN FIGURE 7.2

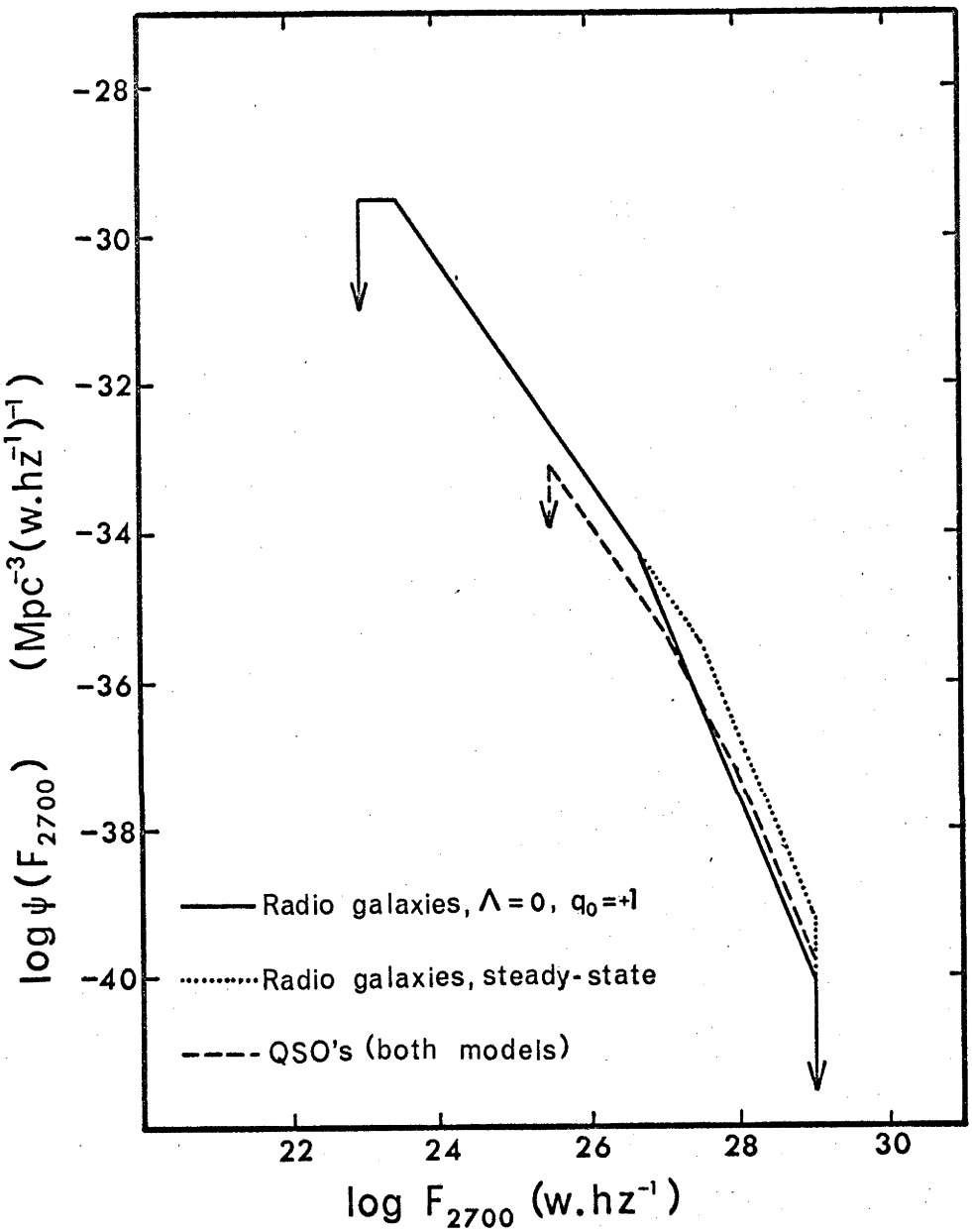

Figure 7.4. Radio luminosity functions derived at 2700 MHz for the two models of the universe considered.

TABLE 7.2 THE 2700 MHZ S-Z ARRAY FOR THE RADIO GALAXY RLF OF FIGURE 7.4
(FRIEDMANN MODEL, LAMBDA = 0, DECELERATION PARAMETER +1.0)

S(I) = / Z(J)	1.1218	0.7945	0.5627	0.3985	0.2822	0.1998	0.1415	0.1002
0.00068	0.000	0.000	0.000	0.000	0.000	0.000	0.000	0.000
0.00162	0.000	0.000	0.000	0.000	0.000	0.000	0.000	0.000
0.00256	0.000	0.000	0.000	0.000	0.000	0.000	0.000	0.000
0.00406	0.000	0.000	0.000	0.000	0.000	0.000	0.000	0.000
0.00643	0.000	0.000	0.000	0.000	0.000	0.000	0.000	0.000
0.01019	0.008	0.005	0.004	0.000	0.000	0.000	0.000	0.000
0.01615	0.033	0.039	0.039	0.027	0.019	0.000	0.000	0.000
0.02560	0.080	0.095	0.113	0.135	0.160	0.135	0.095	0.067
0.04057	0.191	0.227	0.270	0.320	0.381	0.453	0.538	0.639
0.06430	0.438	0.520	0.618	0.735	0.873	1.038	1.233	1.465
0.10190	0.956	1.136	1.351	1.605	1.907	2.266	2.693	3.200
0.16150	1.949	2.316	2.752	3.270	3.886	4.618	5.488	6.521
0.25600	3.605	4.284	5.090	6.049	7.187	8.541	10.149	12.060
0.40570	5.889	6.997	8.315	9.880	11.741	13.951	16.578	19.699
0.56200	2.541	4.585	5.449	6.475	7.694	9.142	10.864	12.909
0.70750	1.820	3.054	5.125	7.350	8.733	10.378	12.332	14.654
0.89060	1.262	2.118	3.555	5.965	9.600	11.407	13.555	16.107
1.12120	0.823	1.380	2.316	3.887	6.522	11.781	14.000	16.635
1.61500	0.755	1.266	2.125	3.566	5.984	10.040	16.846	31.669
2.56000	0.251	0.422	0.708	1.188	1.994	3.346	5.614	9.420
4.05700	0.072	0.120	0.202	0.340	0.571	0.958	1.608	2.698
6.43000	0.018	0.031	0.052	0.088	0.147	0.248	0.416	0.698
9.19100	0.000	0.000	0.017	0.028	0.047	0.080	0.134	0.226
15.15000	0.000	0.000	0.000	0.000	0.000	0.015	0.026	0.044
1	20.70	28.61	38.11	50.92	67.46	88.40	112.18	148.72
2	69.99	98.60	136.00	187.60	255.00	343.40	455.60	604.30
3	53.21	103.80	195.00	368.40	689.30	1275.00	2285.00	4278.00

ROW 1 - SUM (N/SR) OF THE CONTRIBUTIONS FROM ALL Z IN THE INTERVAL ABOUT S(I)
ROW 2 - INTEGRAL SOURCE COUNT (N/SR) DOWN TO LOWER LIMIT OF THE INTERVAL S(I)
ROW 3 - DIFFERENTIAL SOURCE COUNT (DN/DS) FOR EACH S(I)
THE LINES CORRESPOND TO THOSE DRAWN IN FIGURE 7.2

to that described above was found to approximate the steady-state analogue of Figure 7.2 quite well. This RLF is also shown in Figure 7.4.

In Figure 7.5, the $\Lambda = 0$, $q_o = +1$ RLF of Figure 7.4 for radio galaxies has been transformed* to 178 MHz with the spectral index of 0.78. The RLF's derived by Petrosian (1969) and Longair (1966) (with modification by Caswell and Wills (1967)) are also shown. The latter, presented in steps of half radio-magnitude out to $z = 0.01$, has been converted to the form used herein. In comparison with the other two, the RLF derived in the present work is seen to be flatter in the region of the low luminosities, and to contain a much larger proportion of high luminosity radio galaxies. At galactic latitudes higher than 15°, the 3CR catalogue contains about 150 sources identified with galaxies and some 38 unidentified sources (Sandage 1968b), many of which are likely to be distant radio galaxies (Bolton 1966). Petrosian has derived an RLF for these by considering only the 66 radio galaxies for which redshifts were available to him. It is thus almost certain

---

* In this transformation, and in those subsequently mentioned, the form of the original RLF is retained, the limits and "break" points are shifted according to the effective index, and the normalization is such that integration of the function between luminosity limits yields the same volume density of the class of object as that given by the original RLF.

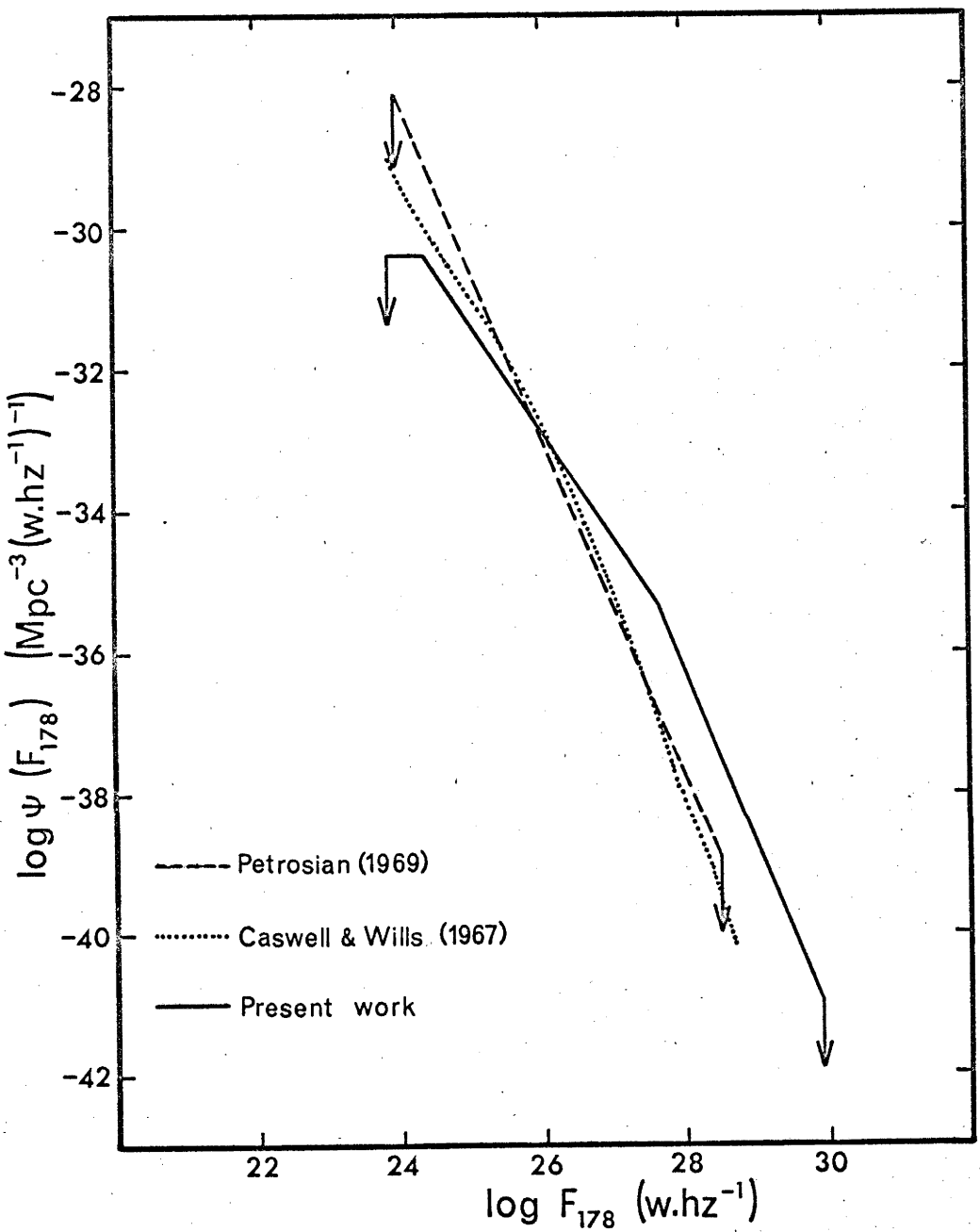

Figure 7.5. A comparison of radio luminosity functions by translation of the results of the present work to 178 MHz.

that his RLF is deficient in high luminosity objects. The RLF presented by Longair is a "local" or "present epoch" one, and provides the best fits to the source counts for the various types of evolution which he finds necessary to invoke. Since he proposes evolution in power or density of a class of the most luminous sources, the local RLF is certain to contain a lesser proportion of such objects than the RLF derived in the present work. Conversely, because no evolution has been assumed, "local" or "present epoch" is implicit in the term luminosity function as used herein. If evolution is present, the procedures to obtain RLF's described above and by Petrosian are both erroneous, but each may be modified to produce present epoch RLF's for any specified form of evolution.

In Chapter 5 it has been shown that between the frequencies of 178 and 2700 MHz, most radio galaxies have spectra which either obey power laws or steepen with increasing frequency. The few exceptions generally show low frequency cut-offs due (probably) to synchrotron self-absorption. In computing the S - z arrays at 178 and 2700 MHz, then, 3 types of spectra denoted as RG1, RG2, and RG3 have been considered as representing all radio galaxies. RG1 comprises all spectra which obey power laws or which steepen with frequency, while RG2 and RG3 are the spectral forms shown in Figure 7.6. The latter two spectra were derived by considering the spectral data on radio galaxies in the 2700 MHz catalogues for which spectra could not be classed as RG1. At 2700 MHz the

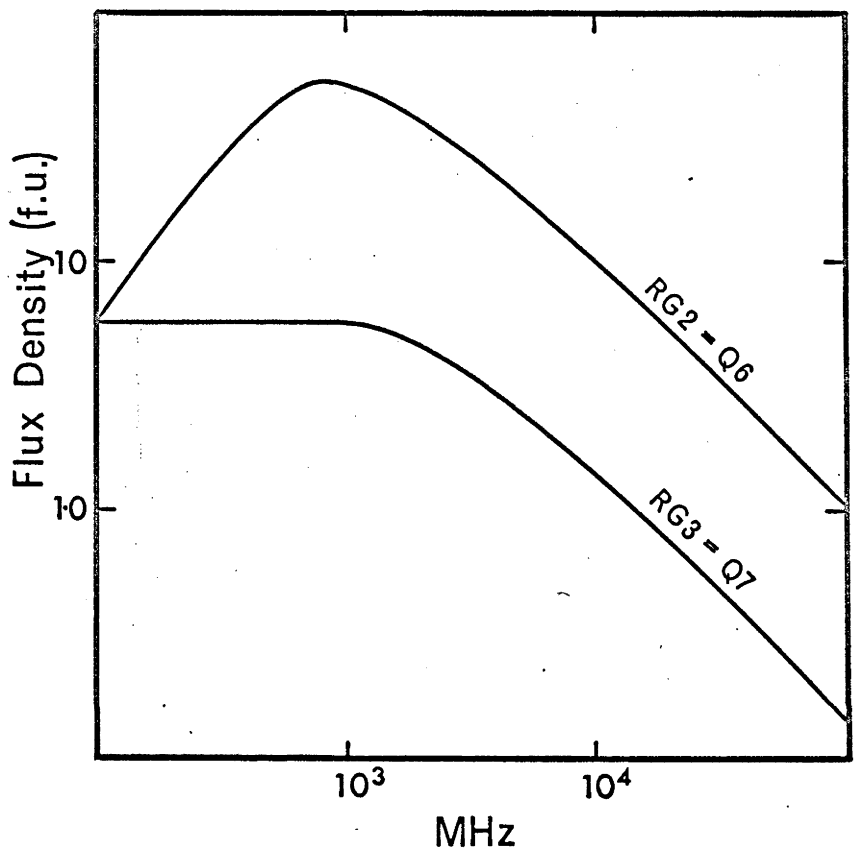

Figure 7.6. Spectral forms used in computation of the S - z arrays.

dispersion in the high frequency spectra of galaxies in RG1 has been represented by subdividing the class into 5 power law spectra with indices 0.6, 0.8, 1.0, 1.2, and 1.4. The RLF derived above for the 2700 MHz radio galaxies (Figure 7.4) is hence that for spectral class RG1, $\alpha = 1.0$ alone. However, as noted previously, computation of the S - z arrays for all other spectral indices of RG1 indicated no significant differences in form. Above 2700 MHz the spectra RG2 and RG3 are such that S - z arrays computed for them at 2700 MHz likewise showed no significant difference in form from that of Figure 7.2. Consequently S - z arrays for radio galaxies at 2700 MHz were computed for these three spectral types using the same RLF's for each.

In computing the S - z arrays at 178 MHz, the RLF's were derived as follows. For spectral type RG1, the 2700 MHz RLF was translated to 178 MHz as described previously with the single effective index of 0.78 (see Figure 7.5). S - z diagrams at 178 MHz were then computed for subdivisions of RG1 into power law spectra with indices 0.4, 0.6, 0.8, 1.0, and 1.2. Note that these subdivisions are shifted to smaller indices because of the shift to steeper spectra with increased frequency illustrated in Figures 5.4(a) and (b). Although many spectra in RG1 steepen in the frequency range 178 to 2700 MHz, little error is introduced by approximating the spectrum above 178 MHz by a power law in the present computations. This is due to the fact that in the range of flux densities considered here, the

computed arrays show very few galaxies beyond redshifts of 4. For observation at 178 MHz this redshift corresponds to a frequency in the radio source frame of less than 900 MHz; even the spectra of radio galaxies which exhibit pronounced steepening can be approximated quite well by power laws in the range 178 to 900 MHz. The RLF's at 178 MHz for spectral classes RG2 and RG3 were derived from the 2700 MHz RLF in the same fashion as the RLF for RG1. Simple translations to 178 MHz as previously described were used, the effective indices being directly obtained from Figure 7.6. S - z arrays at 178 MHz were computed as for the sub-classes of RG1.

All S - z arrays for 2700 MHz were computed for $100 \leq S_{2700} \leq 0.10$, and all those for 178 MHz for $1000 \leq S_{178} \leq 1.0$. The normalizations of the arrays and their subsequent combination to construct the number - flux density relations are described in §7.5.

7.4 Luminosity Functions for QSO's

7.4 (i) Optical Luminosity Functions for QSO's

It is well known that unlike the radio galaxies, plots of log z versus optical apparent magnitude for QSO's exhibit enormous scatter (e.g. Hoyle and Burbidge 1966, Longair and Scheuer 1967). The formulation of optical luminosity functions to account for this scatter has proved to be difficult (Longair and Scheuer 1967). Schmidt (1968) has suggested a very broad optical luminosity function; Wall (unpublished calculations)

finds such a luminosity function almost impossible to reconcile with the known distributions in redshift (Burbidges 1969) and the relatively narrow apparent magnitude distributions obtained in the present work (Figure 5.9). If the cosmological interpretation of the redshift is to be retained, the implication of this result is similar to that mentioned by Longair and Scheuer; i.e. a dependence of luminosity on redshift in the sense that optical luminosities are required to be greater at earlier epochs.

In the present context the preceding discussion is relevant from two aspects which are interrelated. Firstly it emphasizes once again the principal problem posed by the QSO's - the interpretation of redshifts. The results imply either (1) a non-cosmological interpretation of the redshift, (2) a cosmological interpretation with some form of evolution, or (3) the presence of selection effects which have not been recognized. In deriving an RLF for the QSO's the cosmological interpretation has been adopted for two simple reasons: (1) no non-cosmological interpretation presently suggested permits determination of an RLF, and (2) the results of §7.5 suggest that some form of evolution is necessary even for the radio galaxies. Secondly the preceding discussion has illustrated that there is no hope of estimating redshifts from apparent magnitudes as was done for the radio galaxies. The 28 redshifts obtained for the QSO's in the first two parts of the 2700 MHz catalogue provide a very sparsely populated

S - z diagram for RLF determination.

7.4 (ii) Radio Luminosity Functions for QSO's

The 28 QSO's with measured redshifts are shown in the S - z diagram for the $\Lambda = 0$, $q_o = +1$ geometry in Figure 7.2. The sample should be representative of QSO's catalogued at 2700 MHz in terms of redshifts and flux densities. The very limited data appear to indicate that two simple criteria which must be met for an RLF to be considered satisfactory are (1) an even distribution across the band in the S - z diagram where the QSO population appears, and (2) an approximate cut-off throughout the diagram at redshifts of $\sim$2.5. The luminosity function shown in Figure 7.4 meets these criteria quite well. It was obtained by comparison of computed S - z arrays with Figure 7.2 on the assumption of a high frequency spectral index of 0.6, and normalized so that the number - flux density relation derived from its S - z diagram passed through the point N = 43.0, S_{2700} = 0.94 f.u. on the QSO log N - log S curve of Figure 6.13. A portion of the resulting S - z array is shown in Table 7.3. An S - z diagram computed for the steady-state model with the same RLF provides a satisfactory representation of the QSO data in the steady-state analogue of Figure 7.2.

The width of the RLF derived indicates that there should be considerable scatter in the plot of log z versus S_{2700}. This has been found by Bolton and Wall, and the

TABLE 7.3 THE 2700 MHZ S-Z ARRAY FOR THE QSO RLF OF FIGURE 7.4
(FRIEDMANN MODEL, LAMBDA = 0, DECELERATION PARAMETER +1.0)

S(I) = / Z(J)	1.1218	0.7945	0.5627	0.3985	0.2822	0.1998	0.1415	0.1002
0.00068	0.000	0.000	0.000	0.000	0.000	0.000	0.000	0.000
0.00162	0.000	0.000	0.000	0.000	0.000	0.000	0.000	0.000
0.00256	0.000	0.000	0.000	0.000	0.000	0.000	0.000	0.000
0.00406	0.000	0.000	0.000	0.000	0.000	0.000	0.000	0.000
0.00643	0.000	0.000	0.000	0.000	0.000	0.000	0.000	0.000
0.01019	0.000	0.000	0.000	0.000	0.000	0.000	0.000	0.000
0.01615	0.000	0.000	0.000	0.000	0.000	0.000	0.000	0.000
0.02560	0.000	0.000	0.000	0.000	0.000	0.000	0.000	0.000
0.04057	0.000	0.000	0.000	0.000	0.000	0.000	0.000	0.000
0.06430	0.000	0.000	0.000	0.000	0.000	0.000	0.000	0.000
0.01019	0.000	0.000	0.000	0.000	0.000	0.000	0.000	0.000
0.16150	0.543	0.645	0.000	0.000	0.000	0.000	0.000	0.000
0.25600	1.020	1.212	1.440	1.711	2.033	0.000	0.000	0.000
0.40570	1.704	2.025	2.406	2.859	3.397	4.037	4.797	0.000
0.56200	1.140	1.355	1.610	1.913	2.274	2.702	3.210	3.815
0.70750	1.318	1.566	1.861	2.211	2.627	3.122	3.710	4.408
0.89060	1.284	1.756	2.087	2.480	2.947	3.502	4.162	4.945
1.12120	1.103	1.557	2.199	2.621	3.115	3.701	4.398	5.227
1.61500	1.585	2.238	3.160	4.462	6.184	7.348	8.731	10.375
2.56000	0.947	1.337	1.888	2.666	3.765	5.317	7.507	9.242
4.05700	0.365	0.612	0.986	1.393	1.967	2.778	3.922	5.538
6.43000	0.119	0.199	0.335	0.562	0.943	1.329	1.876	2.649
9.19100	0.046	0.078	0.131	0.220	0.369	0.619	0.986	1.392
15.15000	0.000	0.000	0.034	0.057	0.096	0.161	0.270	0.454
1	11.18	14.58	18.14	23.16	29.74	34.66	43.64	48.19
2	42.95	57.54	75.60	98.84	128.50	163.20	206.80	255.00
3	28.73	52.94	92.90	167.60	303.90	500.00	889.00	1386.00

ROW 1 - SUM (N/SR) OF THE CONTRIBUTIONS FROM ALL Z IN THE INTERVAL ABOUT S(I)
ROW 2 - INTEGRAL SOURCE COUNT (N/SR) DOWN TO LOWER LIMIT OF THE INTERVAL S(I)
ROW 3 - DIFFERENTIAL SOURCE COUNT (DN/DS) FOR EACH S(I)
THE LINES CORRESPOND TO THOSE DRAWN IN FIGURE 7.2

diagram for the 28 objects in the present sample is shown in Figure 7.7. The disturbing feature, however, is that any RLF, in the absence of evolutionary effects, will predict increasing numbers of high redshift objects at the lower flux densities. If the RLF derived above is even a first approximation, then it is difficult to understand why redshifts >3 have not been found among "radio-quiet" QSO's.

For the present calculations, 16 spectral classes have been adopted to represent the wide variety of spectral forms exhibited by QSO's. Five of these are power laws (Q1, Q2, Q3, Q4, Q5; α = 0.2, 0.6, 0.8, 1.0, 1.2) from 178 MHz to $(1 + z_{max}) \times 2700$ MHz, where z_{max} is the highest redshift contributing to the count at the lowest level of flux density considered. Q6 and Q7 are the same as RG2 and RG3 (Figure 7.6); the remainder (Q8 to Q16) are illustrated in Figures 7.8 and 7.9. Spectral types Q6 to Q16 have been obtained by dividing the radio sources with non - power law spectra in Figure 4.4 into groups of similar form, and assuming all the sources in Figure 4.4 not identified with galaxies to be QSO's with $z = 1.0$.

The question arises as to whether all these spectral types should have the same RLF at 2700 MHz. When each of the 16 spectra is normalized to the same flux density at 2700 MHz and then integrated from 10 to 10^5 MHz, a variation in "bolometric radio luminosity" by a factor of only 5 is obtained. Hence the 2700 MHz flux density represents quite a good estimate

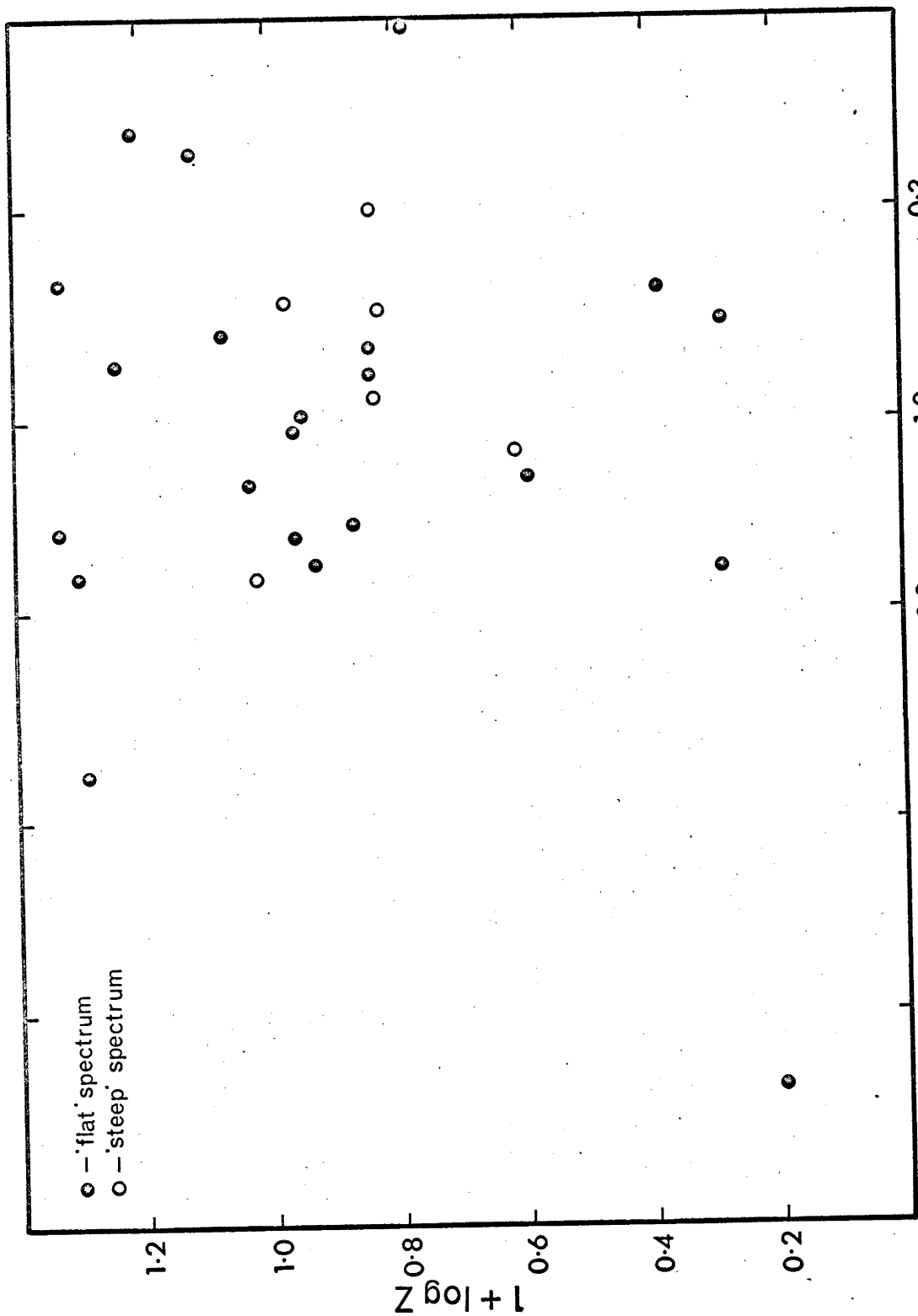

Figure 7.7. Redshift versus flux density for QSO's in the 2700 MHz survey (from Bolton and Wall, §3.2). The suggestion by Bolton (1966) of a correlation between redshift and flux density for the "flat" spectrum ($\alpha_{HF} \leq 0.5$) QSO's is

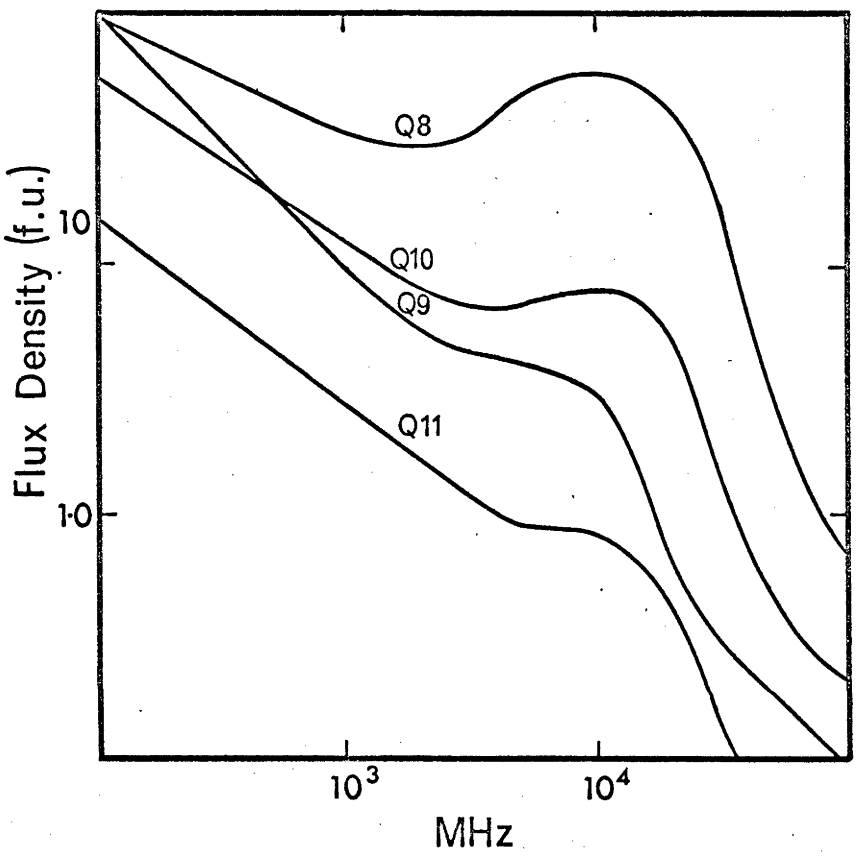

Figure 7.8. Spectral forms used in computation of the S - z arrays.

of the "bolometric radio luminosity", and there appears to be little justification for any assumption other than that of the same RLF at 2700 MHz for each spectral class. The very limited amount of data from which the original RLF was derived further indicates that any other assumption would be pure speculation.

The RLF's at 178 MHz for each spectral class of QSO have been obtained by translation of the single 2700 MHz RLF to 178 MHz with the effective index $\alpha_{178-2700}$ appropriate to each spectral class. For the non - power law classes, these effective indices have been obtained directly from the spectral forms shown in Figures 7.6, 7.8, and 7.9.

The S - z arrays at 2700 and 178 MHz for the 16 assumed QSO spectral classes were computed with the RLF's derived above. The normalizations appropriate to the combination of all the QSO and galaxy arrays at each frequency are now introduced, and the resulting number - flux density relations are discussed.

7.5 The Computed Number - Flux Density Relations

The 2700 MHz S - z arrays for both radio galaxies and QSO's have been normalized so that the sums of the contributions from each spectral class give the source densities at $S_{2700} = 0.94$ f.u. which are indicated by the counts of these objects in Figure 6.13. For the radio galaxies this source density is 70.0/sr.; for the QSO's it is 43.0/sr. The normalization has been carried out in the following manner.

The relative proportions in each spectral class of the radio galaxies and the QSO's have been derived from the spectral statistics of Chapters 4 and 5, and are shown in Tables 7.4 and 7.5. These proportions were then converted to corresponding source densities which the integrated source count of each S - z array was required to produce at $S_{2700} = 0.94$ f.u., and each of the arrays was scaled accordingly. The counts resulting from each array were summed to obtain the complete number - flux density relations for QSO's and radio galaxies at the frequencies of 178 and 2700 MHz, and these are now discussed.

The dashed curves shown in Figure 6.13 represent the 2700 MHz number - flux density relations computed for QSO's and radio galaxies in the $\Lambda = 0$, $q_o = +1$ universe. For both classes of object, the agreement is very poor. There is agreement between the computed curve for the radio galaxies and the radio galaxy counts with no unidentified sources added, but it must be regarded as purely fortuitous. The arguments of §5.6 and §7.3 indicated that ∿75% of the unidentified sources must be galaxies beyond the plate limit, and the RLF from which the computed curve was derived was based on this hypothesis. Furthermore, the transfer of many of the unidentified sources to the QSO class serves only to increase the divergence between calculation and observation which is apparent in Figure 6.13.

TABLE 7.4 PROPORTIONS OF RADIO GALAXIES IN EACH SPECTRAL CLASS

Spectral Class	Proportion in Spectral Class (%)		Contribution to Count at S_{2700} = 0.94 f.u. (N/sr.)
RG1		94.9	66.4
α = 0.6	17.3		
0.8	31.0		
1.0	27.6		
1.2	13.8		
1.4	5.2		
RG2		1.7	1.2
RG3		3.4	2.4
	94.9	100.0	70.0

TABLE 7.5 PROPORTIONS OF QSO's IN EACH SPECTRAL CLASS

Spectral Class	Proportion in Spectral Class (%)	Contribution to Count at S_{2700} = 0.94 f.u. (N/sr.)
Q1 (α = 0.2)	6.8	2.9
Q2 (α = 0.6)	10.0	4.4
Q3 (α = 0.8)	10.5	4.5
Q4 (α = 1.0)	3.4	1.5
Q5 (α = 1.2)	0.9	0.4
Q6 (RG2)	4.8	2.0
Q7 (RG3)	7.0	3.0
Q8	6.8	2.9
Q9	6.8	2.9
Q10	6.8	2.9
Q11	6.8	2.9
Q12	6.3	2.7
Q13	7.4	3.2
Q14	3.2	1.4
Q15	6.9	3.0
Q16	5.3	2.3
	99.7	42.9

The poor agreement found on completing the calculations for this geometry led to the calculations for the steady-state model being carried no further than the determination of RLF's (§7.3, 7.4). Figure 7.10 illustrates why. With a spectral index of 1.0, the radio galaxy S - z array computed at 2700 MHz for each model yields the integrated number - flux density relations (normalized to (70.0, 0.94)) shown in this diagram. It is apparent that the steady-state RLF for radio galaxies which contains increased numbers of high luminosity sources (Figure 7.4) conspires with the geometrical effects to produce a count which is considerably flatter than that of the $\Lambda = 0$, $q_o = +1$ model. The QSO relations (computed for indices of 0.6 and normalized to (43.0, 0.94)) diverge only at the lowest source densities, but again in the sense that the steady-state model exhibits the flatter slope. Hence the poor agreement between computation and observation for the $\Lambda = 0$, $q_o = +1$ geometry which is evident in Figure 6.13 indicates that even worse agreement would result for the steady-state model.

In Figure 7.11 the number - flux density relations computed at 2700 MHz (in the $\Lambda = 0$, $q_o = +1$ geometry) for the radio galaxies and QSO's have been summed to produce the composite relation. The observed number - flux density relation (Figure 6.1) is shown for comparison. In Figure 7.12 the same number - flux density relations are illustrated for 178 MHz - those computed for radio galaxies and QSO's, their sum, and that obtained from observation by Gower (1966). In

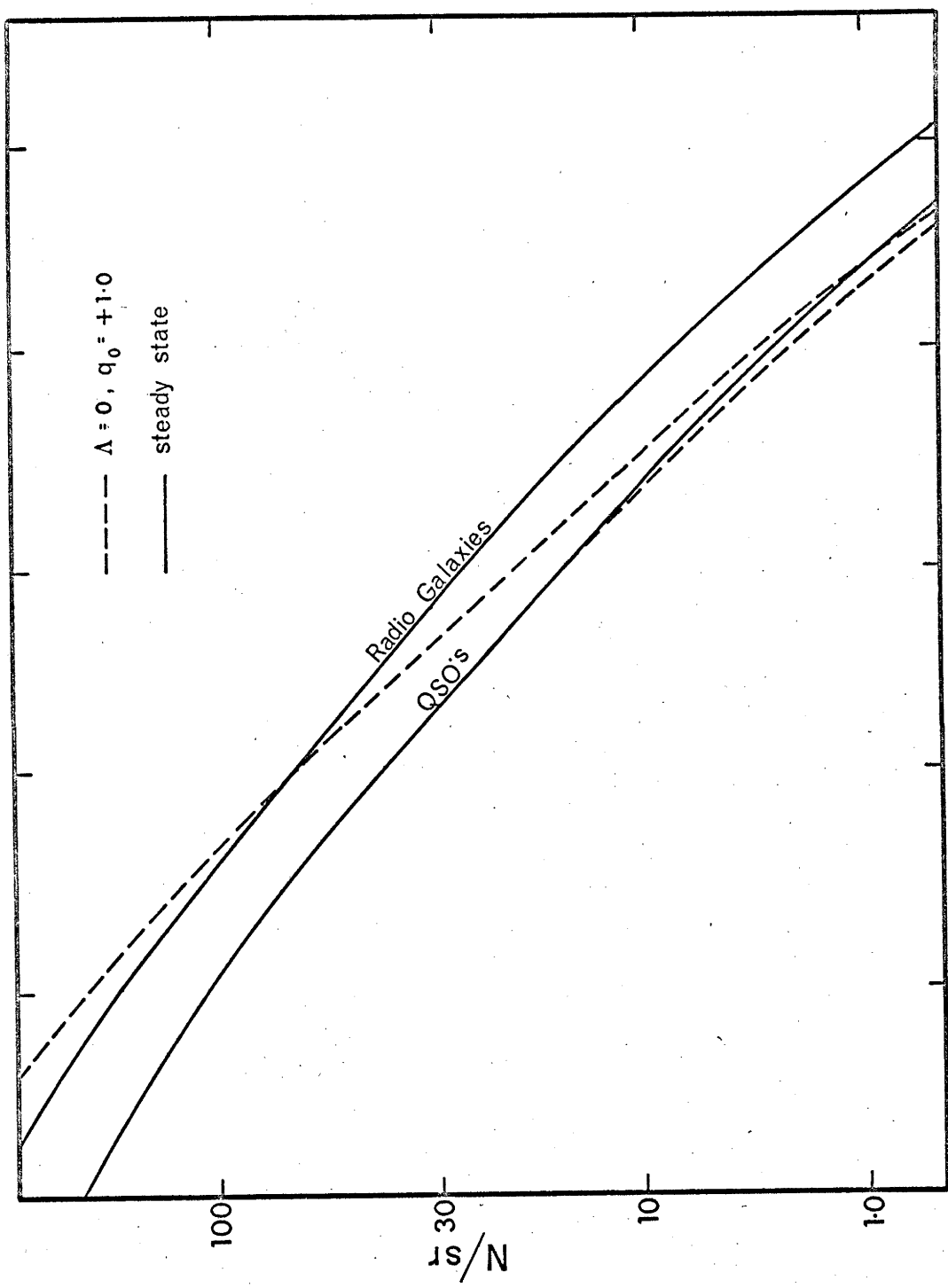

Figure 7.10. The 2700 MHz number - flux density relations from the S - z arrays (computed with a single spectral class for radio galaxies and QSO's; see text) for the two models of the universe assumed.

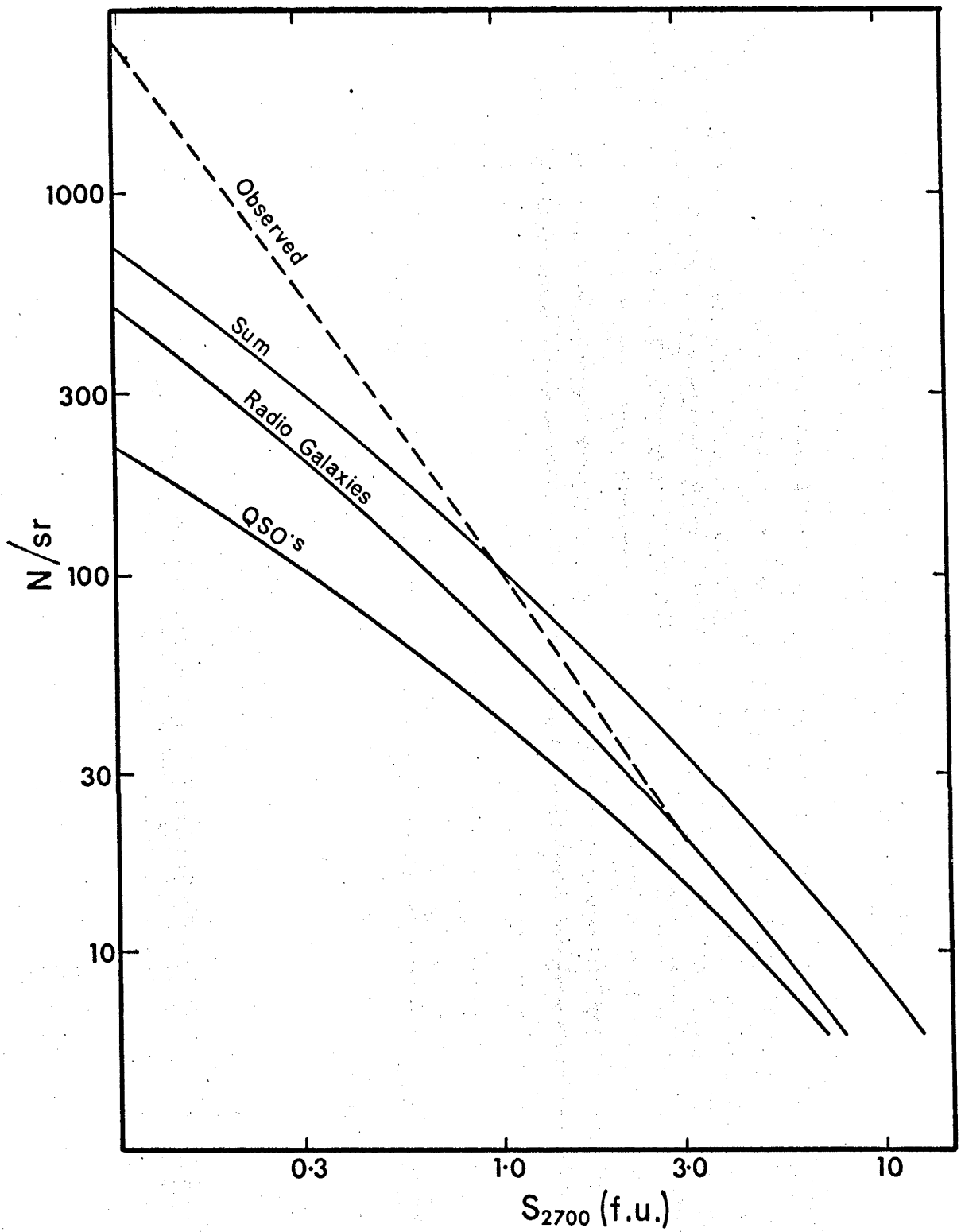

Figure 7.11. The number - flux density relations computed from the 2700 MHz S - z arrays. The dashed line is the solid line of Figure 6.1, the observed number - flux density relation.

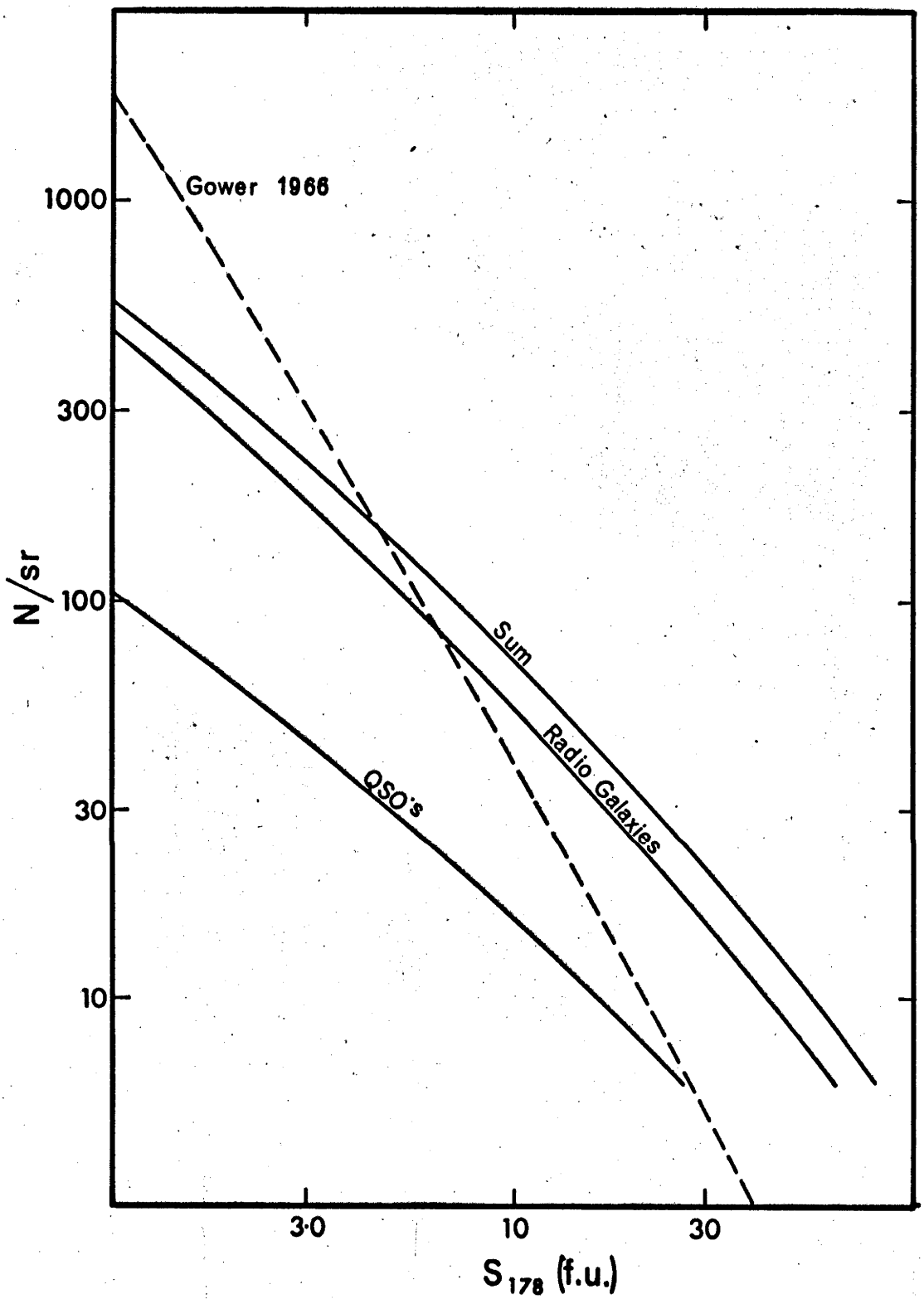

Figure 7.12. The number - flux density relations computed from the 178 MHz S - z arrays. The dashed line is the observed number - flux density relation derived by Gower (1966).

each diagram the difference between computation and observation is so large that no change in normalization of the calculations, or statistical fluctuation of the observed counts, can possibly reconcile them.

There are three methods by which it might be possible to derive steeper number - flux density relations in these two model universes considered.

(1) A different value for the Hubble constant may be assumed. However, some trial computations for H_o = 50 and 125 km $sec.^{-1}$ Mpc^{-1} indicated that only minor changes in the above results could be so derived.

(2) Suppose that the classes "radio galaxies" and "QSO's" are in fact composed of a large number of sub-classes of object which are not related. Suppose further that each of these classes has its own RLF and spectral form. Then the added constraint of having to treat each computed element of the S - z diagram as a discrete number of sources rather than as a probability as has been assumed here will lead to an initial steepening of the computed number - flux density relation. Observationally the effect is that of having to survey down to a particular flux density before counting the first source of each sub-class, and the result is an initially steep source count. However, it appears probable that all objects classed as radio galaxies and as QSO's belong to the same population, and indeed that some form of evolution may relate QSO's and radio galaxies. The effect must nevertheless

produce an initially steep portion of the observed count; it is hard to see how to treat this in the calculations, but likewise hard to see how it can be of significance at source densities above 10 or 20 per steradian.

(3) Hoyle and Narlikar (1961, 1962) invoked a "hierarchal" concept of the steady-state universe in which large scale condensations of different generations are postulated. They showed that in such a model a particular observer may obtain a source count in which the initial portion is considerably steeper than that computed from the conventional steady-state model. The average source count of observers spread throughout the universe, however, is that of the conventional steady-state model. The model appears to have been constructed solely to explain the source counts, and this seems to have contributed more to the general lack of acceptance than any direct attack.*

---

* A direct attack has been made by McVittie (1965) who states that the concepts appear to contradict the basic assumption of the steady-state theory, namely that all positions in space are at all times indistinguishable from one another. The applicability of the assumption to any point is evidently a matter of degree; the same assumption (with the omission of the phrase "at all times") is also basic to all other uniform model universes. McVittie also states that "Hoyle and Narlikar's treatment has still to be supplemented by the discovery of the metric of a space - time in which the material is distributed irregularly in space." On this argument, the presence of "island universes" unfortunately rules out all cosmological models which are based on the Robertson-Walker metric.

Scheuer (1968) pointed out that the astrophysical framework for the model was based on the "hot universe" (kinetic temperature of $\sim 10^9$ °K. for the intergalactic plasma) which is now no longer accepted (see, e.g. Field and Henry 1964). If a similar model (from the point of view of radio source counts) could be derived in a "cooler" universe, the following consideration indicates that the present results would not support it. The calculations of Hoyle and Narlikar (1962) showed that the "fluctuations" in the initial portion of the slope which enable some observers to derive steep source counts diminish at redshifts >0.3. The S - z tables calculated for both QSO's and radio galaxies at 2700 MHz indicate that the greatest contribution to the counts for source densities above 100/sr. is from redshifts >0.3; and it is this region of the count for which complete incompatibility with observation is present.

Some additional cosmological models are briefly considered in relation to the source counts in the final section of this chapter. The dependence of spectrum on flux density (computed versus observed) is first discussed.

7.6 The Dependence of Spectrum on Flux Density

In the previous chapter it has been shown that an apparent difference in the initial slopes of the number - flux density relations at 178 and 2700 MHz is mostly due to a dependence of the spectrum of the QSO's on 2700 MHz flux

density. One of the few points of agreement between observation and the computations described above is that the calculated number - flux density relation for 178 MHz does have a steeper initial portion than does that for 2700 MHz. However, the result is not caused by the dependence of spectrum on flux density for any class of object; it is due to the greater contribution of the QSO's to the 2700 MHz source counts, which in turn results from the spectral selection effect of survey frequency. At both frequencies the number - flux density relations computed for the QSO's are flatter than those for the radio galaxies because the generally greater redshifts of these objects increase the severity of the geometrical effects.

As a first step in examining whether the computations indicate the spectral dependence in flux density for QSO's which was discussed in §6.7, the number - flux density relations computed for these objects (Figures 7.11 and 7.12) were compared. At source densities above 10/sr. they are identical in form; at lower source densities the 178 MHz relation is slightly flatter. The agreement in form appears surprising on first consideration because the relation computed at 178 MHz is dominated by those QSO's whose spectral types have the largest effective indices between 178 and 2700 MHz. These spectral classes should tend to flatten the computed count over that of the 2700 MHz computation because of the increased "K - dimming" effect for such spectra. However, examination of the spectral types indicates that for most of

them, at redshifts of ∿1.0 or less the "K - dimming" at 2700 MHz will be in the same sense because the frequency of the peak in the spectrum has been surpassed. It is clear that the curves do not indicate a significant change in the effective index for the flux density ranges of $S_{2700} \geq 1.01$ f.u. and $0.64 \leq S_{2700} < 1.01$ f.u. which were considered in §6.7.

The lack of dependence of effective index $\alpha_{178-2700}$ on flux density at 2700 MHz which is indicated for the QSO's by the computations may be demonstrated directly. The "observed" effective indices for each QSO spectral class were first obtained from Figures 7.6, 7.8, and 7.9 on the assumption of a redshift of unity for each object. The two ranges in flux density chosen for comparison were $S_{2700} \geq 0.94$ f.u., and $0.46 \leq S_{2700} < 0.94$ f.u. The 2700 MHz S - z array computed for each spectral class was used to determine the ratio of sources (summed over all contributing redshifts) in each of the two ranges of flux density. The solid line of Figure 7.13 shows the distribution in effective indices for sources of $S_{2700} \geq 0.94$ f.u. when the spectral classes are combined in the proportion of Table 7.5. When the different ratios derived above are used to compute the equivalent histogram for the lower range in flux density, the resultant distribution, shown by dots in Figure 7.13, is virtually identical. Examination of the individual S - z arrays indicates that the assumption of a single redshift of unity in determining the apparent effective index for each class of object does not invalidate

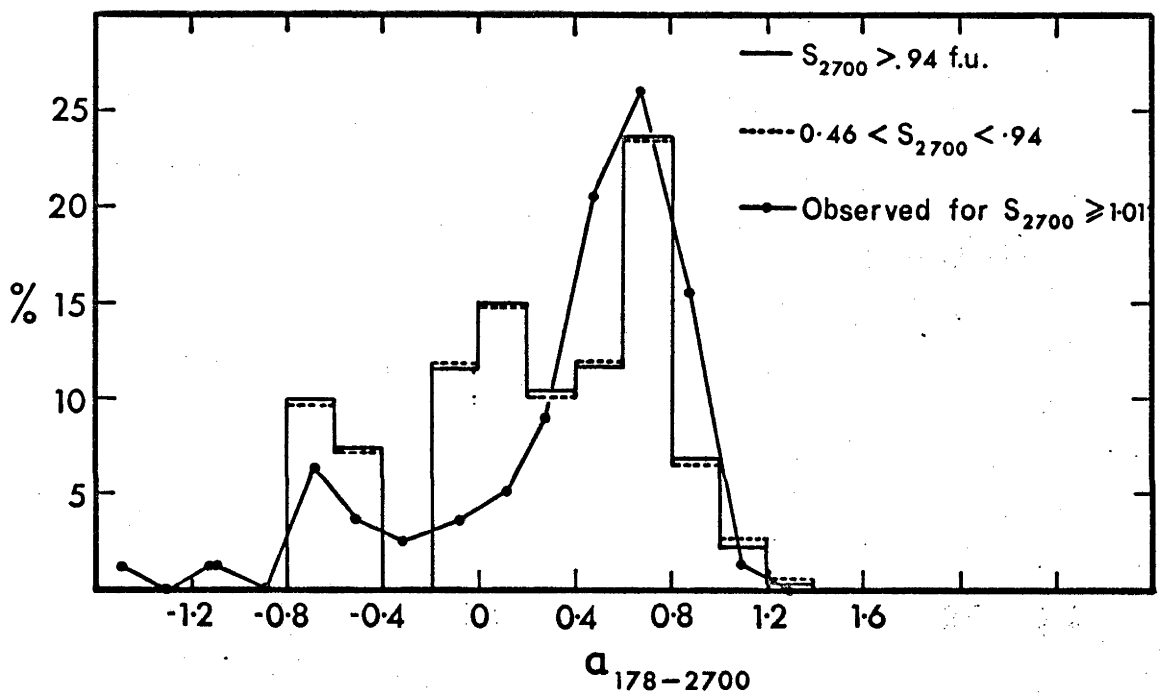

Figure 7.13. The distributions in effective indices for QSO's in different ranges of 2700 MHz flux density from the combination of computed S - z diagrams in the proportions given by Table 7.4.

the result. The distribution in effective indices for the QSO's for which $S_{2700} \geq 1.01$ f.u. in the present sample has been added to Figure 7.13 to illustrate the reasonably good agreement with the estimated proportions of the spectral types.

(That possible changes in spectrum might be observable at different levels of flux density was first suggested by Conway, Shakeshaft, and Whitfield (1960). Calculations were carried out by Stewart (1967) for a frequency of 178 MHz. He assumed power law spectral indices with a Gaussian distribution characterized by $\bar{\alpha} = 0.75$, $\sigma = 0.20$, similar to that found for the stronger sources catalogued at 178 MHz. A hyperbolic universe was used (density parameter $\sigma_o = 0.2$, $q_o = +1.8$, $\Lambda < 0$), and the calculations were made for individual sources of powers $F_{178} = 10^{25}$, 10^{26}, 10^{27}, and 10^{28} w. hz^{-1}. A similar calculation has been carried out with the present computational technique for the flux density range $0.1 \leq S_{178} \leq 100.0$ f.u. S - z arrays were computed for spectral indices 0.3 to 1.4 in steps of 0.1, and scaled to represent the Gaussian distribution described above at $S_{178} = 100$ f.u. Two different RLF's were used: that obtained from Petrosian's (1969) data, and that derived in §7.3 with translation to 178 MHz. The $\Lambda = 0$, $q_o = +1$ geometry was assumed, and the distributions resulting at the lower flux densities were obtained directly from the scaled S - z arrays by summing the columns (which represent narrow ranges in S_{178}; see §7.2) at various flux densities down to 0.1 f.u. The results for the two RLF's are virtually identical

and agree with Stewart's only in that no change in dispersion was found. The change in mean spectral index with flux density in both investigations is shown in Figure 7.14. The present work is seen to result in far less dependence of the mean index on flux density, and this must be due to the use of luminosity functions and a different (possibly more acceptable) geometry.

It is self-evident that unless the computations can reproduce the observed source counts, any prediction of spectral dependence on flux density is of academic interest only. The failure of the present computations in this respect has been discussed; Stewart makes no explicit statement but it is difficult to see how his calculations can be any more successful.)

A spectral dependence of the QSO's on flux density at 2700 MHz thus cannot be explained by redshift selection effects in non-evolutionary universes. Moreover, the lack of correlation of flux density with redshift (if these are interpreted as cosmological in origin) implies that there is no correlation between flux density and luminosity distance, and consequently no correlation between spectral form and luminosity distance. Such a correlation might be expected if certain forms of evolution were to be invoked.

To examine the question further, the "bolometric radio luminosities" for 24 QSO's in the 2700 MHz catalogue for which redshifts and spectral data were available have been computed. These luminosities have been obtained by integrating

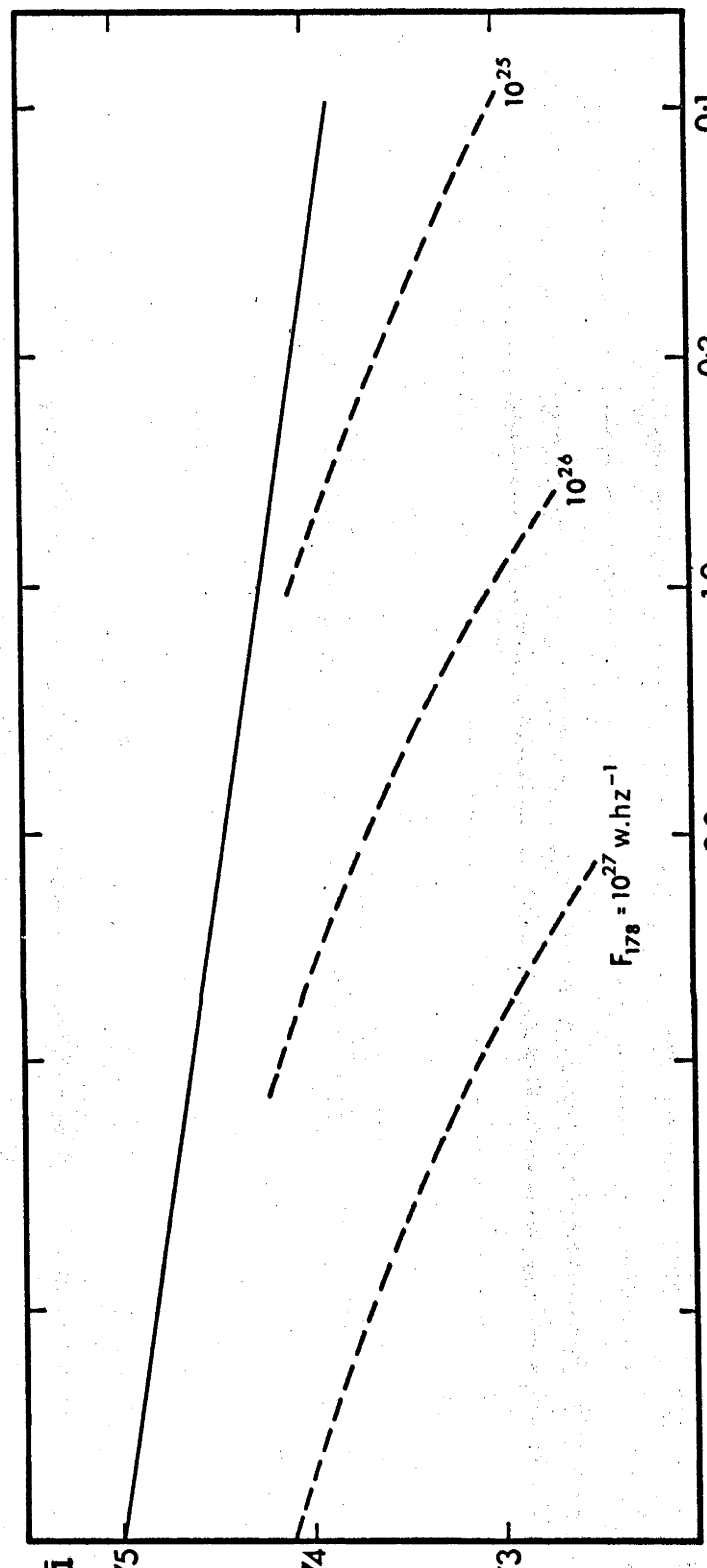

Figure 7.14. The dependence on 178 MHz flux density for the mean of a Gaussian distribution in spectral indices. The solid line is obtained from the present computations (with the geometry of the Friedmann model used), and the same line results from using both the RLF for radio galaxies derived by Petrosian (1969), and that derived in the present work (Figure 7.4) translated to 178 MHz. Dashed lines show the result of Stewart's (1967) computations for a hyperbolic universe and the different luminosities indicated.

the spectrum (blue-shifted to the source frame), and assuming the $\Lambda = 0$, $q_o = +1$ geometry and the redshifts to be cosmological in nature. Weak correlations were found between this luminosity and both high and low frequency spectral indices (α_{HF}, α_{LF}; see §5.1). These correlations then imply (because of the correlation of spectrum with flux density (§6.6, 6.7)) that there might be a further correlation between the observed 2700 MHz flux density and radio luminosity. The diagram is shown in Figure 7.15, and the anticipated correlation appears to be present. If there is a real cut-off at $z = 2.4$, then a 45° line bounds the upper left of the diagram, the position of this line depending on the spectral type assumed in its computation. A horizontal line indicating maximum radio power must provide the upper boundary to the diagram. Because of the greater volumes which correspond to the larger redshifts the population of the diagram will tend to increase towards the region in which the boundary lines for the various spectral types appear. In this manner the weak correlation may be obtained, and the dependence of the spectral form of QSO's on the 2700 MHz flux density is explained.

In physical terms, the argument runs as follows. A broad "bolometric" RLF is confined to a relatively narrow range in luminosity distance. The most luminous sources (which have the "flattest" spectra) then become the apparently brightest, and correlation between spectrum and flux density is effected.

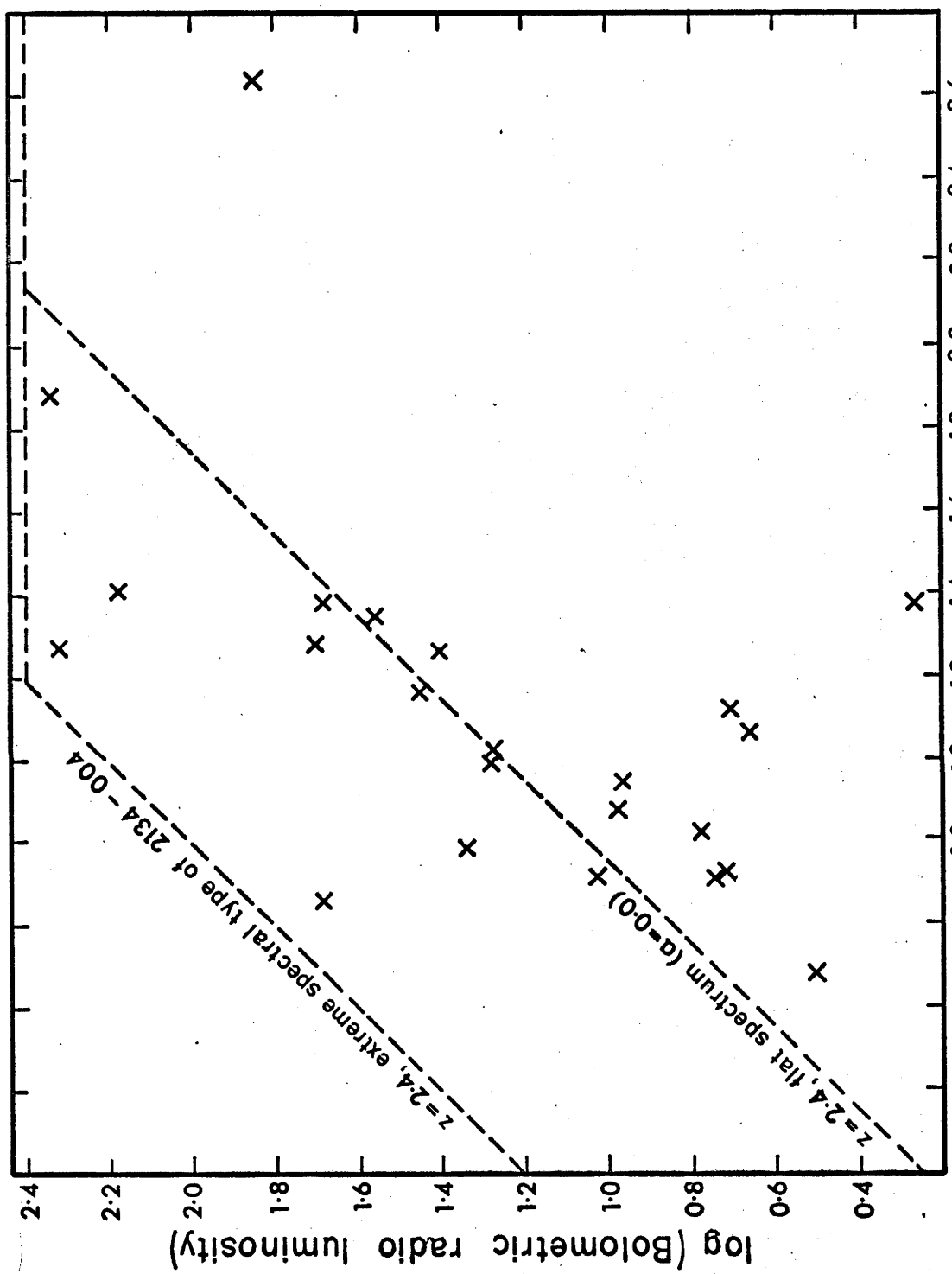

Figure 7.15. The "bolometric radio luminosity" (in arbitrary units) versus flux density at 2700 MHz (in f.u.). The $\Lambda = 0$, $q_o = +1$ geometry has been assumed.

The spectrum - flux density correlation for the QSO's (with the assumption of the cosmological nature of the redshifts) seems to indicate as strong an argument against the uniform models on which the calculations were based as do the source counts themselves.

7.7 Conclusions from the Present Analysis

The difficulty of interpretation of the number - flux density relations observed at low frequencies in uniform models of the universe without invoking evolution has been demonstrated in analyses by several authors (see, e.g., the reviews by Scheuer (1968) and Ryle (1968)). However, the acceptance of evolution on the basis of these analyses has not been universal (e.g. Hoyle 1968, Bolton 1969). Moreover, the probable change in form of the number - flux density relation at 2700 MHz, together with dramatic changes in spectral and identification content, indicated that the results obtained in the low frequency analyses were not necessarily valid at 2700 MHz, and that selection effects of some form possibly had been overlooked.

The foregoing analysis which has used all sources in the 2700 MHz surveys in deriving RLF's, and which has taken all spectral types of each class of identification into consideration, indicates that the difficulty persists. That this would prove to be so was evident as soon as the RLF's of §7.3 and §7.4 were derived; the 2700 MHz catalogues appear to

contain a greater proportion of high luminosity objects than the low frequency catalogues, and geometrical effects are consequently more severe.

The geometrical effects may be somewhat reduced in Friedmann models with $\Lambda = 0$ by decreasing q_o. With q_o as large as +1, the value favoured by Sandage (1968c), the problem of "missing mass" is serious - there is over an order of magnitude between the density of observed matter and the density of matter required to "close" the universe. A much more drastic assumption in terms of the geometry is to assume the cosmological constant $\neq 0$. For instance, Petrosian (1969) has shown how it is possible to derive steep initial portions for number - flux density relations due to the geometrical effects in a Lemaître universe. Such a universe has a cosmological constant slightly larger than the critical value which produces the static Einstein model, and evolves through a quasi-static period. Petrosian finds, however, that some evolution in his model is still required, and it is not clear how he accounts for the relatively rapid turnover of the number - flux density relation revealed by the 5C surveys.

If evolution is implied by the observed number - flux density relation, it seems almost certain from the computations that both the radio galaxies and the QSO's must partake in it. Schmidt's analysis (1968) for 33 QSO's in the 3CR catalogue indicated strong density evolution, but the same analysis carried out by Miss Harris (1969) for 27 QSO's in the Parkes

(408 MHz) catalogue produced the opposite result, an apparently uniform distribution of these objects in space. Luminosity evolution is indicated by the forms of the redshift and apparent magnitude distributions as discussed in §7.4. A form of luminosity evolution with some assumption of spectral dependence on source age might also be devised to obtain the dependence of spectrum on flux density found for the QSO's.

In this regard it is commonly and not unreasonably presumed that scheme of evolution for the individual radio source is from a compact "flat spectrum" object to an extended "steep spectrum" object. It follows that if the form of the source count is largely governed by evolutionary effects (as various analyses including that herein seem to indicate), then one might expect the bias of a high frequency survey towards the detection of objects of flatter spectra to result in a number - flux density relation for such a survey revealing greater evolutionary effects than the lower frequency counterparts. That such is not the case is evident from the results of the preceding chapter. In particular, it is apparent that the source count for the "flat spectrum" objects (which when identified are predominantly QSO's) are flatter than the counts for the "steep spectrum" objects.

The superposition of geometrical effects on evolutionary effects might explain this result if the "flat spectrum" sources occupied a larger volume of space than the "steep spectrum" sources. The division of QSO's into two classes on

the basis of "flat" or "steep" radio spectrum results in apparently identical distributions of redshift. If redshift is indicative of distance, then as noted in the previous section, the same volume of space is occupied by sources of each spectral type. A steeper count for the "flat spectrum" objects would be expected both on the basis of the evolutionary argument and on the basis of a reduced radio "K - dimming". A paradox appears to be unavoidable if the redshift is entirely cosmological in origin.

It is concluded that the observed number - flux density relations indicate three possibilities: (1) evolution of some form for both radio galaxies and QSO's (if redshifts of the latter are cosmological in origin), (2) the presence of selection effects which are not recognized at this stage, or (3) fundamental errors in the formulation of cosmological theory as it is presently accepted.

CHAPTER 8

CONCLUSION

8.1 Results of the Present Investigation

The results of the investigation described in this thesis may be summarized as follows:

(1) Catalogues of extragalactic radio sources have been obtained from 2700 MHz surveys of 0.77 sr. in the $+4^{\circ}$ to -4° declination zone, and of 0.075 sr. in 6 selected regions. The former, complete to 0.35 f.u. at 2700 MHz, contains 500 sources of which 120 do not appear in previously published catalogues. The latter, complete to 0.10 f.u. at 2700 MHz, contains 310 sources of which 240 do not appear in previously published catalogues.

(2) Accurate positions measured for all catalogued sources have enabled complete statistics on optical identifications to be obtained. Identifications have been suggested for approximately 80 additional radio galaxies and 105 additional QSO's. The identifications and suggested identifications are divided equally among the QSO's and radio galaxies; in the 3CR (178 MHz) survey, the ratio of QSO's to radio galaxies is about 1:4.

(3) Investigation of the spectra of about 350 of the sources catalogued has indicated that this dramatic change in identification content from the lower frequency surveys is paralleled by a similar change in spectral content. About half

of these sources show spectra which cannot be described by a single power law between 178 and 5009 MHz. This 50% is comprised of some 25% having spectra which steepen with increasing frequency, 15% having spectra showing low frequency cut-offs, and 10% having spectra which indicate the presence of at least two components, one of which exhibits self-absorption. Among the latter 25%, there are very few sources for which the frequency of maximum flux density is higher than 5000 MHz. Moreover, identifications among this 25% are almost exclusively QSO's. The clear distinction between the radio spectra of QSO's and radio galaxies as classes indicates the reason for the change in identification content with survey frequency, and the present results permit this distinction to be used in predicting the identification content of surveys at other frequencies. It may likewise be used to establish the fraction of unidentified sources which belong to each class of identification; the present analysis suggests that of the unidentified sources in the 2700 MHz catalogues for which $S_{2700} \geq 0.40$ f.u., some 25% are QSO's beyond the plate limit of the Sky Survey, while the remainder are distant radio galaxies.

The spectral investigation has also indicated that several of the newly discovered sources are variable or suspected to be variable at centimeter wavelengths. A further result is a remarkable dependence of the spectrum of the QSO's on flux density in the sense that the proportion of those exhibiting flat or inverted spectra is greater among the sources

having higher flux densities at 2700 MHz.

(4) The 2700 MHz number - flux density relation has a slope in the range of source densities 50 to 2500/sr. of about -1.45. It is suggested that at the high frequencies the number - flux density relation does steepen at the low source densities, but that this steepening takes place either to a lesser extent or at lower source densities than that of the low frequency relations. The classification of the unidentified sources on the basis of their spectral characteristics indicates that the QSO number - flux density relation is flatter than that of the radio galaxies at 2700 MHz. The change in form of the composite number - flux density relations with frequency is then the result of two effects: (1) the spectral selection due to survey frequency which implies increasing proportions of QSO's as survey frequency is raised, and (2) the dependence of the spectrum of the QSO's on flux density as mentioned previously. The latter is the more important.

(5) Preliminary computations to construct number - flux density relations in uniform model universes indicate that if no evolution is assumed, difficulties in reconciling the observed relations at 2700 MHz with those calculated are severe, and are similar to those encountered in previous investigations of the low frequency counts. The computations have been carried out with a simple and versatile technique enabling the incorporation of any geometry, type of evolution, radio luminosity function, or radio spectrum. In the calculations,

radio luminosity functions have been derived for both the QSO's and radio galaxies catalogued in the 2700 MHz survey, and the number - flux density relations obtained by considering all spectral types for each identification class in the proportions found from the analysis of the spectral data. In addition to the poor agreement with the observed number - flux density relations, the computations indicate no dependence of spectrum on flux density of the order of that observed for the QSO's in the 2700 MHz catalogue. A cosmological interpretation of the redshifts of QSO's has been assumed; if this is in error, the difficulty of reconciling the calculated number - flux density relations for radio galaxies with the observed relation persists. If the QSO's are at the distances implied by their redshifts, then there are three possibilities: (1) evolution in some form for both radio galaxies and QSO's; (2) the presence of selection effects which are not recognized at this stage; or (3) fundamental errors in the formulation of cosmological theory as it is presently accepted.

8.2 Lines of Further Investigation

8.2 (i) Radio Observations

(1) Flux densities at frequencies higher than 5000 MHz clearly are desirable for many of the sources whose spectra are illustrated in Figure 4.4. The sources suggested as variable should be incorporated into monitoring programmes at Parkes and other observatories as quickly as possible in

order to obtain the best possible temporal and spectral resolution.

(2) The apparent dependence of QSO spectrum on flux density at 2700 MHz warrants considerable further investigation. In particular, low frequency flux densities of greater accuracy for many of the sources in the 2700 MHz catalogues which have not been detected in other sky surveys should be obtained. A source - by - source comparison with results from the Molonglo Cross of the University of Sydney will prove of great interest in this regard.

Measurement of the flux densities at 5000 MHz should be carried out for QSO's in the present catalogues with flux densities less than $S_{2700} = 0.40$ f.u. to see if the trend of Figure 6.11 continues to still lower intensity levels.

(3) The 2700 MHz number - flux density relation derived in Chapter 6 requires extension to both higher and lower source densities. The southern surveys being carried out by A. J. Shimmins will help in the latter regard. For the higher source densities, it appears that with care, the count could be directly extended to approximately 10^4/sr. at 2700 MHz using the Parkes telescope. With some form of P(D) analysis (see Appendix I), estimates may be possible for a further order of magnitude in source density. If the form of the relation can be established in the region of source densities where the Cambridge 5C survey results (408 MHz) illustrate significant flattening, then comparison should prove of

considerable interest from the point of view of further analyses of the cosmological implications of source counts.

8.2 (ii) Optical Observations

(1) Many of the QSO's discovered in the present work are of bright enough apparent magnitude for optical spectra to be obtained. Additional redshifts for the QSO's in the 2700 MHz catalogues will illustrate how the radio luminosity functions derived in §7.4 should be modified to conform with reality. If such redshifts are obtained for a sample from the 2700 MHz catalogue complete to optical and radio intensity limits, an analysis of spatial distribution as performed by Schmidt (1968) for the 3CR QSO's would be possible. (Note that accurate photometry is also required). The results would be of particular interest because all spectral types of QSO's would be represented as opposed to a sample containing only QSO's with relatively steep spectra, as selected by the low frequency of the 3C survey.

If the redshifts of QSO's are not cosmological in nature, these analyses have no significance. It is still possible that additional spectra for QSO's may provide the evidence on how the redshifts are to be interpreted.

(2) It has been mentioned that if the source counts are accepted as indicating evolution, then both radio galaxies and QSO's probably partake in that evolution. Moreover, examination of the S - z diagrams of the previous chapter

indicates that such evolution may be significant at redshifts of 0.5 or less. The most luminous elliptical galaxies (those of $M_{pg} \leq -20^{m}.0$, some 7% of which are radio galaxies according to Rogstad and Ekers 1969) are visible out to redshifts of $\sim$0.4 with the largest reflectors. It therefore seems reasonable to propose that evolutionary effects should be detectable in the optical region of the electromagnetic spectrum if they are present to the extent that observations in the radio region suggest.

8.2 (iii) Theoretical Investigations

(1) The relative numbers of all spectral types which this investigation has established should enable some refinement of current theories of source evolution. A particular aspect requiring investigation is the great range in expansion velocities shown by source components which exhibit synchrotron self-absorption. It may prove possible to account for the observations by making modifications to the expanding cloud theory which incorporate (i) different mechanisms of injection of the relativistic electrons which have finite time scales, (ii) different structures for the sources, or (iii) possible mechanisms of confining the optically thick plasmas. The observation that the most stable sources exhibiting self-absorption show no additional component having a simple power law spectrum must be a significant datum in this regard.

(2) If the results of Chapter 7 are accepted as indicative of cosmological evolution, then it is possible to carry out an investigation in which reasonable forms of this evolution are assumed. The constraints provided by the present observations are stringent; the forms of the number - flux density relations for each class of identification at both low and high frequencies must be accounted for, and the dependence of QSO spectrum on flux density must be explained. The technique described in Chapter 7 provides a simple framework in which to attempt such an analysis.

The results of this project imply that the "astrophysical" and "cosmological" aspects of the studies of radio source populations mentioned in the opening paragraphs of this thesis are in fact strongly interrelated. It is apparent that detailed surveys of the radio sky still have something to tell us of both.

* * *

REFERENCES

Batchelor, R.A., Brooks, John W., and Cooper, B.F.C. (1968) - IEEE Trans. Antennas and Propagation AP-16, 228

Blum, E.J., and Davis, M.M. (1968) - Astrophys. Lett. 2, 41

Bolton, J.G. (1966) - Nature 211, 917

Bolton, J.G. (1969) - Astron. J. 74, 131

Bolton, J.G., and Ekers, Jennifer A. (1966a) - Aust. J. Phys. 19, 471

Bolton, J.G., and Ekers, Jennifer A. (1966b) - Aust. J. Phys. 19, 559

Bolton, J.G., and Ekers, Jennifer A. (1967) - Aust. J. Phys. 20, 109

Bolton, J.G., Gardner, F.F., and Mackey, M.B. (1963) - Nature 199, 682

Bolton, J.G., Kinman, T.D., and Wall, J.V. (1968) - Astrophys. J. 154, L105

Braccesi, A., Ceccarelli, M., Fanti, R., Gelato, G., Giovanni, C., Harris, D., Rosatelli, C., Sinigaglia, G., and Volders, L. (1965a) - Nuovo Cim. 40B, 267

Braccesi, A., Ceccarelli, M., Fanti, R., and Giovanni, C. (1965b) - Contributions from Laboratorie Nationale di Radioastronomia, Università degli Studi, Bologna (Dec. 1965)

Burbidge, G.R., and Burbidge, E.M. (1969) - Nature 222, 735

Caswell, J.L., and Wills, D. (1967) - Mon. Not. R. astr. Soc. 135, 231

Clarke, Margaret E., Bolton, J.G., and Shimmins, A.J. (1966) - Aust. J. Phys. 19, 375

Clarke, T.W., and Munro, R.E.B. (1968) - Proc. A.S.A. 1, 93

Cole, D.J. (1967) -
Proc. A.S.A. 1, 30

Conway, R.G., Shakeshaft, J.R., and Whitfield, G.R. (1960) -
Obs. 80, 162

Davidson, W. (1959) -
Mon. Not. R. astr. Soc. 119, 665

Davis, M. M. (1967) -
Bull. astr. Insts Neth. 19, 201

Dent, W.A. (1965) -
Science 148, 1458

Dent, W.A. (1968) -
Astrophys. J. 153, L29

Dixon, R.S., and Kraus, J.D. (1968) -
Astron. J. 73, 381

Ekers, R.D. (1967) -
Ph.D. Thesis, the Australian National University

Field, G.B., and Henry, R.C. (1964) -
Astrophys. J. 140, 1002

Fitch, L.I., Dixon, R.S., and Kraus, J.D. (1969) -
Astron. J. 74, 612

Fomalont, E.B. (1967) -
Astrophys. J. Supp. 15, 203

Fomalont, E.B. (1968) -
Bull. astr. Insts Neth. 20, 69

Galt, J.A., and Kennedy, J.E.D. (1968) -
Astron. J. 73, 135

Gardner, F.F., and Whiteoak, J.B. (1969) -
Aust. J. Phys. 22, 107

Gardner, F.F., Morris, D., and Whiteoak, J.B. (1969) -
Aust. J. Phys. 22, 79

Gent, H., Adgie, R.L., and Crowther, J.H. (1969) -
Nature 222, 253

Gower, J.F.R. (1966) -
Mon. Not. R. astr. Soc. 133, 151

Gower, J.F.R., Scott, P.F., and Wills, D. (1967) -
Mem. R. astr. Soc. 71, 49

Harris, Beverley J. (1969) -
Ph.D. Thesis, the Australian National University

Heeschen, D.S. (1968) -
Astrophys. J. 151, L135

Hewish, A. (1961) -
Mon. Not. R. astr. Soc. 123, 167

Hoglund, Bertil (1967) -
Astrophys. J. Supp. 15, 61

Howard, William E., and Maran, Stephen P. (1965) -
Astrophys. J. Supp. 10, 1

Hoyle, F. (1968) -
Proc. R. Soc. 308, 1

Hoyle, F., and Burbidge, G.R. (1966) -
Nature 210, 1346

Hoyle, F., and Narlikar, J.V. (1961) -
Mon. Not. R. astr. Soc. 123, 133

Hoyle, F., and Narlikar, J.V. (1962) -
Mon. Not. R. astr. Soc. 125, 13

Hunstead, R.W. (1969) -
Proc. A.S.A. 1, 231

Jauncey, D.L. (1967) -
Nature 216, 877

Kellermann, K.I. (1964) -
Astrophys. J. 140, 969

Kellermann, K.I. (1966) -
Aust. J. Phys. 19, 195

Kellermann, K.I., and Pauliny-Toth, I.I.K. (1968a) -
Astrophys. J. 152, 639

Kellermann, K.I., and Pauliny-Toth, I.I.K. (1968b) -
Ann. Rev. Astron. Ap. 6, 417

Kellermann, K.I., and Pauliny-Toth, I.I.K. (1969) -
Astrophys. J. 155, L71

Kellermann, K.I., and Read, R.B. (1965) -
Pub. Owens Valley Obs. 1,2

Kellermann, K.I., Pauliny-Toth, I.I.K., and Davis, M.M. (1968) -
Astrophys. Lett. 2, 105

Kellermann, K.I., Pauliny-Toth, I.I.K., and Tyler, W.C. (1968) -
Astron. J. 73, 298

Kellermann, K.I., Pauliny-Toth, I.I.K., and Williams, P.J.S. (1969) -
Astrophys. J. 157, 1

Locke, J.L., Andrew, B.H., and Medd, W.J. (1969) -
Astrophys. J. 157, L81

Long, R.J., Smith, M.A., Stewart, P., and Williams, P.J.S. (1966) - Mon. Not. R. astr. Soc. 134, 371

Longair, M.S. (1966) -
Mon. Not. R. astr. Soc. 133, 421

Longair, M.S., and Scheuer, P.A.G. (1967) -
Nature 215, 919

MacLeod, J.M., and Andrew, B.H. (1968) -
Astrophys. Lett. 1, 243

McVittie, G.C. (1957) -
Aust. J. Phys. 10, 331

McVittie, G.C. (1965) -
General Relativity and Cosmology (2d ed; Chapman and Hall: London)

Maltby, P., and Moffet, Alan T. (1962) -
Astrophys. J. Supp. 7, 141

Merkelijn, Jeannette K. (1968) -
Aust. J. Phys. 21, 903

Merkelijn, Jeannette K. (1969) -
Aust. J. Phys. 22, 237

Mills, B.Y. (1960) -
Aust. J. Phys. 13, 550

Mills, B.Y., Slee, O.B., and Hill, E.R. (1960) -
Aust. J. Phys. 13, 676

Minkowski, R. (1960) -
Proc. 4th Berkeley Symp. on Mathematical Statistics and Probability 3, 245

Minnett, H.C., and Thomas, B.MacA. (1966) -
IEEE Trans. Antennas and Propagation AP-14, 654

Minnett, H.C., and Yabsley, D.E. (1966) -
Proc. I.R.E. (Aust.) 27, 304

Murdoch, H.S., and Large, M.I. (1968) -
Mon. Not. R. astr. Soc. 141, 377

Pauliny-Toth, I.I.K., and Kellermann, K.I. (1966) -
Astrophys. J. 146, 634

Pauliny-Toth, I.I.K., and Kellermann, K.I. (1968) -
Astrophys. J. 152, L169

Pauliny-Toth, I.I.K., Wade, C.M., and Heeschen, D.S. (1966) -
Astrophys. J. Supp. 13, 116

Peterson, Bruce A. (1969) -
Preprint

Petrosian, Vahé (1969) -
Astrophys. J. 155, 1029

Pilkington, J.D.H., and Scott, P.F. (1965) -
Mem. R. astr. Soc. 69, 183

Pooley, G.G. (1968a) -
Nature 218, 153

Pooley, G.G. (1968b) -
Obs. 88, 197

Pooley, G.G., and Ryle, M. (1968) -
Mon. Not. R. astr. Soc. 139, 515

Price, R.M., and Milne, D.K. (1965) -
Aust. J. Phys. 18, 329

Priester, W. (1958) -
Zeit. f. Astr. 46, 179

Refsdal, Sjur (1969) -
Astrophys. J. 155, 373

Rogstad, D.H., and Ekers, R.D. (1969) -
Astrophys. J. 157, 481

Ryle, M. (1968) -
Ann. Rev. Astron. Ap. 6, 249

Ryle, M., and Clarke, R.W. (1961) -
Mon. Not. R. astr. Soc. 122, 349

Sandage, Allan (1961) -
Astrophys. J. 133, 355

Sandage, Allan (1967) -
Astrophys. J. 150, L9

Sandage, Allan (1968a) -
Astrophys. J. 152, L149

Sandage, Allan (1968b) -
"Radio Galaxies and Quasars, II", in Highlights of Astronomy (ed. Perek, L., D. Reidel: Dordrecht)

Sandage, Allan (1968c) -
Obs. 88, 91

Scheer, D.J., and Kraus, J.D. (1967) -
Astron. J. 72, 536

Scheuer, P.A.G. (1957) -
Proc. Camb. Phil. Soc. 53, 764

Scheuer, P.A.G. (1968) -
"Radio Astronomy and Cosmology", to be published in Stars and Stellar Systems Vol. IX (ed. Sandage, A. and M.)

Scheuer, P.A.G., and Williams, P.J.S. (1968) -
Ann. Rev. Astron. Ap. 6, 321

Schmidt, Maarten (1968) -
Astrophys. J. 151, 393

Schorn, Ronald A., Epstein, Eugene E., Oliver, John P., Soter, Steven L., Wilson, William J. (1968) -
Astrophys. J. 151, L27

Searle, Leonard, and Bolton, J.G. (1968) -
Astrophys. J. 154, L101

Shane, C.D., and Wirtanen, C.A. (1967) -
Publ. Lick Obs. 22, 1

Shimmins, A.J. (1968a) -
Aust. J. Phys. 21, 65

Shimmins, A.J. (1968b) -
Astrophys. Lett. 2, 157

Shimmins, A.J., Bolton, J.G., and Wall, J.V. (1968) -
Nature 217, 818

Shimmins, A.J., Clarke, Margaret E., and Ekers, R.D. (1966) -
Aust. J. Phys. 19, 649

Shimmins, A.J., Manchester, R.N., and Harris, Beverley J. (1969) -
Aust. J. Phys. Astrophys. Supp. 8

Shimmins, A.J., Searle, L., Andrew, B.H., and Brandie, G.W. (1968) -
Astrophys. Lett. 1, 167

Shklovsky, I.S. (1965) -
Nature 206, 176

Slish, V.I. (1963) -
Nature 199, 682

Stewart, P. (1967) -
Nature 215, 1364

van der Laan, H. (1966) -
Nature 211, 1131

van der Laan, H. (1969) -
Bull. astr. Insts Neth. 20, 171

Véron, P. (1966) -
Nature 211, 724

von Hoerner, Sebastian (1961) -
Pub. NRAO 1, 19

Wall, J.V., Cole, D.J., and Milne, D.K. (1968) -
Proc. A.S.A. 1, 98

Williams, P.J.S. (1963) -
Nature 200, 56

Williams, P.J.S., and Collins, R.A. (1967) -
Obs. 87, 108

Williams, P.J.S., Collins, R.A., Caswell, J.L., and Holden, D.J. (1968) -
Mon. Not. R. astr. Soc. 139, 289

Wills, D. (1968) -
Astrophys. Lett. 2, 247

Wyllie, D.V. (1969) -
Proc. A.S.A. 1, 234

Wyndham, J.D. (1966) -
Astrophys. J. 144, 459

APPENDIX I

CONFUSION EFFECTS AT 2700 MHZ

An analysis of the confusion effects due to background sources has been carried out by von Hoerner (1961). He assumed no clustering of the background sources, and source counts of the form shown in Figure AI.1. These counts take two forms:

(i) a straight log N - log S to infinitely small flux densities, and

(ii) a straight log N - log S to S_{lim} with no sources of flux density $S < S_{lim}$. Under these assumptions he showed the total standard deviation of the background to be

$$\Delta S = \left\{ \frac{\gamma \, S_o^{\gamma}}{\mu} \int \frac{S_o dS}{S^{\gamma-1}} \right\}^{\frac{1}{2}}$$

where the lower limit of the integral is zero for source counts of form (i) above, and S_{lim} for the counts of form (ii), S_o is the lower limit of flux density to which sources are to be measured, $(-\gamma)$ is the slope of the log N - log S curve and μ is the number of beam areas per source of flux density $\geq S_o$.

The term "confusion limit" suffers from a multitude of definitions. The one adopted here is $S_{conf} = \Delta S$, i.e. the flux density of a source at the confusion limit is the same as the standard deviation of the background. The results on evaluating the integral (after von Hoerner) for $S_o = \Delta S$ are

$$\mu = \frac{\gamma}{2-\gamma} \left[1 - \left[\frac{S_{lim}}{S_o} \right]^{2-\gamma} \right] \qquad \gamma < 2$$

$$\mu = 2 \ln \left[\frac{S_o}{S_{lim}} \right] \qquad \gamma = 2$$

Calculation of μ for the source counts of Figure AI.1 yields the values in Table AI.1.

TABLE AI.1

BEAM AREAS PER SOURCE (μ) AT CONFUSION LIMIT

γ \ S_o/S_{lim} =	10	100	1000	∞
1.2	1.27	1.46	1.49	1.50
1.3	1.49	1.79	1.85	1.86
1.4	1.74	2.18	2.29	2.33
1.5	2.05	2.70	2.90	3.00
1.6	2.42	3.37	3.75	4.00
1.7	2.83	4.25	4.96	5.68
1.8	3.32	5.41	6.74	9.00
1.9	3.91	7.01	9.52	19.00
2.0	4.60	9.20	13.81	-

The families of log N - log S curves of Figure AI.1 have been normalized to the point (N,S) of (110, 1.0), taken from the 2700 MHz counts of Chapter 6. This point is reasonably free from the effects of confusion and statistical uncertainty. At 2700 MHz the Parkes telescope has a half power beamwidth of 7.9 arc minutes, and the corresponding beam area is 4.15×10^{-6} steradians. Calculation of S_o from this beam area and source count normalization, and from Table AI.1,

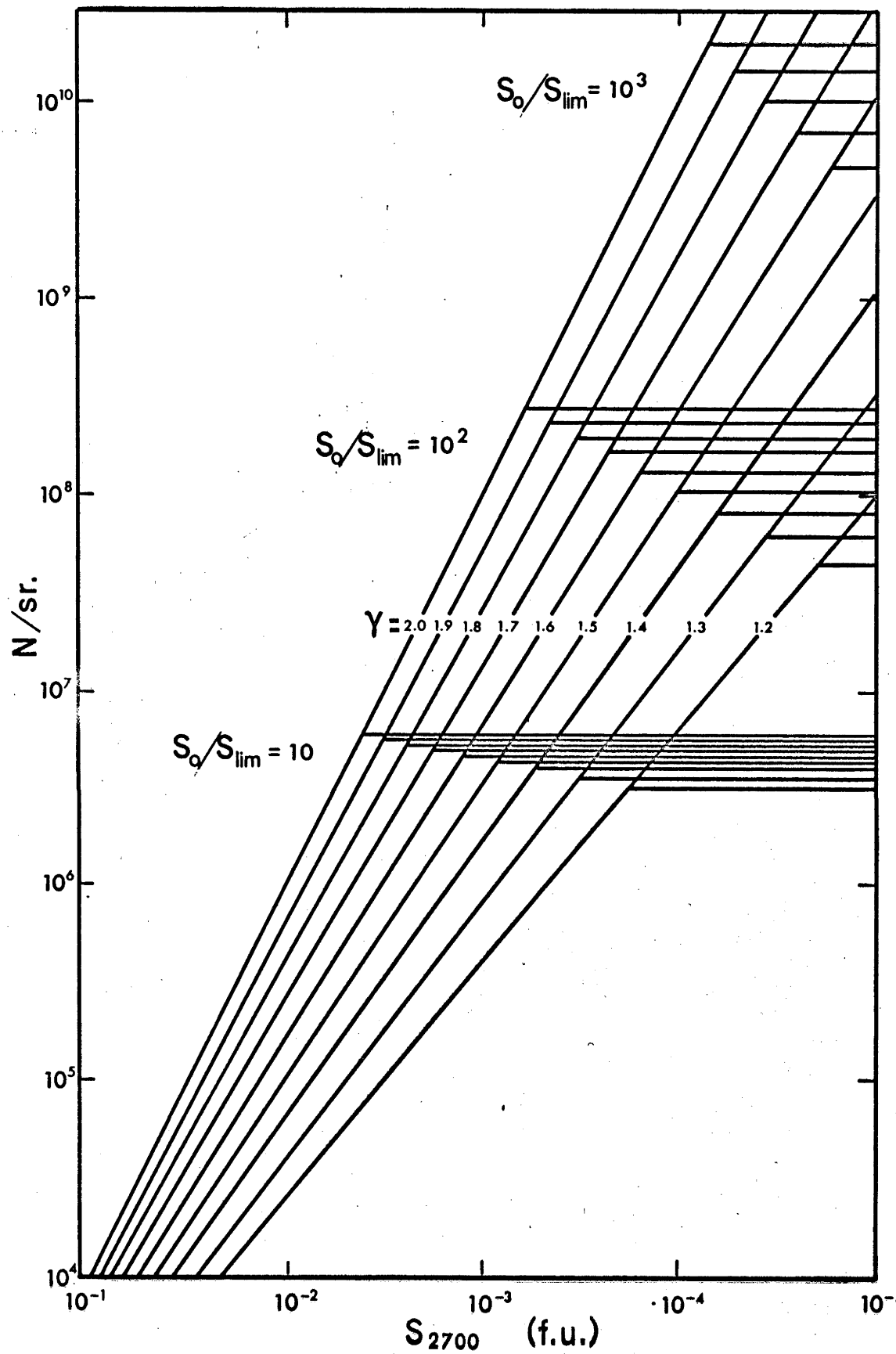

Figure AI.1. The families of number - flux density relations used in the confusion limit computations.

yields the values of the confusion limit in Table AI.2.

TABLE AI.2

CONFUSION LIMIT IN F.U.

S_o/S_{lim} =	10	100	1000	∞
γ				
1.2	.00200	.00229	.00230	.00231
1.3	.00367	.00423	.00434	.00435
1.4	.00614	.00715	.00741	.00747
1.5	.00946	.0116	.0120	.0122
1.6	.0140	.0174	.0188	.0195
1.7	.0197	.0255	.0278	.0299
1.8	.0271	.0388	.0403	.0474
1.9	.0335	.0486	.0572	.0822
2.0	.0458	.0647	.0794	-

Figures AI.2 and AI.3 show the confusion limit plotted against (S_o/S_{lim}) and against the slope of the log N - log S curve. Figure AI.2 indicates that the dependence on (S_o/S_{lim}) is not very marked for log N - log S slopes less steep than $\gamma = 1.5$. The strong dependence of the confusion limit on the slope of the source counts is evident from Figure AI.3. Also apparent is the fact that the confusion limit is virtually determined by the first decade of sources underlying it.

Two conclusions are drawn from the calculations:

(1) With a single beam receiver configuration a reasonable estimate for the confusion limit at 2700 MHz is 0.007 f.u.

(2) There exists the possibility of estimating the source

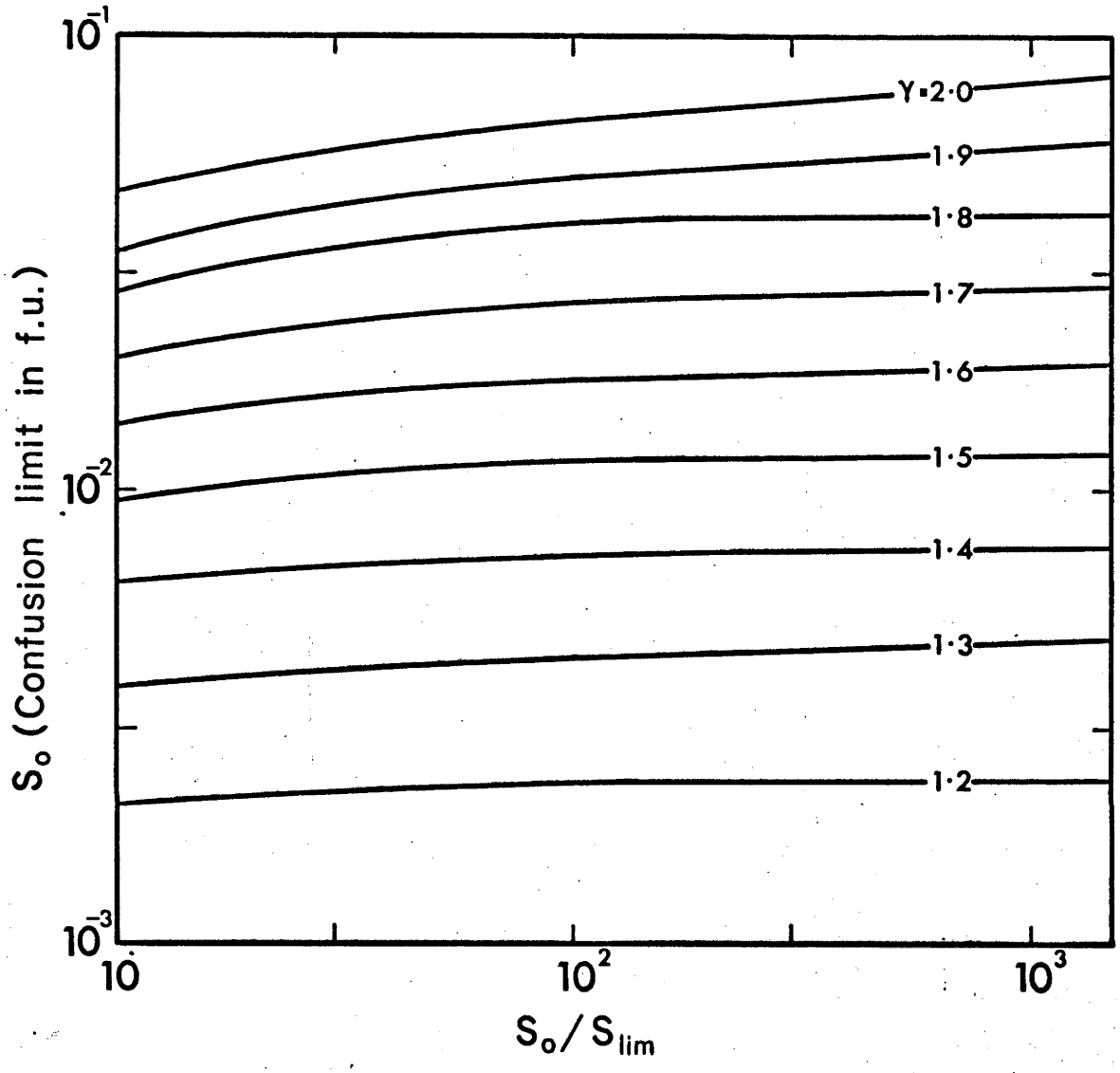

Figure AI.2. The dependence of the confusion limit on the limiting flux density for the source counts.

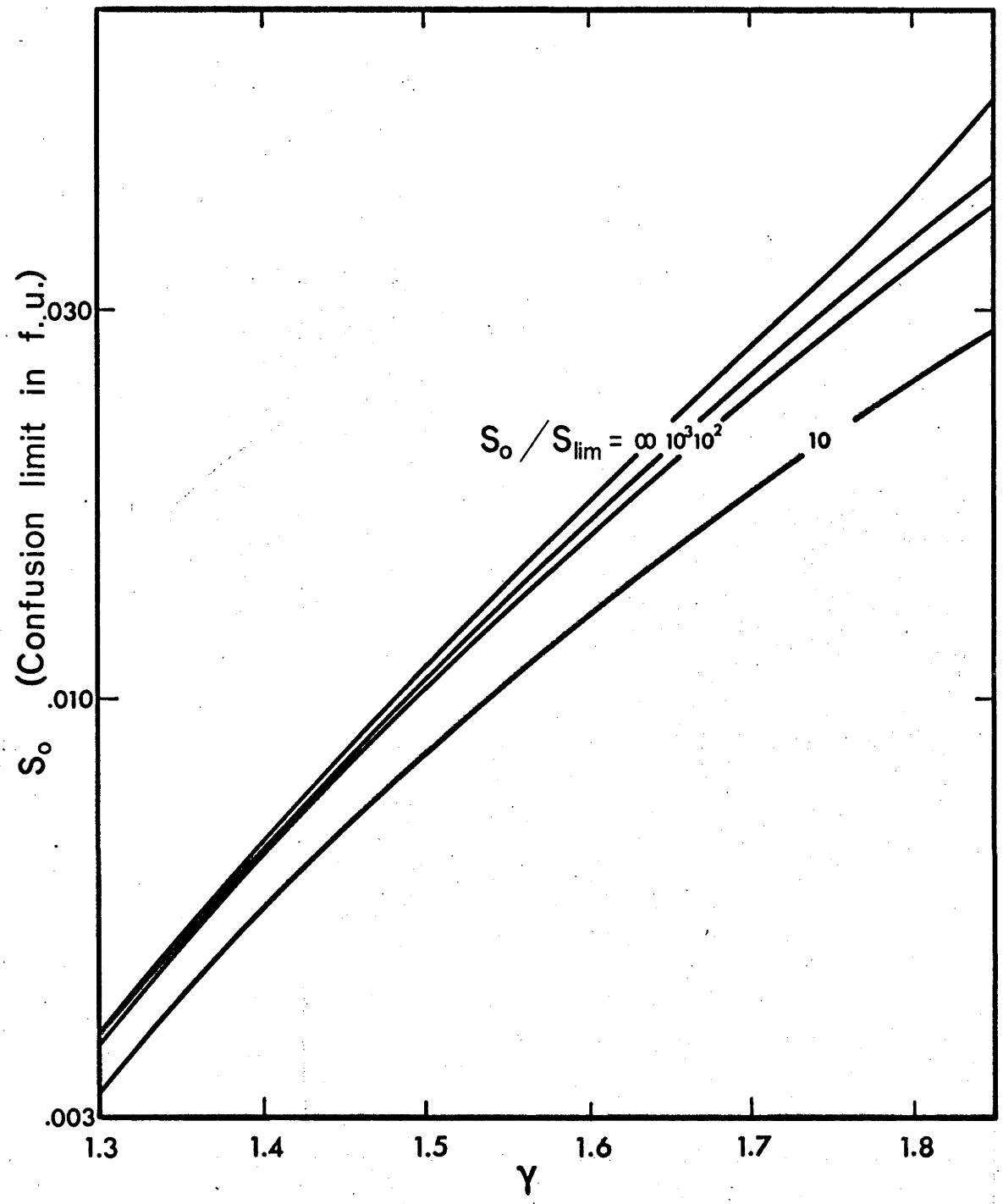

Figure AI.3. The dependence of the confusion limit on the slope of the number - flux density relation.

counts about a decade below the confusion limit by an experimental determination of the confusion limit. The direct source counts of the selected region surveys could thus be extended about two orders of magnitude below the survey limit of 0.10 f.u. A measurement of some significance could be made in only 24 hours of observing time. It is noted that the experiment is the pencil beam analogue of Scheuer's (1957) P(D) analysis for an interferometer survey (Hewish 1961).

Suppose that the flux densities of a series of sources are measured by pointing a telescope at each known source position and at several positions in the sky more than one beamwidth away from each source. The flux density measurement for each source is given by the difference between the on-source receiver output and the mean of the off-source outputs. With no a priori knowledge of the sky map, and with the use of several off-source positions, the distribution of confusion errors in such flux densities is identical to the distribution of deviations from the mean background at random points in the sky. These background fluctuations are known to obey a roughly Poissonian distribution, the tail being due to discrete sources stronger than the confusion limit.

For the sources in the 2700 MHz survey, the tail in this distribution has been largely eliminated by

(i) setting the survey limit at about 10 times the confusion limit, and

(ii) having a priori knowledge of the sky map about the sources, (a) from the original survey, and (b) from measuring the flux densities by scans through the sources (§2.7). The elimination of confusion effects was greatly aided by the ability of the receiver to detect sources down to 0.05 f.u. (half the flux density at the catalogue limit) without integration. From the point of view of noise and confusion, it is evident that measurement of flux densities by scans is the same as measurement by on-off techniques. The equivalent number of off-source positions depends on the length of scan baseline on either side of the source. The scans made for each catalogue source (Tables AII.1 and AII.2) are equivalent to about 6 off-source positions.

From these considerations it is estimated that the distribution of confusion errors in flux density is nearly Gaussian, with a standard deviation approximated by the confusion limit calculated above. The use of the dual beam system in the flux density measurements increases the confusion errors by a factor of $\sqrt{2}$, since each beam sees independent fluctuations in the background. The standard deviation of confusion errors in flux density is hence estimated as $\sqrt{2} \times 0.007 = 0.010$ f.u.

Similar arguments apply to confusion errors in the position measurements (§2.4). Since these errors are generally smaller than those due to calibration and receiver noise, no

formal evaluation has been attempted.

Observations shown in Figure AI.4 indicate very limited statistical support of the estimated scale of the background fluctuations. Ten 2700 MHz scans have been integrated by the author and D.J. Cooke with the PDP-9 on-line computer at the ANRAO. The principal aim was to examine integration techniques for further observations of this type. The 2700 MHz receiver was used in the dual beam mode, and the scans were made in declination between $00^{o}\ 00'$ and $-01^{o}\ 30'$ with the main and off-axis beams at right ascensions $17^{h}40^{m}32^{s}$ and $17^{h}39^{m}20^{s}$ (1969.5) respectively. Scan rate was 30 arc minutes per minute with an effective time constant (see §2.2) of 2 seconds. The drift is instrumental. Samples at beam-width intervals along the scan give an r.m.s. deviation from the mean of about 0.010 f.u., as estimated above.

Two further considerations indicate that the confusion error in the 2700 MHz flux densities has not been significantly underestimated. These are (i) the comparison of the flux densities with those measured at Green Bank (§2.9), and (ii) the form of the number - flux density relation near the lower limit to the selected region catalogues (§6.2).

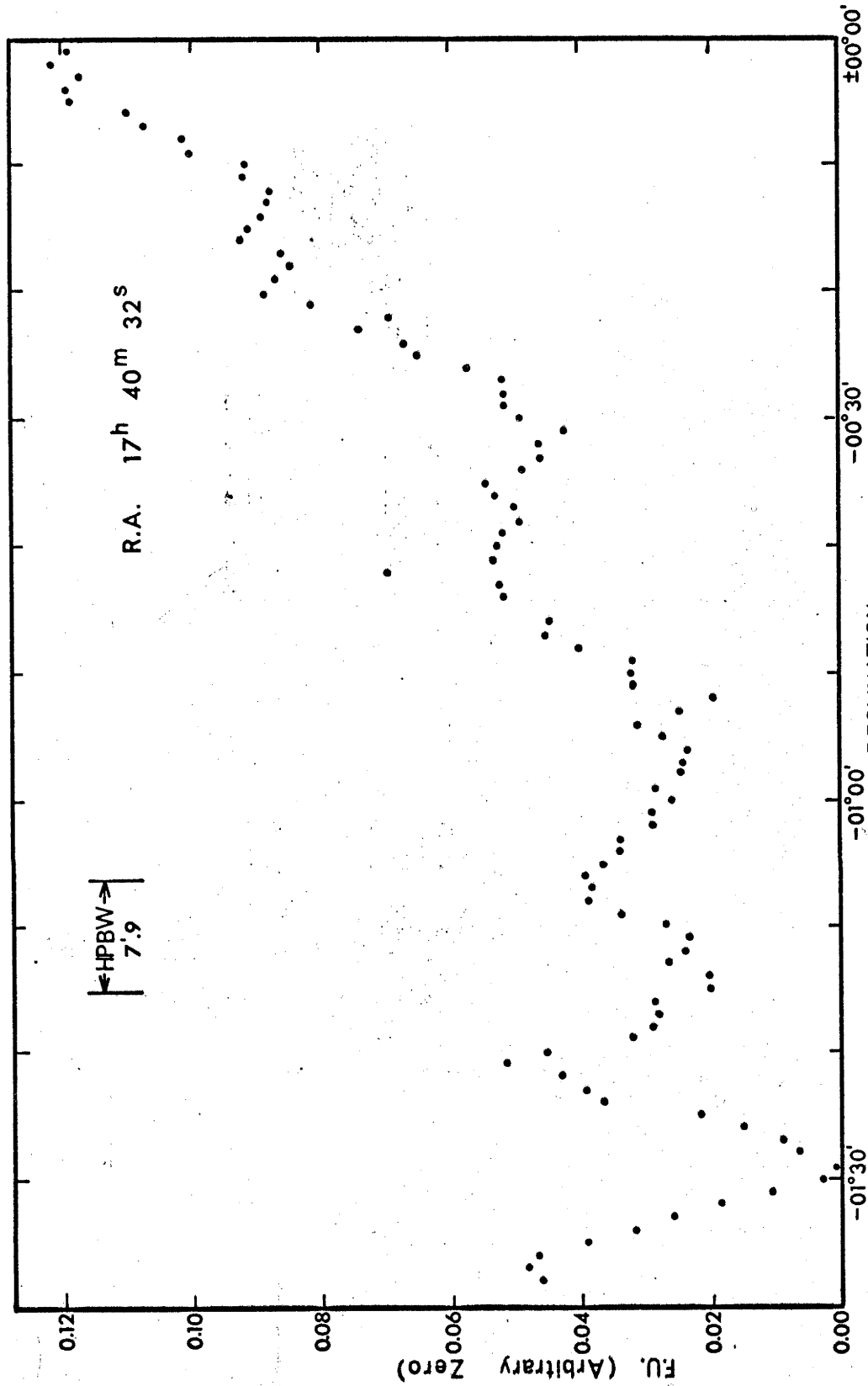

Figure AI.4. Integration of 10 scans with the 2700 MHz receiver in the dual beam configuration. Scan rate was 30 arc seconds per minute, and effective time constant 2 seconds. The drift is instrumental, and the r.m.s. fluctuation about the mean is about 0.01 f.u.

APPENDIX II

THE CATALOGUES

The first two parts of the Parkes 2700 MHz catalogue are presented in Tables AII.1 (the selected regions) and AII.2 (the $\pm 4^{\circ}$ declination zone). Sources common to both surveys are repeated in the tables. The contents of each column are as follows:

(1) Parkes source number. Sources which have been discovered in the course of the 2700 MHz survey are distinguished by an additional digit which represents tenths of degrees in declination.

(2) 4C catalogue number.

(3) Other catalogue designations.

(4), (5) Measured Coordinates, epoch 1950.0 (§2.4). Accurately measured coordinates of well established optical identifications are used where available; references are given in column 13.

(6) Session in which the position and flux density were measured. Corresponding dates are in Table 2.2.

(7) Position angle of the feed (measured north through east) during the position/flux density observation. For sessions 9, 10, and 11, no entry in this column means measurement at two orthogonal feed angles; for earlier sessions no entry indicates that the peak flux density has been corrected for polarization from the data

of Gardner, Whiteoak, and Morris (1969 and unpublished data).

(8) Peak flux density (f.u.) at 2700 MHz (§2.6).

(9) Standard error in the peak flux density (§2.7).

(10) Size factor (§2.6). Data on angular structure used in the calculation of size factors is given in Table 4.3.

(11) Integrated flux density at 2700 MHz (f.u.), i.e. peak flux density multiplied by size factor.

(12) Results of the optical identification programme (Chapter 3). The appearance of the 2 arc minutes error square is described in the following notation (after Wills and Bolton 1969):

QSO - quasi-stellar object, confirmed by ultraviolet excess from photometry, two-colour (blue - ultraviolet) photography, or optical spectrum.

QSO? - a blue stellar object within estimated position errors.

S,D,E,DB,N - galaxies of the corresponding optical classification.

G - a faint galaxy of indeterminate class.

II - several faint galaxies within positional errors, the accuracy of the radio position not permitting a unique identification.

III - a few stars of normal colour.

IIIa - as above, some obscuration possibly present.

IIIb - blank.

IIIc - very crowded star field.

IV - obscured.

Other abbreviations used are: BSO - blue stellar objects; UV - ultraviolet excess; and N - north, S - south, P - preceding, F - following. The magnitudes given are photographic magnitudes for galaxies and visual magnitudes for QSO's as estimated from the Palomar Sky Survey prints. Standard errors in the estimates are $0^{m}.5$. Redshifts are given where available.

(13) Remarks; the numbers given refer to the catalogue references, listed after Tables AII.1 and AII.2. The first reference number refers to the original identification of the source; it is sometimes difficult to establish this and apologies are offered for errors in this respect. Second and third reference numbers respectively indicate the source of the accurate optical position and the redshift where these have been measured.

TABLE AII.1

2700 MHZ SURVEY - SELECTED AREAS

(1) PKS SOURCE NUMBER	(2) OTHER CATALOGUE NUMBERS 4C	(3) OTHER	(4) POSITION (1950) R.A.	DEC.	(6) RUN	(7) PA	(8) 2700 MHZ PEAK FLUX DENSITY F.U.	(9) FLUX R.M.S. ERROR F.U.	(10) DENSITY SIZE FACTOR	(11) FLUX DENSITY F.U.	(12) IDENTIF-ICATION	(13) REMARKS
0038-020			00 38 23.8	-02 2 42	5	135	.610	.030	1.000	.610	QSO 18.5M	Z=1.176 (1) NOT IN SELECTED AREA
0038-019	-02.4	DA20	00 38 49.2	-01 59 18	5		.650	.020	1.000	.650	S 15.0M	
0039-020			00 39 48.7	-02 1 0	5	00	.073	.011	1.000	.073	III	
0040+031		08067	00 40 13.3	+03 10 42	5	135	.146	.012	1.000	.146	IIIB	
0040+017			00 40 15.1	+01 46 0	5	135	.117	.011	1.000	.117	N 18.7M	
0040-005			00 40 51.5	-00 32 0	5	135	.064	.011	1.000	.064		BSO WITH UV EXCESS 2'NP.
0041+001			00 41 1.9	+00 7 54	5	135	.076	.011	1.000	.076	QSO 19 M	
0041+007		08069	00 41 29.5	+00 45 24	5	135	.212	.013	1.000	.212		17.5M G 1.5'SP.
0041-000	-00.4		00 41 54.7	-00 1 36	5	135	.075	.011	1.000	.075		FAINT BSO NEAR POSITION. NO UV EXCESS
0041+015			00 41 57.6	+01 35 30	5	135	.065	.011	1.000	.065	G 19.5M	
0043+000	-00.5		00 43 8.0	+00 4 36	5	135	.269	.014	1.000	.269	E 17.8M	
0043-005			00 43 14.5	-00 30 6	5	45	.096	.011	1.000	.096	IIIB	
0043-029			00 43 29.4	-02 54 0	5	135	.108	.011	1.000	.108	IIIB	NOT IN SELECTED AREA
0043-010			00 43 33.2	-01 0 0	5	45	.188	.013	1.000	.188	IIIB	
0043-003			00 43 54.0	-00 21 18	5	135	.100	.011	1.000	.100	G 18.5M	
0044+030			00 44 27.6	+03 3 54	5	135	.089	.011	1.000	.089	III	
0045-009			00 45 29.8	-00 58 42	5	45	.144	.012	1.000	.144	III	
0045-000			00 45 44.7	-00 0 54	5	135	.110	.011	1.000	.110	QSO? 19M	POSSIBLE UV EXCESS
0045-025			00 45 48.0	-02 30 6	5	135	.157	.012	1.000	.157		3 FAINT RED OBJECTS
0045-002			00 45 53.1	-00 14 48	5	45	.087	.011	1.000	.087	III	
0046+011			00 46 5.7	+01 8 42	5	45	.078	.011	1.000	.078	II	CLUSTER OF GALS.
0047+006			00 47 6.5	+00 41 54	5	135	.091	.011	1.000	.091	III	

TABLE AII.1 CONTINUED

2700 MHZ SURVEY - SELECTED AREAS

(1)	(2)	(3)	(4)	(5)	(6)	(7)	(8)	(9)	(10)	(11)	(12)	(13)
PKS SOURCE NUMBER	OTHER CATALOGUE NUMBERS 4C	OTHER	POSITION (1950) R.A.	DEC.	RUN	PA	2700 MHZ PEAK FLUX DENSITY F.U.	FLUX R.M.S. ERROR F.U.	DENSITY SIZE FACTOR	FLUX DENSITY F.U.	IDENTIF-ICATION	REMARKS
0047+023		08078	00 47 8.0	+02 20 48	5	135	.319	.016	1.000	.319		18.5M G 1.5'SF.
0047-02	-03.2	MSH14	00 47 11.1	-02 59 12	5	135	.730	.030	1.000	.730	III	NOT IN SELECTED AREA
					8	45	.630	.030	1.000	.630		18M QSO?IDENT.(8)REVOKED
0049+019			00 49 4.6	+01 59 12	5	135	.111	.011	1.000	.111	G 20.2M	
0050-014			00 50 22.0	-01 26 6	5	135	.100	.011	1.000	.100	III	
0051-008			00 51 48.6	-00 49 36	5	135	.137	.012	1.000	.137		17.5M G 1.2'NF.
0052+011			00 52 22.2	+01 6 12	5	135	.078	.011	1.000	.078	S 14.5M	
0052+020			00 52 34.5	+02 3 0	5	45	.060	.011	1.000	.060	III	
0053-016			00 53 28.2	-01 36 24	5		.690	.060	1.027	.709		SEE TABLE AII.2
0053-025			00 53 32.3	-02 33 6	5	135	.096	.011	1.000	.096	III	
0053-015			00 53 52.8	-01 32 48	5		.760	.060	1.027	.781		SEE TABLE AII.2
0054-011			00 54 24.5	-01 11 18	5	135	.092	.011	1.450	.133		GALS 2.0'NF.
0054-006			00 54 42.8	-00 40 48	5	135	.113	.011	1.000	.113		S 1.4'SP.
0054+006			00 54 53.0	+00 37 42	5	45	.082	.011	1.000	.082	III	
0054+018		08092?	00 54 53.2	+01 53 12	5	135	.274	.015	1.000	.274	III	
0055-01	-01.5	3C29	00 55 1.4	-01 39 51	5		3.210	.080	1.046	3.358	E0 15.0M	Z=.0450 (6)(50)(40)
		MSH17			9		3.430	.080	1.046	3.588		
0055+015		08093	00 55 8.3	+01 34 30	5	45	.158	.012	1.000	.158		E4 1.0'NP.0055+015A
0055+038			00 55 35.1	+03 51 6	5	45	.092	.011	1.000	.092		FAINT G 0.8'NP.
0055+015			00 55 45.6	+01 32 54	5	45	.098	.011	1.000	.098	IIIB	0055+015B
0055-019			00 55 48.7	-01 57 0	5	45	.076	.011	1.000	.076	III	
0056+024			00 56 20.0	+02 24 12	5	135	.072	.011	1.000	.072	IIIB	

TABLE AII.1 CONTINUED

2700 MHZ SURVEY - SELECTED AREAS

(1)	(2)	(3)	(4)	(5)	(6)	(7)	(8)	(9)	(10)	(11)	(12)	(13)
PKS SOURCE NUMBER	OTHER CATALOGUE NUMBERS 4C	OTHER	POSITION (1950) R.A.	DEC.	RUN	PA	2700 MHZ PEAK FLUX DENSITY F.U.	FLUX R.M.S. ERROR F.U.	DENSITY SIZE FACTOR	FLUX DENSITY F.U.	IDENTIF-ICATION	REMARKS
0056-00	-00.6	DA 32	00 56 31.7	-00 9 16	5		1.960	.050	1.000	1.960	QSO 17.3M	Z=.717 (6)(11)(28)
					8		1.780	.050	1.000	1.780		
					9		1.850	.040	1.000	1.850		
0056+020			00 56 45.6	+02 4 18	5	45	.127	.012	1.000	.127	III	
0056+037			00 56 51.5	+03 45 42	5	45	.077	.011	1.000	.077		FAINT RED OBJ.NEAR POSN. NOT IN SELECTED AREA
0056-010			00 56 58.2	-01 2 18	5	135	.093	.011	1.000	.093		18.5M G 1.0'SF.
0057+028			00 57 34.4	+02 48 24	5	135	.065	.011	1.000	.065	QSO 18.5M	OPTICAL VARIABLE
0058-016			00 58 22.8	-01 39 12	5	135	.088	.011	1.000	.088	III	
0058-021			00 58 28.5	-02 8 48	5	135	.065	.011	1.000	.065	III	
0059+017	+01.1	08099	00 59 41.0	+01 47 36	5	135	.400	.020	1.000	.400	III	
0059+027			00 59 53.1	+02 46 36	5	135	.151	.012	1.000	.151	III	
0100-011			01 00 7.0	-01 6 30	5	135	.078	.011	1.000	.078	G 19.5M	
0100+023			01 00 55.8	+02 19 24	5	135	.128	.012	1.000	.128		19M G 1.0'NP.
0101-025			01 01 14.2	-02 32 18	5	135	.234	.014	1.000	.234	III	
0101-006			01 01 29.6	-00 40 24	5	135	.080	.011	1.000	.080	II	FAINT CLUSTER ON POSN. 16.3M G 1.0'SF.
0101+023			01 01 47.1	+02 23 18	5		.105	.011	1.000	.105	III	
0103-021			01 03 48.6	-02 11 48	5	135	.420	.020	1.000	.420	QSO 19M	
0104-004			01 04 32.4	-00 29 30	5	135	.078	.011	1.000	.078	III	
0105+034			01 05 48.9	+03 25 48	5	135	.181	.012	1.000	.181	IIIB	
0105+025	+02.2		01 05 49.8	+02 33 48	5	135	.122	.011	1.000	.122	III	
0105-008	-01.6		01 05 53.2	-00 53 18	5	135	.730	.030	1.000	.730		BSO NEAR POSITION NO UV EXCESS

TABLE AII.1 CONTINUED

2700 MHZ SURVEY - SELECTED AREAS

(1) PKS SOURCE NUMBER	(2) OTHER CATALOGUE NUMBERS 4C	(3) OTHER	(4) POSITION (1950) R.A.	DEC.	(6) RUN	(7) PA	(8) 2700 MHZ PEAK FLUX DENSITY F.U.	(9) FLUX R.M.S. ERROR F.U.	(10) DENSITY SIZE FACTOR	(11) FLUX DENSITY F.U.	(12) IDENTIF-ICATION	(13) REMARKS
0218+007		0D030	02 18 30.9	+00 46 18	3	135	.186	.013	1.000	.186	III	NOT IN SELECTED AREA
0219+013			02 19 33.0	+01 23 48	3	135	.153	.012	1.000	.153	IIIB	NOT IN SELECTED AREA
0219+007			02 19 56.9	+00 46 6	3	135	.103	.012	1.000	.103	III	
0220-029	-02.11		02 20 25.6	-02 56 24	5	135	.219	.013	1.000	.219	III	NOT IN SELECTED AREA
0220-023			02 20 42.3	-02 19 24	3	135	.112	.011	1.000	.112	III	
0222+000			02 22 34.8	+00 3 18	3	135	.142	.012	1.000	.142	QSO 19.0M	
0222-00	-00.12		02 22 35.0	-00 49 6	3 9	135	.660 .680	.030 .020	1.000 1.000	.660 .680	SO 16.5M	(8)
0223-023			02 23 2.2	-02 23 42	3	135	.225	.014	1.000	.225	III	
0223+035			02 23 21.6	+03 33 42	3	135	.142	.012	1.000	.142	IIIB	
0223+012			02 23 34.5	+01 16 6	3	135	.240	.014	1.000	.240	QSO 19M	
0223+018		0D039	02 23 41.3	+01 52 0	3	135	.220	.013	1.000	.220	III	
0225+003		0D043	02 25 31.8	+00 18 24	3	135	.141	.012	1.000	.141	III	
0225-014	-01.11		02 25 34.5	-01 29 6	3	135	.300	.020	1.000	.300	QSO 18M	Z=.685 (10)
0227+002			02 27 7.9	+00 12 24	3	135	.131	.011	1.000	.131	III	
0229+034			02 29 42.5	+03 25 30	5	135	.106	.011	1.000	.106	III	
0230-027			02 30 13.0	-02 46 36	3	135	.330	.020	1.000	.330		S 1.4'SP.
0230-022			02 30 58.5	-02 15 54	3 10	135	.173 .207	.013 .012	1.000 1.000	.173 .207	III	
0231+022			02 31 13.3	+02 15 48	5	135	.069	.012	1.000	.069	QSO 17.5M	
0231+016			02 31 26.7	+01 38 42	5	135	.092	.011	1.000	.092	III	

TABLE AII.1 CONTINUED

2700 MHZ SURVEY - SELECTED AREAS

(1)	(2)	(3)	(4)	(5)	(6)	(7)	(8)	(9)	(10)	(11)	(12)	(13)
PKS SOURCE NUMBER	OTHER CATALOGUE NUMBERS 4C	OTHER	POSITION (1950) R.A.	DEC.	RUN	PA	2700 MHZ PEAK FLUX DENSITY F.U.	FLUX R.M.S. ERROR F.U.	DENSITY SIZE FACTOR	FLUX DENSITY F.U.	IDENTIF-ICATION	REMARKS
0232-010			02 32 15.5	-01 3 24	5	135	.109	.011	1.000	.109		FAINT G 1.0'NP.
0232-02	-02.12		02 32 59.9	-02 32 24	5	135	.580	.020	1.000	.580	QSO 18M	
0235+017			02 35 5.8	+01 46 54	5	135	.177	.012	1.000	.177	E 14.8M	
0235-019	-02.13		02 35 25.0	-01 57 48	5	135	.224	.013	1.000	.224		BSO NEAR POSITION NO UV. EXCESS
0236+02		0D059	02 36 0	+02 21 30	5	45	.293	.015	1.000	.293		TWO 17.5M G'S,0.7'NF. AND 0.7'SP.
0236-015			02 36 45.0	-01 31 54	5	45	.147	.012	1.000	.147		BSO 1.0'NP. POSSIBLE UV EXCESS
0236+026			02 36 37.9	+02 39 24	5	135	.093	.012	1.000	.093	IIIB	
0237-027			02 37 14.5	-02 47 12	5		.400	.010	1.000	.400	QSO 18.5M	
					8	45	.430	.020	1.000	.430		
					9		.420	.010	1.000	.420		
0238-018	-02.14		02 38 23.3	-01 50 30	5	135	.102	.011	1.000	.102		FAINT BSO 0.3'S. POSSIBLE UV EXCESS
0238-005			02 38 26.0	-00 34 6	5	135	.091	.011	1.000	.091		FAINT BSO 0.5'NP. POSSIBLE UV EXCESS
0239+002			02 39 12.4	+00 13 54	5	135	.147	.012	1.000	.147	S 12.0M	NGC 1055
0239-016			02 39 37.0	-01 41 24	5	135	.128	.011	1.000	.128		BSO 0.3'NF. NO UV EXCESS
0240-00	-00.13	3C71 MSH14	02 40 7.0	-00 13 31	3		3.130	.070	1.000	3.130	SC 9,7M	Z=.00344 (35)(19)(22) SEYFERT G NGC 1068
					5		3.150	.050	1.000	3.150		
					8		3.050	.080	1.000	3.050		
					9		3.140	.070	1.000	3.140		

TABLE AII.1 CONTINUED

2700 MHZ SURVEY - SELECTED AREAS

(1) PKS SOURCE NUMBER	(2) OTHER CATALOGUE NUMBERS 4C	(3) OTHER	(4) POSITION (1950) R.A.	(5) DEC.	(6) RUN	(7) PA	(8) 2700 MHZ PEAK FLUX DENSITY F.U.	(9) FLUX R.M.S. ERROR F.U.	(10) DENSITY SIZE FACTOR	(11) FLUX DENSITY F.U.	(12) IDENTIF-ICATION	(13) REMARKS
0240-021			02 40 15.0	-02 10 12	5	135	.122	.011	1.000	.122	QSO?19.5M	WEAK UV,EXCESS. BSO 1,0'F HAS UV EXCESS.
0240+016		OD068	02 40 47.7	+01 39 18	5	135	.065	.011	1.000	.065	III	
0241-027			02 41 7.5	-02 45 42	5	135	.207	.013	1.000	.207	IIIB	
0241+011			02 41 10.0	+01 8 6	5	135	.122	.011	1.000	.122		NEAR NGC 1073
0241+031			02 41 11.2	+03 8 18	5	135	.082	.011	1.000	.082		FAINT RED OBJ. NEAR POSN.
0241-012			02 41 14.6	-01 15 24	5	135	.107	.011	1.000	.107	IIIB	
0242+028		OD071	02 42 50.5	+02 49 24	5	135	.285	.015	1.000	.285		FAINT RED OBJ. NEAR POSN.
0243+009	+00.9	OD072	02 43 .8	+00 55 54	5	135	.164	.012	1.000	.164	III	
0245+013			02 45 14.6	+01 19 0	5	135	.153	.012	1.000	.153	III	
1151+027			11 51 21.2	+02 42 0	8	45	.160	.012	1.000	.160	III	NOT IN SELECTED AREA
1152-011			11 52 28.8	-01 9 18	8	135	.078	.011	1.000	.078	G 18.3M	NOT IN SELECTED AREA
1154-019			11 54 5.6	-01 56 30	7	45	.112	.011	1.000	.112	III	
1154-038			11 54 13.4	-03 48 30	7	45	.167	.012	1.000	.167	D 15.7M	NOT IN SELECTED AREA
1154-011			11 54 36.6	-01 7 42	7 9	45	.106 .084	.011 .011	1.000 1.000	.106 .084	III	
1155-029			11 55 15.0	-02 56 12	7	45	.233	.013	1.000	.233	III	
1157+026			11 57 2.8	+02 36 24	8	45	.133	.012	1.000	.133	IIIB	
1157+014			11 57 11.7	+01 29 0	8	45	.143	.012	1.000	.143		BSO NEAR POSITION NO UV EXCESS
1157-011			11 57 12.9	-01 8 24	8	45	.086	.011	1.000	.086	III	

TABLE AII.1 CONTINUED

2700 MHZ SURVEY - SELECTED AREAS

(1)	(2)	(3)	(4)	(5)	(6)	(7)	(8)	(9)	(10)	(11)	(12)	(13)
PKS SOURCE NUMBER	OTHER CATALOGUE NUMBERS 4C	OTHER	POSITION (1950) R.A.	DEC.	RUN	PA	2700 MHZ PEAK FLUX DENSITY F.U.	FLUX R.M.S. ERROR F.U.	DENSITY SIZE FACTOR	FLUX DENSITY F.U.	IDENTIF-ICATION	REMARKS
1157-008			11 57 47.6	-00 49 12	8	135	.092	.011	1.000	.092	S 11.6M	NGC 4030
1158+007			11 58 50.1	+00 44 54	8	45	.257	.014	1.000	.257	QSO 18.5M	
1159-036			11 59 39.5	-03 37 30	7	45	.118	.011	1.000	.118	QSO 19.5M	
1159-02	-02.50		11 59 57.5	-02 23 36	5	45	.430	.020	1.000	.430	III	18M G IDENT.(8)REVOKED
1200+016			12 00 14.3	+01 40 36	8	135	.067	.011	1.000	.067	III	
1200-033			12 00 14.9	-03 19 24	7	45	.116	.011	1.000	.116	III	
					8	135	.138	.012	1.000	.138		
1201-026	-02.51		12 01 9.5	-02 38 12	7	45	.143	.012	1.000	.143	QSO? 19M	OPTICAL VARIABLE
					8	45	.158	.012	1.000	.158		
1201-002			12 01 30.1	-00 13 0	10		.193	.013	1.000	.193	G 20.5M	
1201+027			12 01 33.1	+02 42 18	8	135	.152	.012	1.000	.152	E 16.9M	NOT IN SELECTED AREA
					9		.163	.011	1.000	.163		
1203+011			12 03 14.4	+01 10 54	8	45	.126	.012	1.000	.126	QSO 18M	
1203+005			12 03 25.5	+00 34 48	8	45	.073	.011	1.000	.073	III	
1203-001			12 03 40.3	-00 6 0	8	135	.065	.011	1.000	.065	III	
1204-038			12 04 49.1	-03 51 6	8	135	.078	.011	1.000	.078	QSO?	NOT IN SELECTED AREA
1205-008			12 05 9.5	-00 51 0	8	45	.138	.012	1.000	.138	III	
1205+011			12 05 59.8	+01 11 12	8	45	.231	.014	1.000	.231	III	
1206-026			12 06 31.6	-02 40 48	8	45	.143	.012	1.000	.143	III	
					9		.159	.011	1.000	.159		
1207-013			12 07 58.0	-01 20 12	5	45	.370	.020	1.000	.370	DB 19.4M	
					9		.400	.010	1.000	.400		
1208-035			12 08 45.2	-03 33 42	8	45	.082	.011	1.000	.082	G 19.6M	
1209-008			12 09 10.7	-00 48 54	8	135	.075	.011	1.000	.075	III	

TABLE AII.1 CONTINUED

2700 MHZ SURVEY - SELECTED AREAS

(1)	(2)	(3)	(4)	(5)	(6)	(7)	(8)	(9)	(10)	(11)	(12)	(13)
PKS SOURCE NUMBER	OTHER CATALOGUE NUMBERS 4C	OTHER	POSITION (1950) R.A.	DEC.	RUN	PA	2700 MHZ PEAK FLUX DENSITY F.U.	FLUX R.M.S. ERROR F.U.	DENSITY SIZE FACTOR	FLUX DENSITY F.U.	IDENTIFICATION	REMARKS
1209-033			12 09 49.0	-03 23 18	8	135	.060	.011	1.000	.060		FAINT G 1.0'SP.
1210-010			12 10 39.4	-01 3 24	8	45	.089	.011	1.000	.089	III	
1211+003			12 11 21.7	+00 22 0	8		.102	.011	1.000	.102	QSO 20M	
1211+00			12 11 24.0	+00 3 48	8	45	.233	.014	1.000	.233		FAINT G 0.3'SP.(33)
1211+024			12 11 33.9	+02 26 6	8	45	.082	.011	1.000	.082	III	
1212-00	-00.48	MSH 7	12 12 14.3	-00 43 36	5	45	.510	.020	1.000	.510	III	
					8	135	.570	.020	1.000	.570		
					9		.540	.020	1.000	.540		
1212-021			12 12 24.3	-02 9 12	8	45	.085	.011	1.000	.085	IIIB	
1212+006	+00.42		12 12 48.3	+00 36 12	8	135	.285	.016	1.000	.285		FAINT BSO 1.0'SP. NO UV EXCESS
1213-023			12 13 33.9	-02 19 48	8	135	.093	.011	1.000	.093	IIIB	
1214-029	-02.52		12 14 36.4	-02 55 24	8	45	.250	.014	1.000	.250	III	
1215-033			12 15 21.1	-03 20 30	8	45	.108	.011	1.000	.108	III	
1215-002			12 15 26.1	-00 13 42	8	45	.286	.015	1.000	.286	III	
					9		.255	.012	1.000	.255		
1215+013			12 15 56.0	+01 19 18	8	45	.104	.011	1.000	.104	III	
1216-010			12 16 2.3	-01 3 12	8	45	.189	.013	1.000	.189	QSO 19.5M	UV NOT MARKED
					9		.226	.012	1.000	.226		
1216-025			12 16 43.7	-02 30 54	8	45	.094	.011	1.000	.094	IIIB	
1217+02			12 17 38.3	+02 20 21	5	45	.470	.020	1.000	.470	QSO 16.5M	Z=.240 (4)(4)(29)
					9		.450	.020	1.000	.450		
					11		.480	.020	1.000	.480		
1218-02	-02.53		12 18 51.5	-02 25 36	5	45	.540	.020	1.000	.540	QSO 20M	OPTICAL VARIABLE (13) NOT IN SELECTED AREA

TABLE AII.1 CONTINUED

2700 MHZ SURVEY - SELECTED AREAS

(1)	(2)	(3)	(4)	(5)	(6)	(7)	(8)	(9)	(10)	(11)	(12)	(13)
PKS SOURCE NUMBER	OTHER CATALOGUE NUMBERS 4C	OTHER	POSITION (1950) R.A.	DEC.	RUN	PA	2700 MHZ FLUX PEAK FLUX DENSITY F.U.	R.M.S. ERROR F.U.	DENSITY SIZE FACTOR	FLUX DENSITY F.U.	IDENTIFICATION	REMARKS
1219-036			12 19 17.4	-03 40 30	8	45	.087	.011	1.000	.087	III	NOT IN SELECTED AREA
1328-001			13 28 27.2	-00 9 12	2	135	.090	.010	1.000	.090	III	
1328-034			13 28 51.5	-03 25 42	1		.257	.011	1.000	.257	QSO 19M	
1329+012	+01.38		13 29 43.1	+01 17 30	1		.210	.012	1.000	.210		FAINT BSO ON POSN. NO UV EXCESS
1330+02	+02.36	MSH 7	13 30 20.5	+02 16 9	9		1.820	.040	1.050	1.911	N 19.1	Z=.2156 (17)(30)(39) 3C287.1
1331+004			13 31 8.6	+00 25 42	1		.140	.011	1.000	.140	QSO 20.0M	
					2	135	.151	.011	1.000	.151		
1331+025			13 31 16.4	+02 34 18	1	135	.145	.012	1.000	.145	QSO 18.5M	
1331-013			13 31 27.7	-01 18 36	2	135	.052	.011	1.000	.052		GALS. NEAR POSITION
1334+008			13 34 59.5	+00 50 54	1	135	.101	.011	1.000	.101	III	
1335+023			13 35 7.3	+02 22 6	2	135	.104	.011	1.000	.104	QSO 17.5M	Z=0.61 (10)
1336+003			13 36 8.8	+00 18 6	1	135	.117	.011	1.000	.117	III	
1336-030			13 36 57.4	-03 0 54	1	135	.190	.013	1.000	.190	III	
					2	135	.208	.014	1.000	.208		
1336+020	+02.37		13 36 58.8	+02 0 36	1	135	.380	.020	1.000	.380	III	
					2	135	.390	.010	1.000	.390		
1336-000			13 36 59.8	-00 1 12	1	135	.132	.012	1.000	.132	QSO 19M	
					2	90	.099	.011	1.000	.099		
1337-013			13 37 30.1	-01 22 18	1	135	.192	.013	1.000	.192	QSO 18.5M	Z=1.607 (1)

TABLE AII.1 CONTINUED

2700 MHZ SURVEY - SELECTED AREAS

(1)	(2)	(3)	(4)	(5)	(6)	(7)	(8)	(9)	(10)	(11)	(12)	(13)
PKS SOURCE NUMBER	OTHER CATALOGUE NUMBERS 4C	OTHER	POSITION R.A.	(1950) DEC.	RUN	PA	2700 MHZ PEAK FLUX DENSITY F.U.	FLUX R.M.S. ERROR F.U.	DENSITY SIZE FACTOR	FLUX DENSITY F.U.	IDENTIF-ICATION	REMARKS
1337-033			13 37 38.1	-03 20 12	1	135	.580	.020	1.000	.580	III	
					2	135	.580	.030	1.000	.580		
1338+011			13 38 58.0	+01 7 48	1	135	.160	.013	1.000	.160	G 20,2M	
1339+015			13 39 43.0	+01 32 30	1	45	.172	.012	1.000	.172		BSO ON POSITION
					2	135	.172	.013	1.000	.172		NO UV EXCESS
1340+022	+02.38	MSH 9	13 40 16.6	+02 13 0	1	135	.540	.020	1.000	.540	III	
1341+005			13 41 40.3	+00 32 12	1	45	.080	.011	1.000	.080		BSO NEAR POSITION
					2	135	.082	.011	1.000	.082		POSSIBLE UV EXCESS
1342-016			13 42 43.2	-01 41 18	2	135	.224	.014	1.000	.224	D 18,0M	
					11		.208	.012	1.000	.208		
1343-00	-00.51		13 43 3.1	-00 41 48	1	45	.620	.030	1.000	.620	III	17.7M QSO? PREV.IDENT. (8) REVOKED. PKS1342-00
1343-026	-02.58		13 43 17.4	-02 37 42	1	135	.245	.014	1.000	.245	IIIB	
1343+011			13 43 47.8	+01 10 12	1	45	.101	.011	1.000	.101	QSO? 20M	
1344+029			13 44 51.7	+02 55 24	1	45	.149	.012	1.000	.149		BSO 0.7'F. NOT IN SELECTED AREA
1345+008	+00.47		13 45 10.3	+00 50 12	1	135	.139	.012	1.000	.139	III	
					2	135	.176	.013	1.000	.176		
1345+002			13 45 13.5	+00 12 24	2	135	.103	.011	1.000	.103	III	
1346-015			13 46 38.9	-01 31 24	2	135	.089	.011	1.000	.089	III	
1346+018			13 46 58.5	+01 49 18	1	135	.147	.012	1.000	.147	III	
1348-011			13 48 22.3	-01 11 0	2	135	.107	.012	1.000	.107	III	
					11		.105	.011	1.000	.105		
1348+007			13 48 30.6	+00 46 12	2	135	.175	.013	1.000	.175	III	

TABLE AII.1 CONTINUED

2700 MHZ SURVEY - SELECTED AREAS

(1) PKS SOURCE NUMBER	(2) OTHER CATALOGUE NUMBERS 4C	(3) OTHER	(4) POSITION (1950) R.A.	DEC.	(5) RUN	(6) PA	(7) 2700 MHZ PEAK FLUX DENSITY F.U.	(8) FLUX DENSITY R.M.S. ERROR F.U.	(9) SIZE FACTOR	(10) FLUX DENSITY F.U.	(11) IDENTIFICATION	(12) REMARKS
1349-019			13 49 23.3	-01 55 12	1	45	.139	.012	1.000	.139	III	PART OF 4C-01.30
					2	135	.118	.012	1.000	.118		
1349-01			13 49 49.4	-01 41 24	2	135	.310	.020	1.000	.310	G 19.6M	PART OF 4C-01.30
1349-008			13 49 52.3	-00 53 18	1	45	.137	.012	1.000	.137		G 0.8'NF.
1349+027			13 49 58.2	+02 47 24	1	45	.810	.030	1.000	.810	III	NOT IN SELECTED AREA
					8	45	.770	.030	1.000	.770		
					9		.720	.020	1.000	.720		
1351+003			13 51 19.0	+00 21 0	2	135	.071	.011	1.000	.071	G 20.2M	IN SMALL CLUSTER
1351+021			13 51 22.1	+02 6 54	2	135	.500	.020	1.000	.500		19.5M BSO 0.7'SP.
					8	45	.440	.020	1.000	.440		UV EXCESS
					11		.460	.020	1.000	.460		
1351-018			13 51 32.8	-01 51 18	2	135	1.000	.040	1.000	1.000		FAINT BSO 1.0'NP.
					8	45	.980	.040	1.000	.980		UV EXCESS
					9		.970	.020	1.000	.970		
					11		.990	.030	1.000	.990		
1352+00			13 52 35.3	+00 55 3	2	135	.400	.020	1.000	.400	QSO?19M	(33)
					8	45	.300	.020	1.000	.300		
1353-005	-00.52		13 53 48.4	-00 34 36	2	135	.320	.020	1.000	.320	III	NOT IN SELECTED AREA
					8	45	.310	.020	1.000	.310		
2149-20			21 49 4.7	-20 0 6	3	135	1.230	.050	1.000	1.230	QSO? 19M	NOT IN SELECTED AREA
2149-158		MSH20	21 49 14.7	-15 51 24	3	135	.320	.020	1.000	.320	DB	17.1M+17.3M NOT IN SELECTED AREA
2150-202			21 50 57.0	-20 15 12	3		.310	.010	1.000	.310	III	
2151-153			21 51 26.7	-15 18 12	3	135	.430	.020	1.000	.430		FAINT G 0.8'NF. NOT IN SELECTED AREA

TABLE AII.1 CONTINUED

2700 MHZ SURVEY - SELECTED AREAS

(1)	(2)	(3)	(4)	(5)	(6)	(7)	(8)	(9)	(10)	(11)	(12)	(13)
PKS SOURCE NUMBER	OTHER CATALOGUE NUMBERS 4C	OTHER	POSITION (1950) R.A.	DEC.	RUN	PA	2700 MHZ PEAK FLUX DENSITY F.U.	FLUX R.M.S. ERROR F.U.	DENSITY SIZE FACTOR	FLUX DENSITY F.U.	IDENTIF-ICATION	REMARKS
2152-218			21 52 16.9	-21 50 48	3	135	.186	.013	1.450	.270	III	
2152-213			21 52 59.9	-21 23 0	3	135	.049	.011	1.000	.049		BSO 1.5'NF.
2153-219			21 53 12.7	-21 58 42	3	135	.114	.011	1.000	.114	N 17.2M	
2153-188			21 53 23.8	-18 50 36	3	135	.141	.012	1.000	.141	III	
2153-204			21 53 48.6	-20 26 36	3	135	.220	.014	1.000	.220	QSO 17M	Z=1.31 (47)
2154-18		MSH23	21 54 13.2	-18 27 54	3		1.080	.040	1.026	1.108	III	16.5M QSO? IDENT.(6) REVOKED
2154-214			21 54 43.3	-21 24 6	3	135	.087	.011	1.000	.087	III	
2154-183			21 54 43.6	-18 21 24	3	135	.990	.040	1.011	1.001	III	
2155-202			21 55 4.7	-20 12 18	3	135	.217	.014	1.000	.217	G 19.6M	
2155-152			21 55 24.0	-15 15 30	3 11	135	1.780 1.560	.070 .040	1.000 1.000	1.780 1.560	III	NOT IN SELECTED AREA
2155-195			21 55 32.9	-19 32 42	3	135	.077	.011	1.000	.077		G 1.5'NP.
2156-203			21 56 3.8	-20 19 48	3	135	.090	.011	1.000	.090		G 1.2'S.
2156-192			21 56 26.3	-19 12 30	3	135	.103	.011	1.000	.103		G 1.0'S.
2156-183			21 56 34.6	-18 22 12	3	135	.090	.011	1.000	.090	QSO 19.5M	
2157-214			21 57 11.1	-21 25 0	3	135	.167	.012	1.000	.167	III	
2157-200			21 57 21.8	-20 0 24	3	135	.133	.012	1.000	.133	QSO 19.5M	OPTICAL VARIABLE
2157-172			21 57 39.4	-17 12 36	3	135	.066	.011	1.000	.066		G 1.3'NF.
2157-191			21 57 54.6	-19 10 6	3	135	.133	.012	1.000	.133	G 20.2M	
2158-160			21 58 4.9	-16 1 30	3	135	.140	.012	1.000	.140	III	
2158-167			21 58 10.8	-16 47 18	3	135	.147	.012	1.000	.147		BSO ON POSITION

TABLE AII.1 CONTINUED

2700 MHZ SURVEY - SELECTED AREAS

(1)	(2)	(3)	(4)	(5)	(6)	(7)	(8)	(9)	(10)	(11)	(12)	(13)
PKS SOURCE NUMBER	OTHER CATALOGUE NUMBERS 4C	OTHER	POSITION (1950) R.A.	DEC.	RUN	PA	2700 MHZ PEAK FLUX DENSITY F.U.	FLUX R.M.S. ERROR F.U.	DENSITY SIZE FACTOR	FLUX DENSITY F.U.	IDENTIF-ICATION	REMARKS
												NO UV EXCESS
2158-206			21 58 41.2	-20 39 48	3	135	.235	.014	1.000	.235		FAINT BSO ON POSN. NOT ON B/UV PLATE
2158-170			21 58 47.1	-17 3 0	3		.178	.012	1.000	.178	III	
2158-17			21 58 54.3	-17 47 36	3	135	.294	.015	1.000	.294	III	
2159-215			21 59 3.7	-21 32 18	3	135	.130	.012	1.000	.130	QSO 19.0M	
2159-187			21 59 5.3	-18 47 30	3	135	.183	.013	1.000	.183	III	
2159-192			21 59 28.1	-19 16 36	3	135	.169	.012	1.000	.169		G 1.2'S.
2159-205			21 59 30.2	-20 31 54	3	135	.081	.011	1.000	.081	III	
2159-163			21 59 35.0	-16 20 6	3	135	.068	.011	1.000	.068		FAINT G NEAR POSN.
2159-219			21 59 52.7	-21 56 48	3	135	.093	.011	1.000	.093	III	
2159-201			21 59 56.5	-20 9 48	3	135	.200	.013	1.000	.200	III	
2159-186			21 59 58.6	-18 37 12	11	135	.070	.011	1.000	.070	III	
2200-189			22 00 6.1	-18 54 42	3	90	.167	.012	1.000	.167	III	
2200-220			22 00 19.8	-22 3 30	3	135	.077	.011	1.000	.077		2 FAINT BSO'S ON POSN. NOT ON B/UV PLATE
2201-217			22 01 16.4	-21 42 42	3	135	.146	.012	1.000	.146	E+E	16.5M+17.3M IN CLUSTER
2201-184			22 01 37.9	-18 26 30	3	135	.078	.011	1.000	.078	III	
2202-179			22 02 12.8	-17 57 18	3	135	.340	.020	1.000	.340	III	
2203-18		MSH11	22 03 25.8	-18 50 16	3		5.200	.110	1.000	5.200	QSO 19.5M	(6)(25)
					4		5.200	.190	1.000	5.200		
					11		5.200	.140	1.000	5.200		
2203-215			22 03 54.9	-21 34 30	3	45	.158	.012	1.000	.158		BSO NEAR POSITION NO UV EXCESS

TABLE AII.1 CONTINUED

2700 MHZ SURVEY - SELECTED AREAS

(1) PKS SOURCE NUMBER	(2) OTHER CATALOGUE NUMBERS 4C	(3) OTHER	(4) POSITION (1950) R.A.	DEC.	(5) RUN	(6) PA	(7) 2700 MHZ PEAK FLUX DENSITY F.U.	(8) FLUX R.M.S. ERROR F.U.	(9) DENSITY SIZE FACTOR	(10) FLUX DENSITY F.U.	(11) IDENTIF-ICATION	(12) REMARKS
2204-182			22 04 10.0	-18 15 36	3	45	.340	.020	1.000	.340	III	
2204-20			22 04 31.1	-20 18 36	3	45	.350	.020	1.000	.350	III	
2204-218			22 04 40.2	-21 49 18	3	45	.083	.011	1.000	.083	E 16.8M	
2204-208			22 04 49.3	-20 53 18	3	45	.145	.012	1.000	.145		BSO NEAR POSITION NOT ON B/UV PLATE
2205-178			22 05 16.5	-17 53 6	3	45	.152	.012	1.000	.152	III	
2207-187			22 07 23.8	-18 45 12	3	45	.079	.011	1.000	.079	III	
2207-203			22 07 33.5	-20 22 6	3	45	.111	.012	1.000	.111		BSO NEAR POSITION NO UV EXCESS
2207-159			22 07 38.1	-15 59 30	3	45	.069	.011	1.000	.069	III	
2209-154			22 09 50.3	-15 26 30	3 4	45 22	.077 .094	.011 .012	1.000 1.000	.077 .094	QSO?20.0M	NOT IN SELECTED AREA
2210-210			22 10 40.2	-21 4 18	3	45	.098	.011	1.000	.098	III	
2211-17		3C444	22 11 42.0	-17 16 42	11		4.470	.120	1.010	4.515	D 19M	(53) MSH7
2211-202			22 11 48.2	-20 17 0	3	45	.093	.011	1.000	.093		FAINT G? 0.5'SP.
2212-159			22 12 14.3	-15 58 30	3	45	.255	.014	1.000	.255		G WITH UV EXCESS 2'S. NOT IN SELECTED AREA
2313-167			23 13 31.6	-16 47 6	3	45	.198	.013	1.000	.198	E 18.3M	
2213-200			22 13 34.1	-20 3 48	3	45	.073	.011	1.000	.073	III	
2213-156			22 13 51.5	-15 39 18	3	45	.281	.015	1.000	.281	III	
2214-192			22 14 21.1	-19 16 36	3	45	.075	.011	1.000	.075	III	
2215-206			22 15 3.3	-20 38 12	3	45	.125	.011	1.000	.125	III	
2215-179			22 15 19.3	-17 58 0	3	45	.234	.014	1.000	.234	III	
2215-185			22 15 37.2	-18 35 0	3	45	.104	.011	1.000	.104	III	

TABLE AII.1 CONTINUED

2700 MHZ SURVEY - SELECTED AREAS

(1)	(2)	(3)	(4)	(5)	(6)	(7)	(8)	(9)	(10)	(11)	(12)	(13)
PKS SOURCE NUMBER	OTHER CATALOGUE NUMBERS 4C	OTHER	POSITION (1950) R.A.	DEC.	RUN	PA	2700 MHZ PEAK FLUX DENSITY F.U.	FLUX DENSITY R.M.S. ERROR F.U.	SIZE FACTOR	FLUX DENSITY F.U.	IDENTIFICATION	REMARKS
2353-003	-00.84		23 53 2.3	-00 19 12	3	135	.163	.012	1.000	.163	III	
2353+028			23 53 16.3	+02 51 0	3	135	.099	.011	1.000	.099	III	
2353+004			23 53 20.2	+00 24 30	3	135	.095	.011	1.000	.095	III	
2353-018			23 53 33.0	-01 48 0	3	135	.118	.012	1.000	.118		E 16M 2.0'NP.
2353+010			23 53 34.1	+01 2 36	3	135	.104	.011	1.000	.104	III	
2354-02	-02.91		23 54 31.9	-02 43 18	2	135	.459	.020	1.000	.459	III	NOT IN SELECTED AREA
2354+008		0Z091	23 54 37.7	+00 48 30	2	135	.157	.013	1.000	.157		FAINT OBJECT WITH POSSIBLE UV.EXCESS
2354-021			23 54 51.1	-02 9 18	2	135	.287	.015	1.000	.287	III	
2355-024			23 55 24.2	-02 28 12	2	135	.151	.012	1.000	.151	III	
2355-010	-00.85		23 55 51.5	-01 1 36	2	135	.423	.019	1.000	.423	III	
2356+023			23 56 2.3	+02 23 48	3	135	.106	.011	1.000	.106	III	
2356+033	+03.61	0Z094	23 56 7.6	+03 20 30	2 3	135 135	.209 .228	.014 .014	1.000 1.000	.209 .228	III	
2356-028	-02.92		23 56 30.0	-02 52 12	3	45	.171	.013	1.000	.171	III	NOT IN SELECTED AREA
2356+030			23 56 30.1	+03 5 54	3	45	.064	.011	1.000	.064		NOT IN SELECTED AREA FAINT G 1.1'NP.
2356+01			23 56 41.3	+01 50 6	2	135	.156	.013	1.000	.156	E4 17.5M	
2356-023			23 56 43.3	-02 21 24	2	135	.108	.011	1.000	.108	III	
2357-007			23 57 4.5	-00 47 54	3	135	.101	.011	1.000	.101	IIIB	
2357+00		0Z095	23 57 24.2	+00 25 30	3	135	.275	.015	1.000	.275	DB 15.6M	(17)
2357-006			23 57 59.3	-00 38 42	3	135	.147	.012	1.000	.147	IIIB	
2358+028			23 58 6.3	+02 51 6	3	135	.073	.011	1.000	.073	III	
2359+017		0Z098	23 59 17.2	+01 46 30	3	135	.174	.012	1.000	.174	IIIB	

TABLE AII.1 CONTINUED

2700 MHZ SURVEY - SELECTED AREAS

(1)	(2)	(3)	(4)	(5)	(6)	(7)	(8)	(9)	(10)	(11)	(12)	(13)
PKS SOURCE NUMBER	OTHER CATALOGUE NUMBERS 4C	OTHER	POSITION (1950) R.A.	DEC.	RUN	PA	2700 MHZ PEAK FLUX DENSITY F.U.	FLUX R.M.S. ERROR F.U.	DENSITY SIZE FACTOR	FLUX DENSITY F.U.	IDENTIF-ICATION	REMARKS
2359-012			23 59 36.2	-01 14 18	3	135	.047	.011	1.000	.047	III	
0000-006			00 00 21.8	-00 41 24	2	135	.236	.014	1.000	.236	III	
0000+035		0B001	00 00 44.7	+03 31 18	3	135	.146	.012	1.000	.146	IIIB	
0000-022			00 00 49.2	-02 13 24	3	135	.156	.013	1.000	.156	III	
0001+037			00 01 6.8	+03 43 48	3	135	.125	.012	1.000	.125	III	NOT IN SELECTED AREA
0003-008			00 03 12.2	-00 51 24	3	135	.073	.011	1.000	.073		18M G 1.1'SF.
0003+006		0B005	00 03 30.3	+00 37 12	2	135	.248	.015	1.000	.248	G 18.3M	
0003-00	-00.1	3C2 MSH 1	00 03 48.7	-00 21 6	2		2.400	.040	1.000	2.400	QS019.5M	Z=1.037 (42)(42)(26)
					3		2.430	.050	1.000	2.430		
					9		2.400	.050	1.000	2.400		
0004-000			00 04 42.2	-00 1 12	3	135	.065	.011	1.000	.065		17.5M G 1.1'NP.
0004-010			00 04 56.9	-01 5 12	3	135	.088	.011	1.000	.088	E 16.3M	
0005+021		0B009	00 05 10.4	+02 10 12	3	135	.117	.012	1.000	.117		TWO BSO'S.NO UV.EXCESS
0005+024			00 05 32.2	+02 28 30	3	135	.066	.010	1.000	.066	III	
0006+021			00 06 6.9	+02 11 24	3	135	.093	.011	1.000	.093	III	
0006-005			00 06 15.2	-00 33 12	11	45	.092	.011	1.000	.092	III	
0006+014			00 06 17.0	+01 25 54	2	135	.094	.011	1.000	.094	QSO 18.5M	
0006-025			00 06 43.0	-02 35 54	3	135	.071	.011	1.000	.071	III	
0007+016		0B014	00 07 23.7	+01 41 6	2	135	.160	.013	1.000	.160	G 20.5M	
0008+009			00 08 3.1	+00 55 30	3	135	.088	.011	1.000	.088	III	
0008-011			00 08 9.0	-01 7 42	3	135	.077	.011	1.000	.077	III	
0008-006			00 08 20.4	-00 36 48	3	135	.106	.011	1.000	.106	III	
0008+034			00 08 36.7	+03 25 30	3	135	.064	.011	1.000	.064	III	NOT IN SELECTED AREA

TABLE AII.1 CONCLUDED

2700 MHZ SURVEY - SELECTED AREAS

(1) PKS SOURCE NUMBER	(2) OTHER CATALOGUE NUMBERS 4C	(3) OTHER	(4) POSITION (1950) R.A.	(5) DEC.	(6) RUN	(7) PA	(8) 2700 MHZ PEAK FLUX DENSITY F.U.	(9) FLUX R.M.S. ERROR F.U.	(10) DENSITY SIZE FACTOR	(11) FLUX DENSITY F.U.	(12) IDENTIFICATION	(13) REMARKS
0008-033			00 08 38.5	-03 18 24	2	135	.182	.013	1.350	.246	III	NOT IN SELECTED AREA
					3	135	.208	.013	1.350	.281		
0008+008		0B015	00 08 52.7	+00 50 48	3	135	.074	.011	1.000	.074	III	
0010+036			00 10 16.8	+03 36 54	3	135	.082	.011	1.000	.082	IIIB	NOT IN SELECTED AREA
0010+00	+00.1	3C5	00 10 35.6	+00 34 54	2	135	.950	.040	1.000	.950	III	
		MSH 2			9		.910	.020	1.000	.910		
0011-023			00 11 50.1	-02 22 30	2	135	.243	.014	1.000	.243	III	
0012+027			00 12 19.6	+02 42 48	3	135	.067	.011	1.000	.067	III	
0012-008			00 12 27.9	-00 51 24	2	135	.120	.012	1.000	.120	E 18.0M	
0013+018			00 13 13.6	+01 49 18	3	135	.087	.011	1.000	.087	III	
0013-00			00 13 36.7	-00 31 48	2	135	.870	.030	1.000	.870		BSO NEAR POSN.NO UV EXC-
					9		.900	.020	1.000	.900		ESS.PREV.IDENT.(8)REVOKED
0014-010			00 14 3.3	-01 5 6	11	45	.098	.012	1.000	.098	III	
0015-021			00 15 1.5	-02 6 6	3	135	.070	.011	1.000	.070	III	
0015-028			00 15 19.2	-02 53 12	3	135	.073	.011	1.000	.073	III	
0015+000			00 15 43.4	+00 4 0	3	135	.079	.011	1.000	.079	III	
0016-028			00 16 14.1	-02 49 42	3	135	.102	.012	1.000	.102	III	NOT IN SELECTED AREA
0016-013			00 16 51.9	-01 21 30	3	135	.116	.012	1.000	.116	III	
0016-022			00 16 54.4	-02 14 24	3	135	.069	.011	1.000	.069	III	
0017+026			00 17 10.7	+02 41 36	3	135	.142	.012	1.000	.142	IIIB	
0017-008			00 17 33.8	-00 50 36	3	135	.093	.011	1.000	.093	III	
0017-001			00 17 37.3	-00 11 42	3	135	.108	.011	1.000	.108	III	
0017-028	-02.2		00 17 47.2	-02 49 36	3	135	.255	.014	1.000	.255	III	NOT IN SELECTED AREA

TABLE AII.2

2700 MHZ SURVEY - +4 TO -4 DEG.DEC. ZONE

(1)	(2)	(3)	(4)	(5)	(6)	(7)	(8)	(9)	(10)	(11)	(12)	(13)
PKS SOURCE NUMBER	OTHER CATALOGUE NUMBERS 4C	OTHER	POSITION R.A.	(1950) DEC.	RUN	PA	2700 MHZ PEAK FLUX DENSITY F.U.	FLUX R.M.S. ERROR F.U.	DENSITY SIZE FACTOR	FLUX DENSITY F.U.	IDENTIF-ICATION	REMARKS
0003-00	-00.1	MSH 1	00 03 48.7	-00 21 6	2		2,40	.04	1.000	2.40	QSO 19.5M	Z=1,037 (42)(42)(26)
					3		2,43	.05	1.000	2.43		OPTICAL VARIABLE (42)
					9		2,40	.05	1.000	2.40		
0010+00	+00.1	3C5	00 10 35.6	+00 34 54	2	135	.95	.04	1.000	.95	III	
		MSH 2			9		.91	.02	1.000	.91		
0013-00			00 13 36.7	-00 31 48	2	135	.87	.03	1.000	.87		BSO NEAR POSITION.NO UV
					9		.90	.02	1.000	.90		EXCESS,IDENT.(8)REVOKED
0018-01	-01.1	MSH 5	00 18 49.9	-01 12 36	3	135	.64	.03	1.000	.64	III	
0019-00	+00.2?	DA9	00 19 51.6	-00 1 42	5		1.89	.05	1.000	1.89		FAINT RED OBJECT ON
					9		1.90	.04	1.000	1.90		POSITION. CLUSTER 2'F.
0025-007	-00.2		00 25 55.4	-00 43 12	5	135	.59	.03	1.059	.62		17M E 1.0'P.
0026-014			00 26 29.6	-01 29 42	9		.29	.01	1.000	.29		E 1.0'SP.
0028-01	-01.2		00 28 58.9	-01 17 30	5	135	.50	.02	1.000	.50	G 19.4M	PKS 0029-01
					11		.55	.02	1.000	.55		
0029+01		MSH 6	00 29 34.3	+01 20 36	9		.32	.01	1.000	.32	III	E4 PREVIOUS IDENT.
		0B050										REVOKED(17)
0031+01	+00.4	0B055	00 31 45.9	+01 2 24	9		.37	.01	1.000	.37		19M N IDENT.REVOKED(17)
												BSO 0.7'S.
0033-000	-00.3		00 33 54.0	-00 3 30	9		.28	.01	1.000	.28	III	
0034-01	-01.3	3C15	00 34 30.5	-01 25 44	5		2.57	.07	1.003	2.58	E0 17.1M	Z=.0733 (6)(50)(15)
		MSH 9			9		2.53	.06	1.003	2.54		
0035-02	-02.3	3C17	00 35 46.8	-02 24 10	5		4.04	.10	1.000	4.04	E 19.6M	Z=.2201 (37)(38)(46)
		MSH 9			9		4.04	.09	1.000	4.04		
0036+03	+03.1	MSH10	00 36 43.4	+03 3 18	5	135	1.08	.04	1.024	1.11	E2 13.5M	Z=.0145 (17)(52)
		0B062										NGC 193
0037-009			00 37 47.1	-00 56 18	9		.26	.01	1.000	.26	III	

TABLE AII.2 CONTINUED

2700 MHZ SURVEY - +4 TO -4 DEG.DEC. ZONE

(1)	(2)	(3)	(4)	(5)	(6)	(7)	(8)	(9)	(10)	(11)	(12)	(13)
PKS SOURCE NUMBER	OTHER CATALOGUE NUMBERS 4C	OTHER	POSITION (1950) R.A.	DEC.	RUN	PA	2700 MHZ FLUX DENSITY PEAK FLUX DENSITY F.U.	FLUX DENSITY R.M.S. ERROR F.U.	SIZE FACTOR	FLUX DENSITY F.U.	IDENTIFICATION	REMARKS
0038-020			00 38 23.8	-02 2 42	5	135	.61	.03	1.000	.61	QSO 18.0M	Z=1.176 (1)
0038-019	-02.4	DA20	00 38 49.2	-01 59 18	5		.65	.02	1.000	.65	S 15.0M	
0047+023		OB078	00 47 8.0	+02 20 48	5	135	.32	.02	1.000	.32		18M G 1.5'SF.
0047-02	-03.2	MSH14	00 47 11.1	-02 59 12	5	135	.73	.03	1.000	.73	III	18M QSO PREVIOUS IDENT.
					8	45	.63	.03	1.000	.63		REVOKED(8)
0051-03	-03.3	3C26	00 51 35.6	-03 50 11	8	5	1.08	.03	1.000	1.08	E 19.1M	Z=.2106 (6)(3)(46)
		MSH15			9		1.14	.03	1.000	1.14		
0053-016	-01.4		00 53 28.2	-01 36 24	5		.69	.06	1.027	.71	N 16.4M	PART OF PKS 0053-01
0053-015	-01.4		00 53 52.8	-01 32 48	5		.76	.06	1.027	.78	N 16.7M	PART OF PKS 0053-01
0055-01	-01.5	3C29	00 55 1.4	-01 39 51	5		3.21	.08	1.046	3.36	E0 15.0M	Z=.0450 (0)(50)(40)
		MSH17			9		3.43	.08	1.046	3.59		
0056-00	-00.6	DA32	00 56 31.7	-00 9 16	5		1.96	.05	1.000	1.96	QSO 17.3M	Z=.717 (6)(11)(28)
					8		1.78	.05	1.000	1.78		
					9		1.85	.04	1.000	1.85		
0059+017	+01.1	OB099	00 59 41.0	+01 47 36	5	135	.40	.02	1.000	.40	III	
0103-021			01 03 48.6	-02 11 48	5	135	.42	.02	1.000	.42	QSO 19M	
0105-008	-01.6		01 05 53.2	-00 53 18	5	135	.73	.03	1.000	.73		BSO NEAR POSITION
0106+01	+01.2	MSH 1	01 06 4.4	+01 19 2	5		1.73	.03	1.000	1.73	QSO 18.4M	Z=2.107 (4)(3)(14)
		OC012			9		1.98	.05	1.000	1.98		
					11		1.93	.05	1.000	1.93		
0109+02	+02.3	OC015	01 09 42.5	+02 42 0	9		.33	.01	1.000	.33	III	
0111+021		OC019	01 11 9.2	+02 6 30	9		.61	.02	1.000	.61	E 16.3M	
0112-017			01 12 44.4	-01 42 54	9		1.38	.03	1.000	1.38	QSO 18M	
0115+02	+02.4	OC026	01 15 43.0	+02 42 6	9		.88	.02	1.000	.88	QSO 17.5M	Z=.673 (47)

TABLE AII.2 CONTINUED

2700 MHZ SURVEY - +4 TO -4 DEG.DEC. ZONE

(1)	(2)	(3)	(4)	(5)	(6)	(7)	(8)	(9)	(10)	(11)	(12)	(13)
PKS SOURCE NUMBER	OTHER CATALOGUE NUMBERS 4C	OTHER	POSITION (1950) R.A.	DEC.	RUN	PA	2700 MHZ PEAK FLUX DENSITY F.U.	FLUX R.M.S. ERROR F.U.	DENSITY SIZE FACTOR	FLUX DENSITY F.U.	IDENTIF-ICATION	REMARKS
0115-01	-01.7		01 15 43.4	-01 35 42	8	45	.52	.02	1.000	.52	N 18.3M	(8)
0118-00	-00.8		01 18 22.0	-00 11 0	8	45	.36	.02	1.000	.36	III	17M S PREVIOUS IDENT,
					9		.42	.01	1.000	.42		REVOKED (8)
0118+03	+03.2	OC031	01 18 26.2	+03 28 29	9		.52	.02	1.000	.52	QSO 18M	Z=.765 (17)(3)(1)
					11		.51	.02	1.000	.51		
0122-005	-00.1		01 22 43.9	-00 34 24	8	45	.28	.02	1.000	.28		BSO NEAR POSITION
					9	135	.32	.02	1.000	.32		
0122-00			01 22 56.0	-00 21 34	8	45	1.42	.05	1.000	1.42	QSO 17.0M	Z=1.070(6)(11)(28)
					9		1.43	.03	1.000	1.43		
0123-01	-01.8	3C40 MSH 5	01 23 26.7	-01 36 9	9		2.26	.05	1.218	2.75	DB 13.2M 13.4M	Z=.0180 (36)(19)(30) SEPN.22"EW,18"NS NGC 545/7
0128+03	+04.7	MSH 6 OC047	01 28 39.7	+03 58 24	9		.81	.10	1.018	.82		POSITION AND FLUX ERRORS HIGH.SEE TABLE 4. FAINT BSO NEAR POSN.
0128+003	+00.5	OC049	01 28 58.2	+00 18 6	9		.33	.01	1.000	.33	E 16.1M	
0131-00	-00.11		01 31 40.4	-00 11 48	9	45	.68	.03	1.000	.68	G 0.7'E	PREV.IDENT.(8)DOUBTFUL
0137+012	+01.4	OC062	01 37 23.0	+01 16 36	9		1.07	.03	1.000	1.07	QSO 17.5M	
0140-01	-01.9		01 40 44.8	-01 34 30	8	45	.46	.02	1.000	.46	III	
0141+019		OC070	01 41 23.7	+01 56 42	9		.28	.01	1.000	.28	III	
0144-02	-02.8	MSH10	01 44 19.6	-02 12 30	9		.42	.01	1.000	.42		FAINT G 1.0'SF.
0144+037	+03.3	OC074	01 44 42.5	+03 46 6	9		.29	.01	1.000	.29	III	
0146+00	+00.7		01 46 50.7	+00 6 24	11		.22	.01	1.000	.22		G 0.7'S.
0150+00		OC084	01 50 11.0	+00 5 48	11		.22	.01	1.000	.22	III	
0150-03	-03.5		01 50 51.0	-03 49 6	8	45	.40	.02	1.000	.40	III	

TABLE AII.2 CONTINUED

(1)	(2)	(3)	(4)	(5)	(6)	(7)	(8)	(9)	(10)	(11)	(12)	(13)
PKS SOURCE NUMBER	OTHER CATALOGUE NUMBERS 4C	OTHER	POSITION (1950) R.A.	DEC.	RUN	PA	2700 MHZ FLUX PEAK FLUX DENSITY F.U.	R.M.S. ERROR F.U.	DENSITY SIZE FACTOR	FLUX DENSITY F.U.	IDENTIFICATION	REMARKS
0152+033	+03.4	MSH13 0C089	01 52 32.4	+03 23 48	9		.63	.02	1.000	.63	III	
0153+03		0C090?	01 53 25.1	+03 17 6	8	45	.38	.02	1.000	.38		G 1.0'SF.
0155+019		0C093	01 55 13.4	+01 55 18	8 10	45	.27 .29	.02 .01	1.000 1.000	.27 .29	III	
0157+01	+01.5	MSH14 0C096	01 57 28.9	+01 11 6	8	45	.44	.02	1.000	.44		DB 1.0'NP.
0158+031			01 58 5.0	+03 8 18	9		.28	.01	1.000	.28	QSO 19M	
0159+034		0C099	01 59 15.5	+03 29 12	9		.31	.01	1.000	.31	III	
0202+011		0D004?	02 02 16.9	+01 6 30	9		.31	.01	1.000	.31	IIIB	
0205-010			02 05 53.0	-01 2 24	9		.38	.01	1.000	.38		BSO 0.5'NF.NO UV EXCESS
0207-018	-01.10		02 07 13.1	-01 51 54	5	135	.48	.02	1.000	.48	III	
0211-031			02 11 7.8	-03 10 0	9		.23	.01	1.000	.23		FAINT CLUSTER 1'NP.
0213-026	-02.9	MSH 5	02 13 10.5	-02 37 6	5	135	.50	.02	1.000	.50	IIIB	
0213+025		0D024?	02 13 59.1	+02 30 36	9		.38	.01	1.000	.38	III	
0215+015		0D026	02 15 14.0	+01 30 54	9		.36	.01	1.000	.36	QSO 18.5M	OPTICAL VARIABLE.(13)
0215+02	+02.7	0D028	02 15 58.9	+02 42 36	9		.41	.01	1.000	.41	III	
0216+011			02 16 32.7	+01 6 54	5	135	.50	.02	1.000	.50	III	
0217+01		0D029	02 17 23.6	+01 42 0	3 9	135	.37 .35	.02 .01	1.000 1.000	.37 .35	E7 15.2M	(17)
0218-02	-02.10	3C63 MSH 7	02 18 21.9	-02 10 33	5 8 9		1.71 1.65 1.69	.04 .04 .04	1.000 1.000 1.000	1.71 1.65 1.69	E 19.1M	(6)(50)
0222-00	-00.12		02 22 35.0	-00 49 6	3 9	135	.66 .68	.03 .02	1.000 1.000	.66 .68	SO 16.5M	(8)

TABLE AII.2 CONTINUED

2700 MHZ SURVEY - +4 TO -4 DEG.DEC. ZONE

(1)	(2)	(3)	(4)	(5)	(6)	(7)	(8)	(9)	(10)	(11)	(12)	(13)
PKS SOURCE NUMBER	OTHER CATALOGUE NUMBERS 4C	OTHER	POSITION (1950) R.A.	DEC.	RUN	PA	2700 MHZ PEAK FLUX DENSITY F.U.	FLUX R.M.S. ERROR F.U.	DENSITY SIZE FACTOR	FLUX DENSITY F.U.	IDENTIF-ICATION	REMARKS
0225-014	-01.11		02 25 34.5	-01 29 6	3	135	.30	.02	1.000	.30	QSO 18M	Z=.685 (10)
0226-038	-03.7		02 26 23.2	-03 51 6	8	45	.66	.03	1.000	.66	QSO 17.5M	Z=.695 (1)
0230-027			02 30 13.0	-02 46 36	3	135	.33	.02	1.000	.33		S 1.4'SP.
0230-03	-03.8		02 30 47.8	-03 34 30	8	45	.34	.02	1.000	.34	III	
0232-02	-02.12		02 32 59.9	-02 32 24	5	135	.58	.02	1.000	.58	QSO 19M	(33)
0237-027			02 37 14.5	-02 47 12	5		.40	.01	1.000	.40	QSO 19.0M	
					8	45	.43	.02	1.000	.43		
					9		.42	.01	1.000	.42		
0240-00	-00.13	3C71	02 40 7.0	-00 13 31	3		3.13	.07	1.000	3.13	SC 9.7M	Z=.00344 (35)(19)(22)
		MSH14			5		3.15	.05	1.000	3.15		SEYFERT GAL. NGC1068
					8		3.05	.08	1.000	3.05		
					9		3.14	.07	1.000	3.14		
0240-034	-03.9		02 40 12.3	-03 24 36	8	45	.27	.01	1.000	.27		TWO FAINT GALS?ON POSN.
0252+02	+02.8	3C74	02 52 33.8	+02 41 36	9		.41	.01	1.000	.41	N 19.9M	(33)
		0D087										
0253-031	-03.10		02 53 20.2	-03 11 36	9		.29	.01	1.000	.29	QSO? 19M	
0256-005			02 56 54.4	-00 31 54	9		.31	.01	1.000	.31	QSO 18.5M	
0300-00	-00.14		03 00 38.2	-00 26 36	5	135	.67	.03	1.000	.67	QSO?18.5M	18M E PREVIOUS IDENT. REVOKED (8)
0303+020	+01.7	0E007	03 03 46.1	+02 4 30	8	45	.46	.02	1.000	.46		G 0.7'NP.
					11		.46	.02	1.000	.46		
0303+033		0E0066	03 03 55.3	+03 18 36	9		.26	.01	1.000	.26	IIIB	
0305+03	+03.5	3C78	03 05 49.0	+03 55 13	5		5.19	.13	1.021	5.30	D 14.4M	Z=.0289 (2)(19)(32)
		MSH 3			9		5.27	.12	1.021	5.38		NGC 1218

TABLE AII.2 CONTINUED

2700 MHZ SURVEY - +4 TO -4 DEG.DEC. ZONE

(1)	(2)	(3)	(4)	(5)	(6)	(7)	(8)	(9)	(10)	(11)	(12)	(13)
PKS SOURCE NUMBER	OTHER CATALOGUE NUMBERS 4C	OTHER	POSITION (1950) R.A.	DEC.	RUN	PA	2700 MHZ PEAK FLUX DENSITY F.U.	FLUX R.M.S. ERROR F.U.	DENSITY SIZE FACTOR	FLUX DENSITY F.U.	IDENTIF-ICATION	REMARKS
0310+013		0E017	03 10 8.4	+01 22 30	9		.25	.01	1.000	.25		BSO NEAR POSITION NO UV EXCESS
0312-03	-03.11	MSH 1	03 12 52.1	-03 27 48	5	135	.68	.03	1.000	.68	QSO 18.5M	
0313-035			03 13 53.2	-03 31 36	5	135	.23	.01	1.000	.23		BSO 1.0'NF.
0317-02	-02.15		03 17 57.1	-02 19 6	5	135	.36	.02	1.000	.36	QSO 19.5M	
0320+015		0E034	03 20 34.0	+01 35 0	5	135	.52	.02	1.000	.52	III	
0322-03	-03.12		03 22 12.2	-03 35 18	5	135	.51	.02	1.000	.51	III	
0325+02	+02.10	3C88 MSH 5	03 25 18.2	+02 23 20	5 9		2.95 2.98	.07 .07	1.074 1.074	3.17 3.20	D 14.9M	Z=.0302 (31)(50)(32)
0331-01	-01.12	3C89 MSH 3	03 31 42.8	-01 21 24	5 9		1.38 1.38	.04 .03	1.008 1.008	1.39 1.39	D 18.3M	(6)(50)
0332-021			03 32 43.7	-02 6 30	5	135	.43	.02	1.000	.43	III	
0336-017			03 36 29.5	-01 43 0	5 9	135	.59 .58	.02 .02	1.000 1.000	.59 .58	III	
0336-01		CTA26 DA110	03 36 59.2	-01 56 19	5 9 11		2.02 2.37 2.35	.05 .05 .06	1.000 1.000 1.000	2.02 2.37 2.35	QSO 17.5M	Z=.852 (6)(25)(1) OPTICAL VARIABLE (25)
0351-032	-03.14		03 51 43.7	-03 16 48	5	135	.46	.02	1.000	.46	QSO?19.5M	
0353+027	+02.11	0E090	03 53 23.4	+02 47 36	5	135	.47	.02	1.000	.47	N 19.1M	GAL. HAS UV EXCESS
0354+000		0E092	03 54 16.6	+00 5 12	9		.31	.01	1.000	.31		E 1.0'NF.
0358+00	+00.14	3C99 MSH12	03 58 32.8	+00 27 54	5	135	1.06	.04	1.000	1.06		G 0.7'S. IDENT.(54) REVOKED
0358+031			03 58 33.0	+03 10 6	5 9	135	.37 .22	.02 .01	1.000 1.000	.37 .22	IIIA	
0358+021	+02.12	0E098	03 58 34.5	+02 8 54	5	135	.37	.02	1.000	.37	IIIA	
0359+028		0E0999	03 59 57.9	+02 53 42	9	45	.36	.02	1.000	.36	IIIA	

TABLE AII.2 CONTINUED

2700 MHZ SURVEY -4 TO +4 DEG.DEC. ZONE

(1)	(2)	(3)	(4)	(5)	(6)	(7)	(8)	(9)	(10)	(11)	(12)	(13)
PKS SOURCE NUMBER	OTHER CATALOGUE NUMBERS 4C	OTHER	POSITION (1950) R.A.	DEC.	RUN	PA	2700 MHZ PEAK FLUX DENSITY F.U.	FLUX R.M.S. ERROR F.U.	DENSITY SIZE FACTOR	FLUX DENSITY F.U.	IDENTIFICATION	REMARKS
0400-03	-03.16		04 00 47.0	-03 8 30	5	135	.45	.02	1.000	.45	IIIA	
0400+032		0F002	04 00 49.5	+03 17 6	9		.27	.01	1.000	.27	IV	
0402+025		0F004	04 02 48.9	+02 32 42	9		.33	.01	1.000	.33	IV	
0404+03	+03.8	3C105 MSH 3	04 04 45.3	+03 33 24	5		3.31	.08	1.076	3.56	IIIA	
					9		3.28	.07	1.076	3.53		
0407+012	+01.8	0F012	04 07 4.5	+01 17 0	5	135	.36	.02	1.000	.36	IIIAB	
0409-01	-01.13	3C107 MSH 6	04 09 49.8	-01 7 6	5	135	.72	.03	1.000	.72	III	
0409+025			04 09 53.7	+02 32 48	9		.26	.01	1.000	.26	IIIB	
0410-02	-02.16		04 10 22.7	-02 29 54	9		.33	.01	1.000	.33		BSO ON POSITION NO UV EXCESS
0416-03	-03.18		04 16 16.3	-03 6 30	5	135	.56	.02	1.021	.57	III	
0420+022			04 20 16.6	+02 12 30	5	135	.34	.02	1.000	.34	QSO 19.5M	
0420-01			04 20 43.1	-01 27 29	5		2.15	.06	1.000	2.15	QSO 18M	Z=.915 (7)(24)(1)
					8	45	1.95	.07	1.000	1.95		
					9		1.76	.04	1.000	1.76		
0421+00	+00.15	0F035	04 21 16.7	+00 24 18	5	135	1.05	.04	1.000	1.05	III	
					9		.99	.02	1.000	.99		
0421+019		0F036	04 21 34.0	+01 57 36	5	135	.76	.03	1.000	.76	QSO 17.5M	Z=.689 (1)
					11		.76	.02	1.000	.76		
0422+00		0F038	04 22 11.9	+00 29 18	5	135	1.24	.05	1.000	1.24		BSO ON POSN.IDENT.GIVEN IN(12)HAS STELLAR SPEC.
					9		1.32	.03	1.000	1.32		
					11		1.20	.03	1.000	1.20		
0428+01	+01.10	MSH 7 3C118	04 28 31.5	+01 6 30	5	135	.90	.04	1.000	.90	III	
0431-02	-02.17	DA141	04 31 23.1	-02 36 18	5	135	1.06	.04	1.000	1.06		FAINT G? ON POSITION

TABLE AII.2 CONTINUED

2700 MHZ SURVEY - +4 TO -4 DEG.DEC. ZONE

(1)	(2)	(3)	(4)	(5)	(6)	(7)	(8)	(9)	(10)	(11)	(12)	(13)
PKS SOURCE NUMBER	OTHER CATALOGUE NUMBERS 4C	OTHER	POSITION (1950) R.A.	DEC.	RUN	PA	2700 MHZ FLUX PEAK FLUX DENSITY F.U.	R.M.S. ERROR F.U.	DENSITY SIZE FACTOR	FLUX DENSITY F.U.	IDENTIFICATION	REMARKS
0432+03	+03.9	MSH 8	04 32 37.0	+03 28 18	9		.27	.01	1.000	.27	IIIB	OFO 54.9
0439-007	-00.18	MSH15	04 39 20.6	-00 43 30	8	45	.38	.02	1.000	.38	III	
					11		.42	.02	1.000	.42		
0439+01	+01.11	3C124	04 39 23.5	+01 15 24	5	135	.57	.02	1.000	.57		E 0.6'S.PREV.IDENT.
					9		.55	.02	1.000	.55		REVOKED.(5)
0440-00		DA145	04 40 5.4	-00 23 16	5		3.73	.09	1.000	3.73	QSO 18.5M	(7)(24) NRAO 190
					9		3.40	.08	1.000	3.40		
					11		3.35	.08	1.000	3.35		
0442+02	+02.16	MSH10	04 42 3.9	+02 42 30	5	135	.58	.02	1.000	.58	III	OF071
0443-00		DA146	04 43 1.2	-00 24 36	9		.27	.01	1.000	.27	QSO 20M	PKS 0442-00
0445-019			04 45 11.4	-01 58 0	9		.20	.01	1.000	.20	QSO 19M	
0447-010			04 47 10.1	-01 2 24	9		.29	.01	1.000	.29	QSO 19.5M	
0448-025	-02.18	MSH19	04 48 50.1	-02 34 0	9		.25	.01	1.000	.25	G 20.2M	
0453-00	-00.19	MSH20	04 53 15.6	-00 14 24	5	135	.62	.03	1.000	.62	III	
0454+039		OF092	04 54 10.4	+03 56 24	9		.40	.01	1.000	.40	QSO?16.5M	
0457+024		OF097	04 57 15.6	+02 25 0	5	135	1.71	.06	1.000	1.71	QSO? 19M	POSSIBLE UV EXCESS
					9		1.62	.04	1.000	1.62		
					11		1.62	.04	1.000	1.62		
0458+01	+01.12	MSH14	04 58 3.9	+01 25 48	5	135	.52	.02	1.000	.52	E 18.5M	OF098
0458-02	-02.19	DA157	04 58 41.1	-02 3 36	5		1.87	.05	1.000	1.87	N? 20 M	BSO ON POSN.NO UV EXCESS
					6		1.94	.05	1.000	1.94		PREV.IDENT.(6).
					9		1.85	.04	1.000	1.85		
					11		1.60	.04	1.000	1.60		
0500+019		OG003	05 00 44.7	+01 58 48	6		2.47	.06	1.000	2.47	III	
					11		2.47	.07	1.000	2.47		

TABLE AII.2 CONTINUED

2700 MHZ SURVEY - +4 TO -4 DEG.DEC. ZONE

(1)	(2)	(3)	(4)	(5)	(6)	(7)	(8)	(9)	(10)	(11)	(12)	(13)
PKS SOURCE NUMBER	OTHER CATALOGUE NUMBERS 4C	OTHER	POSITION (1950) R.A.	DEC.	RUN	PA	2700 MHZ PEAK FLUX DENSITY F.U.	FLUX R.M.S. ERROR F.U.	DENSITY SIZE FACTOR	FLUX DENSITY F.U.	IDENTIF-ICATION	REMARKS
0504+03	+03.10	0G008	05 04 59.7	+03 3 54	6		.75	.02	1.000	.75	QSO? 19M	PROBABLE UV EXCESS (33)
					9		.74	.02	1.000	.74		PREV.IDENT.(17)REVOKED PKS 0505+03
0509-038			05 09 7.0	-03 49 54	6		.39	.02	1.000	.39	IIIA	
0511+00	+00.18	3C135 MSH 2	05 11 33.3	+00 53 18	6		1.65	.05	1.022	1.69	E 17.5M	Z=.1270 (17)(50)(40)
					9		1.67	.04	1.022	1.71		
0519+01		0G033	05 19 41.9	+01 10 42	6		.54	.02	1.000	.54	IIIA	
0534-03	-03.21	DA182	05 34 24.4	-03 11 0	8	45	.39	.02	1.000	.39	IIIA	
					11		.35	.01	1.000	.35		
0550+032		0G083	05 50 12.3	+03 12 42	9		.77	.02	1.000	.77	IV	
					11		.65	.02	1.000	.65		
0554-026			05 54 23.1	-02 41 48	9		.51	.02	1.000	.51	IV	
0559+02	+02.17	0G099	05 59 2.9	+02 27 24	11		.29	.01	1.000	.29	IIIA	PKS 0558+02
0723-008			07 23 17.6	-00 49 0	10		2.99	.07	1.000	2.99	III	DW0723-00
					11		3.07	.08	1.000	3.07		
0723-036			07 23 36.0	-03 38 30	10		.32	.01	1.000	.32	DB	17.5M+18.0M
0724-01	-02.31	3C180 MSH 6	07 24 33.3	-01 58 24	10		1.54	.04	1.013	1.56	G 20.2M	(6)(50)
0725+001		0I041	07 25 1.0	+00 10 54	10		.27	.01	1.000	.27	III	
0726-00	-00.25		07 26 14.2	-00 2 30	10		.40	.02	1.000	.40	G 20.2M	(8)
0727-025			07 27 55.4	-02 35 12	10		.28	.01	1.000	.28	III	
0729+019			07 29 46.6	+01 57 0	10		.32	.01	1.000	.32	III	
0731+02	+02.20	0I052	07 31 17.2	+02 9 18	10		.58	.02	1.000	.58	III	
0736-01	-01.18	MSH 8	07 36 1.7	-01 57 18	10		.64	.02	1.000	.64	QSO 18M	

TABLE AII.2 CONTINUED

2700 MHZ SURVEY - +4 TO -4 DEG.DEC. ZONE

(1)	(2)	(3)	(4)	(5)	(6)	(7)	(8)	(9)	(10)	(11)	(12)	(13)
PKS SOURCE NUMBER	OTHER CATALOGUE NUMBERS 4C	OTHER	POSITION (1950) R.A.	DEC.	RUN	PA	2700 MHZ FLUX DENSITY PEAK FLUX F.U.	R.M.S. ERROR F.U.	DENSITY SIZE FACTOR	FLUX DENSITY F.U.	IDENTIFICATION	REMARKS
0736+01		0I061	07 36 42.4	+01 43 57	7		2.30	.06	1.000	2.30	QSO 18M	Z=.191 (5)(9)(28)
					9		2.60	.05	1.000	2.60		
					10		2.22	.04	1.000	2.22		
					11		2.48	.06	1.000	2.48		
0737-030	-03.27		07 37 58.7	-03 3 54	10		.35	.01	1.000	.35	III	
0738-00	-00.26	MSH 9	07 38 35.3	-00 59 6	11		.38	.02	1.000	.38	III	
0742+02	+02.21	3C187 MSH 4	07 42 27.9	+02 7 45	7	45	.79	.03	1.040	.82	G 19.5M	(54)(50)
0743-006			07 43 20.8	-00 37 0	7	45	1.41	.05	1.000	1.41	QSO? 18M	4C-00.28?
					9		1.37	.03	1.000	1.37		
					11		1.42	.04	1.000	1.42		
0747-00	-00.30		07 47 6.0	-00 2 12	7	45	.43	.02	1.000	.43	III	19M DB IDENT.(8)REVOKED
0752-026	-02.33		07 52 16.8	-02 39 30	7	45	.46	.02	1.000	.46	N 19.4M	PKS 0752-02.7
0752-022			07 52 26.6	-02 14 54	7	45	.42	.02	1.000	.42	DB	15.8M+16.2M PKS 0752-02.3
0753+02	+02.22	3C188 0I086	07 53 9.0	+02 18 42	7	45	.45	.02	1.000	.45	III	
0755+029		0I091	07 55 5.2	+02 59 6	7	45	.49	.02	1.000	.49	III	DW 0755+03
0757+025		0I095	07 57 27.3	+02 31 6	7	45	.27	.02	1.000	.27	III	
0802-010			08 02 46.7	-01 2 54	9	135	.35	.02	1.000	.35	III	
0803-00	-00.32	MSH 2	08 03 4.0	-00 49 42	5	135	.71	.03	1.000	.71	E4 15.4M	(6)
0803-023	-02.34		08 03 41.1	-02 23 24	9		.35	.01	1.000	.35	III	
0808+019		0J014	08 08 51.0	+01 55 48	5	135	.65	.03	1.000	.65		DW0808+01,BSO ON POSN.
					11		.80	.02	1.000	.80		NO UV EXCESS

TABLE AII.2 CONTINUED

2700 MHZ SURVEY - +4 TO -4 DEG.DEC. ZONE

(1)	(2)	(3)	(4)	(5)	(6)	(7)	(8)	(9)	(10)	(11)	(12)	(13)
PKS SOURCE NUMBER	OTHER CATALOGUE NUMBERS 4C	OTHER	POSITION (1950) R.A.	DEC.	RUN	PA	2700 MHZ FLUX PEAK FLUX DENSITY F.U.	R.M.S. ERROR F.U.	DENSITY SIZE FACTOR	FLUX DENSITY F.U.	IDENTIFICATION	REMARKS
0812+02	+02.23	MSH 2 0J021	08 12 47.2	+02 4 11	5 7 9 11	135 45	1.16 1.19 1.21 1.17	.04 .05 .02 .03	1.000 1.000 1.000 1.000	1.16 1.19 1.21 1.17	QSO 18.5M	Z=.406 (17)(11)(26)
0812-02	-02.35	MSH 5	08 12 57.3	-02 59 14	5 9	135	.94 .95	.04 .02	1.000 1.000	.94 .95	D 18.9M	(6)(50).3C196.1
0813+020			08 13 20.8	+02 5 18	5 9	135	.38 .38	.02 .01	1.000 1.000	.38 .38	III	
0819-032			08 19 10.0	-03 13 36	5	135	.42	.02	1.000	.42		BSO ON POSITION NO UV EXCESS
0823+033		0J038	08 23 13.5	+03 19 18	5 9 11	135	.82 .91 .82	.03 .02 .02	1.000 1.000 1.000	.82 .91 .82		18M G 1.0'F. 16.5M DB 1.5'N.
0825+013	+01.22	0J042	08 25 24.7	+01 22 36	9		.30	.01	1.000	.30	III	
0828-03	-03.32		08 28 14.1	-03 30 36	5	135	.53	.02	1.000	.53	QSO? 20M	DOUBTFUL UV EXCESS
0833-01			08 33 3.0	-01 40 42	5	135	.53	.02	1.057	.56	E 13.9M	(8)
0835-013			08 35 58.5	-01 23 54	9		.32	.01	1.000	.32	III	
0836-00	-00.34		08 36 19.9	-00 27 42	9		.31	.01	1.000	.31	III	
0837+035		0J063	08 37 12.8	+03 30 18	5	135	.69	.03	1.000	.69	QSO?20.0M	
0837+012		0J062	08 37 14.2	+01 15 24	9		.25	.01	1.000	.25	QSO 19M	
0849+008	+01.23	0J083	08 49 52.2	+00 53 48	9		.24	.01	1.000	.24	III	
0850-03	-03.34		08 50 56.3	-03 30 6	5	135	.75	.03	1.000	.75		TWO BSO'S NEAR POSN. NO UV EXCESS
0852+029	+03.14		08 52 32.1	+02 56 42	5	135	.38	.02	1.000	.38	III	
0853+03			08 53 .7	+03 23 48	11		.35	.01	1.000	.35	QSO?17.5M	(33)
0854-03	-03.35		08 54 41.6	-03 27 12	5	135	.66	.03	1.000	.66	II	SEVERAL FAINT GALS. 18M QSO IDENT.(8)REVOKED.

TABLE AII.2 CONTINUED

2700 MHZ SURVEY - +4 TO -4 DEG.DEC. ZONE

(1)	(2)	(3)	(4)	(5)	(6)	(7)	(8)	(9)	(10)	(11)	(12)	(13)
PKS SOURCE NUMBER	OTHER CATALOGUE NUMBERS 4C	OTHER	POSITION (1950) R.A.	DEC.	RUN	PA	2700 MHZ PEAK FLUX DENSITY F.U.	FLUX R.M.S. ERROR F.U.	DENSITY SIZE FACTOR	FLUX DENSITY F.U.	IDENTIF-ICATION	REMARKS
0859+032		OJ098	08 59 15.0	+03 16 12	9		.34	.01	1.000	.34	G 20.2M	
0904+039			09 04 4.9	+03 54 30	5	135	.44	.02	1.000	.44	III	
0906+011			09 06 34.3	+01 6 42	9		.28	.01	1.000	.28	III	
0906+01	+01.24		09 06 36.0	+01 33 48	5		1.26	.03	1.000	1.26	QSO 17.5M	(12)
					9		1.18	.03	1.000	1.18		
					11		1.16	.03	1.000	1.16		
0907+022			09 07 5.6	+02 12 18	9		.19	.01	1.000	.19		BSO NEAR POSITION NO UV EXCESS
0907-023			09 07 13.8	-02 19 36	5	135	.57	.02	1.000	.57	QSO 18.0M	
0909+003		OK015	09 09 8.2	+00 23 48	9		.26	.01	1.000	.26	III	
0912+029		OK020	09 12 1.8	+02 58 42	5	135	.54	.02	1.000	.54	QSO 18.5M	
0913-025	-02.38		09 13 48.5	-02 31 36	9		.28	.01	1.000	.28	QSO 18.5M	
0922+005		OK037	09 22 34.4	+00 32 6	5	135	.68	.03	1.000	.68	QSO 18.5M	Z=1.72 (10)
					11		.76	.02	1.000	.76		
0927+02		OK045	09 27 30.5	+02 2 6	11		.32	.01	1.000	.32	III	
0932+02	+02.27	OK055	09 32 42.1	+02 17 18	5	135	.53	.02	1.000	.53	QSO 18M	Z=.659(10)17M E IDENT. (17) REVOKED
0936+02	+02.28	OK061	09 36 39.2	+02 13 42	11		.28	.01	1.000	.28	III	
0937+033			09 37 12.9	+03 19 6	9		.28	.01	1.000	.28	III	
0938-01	-01.19	MSH 7	09 38 50.4	-01 29 24	5	135	.53	.02	1.000	.53		FAINT RED OBJ.ON POSN.
0940+02	+02.29		09 40 37.6	+02 57 12	5	135	.87	.03	1.000	.87	III	
					9		.85	.02	1.000	.85		
0940+00	+00.30	OK067	09 40 45.3	+00 9 18	5	135	.73	.03	1.000	.73	III	
0945+003	+00.31	OK075	09 45 11.8	+00 18 24	5	135	.39	.02	1.000	.39		FAINT BSO 0.2'P.
0949+00	+00.32	3C230 MSH 8	09 49 24.8	+00 12 24	5		1.53	.04	1.006	1.54		18.5M N 0.4'NF. PREV.IDENT.(5)REVOKED
					9		1.51	.04	1.006	1.52		

TABLE AII.2 CONTINUED

2700 MHZ SURVEY - +4 TO -4 DEG.DEC. ZONE

(1)	(2)	(3)	(4)	(5)	(6)	(7)	(8)	(9)	(10)	(11)	(12)	(13)
PKS SOURCE NUMBER	OTHER CATALOGUE NUMBERS 4C	OTHER	POSITION (1950) R.A.	DEC.	RUN	PA	2700 MHZ FLUX PEAK FLUX DENSITY F.U.	R.M.S. ERROR F.U.	DENSITY SIZE FACTOR	FLUX DENSITY F.U.	IDENTIFICATION	REMARKS
0950+00			09 50 13.3	+00 14 30	5	135	.43	.02	1.000	.43	QSO 19.5M	OPTICAL VARIABLE
0955+036A	+03.17	MSH10	09 55 21.1	+03 41 30	5	135	.35	.02	1.000	.35		17M G 0.7'F. PART OF PKS 0955+03
0955+036B	+03.17	MSH10	09 55 48.1	+03 38 48	5	135	.35	.02	1.000	.35		FAINT BSO 0.3'NP. PART OF PKS 0955+03
0955-01	-01.20		09 55 56.2	-01 25 42	5	135	.72	.03	1.000	.72		BSO NEAR POSITION STELLAR SPECT.(47)
0956+015		OK094	09 56 46.3	+01 32 24	9		.30	.01	1.000	.30	DB? 15.8M	
0957+00	+00.34	OK096	09 57 43.8	+00 19 50	5	135	.51	.02	1.000	.51	QSO 17.6M	Z=0.907 (4)(4)(29)
					9		.53	.02	1.000	.53		
					11		.51	.02	1.000	.51		
0958-001	-00.37		09 58 49.9	-00 11 48	5	135	.58	.02	1.000	.58		19M DB 0.5'NF.
1004-018			10 04 32.3	-01 52 42	5	135	.53	.02	1.000	.53	QSO 19.0M	
					11		.59	.02	1.000	.59		
1005+007		OL009	10 05 37.3	+00 44 36	9		.34	.01	1.000	.34	N 16.9M	
1008-01	-01.21		10 08 19.8	-01 46 18	5	135	.77	.03	1.042	.80	S(?) 19.4M	
1008+013		OL014	10 08 41.7	+01 21 42	9		.24	.01	1.000	.24	QSO 19M	
1012+022	+02.30	OL021	10 12 40.9	+02 14 0	8	45	.40	.02	1.000	.40	QSO 18M	
					9		.40	.01	1.000	.40		
1014+018		OL023	10 14 2.0	+01 52 12	9		.32	.01	1.000	.32	III	
1021+028			10 21 18.7	+02 48 24	9		.22	.01	1.000	.22	QSO? 19M	
1021-00			10 21 55.8	-00 37 36	5	135	.95	.04	1.000	.95	QSO?18.5M	(8)
1027+00	+00.35	OL045	10 27 36.6	+00 52 48	5	135	.61	.03	1.000	.61	G 19.4M	
1033+003	+00.37	OL055	10 33 32.5	+00 21 48	9		.34	.01	1.000	.34	E 16.5M	

TABLE AII.2 CONTINUED

2700 MHZ SURVEY - +4 TO -4 DEG.DEC. ZONE

(1)	(2)	(3)	(4)	(5)	(6)	(7)	(8)	(9)	(10)	(11)	(12)	(13)
PKS SOURCE NUMBER	OTHER CATALOGUE NUMBERS 4C	OTHER	POSITION (1950) R.A.	DEC.	RUN	PA	2700 MHZ PEAK FLUX DENSITY F.U.	FLUX R.M.S. ERROR F.U.	DENSITY SIZE FACTOR	FLUX DENSITY F.U.	IDENTIF-ICATION	REMARKS
1039+02	+03.18	DA288	10 39 4.7	+02 58 18	5		1.67	.04	1.000	1.67	G 19.4M	
					9		1.65	.04	1.000	1.65		
1044-00	-00.39	MSH17	10 44 48.8	-00 50 12	9		.32	.01	1.000	.32	III	
1045+019			10 45 49.9	+01 57 36	5	135	.41	.02	1.000	.41	III	OL076?
1046-02	-02.43	MSH18	10 46 53.7	-02 39 12	8	45	.52	.02	1.000	.52	III	
					11		.50	.02	1.000	.50		
1048+00	+00.38	MSH 9 OL080	10 48 5.2	+00 12 18	10		.31	.01	1.000	.31	III	
1051+035	+03.19		10 51 51.8	+03 30 42	9		.29	.01	1.000	.29	DB 20.2M	
1052-004	-00.41		10 52 22.9	-00 29 42	9		.34	.01	1.000	.34	QSO? 18M	
1052+023	+02.31		10 52 44.0	+02 21 42	9		.34	.01	1.000	.34	III	
1054+004		OL091	10 54 41.7	+00 27 54	5	135	.58	.02	1.000	.58	III	
1055+01	+01.28	DA293 OL093	10 55 55.5	+01 50 3	5		3.15	.08	1.000	3.15	QSO 18M	(17)(11)
					7		3.02	.07	1.000	3.02		
					9		3.03	.06	1.000	3.03		
					10		2.88	.07	1.000	2.88		
					11		3.03	.08	1.000	3.03		
1055-028			10 55 38.7	-02 53 18	9		.42	.01	1.000	.42	III	
1059-01	-00.42	3C249 MSH21	10 59 30.9	-01 0 0	7		1.32	.04	1.000	1.32	III	
					9		1.36	.03	1.000	1.36		
1059-023	-02.44		10 59 52.6	-02 19 18	7	45	.50	.02	1.000	.50	IIIB	
1103+002		OM005	11 03 16.8	+00 13 0	10		.29	.01	1.000	.29	S 9.8M	Z=.00205 (22) NGC 3521
1103-006	-00.43		11 03 58.7	-00 36 36	7	45	.68	.03	1.000	.68	QSO?16.5M	
1105-028	-02.45		11 05 4.3	-02 51 54	7	45	.36	.02	1.000	.36	QSO?19.5M	
1105+037			11 05 39.9	+03 43 18	7	45	.43	.02	1.067	.46	III	

TABLE AII.2 CONTINUED

2700 MHZ SURVEY + 4 TO -4 DEG.DEC. ZONE

(1)	(2)	(3)	(4)	(5)	(6)	(7)	(8)	(9)	(10)	(11)	(12)	(13)
PKS SOURCE NUMBER	OTHER CATALOGUE NUMBERS 4C	OTHER	POSITION (1950) R.A.	DEC.	RUN	PA	2700 MHZ FLUX PEAK FLUX DENSITY F.U.	R.M.S. ERROR F.U.	DENSITY SIZE FACTOR	FLUX DENSITY F.U.	IDENTIF-ICATION	REMARKS
1106+023			11 06 10.9	+02 18 54	7	45	.64	.03	1.000	.64	N 18.9M	
1106-003			11 06 17.4	-00 22 30	7	45	.26	.01	1.000	.26	QSO?19.5M	
1108+03	+03.21		11 08 49.4	+03 25 30	7	45	.48	.02	1.000	.48	III	
1110-01	-01.25	MSH 5	11 10 59.4	-01 56 12	7	45	.84	.03	1.000	.84	III	
1111-037	-03.41		11 11 58.5	-03 44 36	7	45	.36	.02	1.000	.36	G18.3M/	BOTH OBJECTS NEAR POSN.
					9		.34	.01	1.000	.34	QSO?18.5M	
1115-023	-02.46		11 15 2.0	-02 19 42	7	45	.62	.03	1.000	.62	III	
1116-02	-02.47	3C255 MSH 8	11 16 52.2	-02 46 30	7	45	.59	.03	1.000	.59		FAINT RED OBJ. ON POSN.
1118+000			11 18 45.0	+00 3 0	7	45	.43	.02	1.016	.44	DB	17.0M+18.5M
1122-037			11 22 10.5	-03 43 24	7	45	.47	.02	1.000	.47		FAINT G 1'F.
1123+012			11 23 21.1	+01 16 6	7	45	.25	.01	1.000	.25		FAINT BSO NEAR POSN.
1127+005	+00.40	MSH 7 OM045	11 27 2.8	+00 31 48	7	45	.58	.02	1.000	.58	G	CLUSTER ON POSN. CANNOT SELECT RADIO GALAXY
1127-032	-03.42	MSH10	11 27 36.0	-03 12 54	7	45	.33	.02	1.000	.33	III	
					9		.31	.01	1.000	.31		
1127+012	+01.30		11 27 47.6	+01 14 54	7	45	.41	.02	1.000	.41	N 17.8M	
1130-037	-03.43		11 30 31.0	-03 44 18	7	45	.54	.02	1.000	.54	E 15.3M	
1130+009			11 30 47.3	+00 57 24	7	45	.32	.02	1.000	.32	QSO? 19M	OM050?
1132-000	-00.45		11 32 40.1	-00 4 54	7	45	.73	.03	1.000	.73	III	
1133-032	-03.44		11 33 42.3	-03 14 12	7	45	.20	.01	1.570	.31	III	
1134+01	+01.31		11 34 56.4	+01 32 42	7	45	.55	.02	1.000	.55		G 1.0'NF.
1138+01	+01.32	MSH 8	11 38 35.1	+01 30 54	7		1.57	.04	1.000	1.57	III	
					9		1.57	.04	1.000	1.57		
1141+011			11 41 35.5	+01 11 12	7	45	.34	.02	1.000	.34	G 19.4M	
					9	45	.32	.02	1.000	.32		
1142-00	-00.46	MSH16	11 42 21.9	-00 15 12	7	45	.43	.02	1.000	.43		BSO 1.0'P.

TABLE AII.2 CONTINUED

2700 MHZ SURVEY - +4 TO -4 DEG.DEC. ZONE

(1)	(2)	(3)	(4)	(5)	(6)	(7)	(8)	(9)	(10)	(11)	(12)	(13)
PKS SOURCE NUMBER	OTHER CATALOGUE NUMBERS 4C	OTHER	POSITION (1950) R.A.	DEC.	RUN	PA	2700 MHZ PEAK FLUX DENSITY F.U.	FLUX DENSITY R.M.S. ERROR F.U.	SIZE FACTOR	FLUX DENSITY F.U.	IDENTIFICATION	REMARKS
1146-037			11 46 23.9	-03 47 30	8	45	.40	.02	1.036	.41	QSO? 17M	
					9		.37	.01	1.036	.38		
1147+015	+01.33		11 47 51.5	+01 32 42	7	45	.31	.02	1.000	.31	G 19.9M	
1148-00	-00.47		11 48 10.2	-00 7 13	7		2.58	.05	1.000	2.58	QSO 17.7M	Z=1.982 (7)(3)(16)
					8		2.55	.04	1.000	2.55		
					9		2.54	.06	1.000	2.54		
					11		2.58	.06	1.000	2.58		
1159-02	-02.50		11 59 57.5	-02 23 36	5	45	.43	.02	1.000	.43	III	18.2M E PREV.IDENT. (8) REVOKED
1207-013			12 07 57.6	-01 20 12	5	45	.37	.02	1.000	.37	DB 19.4M	
					9		.40	.01	1.000	.40		
1212-00	-00.48	MSH 7	12 12 14.3	-00 43 36	5	45	.51	.02	1.000	.51	III	
					8	135	.57	.02	1.000	.57		
					9		.54	.02	1.000	.54		
1215+03	+04.41	MSH 4	12 15 0	+03 54 48	5		1.15	.03	1.071	1.23	D+E	17.3M Z=.0756;17.3M Z= .0771 (19)(15) COMPLEX.
					9		1.12	.03	1.071	1.20		
1217+02			12 17 39.3	+02 20 18	5	45	.47	.02	1.000	.47	QSO 16.5M	Z=.240 (4)(4)(29)
					9		.45	.02	1.000	.45		
					11		.48	.02	1.000	.48		
1218-02	-02.53		12 18 51.5	-02 25 36	5	45	.54	.02	1.000	.54	QSO 20M	OPTICAL VARIABLE
1222+037	+03.23		12 22 19.2	+03 47 30	5	45	.82	.03	1.000	.82	QSO? 19M	
					11		.80	.02	1.000	.80		
1225-02	-02.54		12 25 24.5	-02 20 18	5	45	.40	.02	1.000	.40	QSO? 19.5M	
1226+02	+02.32	3C273 MSH 8	12 26 33.3	+02 19 44	9		38.89	.95	1.000	38.89	QSO 12.8M	Z=.158 (21)(23)(45) OPTICAL VARIABLE

TABLE AII.2 CONTINUED

2700 MHZ SURVEY - +4 TO -4 DEG.DEC. ZONE

(1)	(2)	(3)	(4)	(5)	(6)	(7)	(8)	(9)	(10)	(11)	(12)	(13)
PKS SOURCE NUMBER	OTHER CATALOGUE NUMBERS 4C	OTHER	POSITION (1950) R.A.	DEC.	RUN	PA	2700 MHZ PEAK FLUX DENSITY F.U.	FLUX R.M.S. ERROR F.U.	DENSITY SIZE FACTOR	FLUX DENSITY F.U.	IDENTIFICATION	REMARKS
1229-02	-02.55		12 29 25.9	-02 7 31	5		1.36	.04	1.000	1.36	QSO 16.7M	Z=.388 (7)(9)(26)
					9		1.32	.03	1.000	1.32		
					11		1.32	.03	1.000	1.32		
1229-01			12 29 32.3	-01 18 24	5	45	.47	.02	1.000	.47	III	
1247+025			12 47 58.4	+02 32 30	5	45	.42	.02	1.000	.42	III	
1249+035			12 49 50.0	+03 32 12	5	45	.60	.03	1.000	.60	E2 16.8M	
1250+029	+02.34		12 50 30.3	+02 54 42	5	45	.89	.04	1.000	.89	III	
					9		.92	.02	1.000	.92		
1253+026	+02.35		12 53 31.4	+02 36 54	5	45	.30	.02	1.000	.30		FAINT RED OBJ.ON POSN.
1256+018			12 56 35.9	+01 52 24	9		.29	.01	1.000	.29	III B	
1302-035			13 02 8.9	-03 30 6	5	45	.53	.02	1.000	.53	QSO?19.5M	
1305-012			13 05 38.6	-01 13 0	9		.28	.01	1.000	.28	III	
1307+000	+00.46		13 07 16.5	+00 3 0	5	45	.82	.03	1.000	.82	D 19.4M	PKS 1307-00.1
1307-007			13 07 54.7	-00 43 30	9		.22	.01	1.000	.22		15.6M E 1'P.PREV.IDENT. (3)REVOKED.PKS1307-00.7
1317-00	-00.50	MSH 8	13 17 4.1	-00 34 12	5		1.00	.03	1.000	1.00	QSO 18.5M	Z=.89 (10)
					9		.96	.02	1.000	.96		
1317+019			13 17 53.0	+01 55 54	5	45	.54	.02	1.000	.54	III	
					11		.57	.02	1.000	.57		
1320+03	+03.27		13 20 47.4	+03 23 54	5	45	.76	.03	1.000	.76	D 19.9M	(17)
					9		.74	.02	1.000	.74		
1324-025			13 24 32.0	-02 33 48	5	45	.31	.02	1.000	.31	G 19.4M	
1325-01	-01.29		13 25 4.3	-01 47 24	5	45	.71	.03	1.000	.71	D 18.7M	(8)
1330+02	+02.36	MSH 7	13 30 20.5	+02 16 9	9		1.82	.04	1.050	1.91	N 19.1M	Z=.2156 (17)(50)(39) 3C 287.1

TABLE AII.2 CONTINUED

2700 MHZ SURVEY - +4 TO -4 DEG.DEC. ZONE

(1)	(2)	(3)	(4)	(5)	(6)	(7)	(8)	(9)	(10)	(11)	(12)	(13)
PKS SOURCE NUMBER	OTHER CATALOGUE NUMBERS 4C	OTHER	POSITION R.A.	(1950) DEC.	RUN	PA	2700 MHZ PEAK FLUX DENSITY F.U.	FLUX DENSITY R.M.S. ERROR F.U.	SIZE FACTOR	FLUX DENSITY F.U.	IDENTIF-ICATION	REMARKS
1336+020	+02.37		13 36 58.8	+02 0 36	1	135	.38	.02	1.000	.38	III	
					2	135	.39	.01	1.000	.39		
1337+033			13 37 38.1	-03 20 12	1	135	.58	.02	1.000	.58	III	
					2	135	.58	.03	1.000	.58		
1340+022	+02.38	MSH 9	13 40 16.6	+02 13 0	1	135	.54	.02	1.000	.54	III	
1343+00	-00.51		13 43 3.1	-00 41 48	1	45	.62	.03	1.000	.62	III	17M QSO?PREV.IDENT. (8) REVOKED.PKS 1342+00
1349+01	-01.30		13 49 49.4	-01 41 24	2	135	.31	.02	1.000	.31	G 19.6M	
1349+027			13 49 58.2	+02 47 24	1	45	.81	.03	1.000	.81	III	DW 1349+02
					8	45	.77	.03	1.000	.77		
					9		.72	.02	1.000	.72		
1351+021			13 51 22.1	+02 6 54	2	135	.50	.02	1.000	.50		19M BSO WITH UV EXCESS
					8	45	.44	.02	1.000	.44		0.7'SP.
					11		.46	.02	1.000	.46		
1351+018			13 51 32.8	-01 51 18	2	135	1.00	.04	1.000	1.00		FAINT BSO WITH UV EXCESS
					8	45	.98	.04	1.000	.98		1.0'NP.
					9		.97	.02	1.000	.97		
					11		.99	.03	1.000	.99		
1352+00			13 52 35.3	+00 55 30	2	135	.40	.02	1.000	.40	QSO? 19M	(33)
					8	45	.30	.02	1.000	.30		
1353+005	-00.52		13 53 48.4	-00 34 36	2	135	.32	.02	1.000	.32	III	
					8	45	.31	.02	1.000	.31		
1354+01	+01.39	DA353	13 54 28.5	+01 19 18	1		1.27	.03	1.000	1.27		18.2M E 0.8'N.PREV.
					2		1.32	.03	1.000	1.32		IDENT.REVOKED
					8		1.31	.03	1.000	1.31		
					9		1.30	.03	1.000	1.30		

TABLE AII.2 CONTINUED

2700 MHZ SURVEY - +4 TO -4 DEG.DEC. ZONE

(1)	(2)	(3)	(4)	(5)	(6)	(7)	(8)	(9)	(10)	(11)	(12)	(13)
PKS SOURCE NUMBER	OTHER CATALOGUE NUMBERS 4C	OTHER	POSITION (1950) R.A.	DEC.	RUN	PA	2700 MHZ PEAK FLUX DENSITY F.U.	FLUX R.M.S. ERROR F.U.	DENSITY SIZE FACTOR	FLUX DENSITY F.U.	IDENTIFICATION	REMARKS
1355+01		DA355	13 55 20.6	+01 1 6	8	45	1.00	.04	1.000	1.00		BSO 1.0'NP.
					9		1.01	.03	1.000	1.01		
1356+022			13 56 55.1	+02 14 6	8	45	.66	.03	1.000	.66	QSO? 18.5M	
1359+025	+02.39		13 59 59.4	+02 30 30	8	45	.57	.02	1.000	.57	N 19.4M	
1359+039			13 59 52.9	+03 57 0	8	45	.33	.02	1.000	.33	QSO?19M	
1402-012			14 02 11.7	-01 16 6	8	45	.71	.03	1.000	.71	QSO? 18.5M	
1403-02	-02.59	DA358	14 03 36.9	-02 29 36	8	45	.46	.02	1.000	.46	III	
1404-01	-01.31	MSH 1	14 04 14.7	-01 40 0	8	45	.58	.02	1.000	.58	G 20.2M	G VERY BLUE (8)
1405+01			14 05 59.6	+01 30 24	8	45	.38	.02	1.000	.38		BSO 0.7'P.
1407+022			14 07 32.6	+02 17 18	8	45	.49	.02	1.000	.49	QSO?19M	
1414-03	-03.50	3C297 MSH 7	14 14 46.9	-03 47 0	8	45	1.00	.04	1.000	1.00	III B	
					9		.94	.02	1.000	.94		
1416-000			14 16 41.1	-00 0 36	8	45	.20	.01	1.000	.20	III	
1416-015	-01.33		14 16 49.9	-01 35 42	8	45	.30	.02	1.000	.30	III	
1418-025	-02.60		14 18 39.0	-02 33 36	8	45	.25	.01	1.000	.25	G 18.1M	
1420-005	-00.55		14 20 53.3	-00 35 42	8	45	.23	.01	1.000	.23	III	
1425+03	+03.29		14 25 2.9	+03 29 12	8	45	.33	.02	1.000	.33	QSO?19M	PKS 1424+03
1425-01	-01.34		14 25 56.4	-01 10 42	8		1.66	.04	1.000	1.66	N 17.3M	(6) JET IN PA 260 3C 300.1
					9		1.62	.04	1.000	1.62		
1426+030			14 26 32.5	+03 5 0	8	45	.43	.02	1.000	.43		FAINT RED OBJ.ON POSN.
1427-01	-01.35	MSH11	14 27 14.2	-01 0 24	8	22	.39	.02	1.000	.39	III	PKS 1427-00
1428-03	-03.52	MSH12	14 28 13.7	-03 21 42	8	45	.41	.02	1.000	.41		FAINT BSO 1.0'F.
1431+018			14 31 34.6	+01 50 0	8	45	.32	.02	1.000	.32	E 17.4M	
1434+03	+03.30	MSH10	14 34 25.6	+03 37 18	8		1.93	.05	1.000	1.93		FAINT G 1.0'NF.
					9		1.91	.04	1.000	1.91		

TABLE AII.2 CONTINUED

2700 MHZ SURVEY - +4 TO -4 DEG.DEC. ZONE

(1)	(2)	(3)	(4)	(5)	(6)	(7)	(8)	(9)	(10)	(11)	(12)	(13)
PKS SOURCE NUMBER	OTHER CATALOGUE NUMBERS 4C	OTHER	POSITION (1950) R.A.	DEC.	RUN	PA	2700 MHZ PEAK FLUX DENSITY F.U.	FLUX R.M.S, ERROR F.U.	DENSITY SIZE FACTOR	FLUX DENSITY F.U.	IDENTIF-ICATION	REMARKS
1434+019			14 34 58.8	+01 57 0	8	45	.36	.02	1.000	.36		FAINT G 1.5'NP.
1435+038			14 35 52.4	+03 53 6	8	22	.35	.02	1.000	.35	G 17.8M	
1440-01	-01.36		14 40 32.6	-01 4 54	8	45	.26	.01	1.000	.26	III	
1442-029			14 42 19.8	-02 59 6	8	45	.27	.02	1.000	.27	E 17.6M	
1443-032		MSH16	14 43 5.6	-03 17 30	8	45	.25	.01	1.000	.25	III	
1446+00	+00.52		14 46 6.0	+00 30 30	8	45	1.04	.04	1.000	1.04	E 19.4M	(17)FAINTER G NEAR POSN.
1446-005			14 46 42.0	-00 33 0	8	45	.33	.02	1.000	.33	III	
1449-012			14 49 12.5	-01 15 18	8	45	.35	.02	1.000	.35	QSO?18M	
1449+007	+00.53		14 49 25.2	+00 44 42	8	45	.23	.01	1.000	.23	III	
1454-034	-03.53		14 54 33.5	-03 27 24	8 9	45 45	.30 .29	.02 .02	1.000 1.000	.30 .29	QSO?17M	
1500-023	-02.62		15 00 59.4	-02 18 54	8	45	.59	.02	1.000	.59	III	
1502+036			15 02 35.8	+03 38 24	8 11	45	.46 .51	.02 .02	1.000 1.000	.46 .51	QSO?19M	PART OF 4C+03.31
1502+039			15 02 34.8	+03 59 6	11		.25	.01	1.000	.25		BSO 0.6'NP. PART OF 4C+03.31
1503-001	-00.58	MSH 1	15 03 1.7	-00 6 18	8	45	.55	.02	1.000	.55	III	
1505+01	+01.41		15 05 58.7	+01 13 24	8	45	.56	.02	1.000	.56	III	PREV.IDENT.(12)HAS STELLAR SPECTRUM(10)
1508+004	+00.55	MSH 3	15 08 29.9	+00 25 42	8	45	.43	.02	1.000	.43	IIIB	
1509+022			15 09 44.5	+02 14 36	8	45	.69	.03	1.000	.69	III	
1509+01	+01.42		15 09 53.7	+01 32 18	8 9	45	1.29 1.18	.05 .03	1.000 1.000	1.29 1.18	III	
1514+00	+00.56	MSH 6 DA378	15 14 7.6	+00 25 42	8		1.73	.04	1.058	1.83	E3/QSO	E 13.9M Z=.053;QSO18.8M (12)(47) COMPLEX S.

TABLE AII.2 CONTINUED

2700 MHZ SURVEY - +4 TO -4 DEG,DEC. ZONE

(1)	(2)	(3)	(4)	(5)	(6)	(7)	(8)	(9)	(10)	(11)	(12)	(13)
PKS SOURCE NUMBER	OTHER CATALOGUE NUMBERS 4C	OTHER	POSITION (1950) R.A.	DEC.	RUN	PA	2700 MHZ FLUX PEAK FLUX DENSITY F.U.	R.M.S. ERROR F.U.	DENSITY SIZE FACTOR	FLUX DENSITY F.U.	IDENTIFICATION	REMARKS
1523+03	+03.33		15 23 18.7	+03 18 48	8		1.14	.03	1.000	1.14		19.5M E 0.5'NP.PREV.
					9		1.13	.03	1.000	1.13		IDENT.REVOKED
1523-01	-01.37		15 23 56.6	-01 44 18	8	45	.40	.02	1.000	.40	III	
1523-034			15 23 57.3	-03 27 42	8	45	.21	.01	1.000	.21	III	
1525-020			15 25 48.5	-02 3 0	8	45	.27	.02	1.000	.27	III	
1532+01			15 32 20.5	+01 40 48	8	45	1.08	.04	1.000	1.08		BSO 1.0'S.
1532-000			15 32 58.9	-00 1 18	8	45	.30	.02	1.000	.30	III	
1535+004			15 35 43.2	+00 28 48	8	45	.96	.04	1.000	.96	III	
					11		1.04	.03	1.000	1.04		
1538+010	+00.57		15 38 43.0	+01 0 24	8	45	.41	.02	1.000	.41	III	
1539-022	-02.65		15 39 2.2	-02 13 18	8	45	.25	.01	1.000	.25	III	
1543+01	+01.45	MSH13	15 43 2.3	+01 59 12	8	45	.51	.02	1.000	.51	E 18.5M	(5) PKS 1542+02
1543+005			15 43 37.2	+00 35 30	8	45	1.31	.05	1.000	1.31	QSO?19M	DW 1543+00
					9		1.30	.03	1.000	1.30		
1545-004	-00.61		15 45 49.6	-00 25 18	8	45	.19	.01	1.000	.19	III	
1546+027			15 46 57.2	+02 45 54	8	45	1.36	.05	1.000	1.36	QSO?17.5M	
					9		1.10	.03	1.000	1.10		
1547+032			15 47 51.0	+03 12 0	8	135	.26	.01	1.000	.26		FAINT BSO 0.5'N.
1548+013	+01.46		15 48 3.9	+01 20 42	8	45	.26	.01	1.000	.26	III	
1552-033			15 52 51.4	-03 18 18	8	45	.43	.02	1.000	.43	III	
1555+001		DA393	15 55 16.9	+00 6 30	8	45	1.93	.07	1.000	1.93	III	DW 1555+00
					9		2.05	.05	1.000	2.05		
1556+032			15 56 59.6	+03 13 18	8	45	.46	.02	1.000	.46		BSO 0.5'S.
1557-00			15 57 26.2	-00 29 6	8	45	.54	.02	1.000	.54	III	
1559+02	+02.41	3C327 MSH 1	15 59 55.7	+02 6 12	8		4.42	.08	1.136	5.02	D 16.5M	Z=.1041 (2)(19)(32)
					9		4.46	.10	1.136	5.07		

TABLE AII.2 CONTINUED

2700 MHZ SURVEY - +4 TO +4 DEG.DEC. ZONE

(1)	(2)	(3)	(4)	(5)	(6)	(7)	(8)	(9)	(10)	(11)	(12)	(13)
PKS SOURCE NUMBER	OTHER CATALOGUE NUMBERS 4C	OTHER	POSITION (1950) R.A.	DEC.	RUN	PA	2700 MHZ PEAK FLUX DENSITY F.U.	FLUX R.M.S. ERROR F.U.	DENSITY SIZE FACTOR	FLUX DENSITY F.U.	IDENTIF-ICATION	REMARKS
1601-015			16 01 14.0	-01 31 0	8	45	.34	.02	1.000	.34	III	
1601-00	-00.63		16 01 18.4	-00 22 0	8	45	.45	.02	1.000	.45	N 17.5M	
1601-017			16 01 43.5	-01 47 12	8	45	.31	.02	1.000	.31	E 19.1M	
1602+01	+01.48	MSH 2	16 02 12.5	+01 25 54	8		2.14	.05	1.000	2.14	IIIA	3C 327.1
					9		2.13	.05	1.000	2.13		
1602-00		DA397	16 02 24.0	-00 11 30	8	45	.49	.02	1.000	.49	QSO?17.5M	(33).PKS 1602-00.2
					9		.60	.02	1.000	.60		
1603+005			16 03 12.6	+00 33 48	8	45	.66	.03	1.000	.66	IIIA	BSO NEAR POSITION
1603+00	+00.58	MSH 3 DA400	16 03 39.0	+00 8 29	8		1.51	.04	1.000	1.51	E4 16.5M	(53)(3)
					9		1.50	.04	1.000	1.50		
1608-011			16 08 14.7	-01 6 6	8	45	.31	.02	1.000	.31		BSO 0.7'P.
1611-007	-00.64	MSH 4	16 11 53.1	-00 47 54	8	45	.27	.01	1.000	.27	QSO?18.5M	
1615+029			16 15 18.4	+02 54 6	8	45	.74	.03	1.000	.74	QSO? 18M	
1616-029			16 16 30.1	-02 57 24	8	45	.40	.02	1.000	.40	E 16.6M	
1617-030			16 17 45.8	-03 4 24	8	45	.40	.02	1.000	.40	III	
1618+007			16 18 15.7	+00 43 54	8	45	.21	.01	1.000	.21	QSO?18.5M	
1635-035			16 35 38.7	-03 34 24	8	45	.51	.02	1.000	.51	III	
1636-03	-03.61	DA418	16 36 17.0	-03 7 42	8		.48	.02	1.000	.48	G 19.9M	17.6M DB (8) REVOKED
					9		.42	.01	1.000	.42		
1638-025	-02.69		16 38 1.4	-02 34 6	8		1.04	.03	1.000	1.04	III	
					9		1.02	.03	1.000	1.02		
1643+022	+02.42		16 43 10.0	+02 17 18	8	45	1.22	.05	1.000	1.22	E 18.0M	
					9		1.13	.03	1.000	1.13		
1645+027	+02.43		16 45 57.9	+02 47 36	8	45	.50	.02	1.000	.50	III	
1646+003	+00.59		16 46 48.5	+00 21 0	8	45	.33	.02	1.000	.33	III	
1648+015			16 48 31.7	+01 34 0	8	45	.72	.03	1.000	.72	III	

TABLE AII.2 CONTINUED

2700 MHZ SURVEY -= +4 TO -4 DEG.DEC. ZONE

(1)	(2)	(3)	(4)	(5)	(6)	(7)	(8)	(9)	(10)	(11)	(12)	(13)
PKS SOURCE NUMBER	OTHER CATALOGUE NUMBERS 4C	OTHER	POSITION (1950) R.A.	DEC.	RUN	PA	2700 MHZ FLUX PEAK FLUX DENSITY F.U.	R.M.S. ERROR F.U.	DENSITY SIZE FACTOR	FLUX DENSITY F.U.	IDENTIF-ICATION	REMARKS
1649-039			16 49 28.1	-03 55 30	8	45	.50	.02	1.000	.50	III	
1650+004	+00.60		16 50 22.3	+00 24 6	8	45	.73	.03	1.000	.73	III	
1650+024	+02.44		16 50 29.5	+02 29 36	8	45	.30	.02	1.000	.30	G 14M?	(51).PEC.GAL.NGC 6240 Z=.0261
1654-020	-01.39		16 54 18.2	-02 2 12	8	45	.64	.03	1.000	.64	III	
1659+01	+00.62		16 59 20.7	+01 4 24	8	45	.28	.02	1.000	.28	III	
1701+024			17 01 35.5	+02 26 18	8	45	.33	.02	1.027	.34	III	
1704+001	+00.64		17 04 46.8	+00 7 12	8	45	.42	.02	1.000	.42	III	
1705+018			17 05 2.1	+01 52 48	8	45	.52	.02	1.000	.52		BSO NEAR POSITION
					11		.54	.02	1.000	.54		NO UV EXCESS
1706+006			17 06 9.7	+00 39 12	8	45	.50	.02	1.000	.50		BSO NEAR POSITION NO UV EXCESS
1706-02	-02.72		17 06 10.1	-02 52 12	8	45	.29	.02	1.000	.29	III	
1707-038			17 07 36.4	-03 52 30	8	45	.30	.02	1.000	.30	III	
1708+00	+00.65		17 08 .1	+00 40 18	8	45	.83	.03	1.000	.83	DB 21.0M	(5)
1710-029			17 10 54.7	-02 55 12	8	45	.33	.02	1.000	.33	IIIA	
1711+006	+00.66		17 11 32.2	+00 38 42	8	45	.68	.03	1.000	.68		BSO NEAR POSITION NO UV EXCESS
1712-03	-03.62	MSH 4	17 12 22.4	-03 17 54	8	45	.61	.03	1.000	.61	III	
1714-019			17 14 3.3	-01 57 18	8	45	.40	.02	1.000	.40		BSO NEAR POSITION NO UV EXCESS
1714+025		OT024	17 14 25.5	+02 35 36	8	45	.34	.02	1.000	.34	III	
1714-020	-02.73	DA433	17 14 44.8	-02 1 48	8	45	.30	.02	1.000	.30	IIIA	
1716+006			17 16 48.4	+00 40 24	8	45	1.31	.05	1.000	1.31	III	DW 1716+00
					9		1.29	.03	1.000	1.29		

TABLE AII.2 CONTINUED

2700 MHZ SURVEY -+4 TO -4 DEG.DEC. ZONE

(1)	(2)	(3)	(4)	(5)	(6)	(7)	(8)	(9)	(10)	(11)	(12)	(13)
PKS SOURCE NUMBER	OTHER CATALOGUE NUMBERS 4C	OTHER	POSITION (1950) R.A.	DEC.	RUN	PA	2700 MHZ FLUX DENSITY PEAK F.U.	FLUX DENSITY R.M.S. ERROR F.U.	SIZE FACTOR	FLUX DENSITY F.U.	IDENTIFICATION	REMARKS
1717-00	-00.67	3C353 MSH 6	17 17 53.3	-00 55 50	8 9		30.93 32.64	1.42 .72	1.063 1.063	32.88 34.70	D 16.6M	Z=.0307 (34)(19)(32)
1720+001			17 20 .8	+00 6 36	8	45	.51	.02	1.000	.51	III	DW 1720+00
1721-02	-02.74		17 21 59.9	-02 39 42	8 9		1.47 1.50	.04 .04	1.023 1.023	1.50 1.53		G 1.5'SF.PKS 1722-02
1726-038	-03.64		17 26 9.8	-03 48 30	8	45	.57	.02	1.000	.57	IIIA	
1728+004			17 28 .4	+00 26 30	8	45	.18	.01	1.000	.18	III	
1729+010	+01.52		17 29 48.4	+01 2 0	8	45	.20	.01	1.000	.20	QSO? 19M	
1735+026			17 35 2.1	+02 38 36	8	45	.26	.01	1.000	.26	III	
1735-010	-00.69		17 35 7.4	-01 0 24	8	45	.26	.01	1.000	.26	III	
1735+034	+03.37	0T059	17 35 18.3	+03 27 30	8	45	.80	.03	1.000	.80	III	
1738+032			17 38 8.0	+03 13 30	8	45	.27	.02	1.000	.27	III	
1741-03			17 41 20.0	-03 48 48	8 9 11	45	3.05 2.80 2.99	.11 .05 .08	1.000 1.000 1.000	3.05 2.80 2.99	IIIA	
1748+031	+03.38	0T080	17 48 6.8	+03 11 36	8	45	.80	.03	1.000	.80	III	
1749+023	+02.45		17 49 29.7	+02 20 24	8	45	.55	.02	1.000	.55	III	
1938-012	-01.49		19 38 21.7	-01 12 6	8	45	.57	.02	1.000	.57	IIIC	
1942+038	+03.46		19 42 7.2	+03 49 36	8	45	.50	.02	1.000	.50	QSO?17.5M	
1943+002	+00.73		19 43 45.3	+00 13 0	8 9	45	.87 .82	.03 .02	1.000 1.000	.87 .82	III C	
1946+024	+02.49		19 46 36.2	+02 29 36	8	45	.42	.02	1.000	.42	IIIC	
1949+02	+02.50	3C403 MSH10	19 49 44.6	+02 22 37	8 9		3.61 3.60	.09 .08	1.023 1.023	3.69 3.68	SO 16.4M	Z=.0590 (43)(50)(41)

TABLE AII.2 CONTINUED

2700 MHZ SURVEY - +4 TO -4 DEG.DEC. ZONE

(1)	(2)	(3)	(4)	(5)	(6)	(7)	(8)	(9)	(10)	(11)	(12)	(13)
PKS SOURCE NUMBER	OTHER CATALOGUE NUMBERS 4C	OTHER	POSITION R.A.	(1950) DEC.	RUN	PA	2700 MHZ FLUX PEAK FLUX DENSITY F.U.	FLUX R.M.S. ERROR F.U.	DENSITY SIZE FACTOR	FLUX DENSITY F.U.	IDENTIF-ICATION	REMARKS
1949-01	-01.51		19 49 55.2	-01 25 7	8	45	.78	.03	1.089	.85	E 17.5M	(6)(50) . 3C 403.1
					9		.70	.02	1.089	.76		
1952+017	+01.61		19 52 41.1	+01 46 6	8	45	.54	.02	1.000	.54	IIIC	
1952+007	+00.74		19 52 50.2	+00 42 12	8	45	.34	.02	1.000	.34	QSO?18.5M	POSSIBLE UV EXCESS
1953+035	+03.47		19 53 8.1	+03 35 48	8	45	.29	.02	1.000	.29	QSO? 18M	
1957-013	-01.52		19 57 30.1	-01 18 42	8	45	.46	.02	1.000	.46		BSO NEAR POSITION NO UV EXCESS
2001+00	+00.75		20 01 3.3	+00 19 6	9		.24	.01	1.000	.24	IIIC	PKS 2000+00
2001-023	-02.78		20 01 56.0	-02 18 0	9		.38	.01	1.000	.38	III	
					11		.38	.02	1.000	.38		
2003-025	-02.79		20 03 32.4	-02 32 6	5	45	1.52	.06	1.000	1.52		BSO NEAR POSITION NO UV EXCESS
					9		1.45	.03	1.000	1.45		
2012+01	+00.76	OW020	20 12 2.6	+01 5 18	5	45	.43	.02	1.000	.43	IIIC	
2012-017			20 12 39.5	-01 46 42	5	45	.72	.03	1.000	.72	QSO 17.5M	
2022+031			20 22 38.5	+03 7 12	9		.37	.01	1.000	.37	III	
					11		.35	.01	1.000	.35		
2027-035			20 27 31.0	-03 35 30	9		.23	.01	1.000	.23	III	
2034+039	+04.70	OW058 MSH 5	20 34 23.3	+03 59 36	9		.20	.01	1.000	.20	III	
2037-02	-03.72	MSH 8	20 37 34.6	-02 58 24	9		.30	.01	1.000	.30	IIIA	PKS 2037-03
					11		.30	.01	1.000	.30		
2038-01	-01.54		20 38 38.7	-01 22 18	9		.22	.01	1.000	.22	III	
2044-02	-02.80	MSH 9 DA524	20 44 33.8	-02 47 36	5		1.38	.04	1.000	1.38	III	
					9		1.39	.03	1.000	1.39		
2047-032			20 47 59.7	-03 17 12	5	45	.39	.02	1.000	.39	III	

TABLE AII.2 CONTINUED

2700 MHZ SURVEY - +4 TO -4 DEG.DEC. ZONE

(1)	(2)	(3)	(4)	(5)	(6)	(7)	(8)	(9)	(10)	(11)	(12)	(13)
PKS SOURCE NUMBER	OTHER CATALOGUE NUMBERS 4C	OTHER	POSITION (1950) R.A.	DEC.	RUN	PA	2700 MHZ PEAK FLUX DENSITY F.U.	FLUX R.M.S. ERROR F.U.	DENSITY SIZE FACTOR	FLUX DENSITY F.U.	IDENTIFICATION	REMARKS
2047+039		MSH11 OW080	20 47 34.7	+03 56 36	5	45	.47	.02	1.000	.47	III	
2052+005			20 52 14.9	+00 30 30	5	45	.47	.02	1.000	.47	III	
2056+028		OW095	20 56 33.6	+02 52 36	5	45	.43	.02	1.000	.43	III	
2058+019	+01.64	OW097	20 58 38.1	+01 54 6	11		.32	.01	1.000	.32	III	
2059+034			20 59 8.8	+03 29 48	5	45	.59	.03	1.000	.59	QSO 18M	
2108+039	+03.50	OX014	21 08 42.5	+03 58 54	9 11		.37 .36	.01 .02	1.000 1.000	.37 .36	III	
2110-017	-01.55		21 10 13.1	-01 46 24	9		.31	.01	1.000	.31	QSO?19.5M	POSSIBLE UV EXCESS
2110+023		OX018	21 10 48.8	+02 18 6	9		.34	.01	1.000	.34		FAINT BSO 1.0'P.
2121-01			21 21 2.7	-01 25 36	5	45	.60	.03	1.000	.60		BSO 1'F.(PREVIOUS IDENT.(12))
2121+028	+02.52	OX0352	21 21 9.9	+02 52 12	5	45	.32	.02	1.000	.32		FAINT G 0.6'S.
2123+00	+00.79	OX040	21 23 11.3	+00 43 18	5	45	.38	.02	1.000	.38	DB	17.5M+18.3M.(17)
2123-015			21 23 56.1	-01 32 42	9		.30	.01	1.000	.30		TWO FAINT BSO'S. NO UV EXCESS
2126+010			21 26 17.8	+01 1 30	9		.27	.01	1.000	.27		16M DB 1'N.OX043?
2131-021	-02.81	MSH11	21 31 33.5	-02 6 36	5 11	45	1.98 1.87	.07 .05	1.000 1.000	1.98 1.87	QSO 19M	
2133+010	+01.66	OX055	21 33 18.8	+01 4 48	5	45	.56	.02	1.000	.56	QSO?20M	POSSIBLE UV EXCESS
2134+004		DA553 OX057	21 34 4.2	+00 28 18	9 11		7.60 7.58	.17 .20	1.000 1.000	7.60 7.58	QSO 17M	Z=1.94 (48)
2136+021		OX060	21 36 19.9	+02 6 42	9		.25	.01	1.000	.25		BSO NEAR POSITION NO UV EXCESS

TABLE AII.2 CONTINUED

2700 MHZ SURVEY - +4 TO -4 DEG.DEC. ZONE

(1)	(2)	(3)	(4)	(5)	(6)	(7)	(8)	(9)	(10)	(11)	(12)	(13)
PKS SOURCE NUMBER	OTHER CATALOGUE NUMBERS 4C	OTHER	POSITION (1950) R.A.	DEC.	RUN	PA	2700 MHZ FLUX PEAK FLUX DENSITY F.U.	R.M.S. ERROR F.U.	DENSITY SIZE FACTOR	FLUX DENSITY F.U.	IDENTIF-ICATION	REMARKS
2139+02	+02.53	MSH 7 OX066	21 39 38.2	+02 48 36	5	45	.63	.03	1.000	.63	III	
2150-031	-03.75		21 50 1.5	-03 8 36	9		.30	.01	1.000	.30	G 19.6M	
2154-01	-01.57	MSH18	21 54 13.7	-01 39 54	5	45	.73	.03	1.000	.73	III	
					9		.74	.02	1.000	.74		
2201-006	-00.79		22 01 23.7	-00 36 18	7	45	.33	.02	1.000	.33	III	
2202-003	-00.80		22 02 40.8	-00 19 6	8	45	.26	.01	1.000	.26	III	
2207+020	+02.54	MSH 1 OY011	22 07 .2	+02 4 18	7	90	.44	.02	1.000	.44		BSO NEAR POSITION NO UV EXCESS
2210+01	+01.69	DA575 OY016	22 10 5.6	+01 38 6	7		1.77	.05	1.000	1.77	IIIB	
					9		1.80	.04	1.000	1.80		
2211-035	-03.77		22 11 58.1	-03 33 0	7	45	.43	.02	1.000	.43	III	
2214-035	-03.78		22 14 37.5	-03 35 24	8	45	.31	.02	1.000	.31	III	
2215-027			22 15 10.9	-02 47 36	7	45	.43	.02	1.000	.43		FAINT BSO NEAR POSN.
2215+02		OY026	22 15 14.7	+02 5 18	7	45	.70	.03	1.000	.70	III	
2215-000	-00.81		22 15 53.6	-00 3 6	8	45	.28	.02	1.000	.28	III	
2216-03	-03.79	MSH 6	22 16 16.3	-03 50 43	7	45	1.05	.04	1.000	1.05	QSO 16.9M	Z=.901 (6)(11)(28)
					8	45	1.00	.03	1.000	1.00		
					9		1.06	.03	1.000	1.06		
					11		1.09	.03	1.000	1.09		
2217-011		MSH 7	22 17 10.5	-01 6 6	8	45	.28	.02	1.000	.28	G 20.2M	
2217+018	+01.70	OY030	22 17 57.6	+01 49 54	7	45	.50	.02	1.000	.50	III	
2219-030	-03.80		22 19 47.2	-03 5 6	7	45	.81	.03	1.000	.81	III	
					9		.81	.02	1.000	.81		

TABLE AII.2 CONTINUED

2700 MHZ SURVEY - +4 TO -4 DEG,DEC, ZONE

(1)	(2)	(3)	(4)	(5)	(6)	(7)	(8)	(9)	(10)	(11)	(12)	(13)
PKS SOURCE NUMBER	OTHER CATALOGUE NUMBERS 4C	OTHER	POSITION (1950) R.A.	DEC.	RUN	PA	2700 MHZ FLUX PEAK FLUX DENSITY F.U.	R.M.S. ERROR F.U.	DENSITY SIZE FACTOR	FLUX DENSITY F.U.	IDENTIFICATION	REMARKS
2221-02	-02.83	3C445 MSH 9	22 21 15.5	-02 21 48	7		2.47	.07	1.400	3.46	N 17.5M	Z=.0568 (31)(32)
2224+006	+00.81	OY041	22 24 13.6	+00 36 48	7	45	.44	.02	1.000	.44	III	
2229+029		OY051	22 29 54.3	+02 55 36	8	45	.26	.02	1.000	.26	III	
2243-03	-03.81		22 43 36.0	-03 16 24	8 9	45	.70 .63	.03 .02	1.000 1.000	.70 .63	G 21.0M	VERY BLUE,(8)
2244-002			22 44 57.1	-00 16 12	8	45	.25	.02	1.000	.25		BSO NEAR POSITION NO UV EXCESS
2245-022		MSH16	22 45 24.4	-02 13 54	8	45	.34	.02	1.000	.34	III	
2245+029		OY077	22 45 24.6	+02 55 0	8	45	.66	.03	1.000	.66	III	
2250+03	+03.55	OY083 MSH11	22 50 11.7	+03 28 36	11		.24	.01	1.000	.24	III	
2250+003	+00.83	OY084	22 50 21.4	+00 22 0	8	45	.50	.02	1.000	.50	III	
2250+023		OY086	22 50 46.6	+02 20 24	8	45	.34	.02	1.000	.34	III	
2251+006		MSH12 OY087	22 51 33.7	+00 39 12	8	45	.30	.02	1.000	.30	III	
2252+021	+02.56	OY088	22 52 18.6	+02 9 30	8	45	.27	.02	1.000	.27	III	
2254+024			22 54 43.9	+02 27 12	8	45	.46	.02	1.000	.46	QSO 18M	Z=2.09 (10),OY091.3
2256+017			22 56 24.4	+01 47 30	8	45	.36	.02	1.000	.36		BSO ON POSITION NO UV EXCESS
2300-013			23 00 15.7	-01 21 6	8	45	.19	.01	1.000	.19	III	
2302-025	-02.87	MSH 1	23 02 24.7	-02 35 12	8	45	.25	.01	1.000	.25	III	
2303-008	-01.59	MSH 3	23 03 10.5	-00 52 18	8	45	.33	.02	1.000	.33	III	
2304+00	+00.84	DA592 OZ007	23 04 9.1	+00 40 48	8	45	.31	.02	1.000	.31	III	

TABLE AII.2 CONTINUED

2700 MHZ SURVEY - +4 TO -4 DEG.DEC. ZONE

(1)	(2)	(3)	(4)	(5)	(6)	(7)	(8)	(9)	(10)	(11)	(12)	(13)
PKS SOURCE NUMBER	OTHER CATALOGUE NUMBERS 4C	OTHER	POSITION (1950) R.A.	DEC.	RUN	PA	2700 MHZ FLUX PEAK FLUX DENSITY F.U.	R.M.S. ERROR F.U.	DENSITY SIZE FACTOR	FLUX DENSITY F.U.	IDENTIFICATION	REMARKS
2305+02	+02.57	OZ010	23 05 43.2	+02 12 48	8	45	.32	.02	1.000	.32	III	
2305+033		OZ011	23 05 51.3	+03 20 36	8	45	.27	.02	1.000	.27	IIIB	
2313+01	+01.74	OZ023	23 13 43.9	+01 12 36	8	45	.58	.02	1.000	.58	G 19.4M	(33)
2314+03	+03.57	3C459	23 14 2.3	+03 48 56	8		2.36	.05	1.000	2.36	N 18.7M	Z=.2205 (27)(50)(46)
		MSH 5			9		2.43	.06	1.000	2.43		PKS 2313+03
2318+02	+02.58	OZ030	23 18 13.3	+02 40 36	8	45	.38	.02	1.000	.38	QSO 19M	(17)
2320-021			23 20 30.1	-02 7 0	8	45	.33	.02	1.000	.33	QSO 19.5M	
2320-035			23 20 56.6	-03 33 6	8	45	.42	.02	1.000	.42		BSO NEAR POSITION NO UV EXCESS
2323-038			23 23 18.8	-03 52 24	8		.23	.01	1.000	.23	III	
2324-02		MSH11	23 24 19.4	-02 18 44	8		1.55	.03	1.022	1.58	E 18.0M	(6)(3)
		DA602			9		1.50	.04	1.022	1.53		
2332-017			23 32 45.2	-01 47 48	8	45	.64	.03	1.000	.64	QSO 18.5M	
2335-027			23 35 22.7	-02 47 36	8	45	.60	.02	1.000	.60	QSO 19M	
2335+03	+03.59	OZ061	23 35 33.8	+03 10 24	8	45	.93	.04	1.000	.93	III	
2338-002	-00.83	MSH15	23 38 26.0	-00 12 18	8	45	.38	.02	1.000	.38	DB 17.2M	
					9		.37	.01	1.000	.37		
					11		.38	.02	1.000	.38		
2338+000			23 38 34.7	+00 2 6	8	45	.34	.02	1.000	.34	E 19.1M	
					9		.37	.01	1.000	.37		
2338+03	+03.60	OZ066	23 38 56.3	+03 1 0	8	45	.38	.02	1.000	.38	G 20.2M	
2340-036			23 40 22.3	-03 39 48	8	45	.28	.02	1.000	.28	QSO 17M	
2347-02	-02.90		23 47 51.0	-02 41 12	8	45	.93	.04	1.000	.93	IIIB	
2349-01	-01.61	MSH20	23 49 22.3	-01 25 54	8	45	1.05	.04	1.000	1.05	N 17.1M	Z=.173 (7)(3)(47)
					9		.97	.02	1.000	.97		
					11		1.04	.03	1.000	1.04		

TABLE AII.2 CONCLUDED

2700 MHZ SURVEY - +4 TO -4 DEG.DEC. ZONE

(1)	(2)	(3)	(4)	(5)	(6)	(7)	(8)	(9)	(10)	(11)	(12)	(13)
PKS SOURCE NUMBER	OTHER CATALOGUE NUMBERS 4C	OTHER	POSITION (1950) R.A.	DEC.	RUN	PA	2700 MHZ PEAK FLUX DENSITY F.U.	FLUX DENSITY R.M.S. ERROR F.U.	SIZE FACTOR	FLUX DENSITY F.U.	IDENTIF-ICATION	REMARKS
2351-006			23 51 35.3	-00 36 18	8	45	.51	.02	1.000	.51		BSO NEAR POSITION NO UV EXCESS
2354-02	-02.91		23 54 31.9	-02 43 18	2	135	.46	.02	1.000	.46	III	
2355-010	-00.85		23 55 51.5	-01 1 36	2	135	.42	.02	1.000	.42	III	

References for Tables AII.1 and AII.2

(1) Bolton, J.G. - personal communication

(2) Bolton, J.G. (1960) - Report at XIII General Assembly of URSI, London. Also Obs. Cal. Tech. Radio Obs. 5, 1960

(3) Bolton, J.G. (1968) - Pub. astr. Soc. Pacific 80, 5

(4) Bolton, J.G., Clarke, Margaret E., Sandage, Allan, and Véron, P. (1965) - Astrophys. J. 142, 1289

(5) Bolton, J.G., and Ekers, Jennifer A. (1966) - Aust. J. Phys. 19, 275

(6) Bolton, J.G., and Ekers, Jennifer A. (1966) - Aust. J. Phys. 19, 559

(7) Bolton, J.G., and Ekers, Jennifer A. (1966) - Aust. J. Phys. 19, 713

(8) Bolton, J.G., and Ekers, Jennifer A. (1967) - Aust. J. Phys. 20, 109

(9) Bolton, J.G., and Kinman, T.D. (1966) - Astrophys. J. 145, 951

(10) Bolton, J.G., Kinman, T.D., and Wall, J.V. (1968) - Astrophys. J. 154, L105

(11) Bolton, J.G., Shimmins, A.J., Ekers, Jennifer A., Kinman, T.D., Lamla, E., and Wirtanen, C.A. (1966) - Astrophys. J. 144, 1229

(12) Bolton, J.G., Shimmins, A.J., and Merkelijn, Jeannette (1968) - Aust. J. Phys. 21, 81

(13) Bolton, J.G., and Wall, J.V. (1969) - Astrophys. Lett. 3, 177

(14) Burbidge, E. Margaret (1966) - Astrophys. J. 143, 612

(15) Burbidge, E.M. (1967) - Astrophys. J. 149, L51

(16) Burbidge, E. Margaret, and Kinman, T.D. (1966) - Astrophys. J. 145, 654

(17) Clarke, Margaret E., Bolton, J.G., and Shimmins, A.J. (1966) - Aust. J. Phys. 19, 375

(18) Gent, H., Adgie, R.L, and Crowther, J.H. (1969) - Nature 222, 253

(19) Griffin, Roger F. (1963) - Astron. J. 68, 421

(20) Hazard, C., Mackey, M.B., and Nicholson, W. (1964) - Nature 202, 227

(21) Hazard, C., Mackey, M.B., and Shimmins, A.J. (1963) - Nature 197, 1037

(22) Humason, M.L., Mayall, N.U., and Sandage, A.R. (1956) - Astron. J. 61, 97

(23) Jefferys, W.H. III (1964) - Astron. J. 69, 255

(24) Kinman, T.D. - personal communication to J.G. Bolton

(25) Kinman, T.D., Bolton, J.G., Clarke, R.W., and Sandage, A.R. (1967) - Astrophys. J. 147, 848

(26) Kinman, T.D., and Burbidge, E. Margaret (1967) - Astrophys. J. 148, L59

(27) Longair, M.S. (1965) - Mon. Not. R. astr. Soc. 129, 419

(28) Lynds, C.R. (1967) - Astrophys. J. 147, 837

(29) Lynds, C.R., Hill, S.J., Heere, Karen, and Stockton, A.N. (1966) - Astrophys. J. 144, 1244

(30) Maltby, P., Matthews, T.A., and Moffet, A.T. (1963) - Astrophys. J. 137, 153

(31) Matthews, T.A., reported by Schmidt, Maarten (1965) - Astrophys. J. 141, 1

(32) Matthews, Thomas A., Morgan, William W., Schmidt, Maarten (1964) - Astrophys. J. 140, 35

(33) Merkelijn, Jeannette K. (1969) - Aust. J. Phys. 22, 237

(34) Mills, B.Y. (1960) - Aust. J. Phys. 13, 550

(35) Mills, B.Y., Slee, O.B., and Hill, E.R. (1958) - Aust. J. Phys. 11, 360

(36) Minkowski, R. (1958) - Pub. astr. Soc. Pacific 70, 143

(37) Moffet, A.T., reported by Schmidt, Maarten (1965) - Astrophys. J. 141, 1

(38) Moffet, A.T., Schmidt, M., Slater, C.H., Thompson, A.R. (1967) - Astrophys. J. 148, 283

(39) Sandage, Allan (1966) - Astrophys. J. 145, 1

(40) Sandage, Allan (1967) - Astrophys. J. 150, L145

(41) Sandage, Allan, reported by Petrosian, Vahé (1969) - Astrophys. J. 155, 1029

(42) Sandage, Allan, Véron, Philippe, and Wyndham, John D. (1965) - Astrophys. J. 142, 1307

(43) Sandage, Allan, and Wyndham, John D. (1965) - Astrophys. J. 141, 328

(44) Schmidt, M. - personal communication to J.G. Bolton

(45) Schmidt, M. (1963) - Nature 197, 1040

(46) Schmidt, Maarten (1965) - Astrophys. J. 141, 1

(47) Searle, Leonard, and Bolton, J.G. (1968) - Astrophys. J. 154, L101

(48) Shimmins, A.J., Searle, L., Andrew, B.H., and Brandie, G.W. (1968) - Astrophys. Lett. 1, 167

(49) Smith, Harlan J., and Hoffleit, Dorrit (1963) - Nature 198, 650

(50) Véron, P. (1966) - Astrophys. J. 144, 861

(51) Whiteoak, J.B. - personal communication

(52) Wills, D. (1967) - Astrophys. J. 148, L57

(53) Wyndham, J.D. (1965) - Astron. J. 70, 384

(54) Wyndham, J.D. (1966) - Astrophys. J. 144, 459

APPENDIX III

DATA ON THE OPTICAL IDENTIFICATIONS FROM THE 2700 MHZ SURVEY OF THE SELECTED REGIONS AND THE ±4° DECLINATION ZONE

AIII.1 Galaxy Identifications

The galaxy identifications in the selected regions and in the ±4° declination zone (see §3.1) are listed in Tables AIII.1 and AIII.2. The content of each column is as follows:

(1) Parkes source number.

(2), (3) The coordinates (epoch 1950.0) of the optical centroid of the galaxy as estimated from the Palomar Sky Survey prints with the aid of the transparent overlay (§3.1(ii)). Standard error in these estimates is 6 arc seconds. For the well established identifications, accurate optical positions as measured by other authors are given.

(4), (5) The displacements in right ascension and declination of the measured position of the radio source from the estimated optical position. The symbols used are n - north, s - south, p - preceding, f - following. Displacements are not entered for those sources used as position calibrators (§2.4).

(6) The morphological type as estimated from the Sky Atlas prints: S,E,N,D, and db have the usual meanings, and g indicates that the galaxy is too faint for classification.

(7) The photographic magnitude as estimated from the Palomar Sky Survey prints. The standard error in m_{pg} is $0^m.5$.

(8) The 2700 MHz flux densities (§2.7). Square brackets indicate that the peak flux density has been corrected for partial resolution.

(9) References to the previous identification of the source, to the measurement of the accurate optical position, and to the measurement of the redshift, respectively. The references follow Table AIII.2.

(10), (11) New galactic coordinates.

(12) Comments, including redshifts and Cambridge catalogue numbers.

TABLE AIII.1

DATA FOR GALAXY IDENTIFICATIONS IN SELECTED REGIONS, 2700 MHZ SURVEY

A. PS 1112

(1) Source	(2) Optical Coordinates (1950.0) r.a.	(3) dec.	(4) $\Delta\alpha$	(5) $\Delta\delta$	(6) Type	(7) m_{pg}	(8) S_{2700} (f.u.)	(9) Reference	(10) l^{II}	(11) b^{II}	(12) Comments
2356+01	$23^h56^m38^s.9$	+01° 50.1	2.4f	0.0	E4	17.5	0.16		98°	-58°	
2357+00	23 57 25.0	+00 25.4	.8p	.1n	db	15.6	0.27	9	97	-60	
0003+006	00 03 28.0	+00 37.3	2.3f	.1s	g	18.3	0.25		100	-60	
0004-010	00 04 57.0	-01 04.9	.1p	.3s	E	16.3	0.09		99	-62	
0007+016	00 07 24.0	+01 41.5	.3p	.4s	g	20.5	0.16		102	-59	Bright galaxy 1.5 sf.
0012-008	00 12 29.5	-00 51.5	1.6p	.1n	E	18.0	0.12		104	-60	
					B. PS 891						
0038-019	00 38 48.2	-01 59.3	1.0f	0.0	S	15.0	0.65		117	-64	4C-02.4
0040+017	00 40 15.0	+01 46.0	.1f	0.0	N	18.7	0.12		119	-61	
0041+015	00 41 59.6	+01 35.6	2.0p	.1s	g	19.5	0.06		119	-61	
0043+000	00 43 06.0	+00 04.5	2.0f	.1n	E	17.8	0.27		120	-62	4C-00.5
0043-003	00 43 53.0	-00 21.7	1.0f	.4n	g	18.5	0.10		120	-62	
0046+011	00 46 05.7	+01 08.7			cluster	-	0.08		121	-61	Position given is that of radio source.
0049+019	00 49 02.5	+01 59.2	2.1f	0.0	g	20.2	0.11		123	-61	
0052+011	00 52 25.0	+01 06.3	2.8p	.1s	S	14.5	0.08		125	-61	
0053-016	00 53 29.3	-01 35.9	1.1p	.5s	N	16.4	[0.71]		126	-64	PKS 0053-01, 4C-01.4;
0053-015	00 53 52.4	-01 32.7	.4f	.1s	N	16.7	[0.78]		126	-64	brighter galaxy 1' n.
0055-01	00 55 01.41	-01 39 50.6			EO	15.0	[3.46]	4,27,23	126	-64	3C29.B, 4C-01.5; z =.0450.
0100-011	01 00 08.5	-01 06.5	1.5p	0.0	g	19.5	0.08		130	-62	
0101-006	01 01 29.6	-00 40.4			cluster	-	0.08		130	-62	Brightest galaxy of cluster (m_{pg}=16.3) is 1' sf. Position given is that of radio source.
					C. PS 1114						
0222-00	02 22 32.8	-00 49.6	2.2p	.5n	SO	16.5	0.67	6	167	-55	4C-00.12
0235+017	02 35 06.0	+01 45.9	.2p	1.0n	E	14.8	0.18		168	-51	
0239+002	02 39 12.6	+00 13.9	.2p	0.0	S	12	0.15		171	-52	Prominent dust lane; NGC1055.
0240-00	02 40 07.00	-00 13 31.1			Sc	9.7	3.12	18,10,11	171	-51	3C71, 4C-00.13; NGC1068; z=.00344.
					D. PS 1777						
1152-011	11 52 27.2	-01 09.2	0.4f	.1s	g	18.3	0.08		275	58	Second galaxy 0.3 np. Outside selected region.
1154-038	11 54 14.8	-03 48.9	1.4p	.4n	D	15.7	0.17		278	56	Outside selected region.
1157-008	11 57 49.0	-00 49.2	1.4p	0.0	S	11.6	0.09		276	61	NGC4030
1201-002	12 01 31.6	-00 13.0	1.5p	.1n	g	20.5	0.19		278	61	
1201+027	12 01 32.1	+02 41.4	1.0f	.9n	E	16.9	0.16		276	63	Outside selected region.
1207-013	12 07 57.6	-01 20.1	.4f	.1s	db	19.4	0.39		282	60	
1208-035	12 08 45.6	-03 33.4	.4p	.3s	g	19.6	0.08		284	58	

TABLE AIII.1 CONCLUDED

E. PS 1778

(1) Source	(2) Optical Coordinates (1950.0) r.a.	(3) dec.	(4) $\Delta\alpha$	(5) $\Delta\delta$	(6) Type	(7) m_{pg}	(8) S_{2700} (f.u.)	(9) Reference	(10) l^{II}	(11) b^{II}	(12) Comments
1330+02	$13^h30^m20^s.5$	$+02^\circ 16' 09''$	$0^s.6f$	$.2n$	N	$19^m.1$	[1.91]	9,27,22	326°	63°	3C287.1, 4C+02.36; z=.2156
1338+011	13 38 58.0	+01 07.4	0.0	.4n	g	20.2	0.16		330	61	
1342-016	13 42 43.5	-01 41.0	.3p	.3s	D	18.0	0.21		329	58	
1349-01	13 49 49.0	-01 41.7	.4f	.3n	g	19.6	0.31		332	57	4C-01.30 In small cluster.
1351+003	13 51 18.3	+00 21.1	.7f	.1s	g	20.2	0.07		335	59	
					F. PS 896						
2149-158	21 49 11.0	-15 51.6	3.7f	.2n	db	17.1+17.3	0.32		39	-47	Outside selected region.
2153-219	21 53 12.2	-21 58.8	.5f	.1n	N	17.2	0.11		31	-50	
2155-202	21 55 02.0	-20 12.9	2.7f	.6n	g	19.6	0.22		34	-50	
2157-191	21 57 57.0	-19 10.6	2.4p	.5n	g	20.2	0.13		35	-50	
2201-217	22 01 16.0	-21 41.7	.4f	1.0s	db	16.5+17.3	0.15		32	-52	Brightest of cluster.
2204-218	22 04 42.4	-21 48.8	2.2p	.5s	E	16.8	0.08		32	-52	
2211-17	22 11 41.5	-17 16.8	.5f	.1n	D	19	[4.52]	30	40	-52	3C444

TABLE AIII.2

DATA FOR GALAXY IDENTIFICATIONS IN ±4° DECLINATION ZONE, 2700 MHZ SURVEY

(1)	(2)	(3)	(4)	(5)	(6)	(7)	(8)	(9)	(10)	(11)	(12)
Source	Optical Coordinates (1950.0) r.a.	dec.	Δα	Δδ	Type	m_{pg}	S_{2700} (f.u.)	Reference	l^{II}	b^{II}	Comments
0029-01	$00^h28^m59^s.3$	-01° 17′.4	0s.4p	0′.1s	g	19m.4	0.52		112°	-63°	4C-01.2
0034-01	00 34 30.5	-01 25 44″.3	.1p	.1s	EO	17.1	[2.56]	4,27,8	114	-63	3C15, 4C-01.3; z=.0733.
0035-02	00 35 46.79	-02 24 10.2			E	19.6	4.04	20,21,25	115	-64	3C17, 4C-02.3; z=.2201.
0036+03	00 36 43.8	+03 03.4	.4p	.1s	E2	13.5	[1.11]	9,29	117	-59	4C+03.1; NGC193; z=.0145.
0038-019	00 38 48.2	-01 59.3	1.0f	0.0	S	15.0	0.65		117	-64	4C-02.4
0051-03	00 51 35.6	-03 50 11.3	1.2p	.1n	E	19.1	1.11	4,2,25	124	-66	3C26,4C-03.3;z= .2106.
0053-016	00 53 29.3	-01 35.9	1.1p	.5s	N	16.4	[0.71]		126	-64	PKS 0053-01, 4C-01.4;
0053-015	00 53 52.4	-01 32.7	.4f	.1s	N	16.7	[0.78]		126	-64	brighter galaxy 1′n.
0055-01	00 55 01.4	-01 39 50.6	.5f	.2s	EO	15.0	[3.46]	4,27,23	126	-64	3C29, 4C-01.5; z=.0450.
0111+021	01 11 08.8	+02 06.4	.4f	.1n	E	16.3	0.61		134	-60	Radio spectrum flat or inverted.
0115-01	01 15 41.5	-01 36.0	1.9f	.3n	N	18.3	0.52	6	138	-63	4C-01.7; jet in p.a. ~ 100°.
0123-01	01 23 26.0 27.5	-01 35 59.5 36 17.2	-	-	E+E	12.8	[2.75]	19,10,13	142	-62	3C40, 4C-01.8; NGC545/7; z=.0180.
0128+003	01 28 59.1	+00 17.9	.9p	.2n	E	16.1	0.33		144	-61	4C+00.5
0217+01	02 17 24.5	+01 41.9	.9p	.1n	E7	15.2	0.36	9	163	-54	
0218-02	02 18 21.90	-02 10 33.0			E	19.1	1.68	4,27	167	-57	3C63, 4C-02.10
0222-00	02 22 32.8	-00 49.6	2.2p	.5n	SO	16.5	0.67	6	167	-55	4C-00.12
0240-00	02 40 07.00	-00 13 31.1			Sc	9.7	3.12	18,10,11	171	-51	3C71,4C-00.13; NGC1068; z=.00344
0252+02	02 52 33.7	+02 41.6	.1f	0.0	N	19.9	0.41	16	172	-48	3C74, 4C+02.8
0305+03	03 05 49.03	+03 55 12.7			D	14.4	[5.33]	1,10,15	175	-45	3C78, 4C+03.5; NGC1218; z=.0289.
0325+02	03 25 18.25	+02 23 20.4	1.0f	0.0	D	14.9	[3.18]	14,27,15	181	-42	3C88, 4C+02.10; z=.0302.
0331-01	03 31 43.37	-01 21 26.3	.6p	0.0	D	18.3	[1.39]	4,27	185	-42	3C89, 4C-01.12
0353+027	03 53 23.0	+02 47.7	.4f	.1s	N	19.1	0.47		186	-36	4C+02.11; galaxy shows UV excess.
0448-025	04 48 49.9	-02 33.8	.2f	.2s	g	20.2	0.25		201	-28	4C-02.18
0458+01	04 58 03.5	+01 26.0	.4f	.2s	E	18.5	0.52		198	-24	4C+01.12
0511+00	05 11 33.78	+00 53 07.9	.5p	.1n	E	17.5	[1.70]	9,27,23	200	-21	3C135, 4C+00.19; z=.1270.
0723-036	07 23 35.6	-03 38.5 38.8	.4f	.1s	db	17.5+18.0	0.32		220	6	
0724-01	07 24 33.27	-01 58 24.4	.6p	0.0	g	20.2	[1.56]	4,27	218	6	3C180, 4C-02.31
0726-00	07 26 15.3	-00 02.5	1.1p	0.0	g	20.2	0.40	6	217	8	4C-00.25
0742+02	07 42 27.94	+02 07 44.6	.4f	.2s	g	19.5(?)	[0.82]	31,27	217	13	3C187, 4C+02.21
0752-02.7	07 52 16.4	-02 39.6	.4f	.1n	N	19.4	0.46		223	13	4C-02.33
0752-02.3	07 52 25.3	-02 14.2	1.3f	.7s	db	15.8+16.2	0.42		222	13	
0803-00	08 03 04.6	-00 49.7	.6p	0.0	E4	15.4	0.71	4	222	16	4C-00.32
0812-02	08 12 57.32	-02 59 13.9			D	18.9	0.95	4,27	225	17	3C196.1, 4C-02.35
0833-01	08 33 02.0	-01 40.7	1.0f	0.0	E	13.9	[0.56]	6	227	22	Some jet structure.
0859+032	08 59 15.2	+03 16.2	.2p	0.0	g	20.2	0.34		227	30	

TABLE AIII.2 Cont'd.

(1) Source	(2) Optical Coordinates (1950.0) r.a.	(3) dec.	(4) $\Delta\alpha$	(5) $\Delta\delta$	(6) Type	(7) m_{pg}	(8) S_{2700} (f.u.)	(9) Reference	(10) l^{II}	(11) b^{II}	(12) Comments
0956+015	$09^h56^m46^s.3$	+01° 32'.4	0s.0	0".0	db?	15m.8	0.30		238°	41°	
1005+007	10 05 37.3	+00 44.8	0.0	.2s	N	16.9	0.34		240	43	
1008-01	10 08 18.8	-01 46.2	1.0f	.1s	S?	19.4	[0.80]		243	42	4C-01.21
1027+00	10 27 36.3	+00 53.1	0.3f	.3s	g	19.4	0.61		245	47	4C+00.35
1033+003	10 33 31.9	+00 21.8	.6f	0.0	E	16.5	0.34		247	48	4C+00.37
1039+02	10 39 05.3	+02 58.1	.6p	.2n	g	19.4	1.66		246	51	4C+03.18
1051+035	10 51 51.6	+03 30.7	.2f	0.0	db	20.2	0.29		248	53	4C+03.19
1103+002	11 03 15.0	+00 14.0	1.8f	1.0n	S	9.82	0.29	11	256	53	NGC3521; z=.00205.
1106+023	11 06 11.1	+02 19.0	.2p	.1s	N	18.9	0.64		254	55	
1111-037	11 11 58.9	-03 44.9	.4p	.3n	g	18.3	0.35		262	51	4C-03.41; BSO near position is also marked on finding chart.
1118+000	11 18 46.1	+00 03.1	1.1p	.1s	db	17.0+18.5	0.44		261	55	
1127+005	11 27 02.8	+00 31.8			cluster	-	0.58		263	57	4C+00.40; cluster of faint galaxies. Radio source position is given.
1127+012	11 27 47.3	+01 15.0	.3f	.1s	N	17.8	0.41		263	57	4C+01.30
1130-037	11 30 32.4	-03 44.2	1.4p	.1s	E	15.3	0.54		269	54	4C-03.43
1141+011	11 41 35.0	+01 11.3	.5f	.1s	g	19.4	0.33		268	59	
1147+015	11 47 51.5	+01 32.7	0.0	0.0	g	19.9	0.31		271	60	4C+01.33
1207-013	12 07 57.6	-01 20.1	0.0	.1s	db	19.4	0.39		282	60	
1215+03	12 15 07 14 58.3	+03 56.0 53.8			D+E	17.3,17.3	[1.21]	10,8	283	65	4C+04.41; z=.0756,.0771. Complex source.
1249+035	12 49 50.0	+03 32.2	0.0	0.0	E2	16.8	0.60		304	66	
1307-00.1	13 07 16.5	+00 03.0	0.0	0.0	D	19.4	0.82		313	62	4C+00.46
1320+03	13 20 46.0	+03 23.8	1.4f	.1n	D	19.9	0.75	9	322	65	4C+03.27
1324-025	13 24 33.0	-02 33.8	1.0p	0.0	g	19.4	0.31		320	59	
1325-01	13 25 04.0	-01 47.6	.3f	.2n	D	18.7	0.71	6	321	60	4C-01.29
1330+02	13 30 20.5	+02 16 09".0	.6f	.2n	N	19.1	[1.91]	9,27,22	326	63	3C287.1, 4C+02.36; z=.2156.
1349-01	13 49 49.0	-01 41.7	.4f	.3n	g	19.6	0.31		332	57	4C-01.30
1359+025	13 59 59.2	+02 30.2	.2f	.3n	N	19.4	0.57		340	60	4C+02.39
1404-01	14 04 15.2	-01 39.9	.5p	.1s	g	20.2	0.58	7	338	56	4C-01.31; blue galaxy.
1418-025	14 18 38.3	-02 33.8	.7f	.2n	g	18.1	0.25		342	53	4C-02.60
1425-01	14 25 54.7	-01 10.6	1.7f	.1s	N	17.3	1.64	8	346	53	3C300.1, 4C-01.34; jet in p.a. ~260
1431+018	14 31 36.4	+01 50.1	1.8p	.1s	E	17.4	0.32		351	55	
1435+038	14 35 51.5	+03 53.1	.9f	0.0	g	17.8	0.35		355	55	
1442-029	14 42 20.2	-02 59.2	.4p	.1n	E	17.6	0.27		349	49	
1446+00	14 46 07.4	+00 30.8	1.4p	.3s	E	19.4	1.04	9	354	51	4C+00.52; fainter galaxy closer to radio position.
1514+00	15 14 05.3	+00 26.0	2.3f	.3s	E3	15.9	[1.83]	7,26	1	46	4C+00.56; z=.053. Complex source; QSO 0.7 nf.
1542+02	15 43 03.7	+01 59.2	1.4p	0.0	E	18.5	0.51	3	9	41	4C+01.45

TABLE AIII.2 CONCLUDED

(1) Source	(2) Optical Coordinates (1950.0) r.a.	(3) dec.		(4) Δα	(5) Δδ	(6) Type	(7) m_{pg}	(8) S_{2700} (f.u.)	(9) Reference	(10) l^{II}	(11) b^{II}	(12) Comments
1559+02	$15^h59^m55^s.67$	+02° 06'	12".3			D	$16^m.5$	[5.04]	1,10,15	13	38	3C327, 4C+02.41; z=.1041.
1601-00	16 01 19.1	-00 21.7		0".7p	0'.3s	N	17.5	0.45		11	37	4C-00.63
1601-017	16 01 44.6	-01 47.1		1.1p	.1s	E	19.1	0.31		9	35	
1603+00	16 03 39.02	+00 08	29.3			E4	16.3	1.50	30,2	1	26	4C+00.58
1616-029	16 16 31.4	-02 57.2		1.3p	.2s	E	16.6	0.40		10	32	
1636-03	16 36 18.5	-03 07.6		1.5p	.1s	g	19.9	0.45	16	13	27	4C-03.61
1643+022	16 43 11.4	+02 17.2		1.4p	.1n	E	18.0	1.16		20	29	4C+02.42; $18^m.7$ galaxy 30" p.
1650+024	16 50 27.7	+02 29.1		1.8f	.5n	g	-	0.30	28	21	27	4C+02.44; NGC6240 Peculiar galaxy z=.0261
1708+00	17 08 01.5	+00 40.2		1.4p	.1n	db	21.0	0.83	3	21	23	4C+00.65
1717-00	17 17 53.29	-00 55	49.5	2.4f	0.0	D	16.6	[33.8]	17,10,15	23	21	3C353, 4C-00.67; z=.0307.
1949+02	19 49 44.57	+02 22	37.1			BO	16.4	[3.68]	31,27,24	42	-12	3C403, 4C+02.50; z=.0590.
1949-01	19 49 55.20	-01 25	07.2			E	17.5(?)	[0.79]	4,27	38	-14	3C403.1, 4C-01.51
2123+00	21 23 13.1	+00 43.1		1.8p	.2n	db	17.5+18.3	0.38	9	54	-33	4C+00.79
2150-031	21 50 01.4	-03 08.8		.1f	.2n	g	19.6	0.30		55	-41	4C-03.75
2217-011	22 17 11.4	-01 05.8		.9p	.3s	g	20.2	0.28		62	-45	
2221-02	22 21 14.76	-02 21	26.1	.7f	.4s	N	17.5	[3.46]	14,15	62	-47	3C445, 4C-02.83; z=.0568
2243-03	22 43 37.1	-03 16.6		1.1p	.2n	g	21.0	0.65	6	66	-52	4C-03.81; blue galaxy.
2313+01	23 13 43.2	+01 12.6		.7f	0.0	g	19.4	0.58	16	80	-53	4C+01.74
2313+03	23 14 02.30	+03 48	56.0			N	18.7	2.38	12,27,25	83	-51	3C459, 4C+03.57; z=.2205.
2324-02	23 24 19.40	-02 18	43.7			E	18.0	[1.56]	4,2	80	-57	
2338-002	23 38 26.2	-00 11.8		.2p	.5s	db	17.2	0.38		87	-58	4C-00.83
2338+000	23 38 32.7	+00 01.9		2.0f	.2n	E	19.1	0.36		88	-58	
2338+03	23 38 57.0	+03 00.8		.7p	.2n	g	20.2	0.38		91	-55	4C+03.60
2349-01	23 49 22.30	-01 25	54.2			N	17.1	1.01	4,2,26	91	-60	4C-01.61; z=.174.

References for Tables AIII.1 and AIII.2

(1) Bolton J.G. (1960) - Report at XIII General Assembly of URSI, London. Also Obs. Cal. Tech. Radio Obs. 5, 1960

(2) Bolton, J.G. (1968) - Pub. astr. Soc. Pacific 80, 5

(3) Bolton, J.G., and Ekers, Jennifer A. (1966) - Aust. J. Phys. 19, 471

(4) Bolton, J.G., and Ekers, Jennifer A. (1966) - Aust. J. Phys. 19, 559

(5) Bolton, J.G., and Ekers, Jennifer A. (1966) - Aust. J. Phys. 19, 713

(6) Bolton, J.G., and Ekers, Jennifer A. (1967) - Aust. J. Phys. 20, 109

(7) Bolton, J.G., Shimmins, A.J., and Merkelijn, Jeannette K. (1968) - Aust. J. Phys. 21, 81

(8) Burbidge, E.M. (1967) - Astrophys. J. 149, L51

(9) Clarke, Margaret E., Bolton, J.G., and Shimmins, A.J. (1966) - Aust. J. Phys. 19, 375

(10) Griffin, Roger F. (1963) - Astron. J. 68, 421

(11) Humason, M.L., Mayall, N.U., and Sandage, A.R. (1956) - Astron. J. 61, 97

(12) Longair, M.S. (1965) - Mon. Not. R. astr. Soc. 129, 419

(13) Maltby, P., Matthews, T.A., and Moffet, A.T. (1963) - Astrophys. J. 137, 153

(14) Matthews, T.A., reported by Schmidt, Maarten (1965) - Astrophys. J. 141, 1

(15) Matthews, Thomas A., Morgan, William W., Schmidt, Maarten (1964) - Astrophys. J. 140, 35

(16) Merkelijn, Jeannette K. (1969) - Aust. J. Phys. 22, 237

(17) Mills, B.Y. (1960) - Aust. J. Phys. 13, 550

(18) Mills, B.Y., Slee, O.B., and Hill, E.R. (1958) - Aust. J. Phys. 11, 360

(19) Minkowski, R. (1958) - Pub. astr. Soc. Pacific 70, 143

(20) Moffet, A.T., reported by Schmidt, Maarten (1965) - Astrophys. J. 141, 1

(21) Moffet, A.T., Schmidt, M., Slater, C.H., and Thompson, A.R. (1967) - Astrophys. J. 148, 283

(22) Sandage, Allan (1966) - Astrophys. J. 145, 1

(23) Sandage, Allan (1967) - Astrophys. J. 150, L145

(24) Sandage, Allan, reported by Petrosian, Vahé (1969) - Astrophys. J. 155, 1029

(25) Schmidt, Maarten (1965) - Astrophys. J. 141, 1

(26) Searle, Leonard, and Bolton, J.G. (1968) - Astrophys. J. 154, L101

(27) Véron, P. (1966) - Astrophys. J. 144, 861

(28) Whiteoak, J.B. (1969) - personal communication to J.V. Wall

(29) Wills, D. (1967) - Astrophys. J. 148, L57

(30) Wyndham, J.D. (1965) - Astron. J. 70, 384

(31) Wyndham, J.D. (1966) - Astrophys. J. 144, 459

AIII.2 QSO Identifications

The QSO or possible QSO identifications in the selected regions and in the $\pm 4^{\circ}$ zone (see §3.2) are listed in Tables AIII.3 and AIII.4. The content of each column is as follows:

(1) Parkes source number.

(2), (3) The optical coordinates (epoch 1950.0) of the identification as estimated from the Palomar Sky Survey prints with the aid of the transparent overlay (§3.2(ii)). Standard error in these estimates is 6 arc seconds. For well known QSO's with accurately measured optical positions, the precise coordinates are given in these columns and were used in pointing calibration (§2.4).

(4), (5) The displacements in right ascension and declination of the measured position of the radio source from the estimated optical position. The symbols used are n - north, s - south, p - preceding, and f - following. Displacements are not entered for those sources used as position calibrators.

(6) The visual magnitude as estimated from the Palomar Sky Survey prints, or the photoelectric V magnitude where available from the literature. The latter is given to a tenth of a magnitude and the former to half a magnitude.

(7) The 2700 MHz flux density (§2.7); round brackets indicate that the source is variable or possibly variable at this frequency.

(8) The spectral index in the vicinity of 2700 MHz. For many QSO's in the present list, the spectral index is a function of frequency. A source whose spectrum deviates markedly from power law has a brief description of the form of the spectrum in column 13. Inverted spectrum indicates that the maximum flux density occurs at a frequency of 2700 MHz or higher. HF (high frequency) enhancement indicates that the spectrum flattens towards the high frequencies, and LF (low frequency) cut-off indicates the possibly of synchrotron self-absorption towards the low frequency end of the spectrum.

(9) References to the original identification of a known QSO, and to the accurate measurement of the optical position.

(10) Alternative catalogue numbers.

(11), (12) New galactic coordinates.

(13) Comments. Redshifts are given where available, together with references. UVX and UVX? in this column indicate definite or probable ultraviolet excess as discussed in §3.2(ii). Comments on the form of the radio spectrum are discussed above.

References for Tables AIII.3 and AIII.4 follow Table AIII.4.

TABLE AIII.3

DATA FOR QSO IDENTIFICATIONS IN SELECTED REGIONS, 2700 MHz SURVEY

A. PS 1112

(1) Source	(2) Optical coordinates (1950.0) r.a.	(3) dec.	(4) $\Delta\alpha$	(5) $\Delta\delta$	(6) m_{pg}	(7) S_{2700} (f.u.)	(8) α_{2700}	(9) Ref.	(10) Other Catalogue Number	(11) (12) Galactic coords. l^{II}	b^{II}	(13) Comments
0003-00	$00^h03^m48^s.70$	$-00°21'06".6$			$19^m.5$	2.41	.80	24	3C2	99	-61	z=1.037(20), optical variable (25)
0006+014	00 06 19.0	+01 25 20	2".0p	0'.6n	18.5	.09				101	-59	UVX

B. PS 891

0041+001	00 41 00.0	+00 08 30	1.9p	0.6s	19	.08				118	-62	UVX
0045-000	00 45 46.0	-00 01 06	1.3p	0.2n	19	.11				121	-63	UVX?
0056-00	00 56 31.70	-00 09 16			17.3	(1.80)	.45	5,10	4C-00.6	127	-63	z=0.717 (21)
0057+028	00 57 34.5	+02 49 00	0.1p	0.6s	19.5	.06				127	-60	UVX,optical variable
0103-021	01 03 48.6	-02 11 48	-	-	19	.42	.50			131	-64	UVX

C. PS 1114

0222+000	02 22 34.3	+00 03 24	0.5f	0.1n	19	0.14				166	-55	UVX
0223+012	02 23 34.0	+01 16 06	0.5f	-	19	0.24				165	-53	UVX
0225-014	02 25 35.0	-01 29 06	0.5p	-	18	0.30	0.8		4C-01.11	168	-55	z=0.685 (9)
0231+022	02 31 14.6	+02 16 18	1.3p	0.5s	17.5	0.07				171	-54	UVX
0232-02	02 32 59.9	-02 32 24	-	-	18	0.58	0.85		4C-02.12	172	-55	UVX
0237-027	02 37 14.2	-02 47 12	1.0f	-	18.5	0.41	-.70			174	-54	UVX, inverted spectrum, optical variable ?
0240-021	02 40 15.0	-02 10 24	-	0.2n	19.5	0.12				174	-53	UVX?, object 4[e] f has UVX

D. PS 1777

1158+007	11 58 49.7	+00 45 10	0.4f	0.3s	18.5	0.26				276	61	UVX
1159-036	11 59 38.4	-03 37 50	1.1	0.3n	19.5	0.12				280	57	UVX
1201-026	12 01 08.6	-02 37 55	0.9f	0.3s	19	0.15			4C-02.51	280	58	Optical variable
1203+011	12 03 15.3	+01 10 27	0.9p	0.4n	18	0.13				278	61	UVX
1211+003	12 11 22.9	+00 22 29	1.2p	0.5s	20	0.10				283	61	UVX
1216-010	12 16 01.0	-01 03 28	1.3f	0.3n	19.5	0.21				286	60	UVX?
1217+02	12 17 38.35	+02 20 20.9	1.3f	-	16.5	0.47	-.05	3		284	65	z=0.240 (22),HF enhancement

E. PS 1778

1328-034	13 28 54.0	-03 25 54	2.5p	0.2n	19	0.26				321	58	UVX
1331+004	13 31 07.7	+00 25 42	0.9f	-	20	0.14				325	60	UVX
1331+025	13 31 17.3	+02 34 06	0.9p	0.2n	18.5	0.14				326	63	UVX
1335+023	13 35 06.9	+02 22 17	0.4f	0.2s	17.5	0.10				329	63	z=0.61 (9)
1336-000	13 37 00.3	-00 00 54	0.5p	0.3s	19	0.11				328	60	UVX
1337-013	13 37 30.4	-01 22 36	0.3p	0.3n	18.5	0.19				327	59	z=1.607 (23)
1343+011	13 43 48.0	+01 09 13	0.2p	1.0n	20	0.10				332	61	Below limit of 2 colour plate
1352+00	13 52 34.7	+00 55 13	0.6f	0.3n	19	0.35	1.15	23		336	60	UVX?, inverted spectrum

TABLE AIII.3 Concluded

(1) Source	(2) Optical coordinates (1950.0) r.a.	(3) dec.	(4) $\Delta\alpha$	(5) $\Delta\delta$	(6) m_{pg}	(7) S_{2700} (f.u.)	(8) α_{2700}	(9) Ref.	(10) Other Catalogue Number	(11) (12) Galactic coords. l^{II}	b^{II}	(13) Comments
						F. PS 896						
2153-204	$21^h53^m47^s.1$	$-20^o26'50''$	1s5f	0.2n	17m	0.22		26		33	-50	z=1.31 (27)
2156-183	21 56 31.6	-18 21 53	3.0f	0.3s	19.5	0.09				36	-49	UVX
2157-200	21 57 21.7	-20 00 15	0.1f	0.1s	19.5	0.13				34	-50	UVX,optical variable
2159-215	21 59 05.7	-21 32 41	2.0p	0.4n	19	0.13				32	-51	UVX, finding chart from red print
2203-18	22 03 25.8	-18 50 16			19.5	5.20	0.40	5,19	MSH22-11	36	-51	UVX?

TABLE AIII.4

DATA FOR QSO IDENTIFICATIONS IN ± 4° DECLINATION ZONE, 2700 MHz SURVEY

(1) Source	(2) Optical coordinates (1950.0) r.a.	(3) dec.	(4) $\Delta\alpha$	(5) $\Delta\delta$	(6) m_{pg}	(7) S_{2700} (f.u.)	(8) α_{2700}	(9) Ref.	(10) Other Catalogue Number	(11) (12) Galactic coords. l^{II}	b^{II}	(13) Comments
0003-00	$00^h03^m48^s.70$	$-00°21'06".6$			19.5	2.41	.80	24	3C2	99	-61	z=1.037 (20), optical variable (25)
0038-020	00 38 23.8	-02 02 54	-	0.2n	18	0.61	-.40			117	-64	z=1.176 (1), inverted spectrum
0056-00	00 56 31.70	-00 09 16			17.3	(1.80)	.45	5,10	4C-00.6	127	-63	z=0.717 (21)
0103-021	01 03 48.6	-02 11 48	-	-	19	.42	.50			131	-64	UVX
0106+01	01 06 04.39	+01 19 01.9			18.4	(1.88)	-.65	3,2	4C+01.2	132	-61	z=2.107(13), HF enhancement
0112-017	01 12 43.5	-01 43 01	0.9f	0.1n	18	1.38	-.25			136	-64	UVX, HF enhancement
0115+02	01 15 42.8	+02 42 35	0.2f	0.5s	17.5	0.88	.85	11	4C+02.4	136	-59	z=0.673 (27)
0118+03	01 18 26.15	+03 28 29.3			18	0.51	1.20	15,2	4C+03.2	137	-58	z=0.765 (1)
0122-00	01 22 55.5	-00 21 34			17	1.43	.25	5,10		140	-62	z=1.070 (21), HF enhancement,LF cut-off
0137+012	01 37 22.8	+01 16 29	0.2f	0.1n	17.5	1.07	.50		4C+01.4	147	-59	UVX
0158+031	01 58 05.0	+03 08 14	-	-	19	0.28				154	-55	UVX
0215+015	02 15 13.4	+01 30 56	0.6f	-	18.5	0.36	.23	12		162	-54	Optical variable (12), LF cut-off
0225-014	02 25 35.0	-01 29 07	0.5p	-	18	0.30	0.8	9	4C-01.11	168	-55	z=0.685 (9)
0226-038	02 26 22.5	-03 50 58	0.7f	0.1s	17.5	0.66	0.30		4C-03.7	172	-57	z=0.695,(1),HF enhancement
0232-02	02 32 59.9	-02 32 23	-	-	19	0.58	0.85	23	4C-02.12	172	-55	UVX
0237-027	02 37 14.2	-02 47 34	0.3f	0.4n	19.5	0.41	-.70			174	-54	UVX, inverted spectrum
0253-031	02 53 20.0	-03 11 37	0.2f	-	19	0.29	1.15		4C-03.10	179	-52	
0256-005	02 56 54.8	-00 31 52	0.4p	-	17.5	0.31	0.55			177	-49	UVX
0300-00	03 00 39.5	00 26 38	1.3p	-	18.5	0.67	0.95		4C-00.14	178	-48	UVX?, galaxy previously suggested (7)
0312-03	03 12 51.9	-03 27 51	0.2f	0.1n	18.5	0.68	1.10		4C-03.11	184	-48	UVX
0317-02	03 17 56.5	-02 19 24	0.6f	0.3n	19.5	0.36	0.45		4C-02.15	184	-46	UVX, HF enhancement
0336-01	03 36 59.2	-01 56 19			18.4	(2.23)	-.10	5,19	CTA26	188	-42	z=0.852 (1), optical variable (19),LF cut-off
0351-032	03 51 43.3	-03 16 43	0.4f	0.1s	19.5	0.46	1.15		4C-03.14	192	-40	
0420+022	04 20 16.8	+02 12 24	0.2p	0.1n	19.5	0.34	-.40			191	-31	UVX, inverted spectrum
0420-01	04 20 43.1	-01 27 29			18	(1.92)	-.10	6,18		195	-33	z=0.915 (1), HF enhancement
0421+019	04 21 33.0	+01 57 33	1.0f	0.1n	17.5	0.76	0.20		OF036	192	-31	z=0.689 (1), LF cut-off
0440-00	04 40 05.4	-00 23 22			19.2	(3.53)	0.10	6,18	NRAO190	197	-29	UVX, inverted spectrum
0442-00	04 43 01.4	-00 24 53	0.2p	0.3n	20	0.27	0.4		DA146	198	-28	UVX
0445-019	04 45 11.2	-01 58 02	0.2f	-	19	0.20				200	-28	UVX
0447-010	04 47 10.1	-01 02 32	-	0.1n	19.5	0.29	0.50			199	-27	UVX
0454+039	04 54 08.8	+03 56 13	1.6f	0.2n	16.5	0.40	0.15		OF092	195	-23	
0457+024	04 57 16.5	+02 25 02	0.9p	-	19	1.63	0.20		OF097	197	-23	UVX?,inverted spectrum
0505+03	05 04 59.1	+03 04 00	0.6f	0.1s	19	0.74	0.50	23	4C+03.10	198	-21	UVX?,galaxy previously suggested (15)

TABLE AIII.4 Cont'd.

(1) Source	(2) Optical coordinates (1950.0) r.a.	(3) dec.	(4) $\Delta\alpha$	(5) $\Delta\delta$	(6) m_{pg}	(7) S_{2700} (f.u.)	(8) α_{2700}	(9) Ref.	(10) Other Catalogue Number	(11) (12) Galactic coords. l^{II}	b^{II}	(13) Comments
0736-01	$07^h36^m02^s6$	$-01^o57'30''$	0.9p	0.2n	18^m	0.64	0.8		4C-01.18	217	10	UVX
0736+01	07 36 42.4	+01 43 57			18	(2.42)	0.10	4,8	OI061	217	11	z=0.191 (21), LF cut-off
0743-006	07 43 21.0	-00 36 57	0.2p	0.1	18	1.40	-.40		4C-00.287	220	12	UVX?,inverted spectrum
0808+019	08 08 51.1	+01 55 47	0.1p	-	18	(0.71)	-.40		OJO14	221	19	UVX?,inverted spectrum
0812+02	08 12 47.20	+02 04 11			18.5	1.18	0.70	15,10	4C+02.23	222	19	z=0.406 (20)
0828-03	08 28 15.2	-03 30 40	1.1p	0.1n	18.5	0.53	0.85		4C-03.32	228	20	UVX
0837+035	08 37 12.6	+03 30 31	0.2f	0.2s	20	0.69	0.25		OJO63	223	25	LF cut-off
0837+012	08 37 14.3	+01 15 08	0.1p	0.3n	19	0.25	-.05		OJO62	225	24	UVX
0853+03	08 53 01.3	+03 23 52	0.6p	0.1s	17.5	0.35	1.00	23		225	29	LF cut-off
0906+01	09 06 35.3	+01 33 40	0.7f	0.1n	17.5	1.20	0.25	11	4C+01.24	229	31	UVX
0907-023	09 07 13.6	-02 19 10	0.2f	0.4s	18	0.57	0.50			233	29	UVX
0912+029	09 12 01.4	+02 58 37	0.4f	0.1n	18.5	0.54	0.25		OKO20	228	33	LF cut-off
0913-025	09 13 48.5	-02 32 02	-	0.4n	18.5	0.28	0.9		4C-02.38	234	30	UVX
0922+005	09 22 34.1	+00 32 09	0.3f	0.1s	18	0.74	0.05	9	OKO37	232	34	z=1.72 (9), inverted spectrum
0932+02	09 32 42.9	+02 17 35	0.8p	0.3s	17.4	0.53	0.85	9	4C+02.27	232	37	z=0.659 (9)
0950+00	09 50 12.0	+00 14 30	1.3f	-	20	0.43	1.50	12		238	39	UVX, optical variable (12)
0957+00	09 57 43.84	+00 19 50.0			17.6	0.51	0.75	3	4C+00.34	239	41	z=0.907 (22)
1004-018	10 04 31.6	-01 52 37	0.7f	0.1s	19	0.56	-.10			243	41	UVX, LF cut-off
1008+013	10 08 41.5	+01 21 35	0.2f	0.1n	19	0.24	0.70		OLO14	240	44	UVX
1012+022	10 12 41.6	+02 13 50	0.7p	0.2n	18	0.40	0.40		4C+02.30	240	45	UVX
1021+028	10 21 18.0	+02 48 18	0.7f	0.1n	19	0.22				242	47	LF cut-off
1021-00	10 21 57.0	-00 37 36	1.2p	-	18.5	0.95	0.30	7		245	45	UVX?,inverted spectrum
1052-004	10 52 23.3	-00 29 54	0.4p	0.2n	18	0.34	0.95		4C-00.41	253	50	
1055+01	10 55 55.5	+01 50 03			18.3	(3.02)	0.00	15,10	4C+01.28	251	53	UVX, HF enhancement
1103-006	11 03 58.0	-00 36 40	0.7f	0.1n	16.5	0.68	0.70		4C-00.43	257	52	UVX
1105-028	11 05 03.9	-02 51 55	0.4f	-	19.5	0.36	1.05		4C-02.45	259	51	
1106-003	11 06 18.3	-00 22 23	0.9p	0.1s	19.5	0.26	0.8			257	53	
1111-037	11 11 58.0	-03 44 47	0.5f	0.2n	18.5	0.35	0.7		4C-03.41	262	51	18^m galaxy also near position
1130+009	11 30 46.6	+00 57 25	0.7f	-	19	0.32	0.50			264	57	LF cut-off
1146-037	11 46 22.5	-03 47 29	1.4f	-	17	0.40	0.35			274	55	
1148-00	11 48 10.23	-00 07 13.1			17.6	2.56	0.40	6,2	4C-00.47	272	59	z=1.982 (14), inverted spectrum
1217+02	12 17 38.35	+02 20 20.9	1.3f	-	16.5	0.47	-.05	3		284	65	z=0.240 (22), HF enhancement
1218-02	12 18 51.0	-02 25 12	0.5f	0.4s	20	0.54	0.20	12	4C-02.53	288	59	UVX, optical variable (12), HF enhancement
1222+037	12 22 19.0	+03 47 24	0.2f	0.1n	19	0.81	-0.10		4C+03.23	287	65	HF enhancement
1225-02	12 25 22.7	-02 20 30	1.8f	0.2n	19.5	0.40	0.80		4C-02.54	291	59	UVX
1226+02	12 26 33.3	+02 19 44			12.8	(43.4)	0.05	16,17	3C273	289	65	z=0.158 (26), optical variable (29)
1229-02	12 29 25.9	-02 07 31			16.8	1.33	0.45	6,8	4C-02.55	293	60	z=0.388 (20), HF enhancement
1302-035	13 02 08.9	-03 29 56	-	0.2s	19.5	0.53	0.60			309	59	
1317-00	13 17 04.5	-00 34 18	0.4p	0.1n	17.3	0.97	0.55	9	4C-00.50	318	61	z=0.89 (9)
1352+00	13 52 34.7	+00 55 13	0.6f	0.3n	19	0.35	1.15	23		336	60	UVX?,inverted spectrum
1356+022	13 56 55.1	+02 14 17	-	0.2s	18.5	0.66	0.45			339	60	Inverted spectrum

TABLE AIII.4 Concluded

(1) Source	(2) Optical coordinates (1950.0) r.a.	(3) dec.	(4) $\Delta\alpha$	(5) $\Delta\delta$	(6) m_{pg}	(7) S_{2700} (f.u.)	(8) α_{2700}	(9) Ref.	(10) Other Catalogue Number	(11) (12) Galactic coords. l^{II}	b^{II}	(13) Comments
1359+039	$13^h59^m54^s.2$	$+03^o57'13''$	1".3p	0'.2s	19^m	0.33	0.3			341	60	
1402-012	14 02 11.5	-01 16 13	0.2f	0.1n	18.5	0.71	-.25			338	57	Inverted spectrum
1407+022	14 07 32.5	+02 17 16	0.1f	-	19	0.49	0.10			343	59	
1424+03	14 25 02.1	+03 29 27	0.8f	0.3s	19	0.33	0.9		4C+03.29	351	57	
1449-012	14 49 12.1	-01 15 15	0.4f	0.1s	18	0.35	0.30			354	50	
1454-034	14 54 32.8	-03 27 48	1.1n	-	19	0.29	0.9		4C-03.53	352	47	Brighter object with jet 0!5 nf is within error of radio position
1502+036	15 02 35.9	+03 38 04	0.1p	0.3n	19	0.48	-.40			2	50	Inverted Spectrum
1514+00	15 14 06.0	+00 25 51	1.6f	0.2s	18.8	|1.83|	0.50	11,26	4C+00.56	2	46	Part of flux due to nearby galaxy
1543+005	15 43 38.1	+00 35 37	0.9p	0.1s	19	1.30	0.55		DW1543+00	8	40	LF cut-off
1546+027	15 46 58.4	+02 46 07	1.2p	0.2s	18	(1.27)	-.35			11	41	Inverted spectrum
1602-00.2	16 02 22.0	-00 11 02	2.0f	0.5s	18	(0.53)	.40	23	DA397	10	36	HF enhancement
1611-007	16 11 53.5	-00 47 58	0.4p	0.1n	18.5	0.27	0.9		4C-00.64	11	34	
1615+029	16 15 18.8	+02 53 58	0.4p	0.1n	18	0.74	0.15			16	35	
1618+007	16 18 15.3	+00 43 55	0.4f	-	18.5	0.21				14	33	
1729+010	17 29 48.8	+01 01 45	0.4p	0.3n	19	0.20	1.0		4C+01.52	24	18	
1942+038	19 42 06.0	+03 49 30	1.2f	0.1n	17.5	0.50	0.80		4C+03.46	43	-10	
1952+007	19 52 49.8	+00 42 04	0.4f	0.1n	18.5	0.34	0.80		4C+00.74	41	-14	UVX?
1953+035	19 53 03.7	+03 36 04	4.4f	0.3s	18	0.29	1.15		4C+03.47	43	-12	
2059+034	20 59 08.8	+03 29 49	-	-	18	0.59	-.35			53	-27	UVX, inverted spectrum
2110-017	21 10 12.2	-01 46 28	0.9f	0.1n	19.5	0.31	0.8		4C-01.55	49	-32	UVX
2131-021	21 31 35.3	-02 06 36	1.8p	-	19	1.91	-.10		4C-02.81	52	-36	UVX, HF enhancement
2134+004	21 34 05.3	+00 28 24	1.1p	0.1s	17	7.59	-1.00	27	DA553	55	-35	z=1.94 (28),inverted spectrum
2216-03	22 16 16.3	-03 50 43			16.4	1.04	-.30	5,10	4C-03.79	59	-47	z=0.901 (21),HF enhancement
2254+024	22 54 44.6	+02 27 12	0.7p	-	18	0.46	-.20	9	OY091.3	76	-49	z=2.09 (9),inverted spectrum
2318+02	23 18 15.0	+02 39 54	1.7p	0.7n	19	0.38	1.05	15	4C+02.58	83	-53	UVX
2320-021	23 20 30.5	-02 07 09	0.4p	0.2n	19.5	0.33	0.05			79	-57	UVX
2332-017	23 32 46.3	-01 47 47	1.1p	-	18.5	0.64	0.40			84	-58	UVX
2335-027	23 35 23.3	-02 47 39	0.6p	0.1n	19	0.60	-0.15			84	-60	UVX, HF enhancement
2340-036	23 40 22.5	-03 40 20	0.2p	0.5n	17	0.28	0.7			85	-61	UVX

References for Tables AIII.3 and AIII.4

(1) This paper

(2) Bolton, J.G. (1968) - Pub. astr. Soc. Pacific 80, 5

(3) Bolton, J.G., Clarke, Margaret E., Sandage, Allan, and Véron, P. (1965) - Astrophys. J. 142, 1289

(4) Bolton, J.G., and Ekers, Jennifer A. (1966) - Aust. J. Phys. 19, 471

(5) Bolton, J.G., and Ekers, Jennifer A. (1966) - Aust. J. Phys. 19, 559

(6) Bolton, J.G., and Ekers, Jennifer A. (1966) - Aust. J. Phys. 19, 713

(7) Bolton, J.G., and Ekers, Jennifer A. (1967) - Aust. J. Phys. 20, 109

(8) Bolton, J.G., and Kinman, T.D. (1966) - Astrophys. J. 145, 951

(9) Bolton, J.G., Kinman, T.D., and Wall, J.V. (1968) - Astrophys. J. 154, L105

(10) Bolton, J.G., Shimmins, A.J., Ekers, Jennifer A., Kinman, T.D., Lamla, E., and Wirtanen, C.A. (1966) - Astrophys. J. 144, 1229

(11) Bolton, J.G., Shimmins, A.J., and Merkelijn, Jeannette (1968) - Aust. J. Phys. 21, 81

(12) Bolton, J.G., and Wall, J.V. (1969) - Astrophys. Lett. 3, 177

(13) Burbidge, E. Margaret (1966) - Astrophys. J. 143, 612

(14) Burbidge, E. Margaret, and Kinman, T.D. (1966) - Astrophys. J. 145, 654

(15) Clarke, Margaret E., Bolton, J.G., and Shimmins, A.J. (1966) - Aust. J. Phys. 19, 375

(16) Hazard, C., Mackey, M.B., and Shimmins, A.J. (1963) - Nature 197, 1037

(17) Jefferys, W.H. III (1964) - Astron. J. 69, 255

(18) Kinman, T.D. - personal communication to J.G. Bolton

(19) Kinman, T.D., Bolton, J.G., Clarke, R.W., and Sandage, A.R. (1967) - Astrophys. J. 147, 848

(20) Kinman, T.D., and Burbidge, E. Margaret (1967) - Astrophys. J. 148, L59

(21) Lynds, C.R. (1967) - Astrophys. J. 147, 837

(22) Lynds, C.R., Hill, S.J., Heere, Karen, and Stockton, A.N. (1966) - Astrophys. J. 144, 1244

(23) Lynds, C.R. - personal communication to J.G. Bolton

(24) Merkelijn, Jeannette K. (1969) - Aust. J. Phys. 22, 237

(25) Sandage, Allan, Véron, Philippe, and Wyndham, John D. (1965) - Astrophys. J. 142, 1307

(26) Schmidt, M. (1963) - Nature 197, 1040

(27) Searle, Leonard, and Bolton, J.G. (1968) - Astrophys. J. 154, L101

(28) Shimmins, A.J., Searle, L., Andrew, B.H., and Brandie, G.W. (1968) - Astrophys. Lett. 1, 167

(29) Smith, Harlan J., and Hoffleit, Dorrit (1963) - Nature 198, 650

APPENDIX IV

SPECTRAL DATA FOR SOURCES CATALOGUED AT 2700 MHZ

The spectral data obtained for sources catalogued in Tables AII.1 and AII.2 is presented in Table AIV.1. The contents of the columns are as follows:

(1) Parkes source numbers.

(2) Flux densities at 178 MHz from Mullard Observatory, University of Cambridge (§4.7).

(3) Flux densities at 408 MHz from the Molonglo Cross, University of Sydney (§4.6).

(4) Flux densities at 468 MHz from the Parkes interferometer (§4.3).

(5) Flux densities at 635 MHz from the Parkes telescope (§4.5).

(6) Flux densities at frequencies between 1400 and 1425 MHz (§4.3, §4.4).

(7) Flux densities at 2700 MHz (§2.7, §4.2).

(8) Flux densities at 5009 MHz (§4.1). Letters (a) through (f) refer to the observing sessions of Table 4.2.

(9), (10), (11) The spectral indices obtained as described in §5.1. Column 9 contains the index α from fitting a power law to the spectrum over the range 178 to 5009 MHz. Columns 10 and 11 contain α_{LF} and α_{HF}, the indices in the ranges 178 to 1403 MHz and 1403 to 5009 MHz respectively. Entries in 9, 10, and 11 have been made only when examination of the spectral

data indicated them to have some significance.

(12) The optical identifications.

(13) References to footnotes.

The flux densities in columns 2 to 8 are followed by the standard errors, and both are in flux units. Bracketed numbers following the errors indicate the references for the flux densities obtained by other observers. These references follow Table AIV.1.

Flux densities in square brackets have been corrected for partial resolution. Those in round brackets are believed to vary, and the best estimate for epoch 1968.5 has been entered.

TABLE AIV.1 SPECTRAL DATA FOR SOURCES IN THE SELECTED REGIONS AND THE ±4° DECLINATION ZONE, PARKES 2700 MHZ CATALOGUE

(1) Source	(2) S_{178}	(3) S_{408}	(4) S_{468}	(5) S_{635}	(6) S_{1400}	(7) S_{2700}	(8) S_{5009}	(9) $\propto$	(10) $\propto_{LF}$	(11) $\propto_{HF}$	(12) Identification	(13) Footnotes
0000+035				0.6 0.3	0.51 0.15 (9)	.146 .012		1.28		1.89		
0003-00	16.5 1.6 (2)		7.5 0.4 (8)	6.3 0.6 (8)	3.36 0.17	2.41 .04	1.40 .03 a	.71	.75	.78	QSO	
0005+021					.25 .15 (9)	.117 .012				1.13		
0007+016					.37 .15 (9)	.160 .013				1.29	g	
0010+00	7.6 0.8 (1)	4.0 0.4 (6)	4.1 0.4	3.1 0.4	1.53 0.15	.92 .02	0.50 .02 a	.82	.77	.94		
0013-00	0.8 0.4 (4)		1.0 0.4	0.9 0.3	0.91 0.12	.89 .02	0.79 .02 a,c	.15	-.02	.17		
0017-028	4.3 1.1 (3)			1.1 0.4		.25 .01		1.04	1.07			
0018-01	3.6 0.9 (3)			1.5 0.2		.64 .03	0.30 .01 a	.85	.68	1.22		
0019-00	2.4 0.8 (3)		3.1 0.4	3.1 0.4	2.88 0.22	1.90 .04	1.07 .03 a		.07	.86		
0025-007	3.4 1.0 (3)		2.3 0.4	1.7 0.3		[.63] .03	[0.34] .01 a	.80	.53	.99		
0026-014				<0.6		.29 .01	0.26 .01 c			.17		2
0029-01	3.7 0.9 (3)		1.1 0.6	1.7 0.4	0.81 0.11	.52 .02	0.31 .01 a	.77	.73	.80	g	
0029+01	1.6 0.6 (4)			1.3 0.3	0.56 0.10	.32 .01		.76	.59	.85		
0031+01	4.7 1.0 (3)		1.5 0.6	2.2 0.3	0.55 0.10	.37 .01	0.18 .01 c	1.06	1.00	1.09		
0033-000	4.3 0.9 (3)			1.5 0.3		.28 .01		1.04	.82			
0034-01	16.0 1.6 (2)	8.6 0.4 (6)	8.7 0.8 (8)	7.0 0.2 (8)	4.00 0.14 (8)	[2.56] .05	[1.56] .04 a	.69	.60	.75	E0	
0035-02	23.0 2.3 (2)	14.7 0.8 (6)	14.0 0.4 (8)	11.4 0.2 (8)	6.21 0.13 (8)	4.04 .08	2.59 .06 a	.70	.58	.68	E	
0036+03	4.6 0.5 (1)		3.6 0.4	3.0 0.4	1.81 0.13	[1.10] .04	[0.62] .02 a	.68	.47	.87	E2	
0037-009				<0.7		.26 .01	0.18 .01 c			.59		2
0038-020						.61 .03	0.78 .02 a,c			-.39	QSO	1
0038-019						.65 .02	0.25 .01 b			1.54	S	1
0040+031					0.24 0.15 (9)	.146 .012				.72		
0041+007				0.8 0.4	0.52 0.15 (9)	.212 .013		1.10		1.40		
0041-000	2.5 0.8 (3)					.075 .011		1.26				
0043+000	3.0 0.9 (3)			0.8 0.4		.27 .01		.87	1.03		E	
0047+023				<0.8	0.34 0.15 (9)	.32 .02				.09		
0047-02	7.2 0.8 (3)	3.5 0.4 (6)	3.5 0.4	2.6 0.4	1.22 0.11	.68 .08	0.32 .01 b	.96	.79	1.07		
0051-03	10.6 1.6 (3)	5.6 0.4 (6)	5.1 0.8 (8)	4.5 0.1 (8)	2.15 0.08 (8)	1.11 .03	0.57 .02 b	.96	.60	1.04	E	
0053-016					1.3 0.3 (11)		[0.35] .01 b			1.03	E	1,3
0053-015					1.3 0.3 (11)		[0.45] .01 b			.83	E	1,3
0055+015A					0.25 0.15 (9)	.158 .012				.69		
0055-01	16.5 1.5 (2)	13.4 0.7 (6)	9.0 1.5	9.8 0.8 (8)	5.28 0.12 (8)	[3.46] .07	[2.58] .05 b	.60	.40	.56	E0	
0056-00	5.7 0.9 (3)	3.4 0.4 (6)	4.0 0.8 (8)	3.2 0.2 (8)	2.51 0.12 (8)	(1.80) .08	(1.37) .02 a,b	.42	.42	.47	QSO	
0059+017	4.1 0.9 (3)		2.6 0.4	1.6 0.4	0.61 0.11	.40 .02	0.17 .01 b	1.05	.97	1.23		

TABLE AIV.1 continued

(1)	(2)	(3)	(4)	(5)	(6)	(7)	(8)	(9) (10) (11)	(12)	(13)
0215+015				<0.5	0.54 0.08	.36 .01	0.32 .01 b	.23	QSO	
0215+02	3.9 0.9 (3)		1.9 0.5	1.4 0.3	0.85 0.10	.41 .01	0.20 .01 c	.97 .73 1.15		
0216+011				<0.5	0.40 0.10	.50 .02	0.64 .01 b	-.39		
0217+01				<0.6	0.47 0.08	.36 .01	0.22 .01 b	.75	E?	
0218-02	16.5 1.6 (2)	11.1 0.6 (6)	9.8 0.8 (8)	7.8 0.1 (8)	3.54 0.07 (8)	1.68 .03	0.80 .02 b	1.05 .64 1.17	E	
0218+007					0.26 0.15 (9)	.186 .013		.48		
0220-029	2.8 0.9 (3)			0.7 0.3		.22 .01		.91 1.08		
0222-00	5.2 0.8 (3)		2.5 0.4	1.3 0.3	1.08 0.10	.67 .02	0.41 .03 b	.73 .75 .76	SO	
0223+018				<0.6	0.45 0.15 (9)	.220 .013		1.10		
0225+003					0.31 0.15 (9)	.141 .012		1.23		
0225-014	2.9 0.7 (3)			0.4 0.3		.30 .02		.81	QSO	
0226-038	3.5 0.9 (3)		1.3 0.5	0.6 0.3	0.74 0.08	.66 .03	0.53 .01 b	.39 .70 .31	QSO	
0230-027				1.5 0.4		.33 .02		1.04		
0230-03	3.5 1.0 (3)			1.2 0.3		.34 .02	0.18 .01 b	.92 .84 1.02		
0230-022	1.2 0.6 (4)			0.9 0.4		.190 .011	0.11 .01 b	.83 .22 .88		
0232-02	3.7 1.1 (3)		2.0 0.8	1.4 0.4	0.90 0.12	.58 .02	0.33 .01 b	.80 .67 .87	QSO	
0235-019	2.3 0.6 (3)			0.5 0.3		.22 .01		.84		
0236+02					0.47 0.15 (9)	.29 .02		.74		
0237-027			<0.6	<0.5	0.37 0.10	.41 .01	0.64 .01 b	-.70	QSO	
0238-018	2.7 0.9 (3)			0.4 0.2		.102 .011		1.18		
0240-00	14.8 1.5 (2)	10.6 0.5 (6)	10.2 0.8 (8)	8.5 0.2 (8)	5.12 0.12 (8)	3.12 .05	1.93 .04 b	.69 .46 .76	Sc	
0240-034	2.4 0.7 (3)			0.5 0.2		.27 .01		.75		
0240+016					0.20 0.15 (9)	.065 .011				
0242+028				0.8 0.3	0.46 0.15 (9)	.28 .02		.72 .73		
0243+009	2.5 0.8 (3)				0.26 0.15 (9)	.164 .012		1.00 .75		
0252+02	3.6 0.9 (3)		3.8 0.5	1.2 0.3	0.89 0.22 (9)	.41 .01	0.21 .01 c	1.06 .46 1.08	N	2
0253-031	4.9 1.2 (3)			0.8 0.4		.29 .01	0.14 .01 c	1.07 1.17	QSO?	2
0256-005				<0.5		.31 .01	0.22 .01 c	.55	QSO	2
0300-00	4.0 1.0 (3)		2.4 0.4	2.2 0.3	0.91 0.12	.67 .03	0.35 .01 a	.83 .78 .93	QSO?	
0303+020	3.2 0.8 (3)			1.1 0.2	0.53 0.15 (9)	.46 .01		.66 .83 .21		
0303+033				0.9 0.3	0.27 0.15 (9)	.26 .01		.80 .05		
0305+03	19.2 1.9 (1)		12.9 1.3 (8)	10.8 0.3 (8)	6.99 0.21 (8)	[5.33] .10	[3.60] .07 a	.51 .45 .54	D	
0310+013	0.8 0.4 (4)			0.9 0.2	0.24 0.15	.25 .01	0.29 .02 c	.25 -.23		2
0312-03	6.9 1.0 (3)	3.3 0.4 (6)		3.0 0.4	1.26 0.15	.68 .03	0.33 .01 a	.96 .80 1.11	QSO	
0313-035				0.9 0.4	0.45 0.10	.23 .01		.97 1.02		
0317-02	2.4 0.6 (3)		1.1 0.4	0.5 0.2	0.45 0.10	.36 .02	0.27 .01 a	.56 .82 .44	QSO	
0320+015			0.7 0.4	<0.5	0.42 0.10	.52 .02	0.41 .01 b	.33 .34		

TABLE AIV.1 continued

(1)	(2)	(3)	(4)	(5)	(6)	(7)	(8)	(9) (10) (11)	(12)	(13)
0322-03	7.7 1.2 (3)		2.7 0.4	2.2 0.3	0.80 0.14	.51 .02	0.26 .01 b	1.01 1.07 1.03		
0325+02	16.5 1.7 (1)		9.5 1.1 (8)	7.9 0.3 (8)	4.66 0.09 (8)	[3.18] .05	[1.93] .03 b	.67 .57 .70	D	
0331-01	20.4 1.5 (2)		9.4 0.6	5.5 0.2 (8)	[3.17] 0.12 (8)	[1.39] .03	[0.72] .01 b	1.02 1.04 1.13	D	
0332-021			2.0 1.0	1.4 0.3	0.91 0.15	.43 .02	0.29 .01 b	.74 .59 .71		
0336-017	2.6 1.0 (4)				0.60 0.20	.58 .02	0.45 .01 b	.42 .71 .40		
0336-01			1.9 0.8 (8)	2.7 0.1 (8)	(1.96) 0.04 (8)	(2.23) .10	(2.28) .04 b	0.00 -.11	QSO	
0351-032	2.7 0.7 (3)		1.5 0.4	0.9 0.3	0.88 0.15	.46 .02	0.22 .01 c	.87 .53 1.16	QSO?	
0353+027	3.6 0.9 (3)		2.4 0.4	0.9 0.3	0.82 0.14	.47 .02	0.21 .01 c	.97 .77 1.22	N	
0354+000				0.9 0.3	0.82 0.21 (9)	.31 .01		.92 1.50	N	
0358+00	11.7 2.3 (1)	6.1 0.4 (6)	3.7 0.4	2.4 0.4	1.85 0.24	1.06 .04	0.53 .01 b	.93 .96 1.08		
0358+031	<1.5 (4)		<0.9	1.3 0.4	<0.3	(.28) .05	(0.25) .01 b			
0358+021	2.5 0.8 (3)			2.1 0.4	0.68 0.11	.37 .02	0.18 .01 c	1.01 .74 1.11		
0359+028				0.7 0.4		.36 .02		.45		
0400-03	4.1 1.0 (3)		2.3 0.4	1.6 0.4	0.79 0.14	.45 .02	0.18 .01 a	1.04 .82 1.37		
0400+032	1.9 0.9 (4)			1.2 0.5	0.47 0.15 (9)	.27 .01		.80 .36 .85		
0402+025				1.1 0.4	0.62 0.10	.33 .01	0.17 .01 c	1.02 .72 1.05		
0404+03	19.2 1.9 (1)		10.9 0.6	8.9 0.3 (8)	[5.41] 0.17 (8)	[3.52] .06	[2.39] .04 a	.63 .60 .63		
0407+012	3.8 0.9 (3)		1.5 0.4	1.1 0.3	0.66 0.13	.36 .02	0.18 .01 a	.92 .84 1.08		
0409-01	12.1 1.5 (2)		4.7 0.4	3.5 0.4	1.91 0.25	.72 .03	0.29 .01 a	1.16 .90 1.47		
0409+025				<0.5		.26 .01				
0410-02	3.9 0.9 (3)		1.7 0.4	1.2 0.4	0.60 0.10	.33 .01		.91 .91 .91		
0416-03	7.6 1.1 (3)		3.6 0.4	2.8 0.4		[.57] .02	[0.30] .01 b	1.01 .78 1.03		
0420+022				<0.4	0.25 0.11	.34 .02	0.44 .02 a	-.41	QSO	
0420-01	1.8 0.8 (4)		2.0 0.4	1.2 0.3	2.24 0.29	(1.92) .10	(2.14) .05 a	-.08 -.17 -.08	QSO	
0421+00	6.7 1.0 (3)			1.8 0.4	1.96 0.26	1.00 .02	0.59 .01 b	.78 .60 .86		
0421+019	<0.7 (4)			0.8 0.3	1.36 0.19	.76 .02	0.70 .02 a	-.66 .21	QSO	
0422+00	1.5 0.7 (4)			1.9 0.4	0.75 0.25	(1.29) .05	(1.57) .05 b	-.15 .37 -.33		
0428+01	9.5 1.0 (1)	4.4 0.4 (6)	3.9 0.4	2.7 0.4	1.64 0.41 (9)	.90 .04	0.44 .01 b	.92 .95 1.14		
0431-02	2.5 0.8 (3)		3.1 0.4	2.3 0.3	1.86 0.16	1.06 .04	0.59 .03 b	.31 .91		
0432+03	5.2 1.0 (1)			1.9 0.3	1.06 0.26 (9)	.27 .01	<.05 c	.79 2.11		
0439-007	3.1 0.8 (3)			1.5 0.5		.40 .02		.77		
0439+01	11.1 1.1 (1)	5.9 0.4 (6)	2.9 0.4	2.1 0.5	1.17 0.13	.56 .02	0.25 .01 b	1.17 1.12 1.26		
0440-00	<1.0 (4)		1.4 0.8 (8)	(1.9) 0.2 (8)	(3.4) 0.2 (8)	(3.53) .20	(3.13) .09 a	-1.00 .08	QSO	
0442+02	7.4 0.7 (1)		3.1 0.4	2.3 0.4	0.91 0.12	.58 .02		.93 .99 .68		
0442-00				0.5 0.2		.27 .01		.42	QSO	
0445-019	0.7 0.3 (4)			0.9 0.3		.20 .01		-.19	QSO	
0447-010			1.1 0.4	0.5 0.2	0.37 0.10	.29 .01	0.21 .01 c	.53 .51	QSO	

TABLE AIV.1 continued

(1)	(2)	(3)	(4)	(5)	(6)	(7)	(8)	(9)	(10)	(11)	(12)	(13)
0448-025	2.6 0.8 (3)			1.1 0.4		.25 .01		.88	.67		E	
0453-00	7.6 1.1 (3)		3.6 0.4	3.1 0.4	1.02 0.12	.62 .03	0.30 .01 a,b	1.02	.97	1.06		
0454+039			1.1 0.4	<0.5	0.45 0.10	.40 .01	0.37 .03 c	.25		.13	QSO?	2
0457+024	<0.4 (4)		<0.6	0.4 0.4	1.89 0.17	1.63 .04	1.44 .04 a			.20	QSO?	
0458+01	4.2 0.8 (1)		1.9 0.6	1.5 0.3	0.89 0.12	.52 .02	0.28 .01 b	.85	.74	.96	E	
0458-02	5.2 1.3 (3)		2.5 0.4	2.60 0.2 (8)	2.15 0.11 (8)	(1.99) .08	(1.76) .05 a	.19	.28	.16	N?	
0500+019	<0.7 (4)		0.7 0.4	0.9 0.3	2.10 0.12	2.47 .05	1.85 .04 a		-1.04	.28		
0505+03	3.2 1.0 (3)		1.6 0.4	1.6 0.4	0.81 0.10	.74 .02	0.51 .02 a		.67	.52	QSO?	
0509-038			0.6 0.3	0.4 0.2	0.65 0.08	.39 .02	0.22 .01 a		-.25	.88		
0511+00	18.7 1.9 (1)			5.3 0.2 (8)	2.97 0.09 (8)	[1.70] .04	[0.99] .03 a	.83	.99	.86	E	
0519+01	0.7 0.3 (4)		1.7 0.4	1.4 0.3	0.84 0.11	.54 .02	0.42 .01 a	.46	.27	.44		
0534-03	8.6 1.3 (3)		2.8 0.5		0.68 0.10	.37 .01	0.11 .01 a	1.23	1.23	1.63		
0550+032	<0.7 (4)		<0.7	<1.5	0.61 0.10	(.90) .10	[0.88] .02 a			-.25		
0554-026			0.8 0.4	<1.8	0.75 0.10	.51 .02	0.22 .01 a		.05	1.19		
0558+02	3.0 0.8 (3)		1.6 0.4	0.8 0.3	0.55 0.10	.29 .01	0.13 .01 a	.99	.84	1.23		
0723-008	2.2 0.6 (4)				3.7 0.2 (10)	3.01 .06			-.25	0.21		
0724-01	15.4 1.5 (2)		6.5 0.5 (8)	5.4 0.2 (8)	2.86 0.09 (8)	[1.56] .04	[0.89] .03 g	.86	.81	.92	g	
0726-00	4.0 1.0 (3)					.40 .02		.84			g	
0731+02	7.0 0.7 (1)	4.4 0.4 (6)			0.89 0.22 (9)	.58 .02		.96		.66		
0736-01	6.6 1.7 (3)					.64 .02		.85			QSO	
0736+01	1.1 0.5 (4)		2.9 0.4 (8)	2.7 0.1 (8)	(2.30) 0.08 (8)	(2.42) .10	(2.06) .05 g		-.36	.09	QSO	
0737-030	5.5 0.8 (3)					.35 .01		1.01				
0738-00	4.6 0.7 (3)					.38 .02		.91				
0742+02	8.7 0.9 (1)	6.0 0.4 (6)	4.4 0.6	2.7 0.4	1.59 0.40 (9)	[.82] .03	[0.37] .01 a	1.03	.72	1.27	g	
0743-006			<0.8	0.6 0.3	0.86 0.08	1.40 .03	1.76 .04 a	-.42		-.42	QSO?	
0747-00	3.1 0.9 (3)		1.7 0.6	1.1 0.3	0.76 0.10	.43 .02	0.18 .01 a	.98	.67	1.26		
0752-02.7	3.8 1.3 (3)			1.6 0.5	0.45 0.10	.46 .02	0.24 .01 c	.89	1.05	.94	N	
0752-02.3	≤0.8 (4)			2.0 0.5	0.59 0.10	.42 .02	0.20 .01 c	1.08		1.07	db	
0753+02	6.6 0.7 (1)		2.6 1.0	1.3 0.3	0.73 0.10	.45 .02	0.24 .01 c	.97	1.08	.95		2
0755+029			1.3 0.6	1.4 0.4	0.84 0.10	.49 .02	0.26 .01 a	.92	.53	.97		
0757+025				0.7 0.3	0.62 0.15 (9)	.27 .02		.88		1.26		
0802-010				1.2 0.4	0.64 0.10	.35 .02	0.22 .01 c	.79		.79		
0803-00	7.6 1.1 (3)			3.4 0.4	1.54 0.21	.71 .03	0.38 .02 a	.95	.76	1.05	E4	
0803-023	2.5 0.8 (3)		0.8 0.4	0.9 0.3	0.61 0.10	.35 .01		.70	.64	.84		
0808+019	<0.5 (4)		1.5 0.4	<0.8	0.45 0.11	(.71) .05	(0.89) .02 a			-.41	QSO	
0812+02	7.9 0.8 (1)	4.4 0.4 (6)		3.8 1.0 (8)	2.05 0.08 (8)	1.18 .02	0.79 .01 a	.69	.66	.70	QSO	
0812-02	15.9 1.5 (2)			4.5 1.0 (8)	1.89 0.08 (8)	.95 .02	0.41 .01 a	1.14	.99	1.24	D	

TABLE AIV.1 continued

(1)	(2)	(3)	(4)	(5)	(6)	(7)	(8)	(9) (10) (11)	(12)	(13)
0813+020				<1.2		.38 .01	0.22 .01 a,c	.88		
0819-032			<0.8	<0.5	0.49 0.10	.42 .02	0.24 .01 a	.81		
0823+033	0.8 0.4 (4)		0.6 0.3	0.5 0.2	0.81 0.14	(.87) .05	(1.14) .03 a	-.31 -.11 -.37		
0825+013	3.9 0.9 (3)		1.8 0.4	0.6 0.3	0.66 0.10	.30 .01		.96 .86 1.20		
0828-03	4.4 0.7 (3)		1.8 0.4	1.3 0.3	0.81 0.14	.53 .02	0.31 .01 a	.78 .82 .84	QSO?	
0833-01				1.6 0.4		[.56] .02	[0.22] .01 a	1.32 1.51	E	
0835-013			0.6 0.3	0.8 0.4	0.79 0.10	.32 .01		-.16 1.38		
0836-00	2.6 0.7 (3)		1.0 0.4	0.9 0.3	0.65 0.10	.31 .01		.79 .64 1.13		
0837+035	<0.5 (4)		0.9 0.4	0.9 0.3	0.70 0.13	.69 .03	0.58 .02 a	.23 .26 .24	QSO?	
0837+012				<0.6	0.24 0.15 (9)	.25 .01		-.06	QSO	
0849+008	3.7 1.1 (3)			0.6 0.2	0.28 0.15 (9)	.24 .01		.92		
0850-03	5.6 0.8 (3)	3.8 0.4 (6)	3.6 0.6	2.7 0.4	1.35 0.11	.75 .03	0.32 .02 a	.90 .74 1.16		
0852+029	3.8 1.0 (3)			1.0 0.3	0.81 0.14	.38 .02	0.19 .01 c	.95 .73 1.12		2
0853+03				<0.9	0.69 0.10	.35 .01	0.19 .01 c	.99	QSO?	2
0854-03	3.8 1.0 (3)	3.5 0.4 (6)	2.8 0.4	1.6 0.3	1.24 0.18	.66 .03	0.37 .02 c	.83 .70 .94	g cluster	2
0859+032			0.6 0.3	0.6 0.3	0.72 0.10	.34 .01	0.21 .01 c	-.18 .84	g	
0904+039			1.3 0.4	0.8 0.2	0.94 0.15	.44 .02	0.18 .01 a	.10 1.38		
0906+011				1.3 0.3		.28 .01		1.06		
0906+01			1.3 0.4	1.1 0.3	1.35 0.19	1.20 .03	1.02 .04 a	.25	QSO	
0907+022				<0.5		.19 .01				
0907-023	0.9 0.4 (4)		<0.6	0.6 0.3	0.55 0.11	.57 .02	0.40 .02 a	.40 .22 .50	QSO	
0909+003				0.6 0.3	0.30 0.15	.26 .01		.51 .21		
0912+029	<0.7 (4)		1.3 0.4	<0.6	0.55 0.10	.54 .02	0.45 .02 a	.26	QSO?	
0913-025	3.6 0.9 (3)			1.1 0.3		.28 .01		.94 .93	QSO	
0922+005	<0.5 (4)		<0.6	<0.7	0.80 0.11	.74 .02	0.71 .03 a	.07	QSO	
0927+02	<2.0 (4)			1.3 0.3	0.39 0.15	.32 .01		.92 .30		
0932+02	4.0 1.0 (3)	3.5 0.4 (6)	2.5 0.4	1.1 0.4	0.82 0.14	.53 .02	0.30 .02 a	.89 .93 .86	QSO	
0936+02	2.3 0.6 (3)			0.7 0.3	0.42 0.15	.28 .01		.75 .83 .61		
0937+033				0.9 0.3		.28 .01		.80		
0938-01	3.4 1.0 (3)		0.7 0.4	0.9 0.3	0.71 0.11	.53 .02	0.35 .02 c	.60 .70 .62		2
0940+02	3.2 0.8 (3)		2.5 0.4	1.5 0.4	1.28 0.18	.86 .02	0.50 .02 a	.67 .48 .84		
0940+00	5.3 0.5 (1)		2.7 0.5	1.7 0.3	1.18 0.10	.73 .03	0.38 .02 c	.77 .73 .93		2
0945+003	8.2 0.8 (1)		2.7 0.4	1.7 0.3	0.80 0.14	.39 .02	0.18 .02 c	1.12 1.14 1.19		2
0949+00	22.8 2.3 (1)				2.90 0.80	[1.53] .03	[0.64] .02 a	1.11 .99 1.39		
0950+00					0.86 0.40	.43 .02	0.17 .01 c	1.48	QSO	
0955+037						.35 .02	0.20 .01 a	.90		
0955+036						.35 .02	0.15 .01 a	1.37		

TABLE AIV.1 continued

(1)	(2)	(3)	(4)	(5)	(6)	(7)	(8)	(9) (10) (11)	(12)	(13)
0955-01	3.7 1.1 (3)		1.7 0.4	1.3 0.3	1.11 0.17	.72 .03	0.44 .01 b	.66 .52 .77		
0956+015			0.9 0.4	<0.6	0.64 0.10	.30 .01		.90 .31 1.15	db	
0957+00	6.9 1.4 (1)		2.3 0.4	1.3 0.3	1.17 0.17	.51 .02	0.34 .01 b	.81 .82 .74	QSO	
0958-001	9.7 2.1 (3)		3.2 0.4	2.2 0.3	1.21 0.18	.58 .02	0.30 .01 b	1.01 .98 1.07		
1004-018	0.9 0.5 (4)		2.2 0.6	0.8 0.3	0.53 0.11	.56 .02	0.60 .02 b	.08 -.10	QSO	
1005+007			1.0 0.5	0.6 0.2	0.60 0.10	.34 .01		.60 .22 .86	N	
1008-01	3.6 0.9 (1)		2.4 0.6	2.0 0.3		[.80] .03	[0.61] .01 b	.51 .46 .43	S	
1008+013				0.3 0.2	0.38 0.15 (9)	.24 .01		.35 .71	QSO	
1012+022	3.3 1.0 (3)		2.1 1.0	0.7 0.3	0.53 0.10	.40 .01		.72 .89 .42	QSO	
1014+018			2.5 1.0	0.8 0.2	0.64 0.10	.32 .01		.88 .73 1.05		
1021+028	0.8 0.4 (4)			1.2 0.2		.22 .01		-.31	QSO?	
1021-00	<0.8 (4)		<0.6	0.5 0.2	1.00 0.12	.95 .04	0.74 .03 a	.26 -.87 .32	QSO?	
1027+00	4.6 0.7 (3)		2.8 0.4	1.9 0.4	0.97 0.24 (9)	.61 .03	0.35 .01 b	.81 .71 .88	g	
1033+003	2.2 0.6 (3)		1.3 0.5	1.0 0.3	0.56 0.10	.34 .01		.71 .67 .76	E	
1039+02	7.9 0.8 (1)	5.9 0.4 (6)	6.9 0.6	5.2 0.5	2.57 0.14	1.66 .04	0.96 .02 c	.73 .61 .82	g	
1044-00	4.5 0.7 (3)		1.1 0.4	1.3 0.3	0.46 0.10	.32 .01		.94 1.08 .55		
1045+019			<1.0	<0.5	0.37 0.10	.41 .02	0.36 .01 b	.18		
1046-02	4.5 1.1 (3)			2.1 0.3		.51 .02		.87 .59		
1048+00	5.7 0.6 (1)	3.2 0.3 (7)	3.2 0.4	1.8 0.4	0.79 0.10	.31 .01		1.16 .95 1.42		
1051+035	2.8 0.8 (3)		1.6 0.5	0.6 0.3	0.84 0.10	.29 .01		.97 .55 1.62	db	
1052-004	3.0 0.8 (3)		1.3 0.4	1.3 0.4	0.64 0.10	.34 .01		.82 .74 .96	QSO?	
1052+023	3.1 0.6 (1)		1.8 0.6	0.7 0.4	0.84 0.10	.34 .01		.87 .63 1.38		
1054+004	1.6 0.7 (4)		1.6 0.4	1.5 0.3	0.91 0.12	.58 .02	0.36 .01 b	.68 .41 .75		
1055+01	5.7 0.6 (1)	3.9 0.4 (6)	4.0 0.4 (8)	4.1 0.15 (8)	(3.1) 0.1 (8)	(3.02) .10	(3.07) .07 d	.22 .00	QSO	
1055-028			0.6 0.3	0.4 0.2	0.63 0.10	.42 .01	0.30 .02 c	-.21 .55		2
1059-01	22.0 1.5 (2)		7.7 0.7	5.9 0.2 (8)	2.71 0.09 (8)	1.34 .03	0.67 .02 b	1.04 1.03 1.10		
1059-023	5.1 1.6 (3)		1.6 0.4	1.3 0.3	0.99 0.10	.50 .02	0.29 .01 b	.84 .65 .92		
1103+002				0.9 0.3	0.61 0.15 (9)	.29 .01		.87 1.15	S	
1103-006	4.7 1.0 (3)		2.3 0.6	1.5 0.3	0.95 0.11	.68 .03	0.42 .01 b	.70 .76 .72	QSO	
1105-028	2.9 1.0 (3)		1.6 0.4	1.2 0.3	0.60 0.10	.36 .02	0.18 .01 b	.91 .80 1.04	QSO?	
1105+037			1.3 0.6	0.6 0.3	0.60 0.10	[.46] .02	[0.29] .01 b	.66 .49 .69		
1106+023			1.5 0.4	1.6 0.3	0.71 0.10	.64 .03	0.50 .02 b	.44 .83 .34	N	
1106-003				0.8 0.2		.26 .01		.77	QSO?	
1108+03	8.6 1.7 (1)		2.4 0.8	3.7 0.4	0.94 0.10	.48 .02	0.20 .01 c	1.25 1.14 1.29		2
1110-01	8.3 1.2 (3)		4.2 0.8	2.6 0.4	1.56 0.12	.84 .03	0.45 .01 b	.91 .81 .99		
1111-037	2.2 0.6 (3)			0.7 0.4		.35 .01		.66	[g? QSO?	
1115-023	4.5 1.1 (3)		3.4 1.5	1.7 0.3	1.09 0.11	.62 .03	0.35 .01 b	.83 .68 .90		

TABLE AIV.1 continued

(1)	(2)	(3)	(4)	(5)	(6)	(7)	(8)	(9) (10) (11)	(12)	(13)
1116-02	18.1 1.8 (2)		7.2 2.0	5.5 0.5	1.59 0.12	.59 .03	0.17 .01 c	1.44 1.18 1.78		
1118+000			1.2 0.4	0.9 0.3	0.72 0.10	[.44] .02	[0.31] .01 b	.58 .40 .60	db	
1122-037	1.7 0.7 (4)		1.6 0.4	1.3 0.3	0.79 0.10	.47 .02	0.30 .01 b	.69 .49 .74		
1123+012				1.5 0.4		.25 .01		1.23		
1127+005	4.3 1.0 (3)		2.3 0.4	1.3 0.3	1.02 0.11	.58 .02	0.30 .02 c	.81 .69 .99	g cluster	2
1127-032	5.0 0.8 (3)			1.3 0.3		.31 .01		1.01 1.05		
1127+012	2.2 0.6 (3)		1.4 0.6	0.3 0.2	0.66 0.10	.41 .02			N	
1130-037	2.2 0.6 (3)		1.4 0.7	1.5 0.4	0.28 0.10	.54 .02	0.28 .01 c	1.60 1.42 1.81	E	2
1130+009			<0.8	0.5 0.3	0.45 0.10	.32 .02		.43 .52	QSO?	
1132-000	3.0 0.8 (3)		2.3 0.4	2.1 0.3	1.34 0.11	.73 .03	0.45 .01 c	.73 .44 .82		
1133-032	2.8 0.6 (3)			0.6 0.3		[.31] .01		.79		
1134+01	5.0 0.5 (1)		2.9 0.6	2.7 0.4	1.12 0.11	.55 .02	0.28 .01 c	.91 .71 1.09		2
1138+01	7.6 0.8 (1)	6.0 0.4 (6)	5.6 0.8 (8)	4.0 0.2 (8)	2.40 0.12 (8)	1.57 .04	0.96 .02 c	.69 .55 .74		
1141+011				0.9 0.3		.33 .02		.69	g	
1142-00	6.2 0.9 (3)		2.3 0.4	1.9 0.3	1.09 0.11	.43 .02	0.14 .01 c	1.14 .82 1.65		2
1146-037	1.2 0.6 (4)		1.5 0.4	1.4 0.4	0.60 0.10	[.40] .01	[0.33] .01 b	.42 .60 .33	QSO?	
1147+015	2.4 0.6 (3)			0.7 0.2		.31 .02		.72 .96	g	
1148-00	2.7 0.7 (3)		3.4 0.4 (8)	3.5 0.2 (8)	3.09 0.13 (8)	2.56 .04	1.95 .04 c	-.18 .39	QSO	
1159-02	3.8 1.0 (3)		2.5 0.4	1.0 0.3	0.77 0.14	.43 .02		.87 .84 .88		
1201-026	2.8 0.7 (3)			0.5 0.3		.150 .011		1.06	QSO?	
1207-013			1.0 0.4	0.5 0.3	0.55 0.10	.39 .01		.47 .43 .52	db	
1212-00	6.0 0.9 (3)		2.7 0.4	2.7 0.5	0.94 0.15	.54 .02	0.28 .01 c	.96 .87 1.03		
1212+006	3.9 0.9 (3)			0.9 0.5		.28 .02		.96		
1214-029	2.7 0.7 (3)			<1.6		.25 .01		.87		
1215+03	13.9 1.4 (1)		5.7 0.8 (8)	4.6 0.5		[1.21] .02	[0.53] .02 e	.98 .87 1.33	D+E	
1217+02	2.0 0.7 (4)	1.0 0.3 (7)	1.8 0.4	0.4 0.3	0.61 0.12	.47 .02	0.50 .01 c	.62 -.05	QSO	
1218-02	2.8 0.7 (3)		1.4 0.4	1.4 0.3	0.64 0.12	.54 .02	0.47 .01 c	.71 .22	QSO	
1222+037	2.5 0.6 (3)			0.9 0.3	0.72 0.13	.81 .02	0.86 .02 b	.60 -.10	QSO?	
1225-02	2.2 0.7 (3)		1.4 0.4	1.4 0.3	0.63 0.12	.40 .02	0.24 .01 c	.76 .63 .80	QSO?	
1226+02	67.8 6.8 (1)	57.0 2.9 (6)	54.5 0.5 (8)	51.3 0.5 (8)	(43.0) 0.5 (8)	(43.4) .8	(40.0) .8 c	.20 .04	QSO	4
1229-02	8.0 2.0 (3)		3.3 0.8	3.0 0.2 (8)	1.90 0.11 (8)	1.33 .03	1.05 .05 c	.53 .75 .45	QSO	
1229-01	2.0 1.0 (4)		2.1 0.8	1.9 0.3	0.81 0.14	.47 .02	0.27 .01 c	.87 .70 .88		2
1247+025			<0.5	0.5 0.3	0.51 0.10	.42 .02	0.29 .01 b	-.02 .56		
1249+035	1.9 0.9 (4)		2.2 0.8	1.3 0.4	0.78 0.14	.60 .03	0.36 .01 b	.69 .57 .76	E2	
1250+029	5.6 0.6 (1)		4.0 1.0	2.2 0.3	1.20 0.18	.91 .02	0.51 .01 b	.76 .73 .90		
1253+026	4.0 0.9 (3)		2.5 0.8	1.0 0.3	0.66 0.13	.30 .02		.98 .89 1.20		
1256+018			0.9 0.4	0.7 0.2	0.50 0.10	.29 .01		.66 .47 .83		

TABLE AIV.1 continued

(1)	(2)	(3)	(4)	(5)	(6)	(7)	(8)	(9) (10) (11)	(12)	(13)
1302-035	2.0 0.7 (4)		1.4 0.4	1.3 0.3	0.79 0.14	.53 .02	0.37 .01 b	.56 .47 .58	QSO?	
1305-012				0.8 0.3		.28 .01		.72		
1307-00.1	11.4 1.1 (1)		4.6 1.0	3.8 0.4	1.57 0.21	.82 .03	0.41 .01 c	1.02 .93 1.10	D	
1307-00.7	1.9 0.7 (4)		1.2 0.5	1.1 0.3		.22 .01		.91 .43		
1317-00	4.7 0.7 (3)		2.2 0.4	3.6 0.4	1.40 0.20	.97 .02	0.68 .02 c	.62 .52 .57	QSO	
1317+019	<0.5 (4)		1.2 0.4	0.7 0.3	0.63 0.13	.55 .02	0.62 .03 b	-.02 .49 -.15		
1320+03	8.3 0.8 (1)		3.0 0.4	2.9 0.4	1.33 0.19	.75 .02	0.38 .01 b	.93 .88 1.07	D	
1324-025			1.7 0.6	0.9 0.3	0.39 0.11	.31 .02		.81 1.26 .35	g	
1325-01	7.0 1.7 (3)		2.8 0.6	1.8 0.4	0.89 0.15	.71 .03	0.43 .01 b	.77 1.00 .75	D	
1329+012	2.5 0.8 (3)			0.5 0.3		.21 .01		.88		
1330+02	8.8 0.9 (1)		5.8 0.8 (8)	4.8 0.5	2.83 0.15	[1.91] .04	[1.47] .07 g	.56 .56 .50	N	
1336+020	3.5 0.9 (3)		1.8 0.5	1.3 0.3	0.86 0.10	.39 .01		.87 .66 1.20		
1337-033	0.8 0.4 (4)		1.4 0.4	0.3 0.3	0.86 0.14	.58 .02	0.30 .01 b	.13 1.01		
1340+022	3.9 0.8 (1)		2.7 0.6	1.9 0.3	0.98 0.15	.54 .02	0.30 .01 c	.86 .69 .94		
1342-00	3.8 1.0 (3)		2.4 0.4	2.0 0.3	0.92 0.15	.62 .03	0.38 .01 b	.75 .73 .76		
1343-026	3.0 1.0 (3)			1.1 0.4		.24 .01		.95		
1345+008	3.0 0.9 (3)			0.5 0.3		.157 .011		1.05		
1349-01				2.3 0.5		.31 .02		1.38	g	1
1349+027	2.5 0.6 (5)		2.5 0.8	2.0 0.4	1.02 0.11	(.76) .05	(0.46) .01 b	.63 .50 .69		
1351+021	<0.6 (4)		1.1 0.6	0.4 0.2	0.52 0.10	.47 .02	0.38 .01 b	.31 .32		
1351-018	<0.6 (4)		1.1 0.4	<0.7	0.85 0.14	.98 .02	0.94 .02 b			
1352+00				0.6 0.3	0.73 0.20	.35 .02	0.17 .01 b	-.24 1.16	QSO?	
1353-005	2.9 0.8 (3)			0.9 0.3		.31 .02		.80 .91		
1354+01				5.0 0.2 (8)	2.31 0.12 (8)	1.30 .02	0.71 .02 b	.94 .97 .95		1
1355+01				2.5 0.8	1.72 0.12	1.01 .03	0.48 .01 b	1.07 .47 1.10		1
1356+022	≤0.7 (4)			<0.8	0.79 0.08	.66 .03	0.47 .01 b	.47	QSO?	
1359+025	4.0 0.9 (3)		2.9 1.0	2.2 0.4	0.92 0.11	.57 .02	0.34 .01 c	.81 .76 .81	N	
1402-012	≤0.7 (4)		1.0 0.4	<0.5	0.51 0.06	.71 .03	0.80 .02 b	-.25	QSO?	
1403-02	7.2 1.8 (3)		2.0 0.8	1.7 0.3	0.77 0.10	.46 .02	0.23 .01 b	1.00 1.06 1.04		
1404-01	6.6 1.7 (3)	3.7 0.4 (6)	3.0 0.8	2.6 0.4	1.02 0.11	.58 .02	0.28 .01 b	1.02 .98 1.10	g	
1405+01		1.4 0.3 (7)	1.3 0.7	1.3 0.3	0.56 0.10	.38 .02		.72 .59		
1407+022	1.5 0.7 (4)		1.0 0.5	0.7 0.2	0.48 0.10	.49 .02	0.45 .01 b	.55 .12	QSO?	
1414-03	10.5 1.5 (2)	4.1 0.4 (6)	2.8 0.4	2.2 0.4	1.71 0.12	.95 .02	0.63 .02 c	.75 .78 .72		
1416-000				1.2 0.3		.20 .01		1.23		
1416-015	2.2 0.6 (3)			1.1 0.3		.30 .02		.76 .54		
1418-025	2.6 0.7 (3)			0.6 0.3		.25 .01		.84	g	
1420-005	3.0 0.8 (3)			1.7 0.4		.23 .01		1.05 .44		

TABLE AIV.1 continued

(1)	(2)	(3)	(4)	(5)	(6)	(7)	(8)	(9) (10) (11)	(12)	(13)
1424+03	3.7 0.9 (3)	1.9 0.3 (7)		0.9 0.3		.33 .02		.89 .98	QSO?	
1425-01	11.6 1.5 (2)		6.2 1.5	6.8 0.7	2.91 0.15	1.64 .03	0.85 .02 d	.91 .71 1.00	N	
1426+030				0.4 0.2	0.75 0.10	.43 .02	0.26 .01 b	.82		
1427-00	3.5 1.1 (3)			0.8 0.4	0.68 0.10	.39 .02		.78 .77 .84		
1428-03	3.8 1.1 (3)		3.1 0.4	1.8 0.3	0.85 0.11	.41 .02	0.20 .02 c	1.05 .92 1.14		2
1431+018				0.8 0.2		.32 .02		.63	E	
1434+03	8.3 1.7 (1)	5.2 0.4 (6)	4.4 1.0	4.5 0.6	2.63 0.15	1.92 .04	1.27 .02 b	.58 .55 .62		
1434+019			2.0 0.7	0.9 0.3	0.61 0.10	.36 .02	0.12 .01 b	.88 1.48		
1435+038			<1.0	1.0 0.4	0.89 0.11	.35 .02		.14 1.42	g	
1440-01	2.6 0.7 (3)			<0.6		.26 .01		.84		
1442-029				1.2 0.3		.27 .02		1.03	E	
1443-032				1.3 0.3		.25 .01		1.13		
1446+00	5.0 0.5 (1)		3.8 0.8	2.6 0.4	1.64 0.12	1.04 .04	0.57 .01 b	.72 .54 .89	E	
1446-005				<0.6		.33 .02				
1449-012				0.8 0.3	0.61 0.10	.35 .02	0.32 .01 b	.31 .28	QSO?	
1449+007	6.4 0.6 (1)			0.8 0.2		.23 .01		1.21 1.63		
1454-034	3.7 0.9 (3)			0.7 0.3		.29 .02		.91 1.30	QSO?	
1500-023	3.2 0.8 (3)		1.7 0.4	0.9 0.3	0.96 0.11	.59 .02	0.29 .01 c	.85 .55 1.06		
1502+036						.48 .02	0.61 .02 c	-.38	QSO?	1
1502+039						.25 .01				1
1503-001	3.5 0.9 (3)		2.2 0.4	0.8 0.3	0.93 0.11	.55 .02	0.30 .01 c	.82 .66 .94		
1505+01	7.0 0.7 (1)	3.4 0.3 (7)	3.0 0.5	1.6 0.4	1.14 0.11	.56 .02	0.29 .01 b	.96 .86 1.07		
1508+004	7.0 0.7 (1)		2.8 0.4	1.5 0.4	0.87 0.10	.43 .02		1.02 1.01 1.07		
1509+022	4.0 2.0 (4)		2.8 1.2	1.4 0.3	0.91 0.11	.69 .03	0.53 .01 b	.47 .71 .42		
1509+01	8.9 0.9 (1)		4.5 1.5	5.6 0.6	2.20 0.13	1.20 .03	0.66 .02 b	.85 .69 .95		
1514+00	7.7 0.8 (1)		3.9 0.5	2.9 0.5		[1.83] .04	[1.32] .02 c	.50 .73 .52	[E3 QSO	
1523+03	5.2 0.5 (1)	4.3 0.3 (7)	3.7 0.4 (8)	3.8 0.6	1.71 0.12	1.13 .03	0.69 .02 c	.67 .58 .75		
1523-01	3.8 0.9 (3)		1.6 0.7	1.3 0.3	0.54 0.10	.40 .02		.80 .94 .45		
1523-034				<0.8		.21 .01				
1525-020				<1.8		.27 .02				
1532+01	≤0.8 (4)	0.9 0.3 (7)	1.0 0.4	1.0 0.3	1.20 0.11	1.08 .04	0.92 .02 c	-.21 .23		
1532-000				0.8 0.3		.30 .02		.67		
1535+004	<0.5 (4)		<0.6	<0.7	0.79 0.10	1.01 .03	0.86 .03 a	.16		
1538+010	3.8 0.8 (1)		2.1 0.4	1.0 0.3	0.64 0.10	.41 .02		.83 .89 .68		
1539-022	3.7 0.9 (3)			<0.7		.25 .01		.99		
1542+02	4.8 0.5 (1)	1.1 0.3 (7)	1.2 0.4	1.6 0.4	1.01 0.11	.51 .02	0.29 .01 c	.82 .74 .94	E	
1543+005	1.0 0.5 (5)		2.5 0.4	2.2 0.4	1.47 0.12	1.30 .03	0.86 .03 a	.55	QSO?	

TABLE AIV.1 continued

(1)	(2)	(3)	(4)	(5)	(6)	(7)	(8)	(9)	(10)	(11)	(12)	(13)
1545−004	2.8 0.8 (3)			0.7 0.2		.19 .01		0.97	1.08			
1546+027	≤0.7 (4)		<1.0	0.6 0.3	0.77 0.10	(1.27) .10	(1.41) .05 a	−.37		−.36	QSO?	
1547+032	1.9 0.7 (4)			2.7 0.5		.26 .01		−.27				
1548+013	2.4 0.6 (3)			0.5 0.3		.26 .01		1.23				
1552−033	≤0.4 (4)		0.6 0.3	0.5 0.2	0.71 0.10	.43 .02	0.42 .01 b	.16	−.27	.16		
1555+001	0.4 0.3 (5)		<1.0	<0.6	1.46 0.12	2.01 .05	2.29 .09 a	−.30		−.28		
1556+032			<1.0	0.5 0.2	0.56 0.10	.46 .02		.17		.30		
1557−00	<0.6 (4)		<1.0	1.5 0.4	1.06 0.11	.54 .02	0.14 .01 b		.43	1.73		
1559+02	38.1 3.8 (1)		23.5 3.0 (8)	16.9 0.2 (8)	[8.81] 0.11 (8)	[5.04] .07	[3.24] .10 a	.81	.65	.82	D	
1601−015				0.5 0.3	0.58 0.10	.34 .02		.64		.81		
1601−00	5.5 1.2 (3)			1.0 0.4	0.57 0.10	.45 .02	0.26 .01 b	.85	1.09	.81	N	
1601−017				0.8 0.3		.31 .02		.65			E	
1602+01	25.5 2.6 (1)		12.6 0.6 (8)	8.9 0.2 (8)	3.94 0.10 (8)	2.13 .05	1.11 .02 b	1.00	.87	1.00		
1602−00.2			2.5 0.8	2.3 0.6	0.68 0.10	(.53) .08	(0.41) .02 b		1.32	.40	QSO?	
1603+005				1.2 0.3	1.15 0.12	.66 .03	0.31 .01 b	1.01	.05	1.12		
1603+00	13.5 1.4 (1)	4.8 0.4 (7)	5.1 0.6	3.6 0.9	2.07 0.13	1.50 .04	1.01 .02 b	.68	.85	.60	E4	
1608−011				<1.0		.31 .02						
1611−007	3.1 0.9 (3)			0.8 0.3		.27 .01		.87	1.06		QSO?	
1615+029	0.8 0.4 (4)		<0.6	<0.7	0.61 0.10	.74 .03	0.65 .02 b	.12		.14	QSO?	
1616−029	1.7 0.7 (4)			0.8 0.3	0.61 0.10	.40 .02	0.24 .01 b	.70	.48	.79	E	
1617−030				<0.7	0.51 0.10	.40 .02	0.21 .01 b			.93		
1618+007				<0.7		.21 .01					QSO?	
1635−035			<1.5	0.5 0.3	0.44 0.10	.51 .02	0.47 .02 b	.09		.10		
1636−03	5.6 1.4 (3)	3.4 0.4 (6)	1.9 0.8	0.6 0.3	0.88 0.10	.45 .01	0.20 .01 b	1.08	.98	1.24	g	
1638−025	6.5 1.6 (3)		3.1 1.0	3.9 0.4	1.71 0.13	1.03 .03	0.54 .02 c	.89	.76	.96		
1643+022	9.2 1.3 (3)		4.7 1.0	2.3 0.8	1.78 0.13	1.16 .03	0.70 .02 c	.76	.79	.77	E	
1645+027	3.7 0.9 (3)		2.8 0.8	2.8 0.8	1.15 0.12	.50 .02	0.23 .01 b	1.05	.62	1.26		
1646+003	2.4 0.6 (3)		1.0 0.4	1.1 0.5	0.58 0.08	.33 .02		.73	.67	.86		
1648+015			<0.8	0.9 0.5	0.90 0.11	.72 .03	0.68 .01 b	.13		.13		
1649−039			1.4 0.4	0.8 0.4	0.66 0.10	.50 .02	0.33 .01 b	.61		.63		
1650+004	5.4 0.8 (3)		3.4 0.5	2.8 0.6	1.37 0.11	.73 .03	0.35 .02 c	.88	.69	1.09		
1650+024	2.3 0.7 (3)			1.8 0.6		.30 .02		.83	.19		g	
1654−020	2.4 0.6 (3)		1.1 0.4	0.7 0.3	0.85 0.10	.64 .03	0.51 .02 b	.40	.46	.38		
1659+01	2.2 0.6 (3)			0.9 0.3		.28 .02	0.11 .01 b	.95	.70	1.51		
1701+024				1.5 0.3		[.34] .02	[0.16] .01 b	1.12		1.21		
1704+001	2.8 0.8 (3)		1.7 0.4	0.9 0.3	0.73 0.10	.42 .02		.72	.66	.84		
1705+018	<0.6 (4)			0.6 0.3	0.45 0.10	.53 .02	0.58 .02 b	−.14		−.15		

TABLE AIV.1 continued

(1)	(2)	(3)	(4)	(5)	(6)	(7)	(8)	(9)	(10)	(11)	(12)	(13)
1706+006			1.8 0.6	0.6 0.3	0.47 0.10	.50 .02	0.36 .01 b	.50		.48		
1706-02	3.0 1.0 (3)			1.0 0.3		.29 .02		.85	.86			
1707-038				<0.8		.30 .02						
1708+00	4.3 0.9 (3)		2.2 0.8	2.1 0.4	1.12 0.11	.83 .03	0.56 .02 b	.60	.66	.59	db	
1710-029				1.0 0.3		.33 .02		.76				
1711+006	4.6 0.9 (3)		3.3 1.0	1.6 0.4	1.13 0.11	.68 .03	0.38 .01 b	.81	.69	.89		
1712-03	8.5 1.3 (3)		2.6 0.8	3.1 0.5	1.29 0.11	.61 .03	0.26 .01 b	1.11	.91	1.29		
1714-019					1.2 0.3	.40 .02	0.19 .01 b			1.25		
1714+025				0.6 0.3	0.32 0.15 (9)	.34 .02		.30		-.09		
1714-020	2.6 0.8 (3)					.30 .02		.80				
1716+006	10.0 5.0 (5)		4.8 2.0	3.6 0.7		1.30 .03	0.74 .02 a	.86	.80	.91		
1717-00	223.0 20.0 (2)		91.8 4.6	97.1 1.4 (8)	53.8 0.6 (8)	[33.8] .7	[20.2] .5 a	.72	.53	.76	D	
1720+001	<2.0 (4)			1.5 0.4	0.76 0.10	.51 .02	0.29 .02 b			.82		
1722-02	7.6 1.9 (3)		4.2 1.5	3.8 0.4		[1.52] .04	[0.94] .03 b	.68	.54	.77		
1726-038	5.6 1.2 (3)			0.8 0.4	0.89 0.11	.57 .02	0.45 .02 c	.62	.87	.44		
1728+004				<0.6		.18 .01						
1729+010	3.1 0.9 (3)			<0.8		.20 .01		1.00			QSO?	
1735+026				<0.7		.26 .01						
1735-010	2.2 0.6 (3)			<0.7		.26 .01		.78				
1735+034	3.9 0.9 (3)		2.0 0.6	1.3 0.4	1.05 0.11	.80 .03	0.46 .02 b	.66	.61	.76		
1738+032				<0.8		.27 .02						
1741-03	0.9 0.4 (4)		0.9 0.4	0.9 0.4	1.17 0.11	(2.96) .20	(3.63) .08 a		-.16	-.72		
1748+031	6.8 1.0 (3)		3.2 0.8	<2.5	1.17 0.11	.80 .03	0.40 .01 b	.89	.85	.99		
1749+023	5.0 0.7 (3)		1.9 0.8	0.7 0.4	0.56 0.10	.55 .02	0.29 .01 c	.85	1.07	.92		
1938-012	3.6 0.9 (3)		1.6 0.4	0.5 0.2	0.58 0.10	.57 .02	0.31 .01 a					
1942+038	4.6 0.9 (3)		1.8 0.4	<0.9	0.69 0.10	.50 .02	0.29 .01 a	.81	.91	.81	QSO?	
1943+002	3.2 0.8 (3)		1.9 0.4	2.3 0.4	1.01 0.11	.84 .02	0.50 .01 a	.69	.60	.77		
1946+024	4.5 0.7 (3)			<1.2	0.76 0.11	.42 .02	0.16 .01 a	1.02	.86	1.38		
1949+02	19.2 1.9 (1)	14.2 0.7 (6)	9.8 0.5	10.7 0.3 (8)	5.69 0.18 (8)	[3.68] .07	[2.37] .04 a,c	.68	.45	.69	SO	
1949-01	13.8 1.5 (2)		2.9 0.4	3.3 0.4		[.79] .02	[0.26] .01 a	1.16	1.23	1.79	E	
1952+017	3.8 0.9 (3)		2.2 0.9	1.2 0.3	0.97 0.11	.54 .02	0.26 .02 a	.83	.64	1.07		
1952+007	3.6 1.1 (3)		0.8 0.4	0.7 0.3	0.42 0.10	.34 .02	0.20 .01 a	.78	1.02	.78	QSO?	
1953+035	4.6 0.9 (3)			0.7 0.3		.29 .02	0.14 .01 b	1.03	1.48	1.17	QSO?	
1957-013	3.0 0.8 (3)		1.0 0.4	0.8 0.4	0.40 0.10	.46 .02	0.26 .01 b					
2000+00	6.7 0.7 (1)			1.6 0.4		.24 .01		1.22	1.12			
2001-023	3.2 0.8 (3)			0.9 0.4	0.43 0.10	.38 .01	0.30 .01 b	.51	.97	.37		
2003-025	7.8 2.0 (3)		2.7 0.8	3.3 0.6	1.81 0.12	1.47 .03	0.84 .02 a	.71	.67	.77		

TABLE AIV.1 continued

(1)	(2)	(3)	(4)	(5)	(6)	(7)	(8)	(9)	(10)	(11)	(12)	(13)
2012+01	5.3 0.5 (1)		2.4 0.4	1.8 0.3	0.84 0.14	.43 .02	0.20 .01 a	.98	.87	1.19		
2012-017	1.3 0.6 (4)		1.2 0.4	1.1 0.3	0.81 0.14	.72 .03	0.65 .02 a,c	.20	.28	.16		
2022+031	≤0.4 (4)		0.7 0.4	0.5 0.3	0.27 0.10	.36 .01	0.36 .01 b		.84	.00		
2027-035				<0.6		.23 .01	0.19 .02 c			.30		2
2034+039	2.3 0.7 (3)			0.9 0.3	0.23 0.15 (9)	.20 .01		.91	.73			
2037-03	3.0 0.8 (3)		0.9 0.4	0.6 0.3	0.45 0.10	.30 .01	0.16 .01 c	.87	.91	.97		2
2038-01	4.3 1.1 (3)			1.2 0.3		.22 .01		1.11	1.00			
2044-02	9.7 2.4 (3)	4.6 0.4 (6)	4.1 0.8	4.5 0.6	1.85 0.11	1.38 .03	0.92 .02 a,c	.64	.77	.60		
2047-032			1.1 0.5	0.9 0.3	0.60 0.12	.39 .02	0.22 .01 b	.81	.53	.88		
2047+039	<0.7 (4)		1.4 0.7	0.5 0.3	0.50 0.12	.47 .02	0.40 .02 b			.24		
2052+005			0.3 0.2	<0.6	0.51 0.12	.47 .02	0.25 .01 b		-.48	.94		
2056+028	1.8 0.7 (4)		1.3 0.4	2.3 0.4	0.80 0.14	.43 .02	0.19 .01 b	1.03	.54	1.25		
2058+019	2.5 0.6 (3)			<1.0	0.50 0.15 (9)	.32 .01		.75		.69		
2059+034	<0.5 (4)		0.5 0.3	<0.6	0.53 0.12	.59 .03	0.74 .02 b	-.32	-.05	-.34	QSO	
2108+039	3.8 0.9 (3)		1.2 0.4	1.3 0.3	0.60 0.10	.36 .01	0.18 .01 b	.93	.87	1.07		
2110-017	2.8 0.7 (3)			1.2 0.3		.31 .01		.83	.66		QSO?	
2110+023	0.8 0.4 (4)		0.9 0.4	1.0 0.3	0.32 0.10	.34 .01	0.15 .01 b	.90	.54	1.23		
2121-01	<0.6 (4)		1.7 0.6	1.3 0.6	0.81 0.14	.60 .03	0.28 .02 a			1.04		
2121+028	2.8 0.7 (3)		1.5 0.4	1.1 0.3	0.63 0.13	.32 .02	0.17 .01 a	.89	.72	1.02		
2123+00	3.1 0.9 (3)		1.4 0.4	1.1 0.3	0.62 0.13	.38 .02	0.16 .01 a	.96	.77	1.28	db	
2123-015			<0.6	<0.8	0.26 0.10	.30 .01	0.27 .01 c			.16		
2126+010				0.8 0.3		.27 .01	0.17 .01 c	.74		.74		
2131-021	2.9 0.7 (3)		2.0 0.4	1.6 0.3	1.42 0.12	1.91 .05	1.96 .05 a,c		.31	-.12	QSO	
2133+010	2.6 0.8 (3)		1.0 0.4	1.8 0.4	0.69 0.10	.56 .02	0.34 .01 a	.69	.67	.74		
2134+004			0.9 0.4	1.1 0.3	2.44 0.13	7.59 .15	12.38 .22 a		-.96	-1.02	QSO	
2136+021				0.9 0.3	0.38 0.15 (9)	.25 .01		.85		.64		
2139+02	4.3 0.4 (1)		2.5 0.4	1.9 0.3	1.08 0.16	.63 .03	0.33 .01 a	.79	.65	1.00		
2149-20						1.23 .05	0.71 .03 f			.88		
2150-031	3.1 0.8 (3)		0.8 0.4	0.6 0.2	0.41 0.10	.30 .01		.77	.98	.47	g	
2154-18						1.11 .04	0.51 .02 f			1.25		
2154-01	8.5 2.1 (3)		3.4 0.4	3.0 0.4	0.96 0.15	.74 .02	0.34 .01 a	1.02	1.07	1.18		
2154-183						1.00 .04	0.55 .03 f			.96		
2201-006	2.2 0.7 (3)			1.0 0.3		.33 .02	0.18 .01 a	.82	.61	.98		
2202-003	2.9 0.7 (3)			<0.6		.26 .01		.88				
2203-18						5.20 .08	4.05 .09 d			.40	QSO	
2207+020	3.2 1.0 (3)		1.4 0.7	0.9 0.3	0.61 0.10	.44 .02	0.22 .01 a	.86	.78	1.00		
2210+01	3.1 0.6 (1)		4.2 0.4 (8)	3.9 0.2 (8)	2.84 0.12 (8)	1.79 .04	1.07 .02 a		-.12	.79		

TABLE AIV.1 continued

(1)	(2)	(3)	(4)	(5)	(6)	(7)	(8)	(9)	(10)	(11)	(12)	(13)
2211-17		30.2 1.5 (6)	26.7 1.3 (8)	20.0 0.2 (8)	8.90 0.13 (8)	[4.52] .12	[2.05] .05 d	1.06	.93	1.14	D	
2211-035	2.6 0.7 (3)		1.2 0.6	<0.8	0.56 0.10	.43 .02	0.20 .01 a	.88	.74	1.09		
2214-035	3.0 0.8 (3)			0.4 0.3		.31 .02	0.14 .01 a	.96		1.28		
2215-027	≤2.5 (4)		≤0.8	1.3 0.4	0.45 0.10	.43 .02	0.26 .01 a			.73		
2215+02	1.2 0.6 (4)		0.7 0.4	0.6 0.2	0.59 0.10	.70 .03	0.64 .02 a	.08	.27	.08		
2215-000	3.8 1.0 (3)			0.7 0.2		.28 .02		.90	1.33			
2216-03	3.0 0.8 (3)		0.9 0.5	1.8 0.1 (8)	0.98 0.07 (8)	1.04 .03	1.29 .02 a,c		.57	-.28	QSO	
2217-011				0.4 0.2		.28 .02		.24			g	
2217+018	3.7 0.9 (3)		1.3 0.6	1.2 0.3	0.64 0.10	.50 .02	0.26 .01 a	.83	.83	.95		
2219-030	5.9 1.3 (3)		2.0 0.5	2.5 0.4	1.03 0.11	.81 .02	0.43 .01 a	.85	.84	.93		
2221-02	25.3 2.5 (2)			12.2 1.2		[3.46] .07	[2.10] .03 a	.78	.57	.80	N	
2224+006	2.8 0.7 (3)		<0.6	0.6 0.2	0.48 0.10	.44 .02	0.48 .01 b			-.11		
2229+029				0.5 0.2	0.31 0.15 (9)	.26 .02		.43				
2243-03	6.8 1.0 (3)		2.0 0.4	2.4 0.3	0.81 0.10	.65 .02	0.45 .02 b	.76	1.00	.54	g	
2244-002				<0.7		.25 .02						
2245-022			1.5 0.4	1.4 0.3	0.45 0.10	.34 .02	0.20 .01 b	.86	1.20	.79		
2245+029	<0.5 (4)		1.2 0.4	0.7 0.2	0.93 0.11	.66 .03	0.57 .03 b			.32		
2250+03	3.1 0.8 (4)			0.9 0.5	0.45 0.15 (9)	.24 .01		.94	.97	.97		
2250+003	3.5 0.9 (3)			1.4 0.4	0.76 0.10	.50 .02	0.26 .01 b	.86	.74	.97		
2250+023				0.7 0.2	0.20 0.15	.34 .02	0.26 .01 c	.43		.41		
2251+006				0.9 0.2	0.43 0.10	.30 .02	0.39 .01 c			-.28		
2252+021	2.8 0.8 (3)			1.0 0.4	0.32 0.15 (9)	.27 .02		.85	.80			
2254+024	<0.5		<0.8	<0.6	0.39 0.10	.46 .02	0.52 .02 b			-.20	QSO	
2256+017			<0.6	<0.6	0.56 0.10	.36 .02	0.25 .01 b			.60		
2300-013				<0.6		.19 .01						
2302-025	4.9 1.6 (3)			0.9 0.3		.25 .01		1.05	1.33			
2303-008	2.6 0.8 (3)			0.6 0.3		.33 .02	0.18 .01 a	.83	1.15	.98		
2304+00	4.2 0.8 (3)			0.8 0.2	0.31 0.15 (9)	.31 .02	0.15 .01 a	.97	1.30	1.11		
2305+02	3.0 0.8 (3)			0.7 0.2	0.50 0.15 (9)	.32 .02	0.14 .01 a	.93	1.14	1.25		
2305+033	1.8 0.8 (4)			1.1 0.3	0.35 0.15 (9)	.27 .02	0.12 .01 a	.98	.38	1.23		
2313+01	6.4 1.3 (1)		2.2 0.4	1.8 0.3	1.74 0.44 (9)	.58 .02	0.26 .01 a	1.00	1.01	1.32	g	
2313+03	27.6 2.8 (1)	14.5 0.7 (6)	13.4 1.3 (8)	9.3 0.3 (8)	4.23 0.20	2.38 .05	1.30 .03 a	.94	.95	.94	N	
2318+02	5.1 0.5 (1)		2.3 0.4	0.8 0.2	0.53 0.10	.38 .02	0.18 .01 a	.98	1.11	1.07	QSO	
2320-021				<0.6		.33 .02	0.32 .02 c			.04	QSO	
2320-035	<3.0 (4)		<0.6	0.6 0.2	0.63 0.10	.42 .02	0.38 .01 b	.23	-.06	.23		
2323-038				<0.6		.23 .01						
2324-02			5.2 0.5	4.0 0.1 (8)	3.03 0.09 (8)	[1.56] .03	[1.10] .02 a	.65	.85	.75	E	

TABLE AIV.1 concluded

(1)	(2)	(3)	(4)	(5)	(6)	(7)	(8)	(9)	(10)	(11)	(12)	(13)
2332-017	1.2 0.6 (4)		1.1 0.4	<0.6	0.91 0.10	.64 .03	0.51 .02 a	.37	.14	.41	QSO	
2335-027	1.3 0.6 (4)		0.7 0.4	<1.2	0.52 0.10	.60 .02	0.65 .01 b	-.08	.42	-.13	QSO	
2335+03	6.0 0.6 (1)		2.5 0.7	1.6 0.3	1.34 0.11	.93 .04	0.61 .02 b	.65	.72	.64		
2338-002	3.2 1.0 (3)				0.60 0.20	.38 .01	0.20 .01 b	.93	.81	1.02	db	
2338+000						.36 .01	0.30 .01 c			.29	E	
2338+03	3.7 1.1 (3)		1.5 0.6	1.9 0.3	0.80 0.10	.38 .02	0.18 .01 b	1.05	.79	1.18	g	
2340-036				0.8 0.3		.28 .02		.72			QSO	
2347-02	7.2 1.8 (3)		4.3 0.6	3.5 0.5	1.82 0.12	.93 .04	0.45 .01 b	1.00	.73	1.12		
2349-01	6.5 1.6 (3)		2.8 0.4	1.9 0.4	1.63 0.12	1.01 .02	0.62 .02 a	.69	.57	.77	N	
2351-006	<1.5 (4)		<0.8	<0.6	0.45 0.10	.51 .02	0.46 .02 a			.13		
2353-003	3.1 1.0 (3)			0.7 0.3		.163 .012		1.08	1.17			
2354-02	4.3 1.4 (3)			1.0 0.4		.46 .02		.77	1.14			
2354+008					0.28 0.15 (9)	.157 .013				.86		
2355-010	4.1 1.0 (3)		2.2 0.4	1.7 0.5	0.85 0.10	.42 .02		.90	.79	1.07		
2356+033	2.9 0.9 (3)			0.5 0.2	0.34 0.20 (9)	.22 .01		.89	1.38	.67		
2356-028	2.2 0.7 (3)			<0.8		.171 .013		.94				
2357+00				0.4 0.2	0:36 0.15 (9)	.27 .02		.30		.44	db	
2359+017				<0.8	0.31 0.15 (9)	.174 .012				.93		

Footnotes to Table AIV.1

1. Confusion or resolution, 4C catalogue.

2. Flux density at 5009 MHz measured in only one linear polarization.

3. Observation at 2700 MHz confused.

4. Flux density at 2700 MHz, epoch 1968.5, from Harris (1969).

References for Table AIV.1

(1) Williams, P.J.S., Collins, R.A., Caswell, J.L., and Holden, D.J. (1968) - Mon. Not. R. astr. Soc. 139, 289

(2) Bennett, A.S. (1962) - Mem. R. astr. Soc. 68, 163

(3) Gower, J.F.R., Scott, P.F., and Wills, D. (1967) - Mem. R. astr. Soc. 71, 49

(4) Wills, D. (1969) - personal communication, after examining the original 4C records

(5) Wills, D. (1968) - Astrophys. Lett. 2, 247

(6) Wyllie, D.V. (1969) - Proc. astr. Soc. Aust. 1, 234

(7) Murdoch, H.S. and Large, M.I. (1968) - Mon. Not. R. astr. Soc. 141, 377

(8) Harris, Beverley J. (1969) - Ph.D. Thesis, A.N.U.

(9) Fitch, L.T., Dixon, R.S., and Kraus, J.D. (1969) - Astron. J. 74, 612

(10) Davis, M.M. (1967) - Bull. astr. Insts Neth. 19, 201

(11) Fomalont, E.B. (1967) - Astrophys. J. Supp. 15, 203